5-2006

B cells at the interface of innate and adaptive immunity in systemic lupus erythematosus: requirements for the activation of autoreactive B cells in autoimmune disease

Sean Ryan Christensen
Yale University.

B Cells at the Interface of Innate and Adaptive Immunity in Systemic Lupus Erythematosus: Requirements for the Activation of Autoreactive B Cells in Autoimmune Disease

A Dissertation

Presented to the Faculty of the Graduate School

of

Yale University

in Candidacy for the Degree of

Doctor of Philosophy

By

Sean Ryan Christensen

Dissertation Director: Mark J. Shlomchik

May 2006

Abstract

B Cells at the Interface of Innate and Adaptive Immunity

in Systemic Lupus Erythematosus:

Requirements for the Activation of Autoreactive B Cells

in Autoimmune Disease

Sean Ryan Christensen

2005

Systemic autoimmune disease is characterized by loss of immunologic tolerance to a restricted set of self-nuclear antigens. These macromolecular complexes can be grouped into two categories: DNA-containing autoantigens such as chromatin, and RNA-containing autoantigens such as Smith antigen (Sm) and related ribonucleoprotein complexes. Elucidating the mechanism for selective targeting of these molecules in systemic lupus erythematosus (SLE) may provide clues to the etiology of disease. We hypothesized that Toll-like receptors (TLRs), germline-encoded pattern-recognition receptors of the innate immune system, could dictate target antigen specificity in SLE. Using genetic ablation of various TLRs in murine models of SLE, we have demonstrated that TLRs are critical for directing the autoimmune response against canonical nuclear autoantigens.

In the absence of TLR9, a receptor for CpG sequence motifs in DNA, the generation of autoantibodies to DNA-containing antigens was specifically inhibited. Other autoantibodies specific for RNA-containing antigens were maintained or even increased in TLR9-deficient autoimmune mice. We then investigated whether TLR3, a

receptor for double-stranded RNA, or TLR7, a receptor for single-stranded RNA, were required for the generation of autoantibodies to RNA-containing antigens. While TLR3 did not appear to affect autoantibody production, the absence of TLR7 led to a reduction in anti-ribonucleoprotein antibodies. Genetic deletion of these receptors also had dramatic, but opposing, effects on disease progression. TLR9-deficient mice developed exacerbated disease and systemic inflammation with accelerated mortality, while TLR7-deficient mice had ameliorated clinical disease and decreased immune activation. A critical component of disease pathogenesis in these mice appeared to be the activation of type I interferon-producing plasmacytoid dendritic cells (pDCs), which was increased in the absence of TLR9, but decreased in the absence of TLR7.

Further studies on the mechanism of autoantibody production and pDC activation revealed that TLR9 expression within B cells was required for anti-DNA antibody production, and that circulating serum factors generated in the absence of TLR9 could induce interferon production by pDCs. We have also shown that costimulation by $CD4^+$ helper T cells contributes to autoantibody production in SLE. Integration of innate and adaptive activation signals is thus central to B cell autoantibody production and clinical disease progression in SLE.

Acknowledgements

This work was made possible by the concerted effort of many individuals. I am indebted to our collaborators for providing the genetic knockouts required to perform these studies; TLR9-deficient mice were provided by Shizuo Akira, and TLR3- and TLR7-deficient mice were provided by Richard Flavell. I also gratefully acknowledge the help and guidance of the faculty members of the Section of Immunobiology at Yale, particularly the members of my thesis committee: Kim Bottomly, Joe Craft, Mark Mamula, and Ruslan Medzhitov. I also thank Nancy Ruddle for helpful comments on the written thesis, and Michael Kashgarian for help with scoring renal pathology. Finally, the MD/PhD program at Yale provided continual support throughout the duration of my studies.

The Shlomchik Lab has been a wonderful place to study science, and I must thank each and every member of the lab for their help, advice, or support in one way or another. I am particularly indebted to Ashraf Khalil and Jonathan Shupe for technical assistance. Ashraf provided technical help with the initial analysis of F2 hybrids, allowing the TLR project to gain momentum with large groups of mice. Jon Shupe was instrumental in subsequent stages of the project, and his efficiency and skill allowed multiple different experiments to run simultaneously. Rosemary Tercyak and Pavlina Baevova kept the lab running and well-stocked with reagents, freeing the rest of us to generate and analyze data.

Mark Shlomchik taught me science. He taught me how to design and perform experiments, how to interpret the results with a skeptical eye, and how to communicate

the significance of the findings to the broader research community. He also provided an example of how science could be continually surprising and rewarding amidst finances, bureaucracy, and four hours of lab meetings in one day. But most importantly, Mark believed in this project when no one else, including a discouraged graduate student, did. For that I am always inspired and ever grateful.

Outside the lab, my family sustained me with continual support. My parents, Eric and Janis Christensen and Steven and Sharon Morris, always offered a sympathetic ear for the accomplishments and setbacks, and tried their best to understand why I was alternately exuberant or reserved about science. My brother Michael also helped to make sure I never took myself too seriously. Above all, I owe my perseverance, my success, my sanity, and my very existence to my future wife, Elin Lisska. Elin is my everything and without her I would not be anything.

Table of Contents

List of Figures

Chapter 1: Introduction

Systemic Autoimmune Disease

The mammalian immune system is a powerful defense against infection by a wide variety of invading microbes from viruses to multicellular parasites. The immune arsenal of molecular and cellular effectors must be carefully regulated, however, to prevent immune attack of the host's own tissues. Indeed, this concept of "tolerance to self" is central to the function of the immune system, and is enforced by multiple cooperative and redundant mechanisms (1). Nevertheless, the destructive power of the immune system can, in certain circumstances, be misdirected towards endogenous molecules, cells and organs, with disastrous results for the individual.

Autoimmunity is a condition in which an individual's immune system mounts a response against the body of its host. When this response leads to tissue damage or pathology, it is characterized as autoimmune disease (2). Because the clonally rearranged receptors of B and T lymphocytes can recognize an almost limitless array of molecular targets, nearly any organ system can be affected by the failure of immune regulation. Clinical entities as diverse as diabetes, Graves disease, rheumatoid arthritis, psoriasis, and Sjogren's syndrome can all be classified under the broad heading of autoimmune disease. Perhaps the most intriguing of human autoimmune diseases is systemic lupus erythematosus (SLE). As suggested by its name, the disease is not focused upon a specific organ system or molecular target, but can have a diverse array of clinical manifestations affecting nearly any organ system. Among the most common and

debilitating consequences of lupus are dermatitis, arthritis, generalized fatigue, neuropsychiatric complications, cardiovascular disease, and a progressive nephritis (3).

Although SLE has been extensively studied for over a century, the underlying causes of disease remain unknown. Twin studies have demonstrated that genetic factors are clearly involved, but are not the only causative agents, as appropriate interactions with the environment are also required for disease pathogenesis (4). Commensurate with our lack of understanding of lupus etiology is the lack of effective, specific treatments for the disease. Although therapy for lupus patients has improved with time and 10-year survival rates now approach 90%, there remains no cure, and affected patients have a 3-fold increased risk of early death compared to the general population (5). These figures become particularly tragic when examined in light of the fact that lupus tends to affect patients in the prime of their lives, between the ages of 25 and 55. Elucidation of the mechanisms of disease initiation and pathogenesis could lead to more effective therapies for lupus as well as a host of related autoimmune conditions.

B Cells are Central to SLE Pathogenesis

Several lines of evidence point towards B lymphocytes and their antibody products as critical mediators of lupus pathogenesis. The initial description of the "LE" cell in 1948 (6) set the stage for the notion that antibodies reactive with self nuclear components could lead to tissue damage. It then became clear that hypergammaglobulinemia and the production of a defined set of circulating autoantibodies were central features of disease (7). Of particular interest were antibodies to endogenous DNA, which are present in the vast majority of SLE patients, tend to rise

and fall according to disease activity, and were proposed to be primary mediators of disease (8, 9). The importance of autoantibodies was reinforced by the observation that anti-nuclear antibodies are deposited in diseased kidneys (10), and the demonstration that anti-DNA antibodies could mediate nephritis in adoptive transfer experiments (11).

Definitive experiments in mouse models of autoimmune disease further clarified the role of B cells in pathogenesis. In MRL/MpJ mice--which develop characteristic autoantibodies, nephritis, and dermatitis--a complete lack of B cells due to genetic disruption of the J_H locus abrogated the development of renal disease and increased survival in both Fas-intact and Fas-deficient *lpr/lpr* animals (12, 13). In addition to the secretion pathogenic autoantibodies, B cells can also serve as potent antigen-presenting cells (APCs) in the activation of autoreactive T cells. This has been demonstrated by the ability of self-reactive B cells to break T cell tolerance to self cytochrome-c and snRNP antigens *in vivo* in normal mice (14, 15). The separation of APC function from autoantibody secretion was formally demonstrated in lupus-prone mice with an IgM H chain transgene lacking the exons required for secretion. In the presence of B cells but the absence of serum antibody, these mice developed interstitial nephritis and vasculitis, as well as the accumulation of activated and memory T cells, at a level comparable to mice with intact antibody production (16). Finally, recent clinical trials in human lupus patients have shown a beneficial effect of B cell depletion with anti-CD20 monoclonal antibody therapy, providing direct evidence that B cells, either as antibody-secreting cells or APCs, are central to lupus pathogenesis in humans (17-19).

Selective Targeting of Self Antigens in SLE

Despite the protean clinical manifestations of lupus, a common feature shared by nearly all patients is the presence of a highly restricted set of autoantibodies (20). These antibodies were initially characterized by their ability to bind to nuclear antigens of fixed epithelial cells, and thus the fluorescent anti-nuclear antibody (ANA) test became a staple in the laboratory diagnosis of SLE (7). Further study showed that the various staining patterns of the ANA produced by serum from lupus patients could be correlated with autoantibodies to specific nuclear components (21-23). Surprisingly, of the tens of thousands of potential self antigens, the autoantibodies of SLE recognize a small subset of only a few dozen. Understanding the basis for this selective targeting could provide clues to the etiology of SLE and autoimmune disease in general (24).

Antibodies to single- and double-stranded DNA, to histones, and to the complexes of DNA and histones (either isolated nucleosomes or chromatin en masse) comprise one major subset of autoantibodies in SLE (9). As discussed above, the anti-DNA specificity is found in the majority of lupus patients, and thus is often cited as a primary mediator of pathogenesis. However, when studying multiple interacting factors in a complex disease, causality can be difficult to determine. The other major subset of autoantibodies in SLE, comprised of antibodies that recognize RNA-containing antigens, may be equally or even more important. These antigens include the Smith (Sm) and ribonucleoprotein (RNP) complexes involved in processing of nuclear RNA (25), the Ro/SSA and La/SSB antigens involved in processing of ribosomal RNA and transfer RNA in both the nucleus and cytoplasm, as well as ribosomal P proteins and even naked RNA molecules (23, 26). Because these autoantibodies are found in only a minority of lupus patients and can

occasionally arise in related autoimmune conditions such as Sjogren's syndrome, and because they can produce cytoplasmic rather than the characteristic nuclear ANA staining patterns, their role in disease is less well established. However, the presence of the anti-Ro specificity is clearly associated with distinct pathology such as vasculitis and congenital heart block, antibodies to ribosomal P proteins are correlated with nephritis and neuropsychiatric disease (26), and anti-Sm antibodies have also been linked to nephritis independently of anti-DNA (27). Thus, it has become increasingly clear that antibodies to both DNA- and RNA-containing antigens can contribute to autoimmune pathogenesis.

Although the effects of autoantibodies in lupus are becoming clearer, their etiology remains the focus of much speculation (28). Fairly conclusive evidence has shown, however, that the canonical autoantigens of SLE can be derived from endogenous apoptotic cells. Genomic DNA is cleaved into nucleosome fragments during the process of apoptotic cell death, and there is evidence that residual fragments of apoptotic DNA have a greater immune stimulatory capacity than native genomic DNA (29). In addition, both DNA- and RNA-containing antigens translocate from the nucleus to membrane blebs on the surface of apoptotic cells, where they presumably become available for immune recognition (30). Moreover, autoantibodies derived from lupus-prone mice have been shown to directly bind to these clusters of nuclear antigens on apoptotic blebs (31).

Autoantibodies can also be induced in otherwise normal individuals when a heavy burden of apoptotic and necrotic cells is created. In non-autoimmune mice, immunization with syngeneic apoptotic cells in the absence of any adjuvant can lead to ANA production (32), as can similar immunization with purified DNA from lymphocytes

stimulated to undergo activation-induced cell death (33). Interestingly, immunization with total genomic DNA is much less effective at inducing autoantibody production (34, 35). In a more physiologic setting, apoptotic and necrotic debris can accumulate when normal pathways of clearance are inhibited or overwhelmed. This failure of disposal results in autoimmunity in mice deficient in SAP (36), DNase I (37), or Mer (38), and in humans and mice lacking the early components of complement (39). Such a mechanism may also explain the increased incidence of anti-nuclear antibodies in circumstances of heightened cell death such as chronic viral infection (40).

Thus, it appears that the selectively targeted antigens in SLE are the products of cell death derived from endogenous cells. In addition, the oligoclonal nature and pattern of mutation and selection in autoreactive B cells indicate that autoimmune disease represents a specific and robust response to self antigens, not a chance byproduct of polyclonal activation or cross-reactivity (41, 42). Why then should a sparse collection of DNA- and RNA-containing antigens be targeted while thousands of others are ignored? The answer may lie in the autoantigens themselves. It is possible that a receptor expressed either directly by B cells or by accessory immune cells is specifically activated by molecular patterns present within the canonical lupus autoantigens. Such activation would lead to the induction of autoimmunity directed only against the antigens containing these putative patterns. Because essentially all the targeted antigens of lupus contain some form of nucleic acid, we hypothesized that a class of receptors activated by nucleic acid ligands could be fundamentally responsible for the generation of anti-nuclear antibodies in lupus. Moreover, if such a family of receptors could be activated by endogenous antigens, it would be central to the etiology and pathogenesis of SLE.

Toll-like Receptors and Innate Recognition of Endogenous Antigens

The adaptive immune system, composed of B and T lymphocytes and their somatically-rearranged antigen receptors, can recognize virtually any antigen, including self antigens. Although the majority of autoreactive lymphocytes are purged from the repertoire during development, this negative selection is not complete (43). There must be a mechanism in place to prevent these self-reactive cells from inducing autoimmunity, as well as a mechanism to instruct the adaptive immune system when to mount a protective response to invading microbes. In 1989, Charles Janeway predicted the existence of an "innate" immune system, intrinsically capable of the discrimination of self from non-self antigen (44). Activation of innate immunity in response to foreign antigens inherent in viruses and bacteria (coined pathogen associated molecular patterns) would result in induction of an adaptive immune response, while innate tolerance to self antigens would prevent the development of autoimmunity. Under this hypothesis, an effective immune response cannot be initiated without activation of innate immunity.

A central concept of innate immunity is that microbes are recognized by a small number of germline-encoded pattern-recognition receptors. Unlike B and T cell receptors, which are generated during the lifetime of the organism, innate receptors are selected over an evolutionary time scale, and thus have been purged of gene products that pose an unacceptable risk of autoimmunity (45). The discovery of a human homolog of the Drosophila innate immune receptor Toll, (46), followed by the demonstration that this receptor is required for the immune response to bacterial lipopolysaccharide (47, 48), proved the existence of innate pattern-recognition receptors. It has since been shown that

there are at least 11 different mammalian Toll-like Receptors (TLRs) activated by a wide range of microbial ligands, and that activation of this family of innate receptors is indeed critical for the induction of an adaptive immune response (49-53).

A subset of TLRs has evolved to recognize the nucleic acid ligands of invading bacteria and viruses. These include TLR9, a receptor for hypomethylated CpG sequence motifs in double-stranded DNA (dsDNA) (54), TLR3, a receptor for double-stranded RNA (dsRNA) (55), and TLR7, a receptor for single-stranded RNA (ssRNA) (56-58). TLR8 in humans can also be activated by ssRNA (58), but a role for TLR8 in the mouse immune system has not been identified (59). In addition, a TLR-independent pathway for recognition of RNA and DNA ligands has recently been described (60-63). The exact nature of the receptors in this pathway remains unclear, but it appears that these innate sensors complement the activity of TLRs in the defense against viral infection. Innate recognition of microbial nucleic acids, however, poses a unique problem for the discrimination of self from non-self antigens. Because pathogens and the host utilize the same nucleic acids to transmit genetic information, the risk of autoimmunity by activation of these receptors is high.

Several mechanisms have evolved to prevent activation of TLR3, -7, and -9 by endogenous nucleic acids. The most important appears to be sequestration of these receptors in intracellular compartments, where host-derived antigens are largely excluded (52, 64). The importance of this compartmentalization was shown by the demonstration that mammalian DNA could activate a chimeric TLR9 expressed on the cell surface, but not wild-type TLR9 contained in intracellular compartments (65). In addition, the fine specificity of these receptors appears to favor molecular determinants that are common in

microbial nucleic acids, but underrepresented in endogenous cells. For example, the CpG motifs found in bacterial DNA are potent activators of TLR9, but GC sequences and mammalian genomic DNA are not, and can even inhibit activation of TLR9 by stimulatory DNA (66). Similarly, TLR3, -7, and -8 are preferentially activated by unmodified RNA present in bacteria, while methylation and other common modifications of eukaryotic RNA prevent its recognition by these receptors (67).

Despite these additional checkpoints in the discrimination of self versus non-self, innate immune activation by endogenous nucleic acids may yet occur in certain circumstances. Murine dendritic cells (DCs) can be induced to mature, express activation markers, and efficiently present antigen to T cells both *in vitro* and *in vivo* after exposure to dsDNA from lysed murine fibroblasts (68). Similarly, mRNA released from apoptotic cells can activate signaling pathways downstream of TLR3 (69), and RNA sequences derived from endogenous Sm/RNP complexes can lead to activation of TLR7 and TLR8 (70). Weak or tolerizing signals induced by TLR recognition of endogenous ligands may be converted into overt inflammation and autoimmunity in cases of high ligand concentration or perseverance, such as when normal clearance mechanisms of apoptotic debris are overwhelmed (38, 39). A low level of activation by TLRs may also reach a critical threshold when cells simultaneously receive an additional stimulus. This phenomenon of costimulation is an inherent aspect of immune biology (1), and may be particularly relevant for the activation of autoreactive B cells.

B Cells at the Interface of Innate and Adaptive Immunity in SLE

B lymphocytes occupy a unique niche in the immune system because they express both the germline encoded receptors of the innate immune system as well as a clonally derived receptor of the adaptive immune system: the somatically rearranged B cell receptor (BCR). B cells express TLR7 and TLR9, and are directly stimulated by synthetic ligands for these receptors (71, 72). After ligation of TLRs, B cells are stimulated to proliferate, express costimulatory molecules for antigen presentation to T cells, secrete modest amounts of cytokines, and most importantly, differentiate into antibody-secreting plasma cells (73, 74). TLR signaling is thus an essential aspect of B cell function. In fact, not only is the presence of TLR ligands required for an effective humoral immune response, but TLR activation must occur in a B cell-intrinsic manner for effective antibody production (75). Within a single B lymphocyte, therefore, signaling pathways generated by the innate and adaptive immune system cooperate to generate effective immunity.

The synergy of activation signals generated by innate and adaptive receptors may also facilitate the activation of autoreactive B cells in lupus. In the context of concurrent BCR stimulation, methylated non-stimulatory DNA can assume stimulatory capacity for B cell proliferation and antibody secretion (76). In addition, low concentrations of specific antigen can synergize with non-stimulatory mammalian DNA to induce B cell activation (77). This combination of two sub-optimal stimuli may be particularly relevant for autoreactive B cells, which are unlikely to have strong signals transmitted by the BCR due to the combination of central deletion of high-affinity clones and peripheral anergy of remaining cells (78). Conversely, additional regulatory mechanisms exist

within anergic B cells to prevent their aberrant activation by TLR ligands (79). Whether this regulation can be overcome by simultaneous BCR and TLR signaling *in vivo* is unknown.

Seminal work on the role of TLRs in autoimmunity has shown that autoreactive rheumatoid factor B cells specifically proliferate *in vitro* in response to immune complexes of IgG and self DNA, but not IgG-protein complexes (80). This response is completely dependent upon TLR signaling, and requires TLR9 for full activation of the autoreactive B cells (81). Further study of the mechanism revealed that signaling through both the BCR and TLRs is essential, and indicated that BCR-medicated endocytosis and delivery of DNA complexes to TLR9-containing endosomal compartments is central to the response (29). An analogous response occurs in rheumatoid factor B cells stimulated with RNA-containing immune complexes, and signals through TLR7 instead of TLR9 (82). Importantly, anti-dsDNA B cells are also stimulated by self DNA *in vitro* in a similar fashion, indicating that pre-existing complexes of IgG and nucleic acids are not required (29); anti-nuclear B cells may be directly stimulated by endogenous ligands.

Thus, by virtue of the integration of signals from the innate and adaptive immunity, autoreactive B cells with anti-nuclear specificity are uniquely poised to initiate autoimmune responses. Potentially weak activation signals transmitted by a low-affinity autoreactive BCR can be complemented by TLR signaling, allowing otherwise anergic B cells to break tolerance. Furthermore, the control mechanisms to prevent innate recognition of endogenous nucleic acids (intracellular sequestration and poor activation by mammalian sequence elements) can be overcome by BCR-mediated delivery of nucleic acid ligands to endosomal compartments and concurrent stimulation via the

antigen receptor. This two-signal model of B cell activation emphasizes the importance of B cells at the interface of innate and adaptive immunity in the pathogenesis of SLE. Thus, several investigators have also proposed a role for innate immunity in the induction of autoimmune responses (83-85), and inhibition of TLR signaling has begun to emerge as an attractive therapeutic goal in the treatment of autoimmune disease (86, 87).

Type I Interferons in SLE

Type I interferons (IFN-I) encompass a family of more than twenty related gene products, of which the several interferon-alpha (IFN-α) genes and the single interferon-beta (IFN-β) gene, are most pertinent for the function of the immune system (88). IFN-I have a panoply of effects on nearly every cell type in the immune system, and are critical mediators of resistance to viral infection. The complex biology and signaling pathways of interferons are gradually being elucidated, but it was three decades ago that the important role of IFN-I in SLE was first suggested. It was noted that human lupus patients have elevated circulating interferon titers, and that levels of serum interferon directly correlate with disease activity (89). More recently, gene expression analysis has identified characteristic gene expression patterns in blood cells of lupus patients, and these expression patterns were found to overlap with those genes induced by IFN-I (90, 91). As with the original observation of circulating IFN-I, the level of expression of interferon-inducible genes in these studies correlated with disease severity. Genetic knockouts of the type I interferon receptor in mouse models have also highlighted the importance of these cytokines in autoimmunity. Inability to respond to IFN-α/β dramatically improved symptoms and severity of autoimmune disease in two different

lupus-prone mouse strains (92, 93), although one conflicting report observed a negligible effect on disease in MRL/MpJ mice (94). These observations are supported by the fact that exogenous interferon can induce symptoms and laboratory findings of autoimmune disease in patients treated with IFN-α for unrelated conditions (95, 96).

Besides the clear association of interferon with autoimmunity, several of the known effects of IFN-α/β may directly contribute to autoimmune pathology or disease progression. Firstly, IFN-I facilitates B cell activation, leading to augmented antibody secretion, particularly of the inflammatory immunoglobulin isotypes IgG2a and IgG3 in the mouse (97, 98). The effect of these cytokines on B cells is such that in the presence of concurrent BCR and TLR9 stimulation (as is predicted to occur in B cells with anti-nuclear specificity), IFN-α can induce differentiation to antibody-secreting plasma cells in the absence of T cell costimulation (99). Secondly, IFN-I is a potent activator of monocytes and immature dendritic cells (88). Immature blood-derived monocytes assume the activated phenotype of mature DCs and acquire robust T cell stimulatory capacity when cultured in the presence of IFN-I (100). In the context of autoimmunity, circulating monocytes from lupus patients have an intrinsically high efficiency of antigen presentation, and this elevated APC activity is dependent upon IFN-α (101). Finally, IFN-I appears to polarize the T cell response toward the inflammatory Th1 type (97, 100), and, by virtue of STAT4 activation, can directly prime T cells for production of the prototypical Th1 cytokine, gamma interferon (102).

Although many cells of both hematopoietic and non-hematopoietic origin can produce IFN-I, it was not until recently that a specialized cell type primed for rapid production of high levels of IFN-I was clearly identified. Originally classified as

plasmacytoid T cells for their prominent rough endoplasmic reticulum and histological location in T cell zones of the lymph node, plasmacytoid dendritic cells (pDCs) are now recognized as the central interferon producing cells of the immune system (103-105). Plasmacytoid DCs express TLR7 and TLR9, and upon recognition of viral nucleic acids by these receptors, rapidly produce high levels of IFN-I (52, 106, 107). It is interesting to note that while activation of TLR7 and TLR9 in B cells induces proliferation and antibody secretion, the same receptors lead to the elaboration of IFN-I in pDCs. This difference that has been attributed to expression of the signaling adaptor interferon-regulatory factor 7 (IRF7) in pDCs (108), and may also depend on intracellular sorting of TLR-containing endosomal compartments (109).

Because pDCs, like B cells, express nucleic acid-binding TLRs that may be activated by endogenous ligands, and because IFN-I is implicated in the pathogenesis of SLE, it is likely that activation of TLRs by self nuclear antigens can lead to IFN-I production by pDCs in autoimmune disease. For example, IFN-α produced by pDCs in the skin was found to be essential for the pathogenesis of psoriasis (110), and pDC-derived IFN-I has been similarly proposed to play a central role in lupus (111). Unlike autoreactive B cells, however, pDCs lack a specific antigen receptor capable of transmitting costimulatory signals and delivering endogenous nucleic acids to appropriate intracellular compartments for recognition by TLRs. How then can pDCs be stimulated by host-derived DNA/RNA ligands? Recent work focusing on IgG immune complexes from human lupus patients provides at least one answer, and reinforces the primary role of B cells at the interface of innate and adaptive immunity in SLE.

Initial studies on serum from lupus patients revealed the presence of a circulating inducer of IFN-α production, which appeared to consist of DNA-containing immune complexes (112). Further work revealed that this interferon-inducer could be recreated by the mixture of purified lupus IgG and apoptotic cells or nucleic acids released into the supernatant of dying cell cultures (113, 114). Analogous to the dual signaling of the B cell response, this stimulation of pDCs requires both the ligation of the Fc receptor FcγRIIa by IgG at the cell surface and activation of TLR9 in endosomal compartments for efficient IFN-α production (115, 116). TLR7 also appears to be involved in the production of IFN-α in response to RNA-containing immune complexes (87). Interestingly, in several of these studies, RNA complexes activated more potent induction of IFN-α than DNA-containing complexes (87, 114). The stimulatory capacity of endogenous RNA is further supported by the fact that the presence of anti-RNA antibodies is independently associated with IFN-I production and clinical disease activity in lupus patients (117).

Thus, as is the case for autoreactive B cells with anti-nuclear specificity, a two signal model of activation can bypass the regulatory mechanisms of innate immunity and allow activation by endogenous nucleic acids. Unlike anti-nuclear B cells, however, pDCs require the presence of pre-existing immune complexes to permit TLR stimulation by endogenous ligands. The requirement of autoantibodies for dendritic cell activation positions B cells at the center of a positive feedback cycle in the pathogenesis of SLE: B cells produce autoantibodies, which induce IFN-I production, which promotes autoantibody formation by B cells. It is also important to note that this mechanism of Fc receptor-mediated activation of DCs can also be demonstrated in conventional myeloid

dendritic cells (mDCs), which respond to DNA-containing immune complexes by producing inflammatory cytokines in a TLR9-dependent fashion (118). Stimulated mDCs in these experiments also elaborated the B cell activating factor BAFF, which has been linked to autoimmunity and could promote further expansion of autoreactive B cells (119).

Importance of Cognate T-B Interactions in SLE

Although interaction with dendritic cells can induce B cells to secrete antibodies in the absence of simultaneous T cell activation (99, 120), the provision of cognate help from $CD4^+$ T cells is generally required for the effective generation of a humoral immune response. This central tenet of B cell activation appears to hold true in autoimmunity as well. Early experiments revealed that depletion of $CD4^+$ T cells in lupus-prone mice could prevent disease in young animals as well as ameliorate advanced disease in aged animals (121, 122). It was subsequently shown that MHC-matched, cognate T cell help is required for the production of high titers of class-switched autoantibodies (123), and that the genetic absence of $\alpha\beta$ T cells in lupus-prone mice causes a reduction in rheumatoid factor and IgG anti-DNA titers (124). The availability of helper T cells is also critical in the 3H9 anti-DNA BCR transgene model, wherein anti-DNA B cells break peripheral tolerance only in the presence of cognate $CD4^+$ T cells (125).

Cognate T-B interactions are mediated primarily through two costimulatory receptor-ligand families: the tumor necrosis factor (TNF)-TNF receptor (TNFR) family, and the B7-CD28 family. The TNF family member CD40L appears to play a central role in T cell-dependent B cell costimulation. CD40L-deficient mice are unable to form

germinal centers or class-switched immunoglobulin to T-dependent antigens (126, 127), and deficiency of CD40L in lupus-prone mice causes a marked reduction in IgG anti-DNA titers (128). Although B7-1 and B7-2 costimulatory molecules are critical for the induction of appropriate humoral responses to immunized antigens (129), dual inhibition of these receptors in autoimmune mice produced only a minor decrease in autoantibody formation (130). Another B7 family member, inducible costimulator (ICOS), which is essential for germinal center formation and isotype switching in normal immune responses (131, 132), may be particularly relevant for autoimmune B cell activation. A recent report of lupus-like disease caused by a single gene mutation identified a primary defect in regulation of ICOS in helper T cells, which presumably allowed for inappropriate activation of autoreactive B cells (133). These various costimulatory molecules in cognate T-B interactions are expected to function cooperatively, as combined inhibition of the B7 and CD40 pathways leads to more profound suppression of autoimmune disease than either pathway alone (134, 135).

Besides the ability to costimulate B cell immune responses, certain subsets of $CD4^+$ T cells can also actively suppress autoimmune responses. The inhibitory capacity of these $CD25^+$ Foxp3-expressing regulatory T cells has been conclusively established, as has the critical importance of these cells in the prevention of overt autoimmune disease (136). Thus, the stimulatory effect of helper T cells on autoreactive B cells is balanced by the suppressive effect of regulatory T cells. This competition between activation and regulation of autoreactive B cells has been directly observed in the 3H9 anti-DNA transgene system (125). Similarly, selective depletion of regulatory T cells results in uncontrolled B cell activation and the production of autoantibodies in otherwise normal

mice (137). The relative contribution regulatory and helper T cells in SLE remains unclear. Although it is likely that T cell inhibition could have therapeutic benefit, it remains possible that a blockade of all T cell function could free B cells from T cell-mediated suppression, potentially exacerbating autoantibody production.

Specific Aims of this Study

The ability of autoreactive B cells to be stimulated by the pattern-recognition receptors of the innate immune system and the somatically-rearranged antigen receptors of adaptive immunity places them in a unique position to respond to endogenous nuclear antigens. Moreover, the ability of B cells to prime autoreactive T cells, secrete cytokines, and produce autoantibodies, which can have direct pathogenic effects as well as mediate the activation of pDCs for efficient IFN-I production, positions these cells at the center of known pathogenic effector mechanisms in autoimmune disease. We have sought to define the factors necessary for the activation of autoreactive B cells, as well as the contribution of such B cell activation and autoantibody secretion to disease in a mouse model of SLE. The specific aims of this project are as follows:

1. Determine the importance of TLR3, -7, and -9 in dictating autoantibody target specificity and generalized autoimmune disease in murine lupus.

2. Determine the requirement for B cell-intrinsic expression of TLR9 in the generation of anti-DNA autoantibodies, and the contribution of TLR-mediated autoantibodies to pathogenesis in autoimmune disease.

3. Determine the phenotype and activation state of DNA-specific and non-specific autoreactive B cells in TLR9-deficient lupus-prone mice.

4. Define the role of T cell help in the propagation of an established autoreactive B cell response.

Chapter 2: Initial Analysis of TLR9 and TLR3 in Autoantibody Production in Murine Lupus

Systemic autoimmune disease in humans and mice is characterized by loss of immunologic tolerance to a restricted set of self nuclear antigens. Autoantigens such as double-stranded DNA (dsDNA) and the RNA-containing Smith antigen (Sm) may be selectively targeted in systemic lupus erythematosus because of their ability to activate a putative common receptor. TLR9, a receptor for hypomethylated CpG DNA motifs (54), has been implicated in the activation of autoreactive B cells *in vitro* (29, 80), but its role in promoting autoantibody production and disease *in vivo* has not been determined. TLR3 is a receptor for dsRNA (55), and may be similarly activated by endogenous mRNA or the inherent stem-loop and double-stranded structures of Sm and U1-snRNP autoantigens (69, 138). We have generated lupus-prone mice deficient in either TLR9 or TLR3 in order to investigate the requirements for these receptors in autoantibody production and clinical autoimmune disease *in vivo*.

Generation of Hybrid TLR-Deficient Lupus-Prone Mice

The inbred MRL/Mp mouse strain develops a lupus-like syndrome marked by characteristic autoantibodies, dermatitis, nephritis, and early mortality, which are accelerated in the presence of the $Fas^{lpr/lpr}$ mutation (139). In order to investigate the role of TLR9 in autoimmune disease, we generated lupus-prone TLR9-deficient ($TLR9^{-/-}$) mice by making F2 crosses of $TLR9^{-/-}$ mice and Fas-deficient $MRL/Mp^{lpr/lpr}$ mice. We selected those $TLR9^{-/-}$ x $MRL/Mp^{lpr/lpr}$ F2 littermates that were homozygous for Fas-

deficiency and either TLR9-wild-type ($TLR9^{+/+}$, n = 19) or $TLR9^{-/-}$ (n = 16). The heterogeneous genetic composition of the F2 generation was controlled with the use of large cohorts of littermate controls, such that background genes were evenly divided between the two groups of mice. Furthermore, the development of autoimmunity in Fas-deficient mice has been documented on multiple genetic backgrounds (140). Similar breeding strategies have been used previously to study the effects of single genes on autoimmune disease (12, 128).

ANA Profiles in Autoimmune TLR-Deficient Mice

Because the fluorescent anti-nuclear antibody (ANA) assay is the most sensitive detection method for antibodies to a variety of nuclear components in their native antigenic form (7, 141), we used it as an initial measure of autoantibody production in the serum of F2 mice. By classification of the ANA staining pattern, we were able to determine the specificity of the autoimmune response, and identify the dominant autoantigens targeted by individual mice. Homogenous nuclear staining is known to correlate with anti-dsDNA antibodies, while a coarsely speckled nuclear staining pattern corresponds to antibodies directed against RNA-containing antigens such as snRNPs or Sm (21, 22). Serum from 7 of 19 $TLR9^{+/+}$ mice exhibited homogenous nuclear staining, whereas none of 16 $TLR9^{-/-}$ sera showed this pattern (Fig. 1, A and C, $P = 0.009$, Fisher's exact test), suggesting an impairment in the generation of anti-dsDNA autoantibodies. Moreover, equatorial staining of chromosomes in metaphase cells, indicative of anti-chromatin antibodies, was observed in 17 of 19 $TLR9^{+/+}$ sera and 0 of 16 $TLR9^{-/-}$ sera (Fig. 1, A, B, and D, $P < 0.0001$). The high prevalence of metaphase chromatin staining

in TLR9$^{+/+}$ sera presumably reflects the presence of multiple different anti-DNA and anti-nucleosome antibody specificities. TLR9$^{-/-}$ mice were incapable of producing any of these autoantibodies.

In contrast to the lack of staining for anti-dsDNA and anti-chromatin autoantibodies in TLR9$^{-/-}$ sera, there was no decrease in the proportion of mice with predominantly speckled ANA patterns, although TLR9$^{-/-}$ sera had a qualitatively different speckled pattern compared to TLR9$^{+/+}$ sera. While wild-type sera demonstrated mixed speckled and homogenous staining, TLR9$^{-/-}$ sera had exclusively speckled patterns in the absence of any superimposed homogenous staining (Fig. 1A and data not shown). In addition, TLR9$^{-/-}$ sera had an increased incidence of primarily cytoplasmic staining compared to wild-type littermates (Fig. 1, A and C, $P = 0.013$), although the sera with cytoplasmic patterns also stained nuclei in a faint speckled pattern. These findings indicate that TLR9$^{-/-}$ mice were capable of targeting the typical RNA-containing autoantigens of lupus, and account for the equivalence of quantitative ANA titers in the two groups of mice (median titer greater than 1:2000, data not shown). Furthermore, the distribution of ANA patterns in TLR9$^{-/-}$ mice suggests that in the absence of anti-DNA antibodies, other autoantibody specificities are maintained and may even become more prominent.

TLR3-deficient lupus-prone mice were generated by F2 crosses with MRL/Mp$^{lpr/lpr}$ mice in an analogous fashion to TLR9 mice. Unlike the TLR9 cohort, there was no difference in the distribution of either homogenous or speckled nuclear ANA patterns between TLR3$^{+/+}$ ($n = 15$) and TLR3$^{-/-}$ ($n = 17$) littermates (Fig. 2, A and C). In addition, nearly all mice in both groups produced antibodies to chromatin, as

evidenced by bright staining of metaphase chromosomes in mitotic cells (Fig. 2, A, B, and D). Because TLR3 is a receptor for dsRNA and may be involved in the generation of autoantibodies to RNA-containing antigens, we examined speckled ANA staining patterns in $TLR3^{-/-}$ sera, but could detect no difference in either the quality or intensity of staining for RNA-containing antigens. Both $TLR3^{-/-}$ and $TLR3^{+/+}$ mice produced autoantibodies that stained nuclear substrates with fine speckled, discrete speckled, and mixed speckled/homogenous patterns (Fig. 2A and data not shown). Based on the ANA, the autoantibody profile of $TLR3^{-/-}$ mice was thus indistinguishable from wild-type littermates.

Reduced Anti-dsDNA Autoantibodies in TLR9-Deficient Mice

The loss of homogenous nuclear and mitotic chromatin staining in $TLR9^{-/-}$ sera implied a block in the generation of autoantibodies to DNA-containing antigens, so we sought to confirm this with a specific assay for anti-dsDNA antibodies. Indirect immunofluorescence on *Crithidia luciliae* substrates is an established assay for the detection of anti-dsDNA autoantibodies in SLE (142). Because the kinetoplast organelle of *C. luciliae* is composed exclusively of circular dsDNA in the absence of ssDNA, RNA, or histones, the *Crithidia* assay is clinically the most specific test for antibodies to native dsDNA (143, 144). To further enhance the detection of anti-DNA antibodies, we co-stained the *Crithidia* DNA with 4',6-diamidino-2-phenylindole (DAPI), thus permitting the differentiation of irrelevant cytoplasmic structures from true staining of kinetoplast and nuclear dsDNA (Fig. 2A).

Among the TLR9 F2 mice, a subset of $TLR9^{+/+}$ sera contained specific anti-dsDNA antibodies as detected by strong staining of the *Crithidia* kinetoplast, but these antibodies were absent in sera from $TLR9^{-/-}$ mice (Fig. 3A-B, $P = 0.0121$, Mann-Whitney U test). Seven of 19 wild-type and 3 of 16 $TLR9^{-/-}$ sera were also found to have borderline staining of dsDNA, evidenced by a faint ring around the kinetoplast (Fig. 3A-B, intensity score of 1). It was unclear whether these staining patterns represented low-affinity anti-dsDNA or non-specific antibodies. We therefore analyzed the incidence of anti-dsDNA using intensity scores of either greater than zero or greater than one as positive. With both methods of analysis, we observed a significant reduction in anti-dsDNA antibodies in $TLR9^{-/-}$ sera ($P < 0.05$, Fisher's exact test). In contrast, $TLR3^{-/-}$ mice appeared to have no impairment in the generation of anti-dsDNA autoantibodies, as there was no difference in the incidence or intensity of kinetoplast staining between $TLR3^{+/+}$ and $TLR3^{-/-}$ sera (Fig. 3C). Thus, TLR9, but not TLR3, was required for the generation of specific autoantibodies to dsDNA in the context of murine lupus.

Anti-Sm and Anti-Cardiolipin Autoantibodies in TLR-Deficient Mice

Autoantibodies to Sm are exclusive to SLE and occur in approximately 25% of diseased humans and mice (25, 145). We performed Western blots to detect antibodies against the protein components of the Sm complex. Mice in both the TLR9 and TLR3 F2 cohorts generated antibodies reacting with a cluster of bands in the 29-34 kD region of the gel, corresponding to the complex of B and B' proteins (Fig. 4A-B). As expected, $TLR9^{-/-}$ mice produced anti-Sm autoantibodies. In fact, there was a significant increase in the proportion of $TLR9^{-/-}$ mice with anti-Sm reactivity compared to $TLR9^{+/+}$ littermates

(Fig. 4, A and C, P = 0.0049, Fisher's exact test). We confirmed these findings with a solid phase ELISA, using purified whole Sm antigen as the target, and again found higher levels of anti-Sm autoantibodies in $TLR9^{-/-}$ mice (Fig. 4D, P = 0.0014, Mann-Whitney U test). Consistent with the presence of speckled ANA patterns, $TLR3^{-/-}$ mice also generated anti-Sm autoantibodies at frequencies equivalent to their wild-type counterparts (Fig. 4, B, C, and E). Thus, neither TLR9 nor TLR3 were required for the production of autoantibodies to the RNA-containing Sm antigen, although, unexpectedly, there was a relative increase in anti-Sm autoantibodies in $TLR9^{-/-}$ mice.

Anti-phospholipid antibodies are also commonly found in autoimmune disease, and are associated with coagulation abnormalities and thrombosis (22). Because of the polyanionic nature of the lipid antigen, anti-phospholipid antibodies can cross-react with DNA, and anti-DNA antibodies can likewise have dual specificity for lipids such as phosphatidylserine (146). To determine if TLR9-deficiency or the loss of anti-dsDNA antibodies in $TLR9^{-/-}$ mice affected the generation of anti-phospholipid antibodies, we measured autoantibodies to cardiolipin, a prototypical phospholipid antigen. We found that $TLR9^{-/-}$ mice developed serum titers of anti-cardiolipin antibodies that were comparable to $TLR9^{+/+}$ littermates (Fig. 4F), indicating that anti-dsDNA and anti-phospholipid antibodies are controlled by separate mechanisms in these mice.

Global Immune Activation in TLR-Deficient Lupus-Prone Mice

Anti-chromatin and anti-ribonucleoprotein antibodies are among the earliest detectable autoantibodies in SLE, and are known to precede the appearance of overt clinical disease in both humans and mice (147, 148). The breakdown of tolerance to

DNA-containing antigens may thus be a critical first step in systemic autoimmunity, and the early appearance of anti-chromatin autoantibodies may facilitate disease progression and epitope spreading to other nuclear autoantigens (149). We therefore determined whether the lack of TLR9 or TLR3 had any effect on several parameters of global autoimmune disease. TLR-intact and TLR-deficient mice from both the TLR9 and TLR3 cohorts exhibited massive lymphadenopathy and splenomegaly (Fig. 5A), characteristic of the accumulation of activated lymphocytes in Fas-deficient autoimmunity. Both groups of mice also had elevated levels of total IgG and IgG2a in the serum relative to non-autoimmune C57BL/6 mice (Fig. 5B). To further define the autoimmune phenotype, we enumerated T cells, B cells, and $CD4^-/CD8^-$ double-negative T cells, which accumulate with age in $MRL/Mp^{lpr/lpr}$ mice (139). These cell populations were not decreased in TLR-deficient mice in the spleen (Fig. 5C) or lymph nodes (data not shown), nor was there any block in the accumulation of activated and memory phenotype $CD4^+$ T cells (Fig. 5D). Thus, neither deficiency of TLR9 or TLR3, nor the specific absence of anti-DNA autoantibodies in $TLR9^{-/-}$ mice, inhibited the dysregulated immune activation and aberrant lymphocyte accumulation of systemic autoimmune disease.

There was, however, an unexpected increase in immune activation in $TLR9^{-/-}$ animals compared to wild-type littermates. This was not observed for animals in the TLR3 cohort. Lymph node weight ($P = 0.0016$), splenic T cell count ($P = 0.0277$), double-negative T cell count ($P = 0.0150$), and activated $CD4^+$ T cell count ($P = 0.0327$) were all significantly greater in $TLR9^{-/-}$ mice compared to $TLR9^{+/+}$ littermates. Because the vast majority of the lymph node in these animals is composed of activated and

double-negative T cells (data not shown), these findings all point toward an increased level of T cell activation in TLR9-deficient mice.

In addition to hypergammaglobulinemia and the accumulation of activated lymphocytes, increased production of type I interferons is associated with SLE in humans and mice (90, 91, 150). Moreover, genetic ablation of the type I interferon receptor markedly reduced clinical and immunologic signs of lupus in NZB mice (92), although this was not observed in other autoimmune strains (94). Because activation of TLR9 and TLR3 is known to stimulate the secretion of type I interferons (106, 151), we determined whether lack of either of these receptors influenced spontaneous interferon levels in autoimmune mice. Using an ELISA to detect serum IFN-α, we could not detect any impairment in interferon production by $TLR9^{-/-}$ or $TLR3^{-/-}$ F2 mice (Fig. 5E-F). Although the sensitivity of this assay was limited to IFN-α, it was clear that a subset of mice exhibited markedly elevated levels type I interferons even in the absence of TLR9 or TLR3.

Glomerulonephritis in the Absence of Anti-DNA Autoantibodies

To assess renal disease in TLR9- and TLR3-deficient autoimmune mice, we first measured spot proteinuria at the time of sacrifice. There was no difference between $TLR9^{-/-}$ or $TLR3^{-/-}$ mice and their wild-type counterparts, with most mice exhibiting mild to moderate levels of proteinuria (data not shown). Histologically, interstitial and perivascular lymphocytic infiltrates were present in the kidneys of all mice. There was a moderate increase in glomerular size and cellularity, with no detectable difference in any parameter between $TLR9^{+/+}$ and $TLR9^{-/-}$ (Fig. 6, A, C, and E) or $TLR3^{+/+}$ and $TLR3^{-/-}$ mice

(Fig. 6, G, I, and K). PAS staining of kidney sections further revealed that TLR9$^{-/-}$ (Fig. 6, B, D, and F) and TLR3$^{-/-}$ (Fig. 6, H, J, and L) mice developed significant glomerular protein deposition that was comparable to wild-type littermates, with marked thickening of capillary loops and obliteration of vessel lumens. These findings indicate that neither TLR9 nor TLR3 was essential for the induction of end organ disease in murine lupus.

Although interstitial renal disease and glomerulonephritis were not inhibited in TLR9-deficient mice, it was unclear whether this was due to direct glomerular deposition of immunoglobulin and complement-containing immune complexes. We therefore assessed renal IgG and complement deposition in TLR9$^{-/-}$ mice lacking anti-dsDNA and anti-chromatin autoantibodies. Both TLR9$^{+/+}$ and TLR9$^{-/-}$ mice had immune deposits throughout the glomerulus, in contrast to non-autoimmune C57BL/6 mice (Fig. 7A). Although levels of IgG and C3 deposition varied among individuals, there was no difference in the mean glomerular fluorescence between the two groups of mice (Fig. 7B). Thus, lupus nephritis and glomerular immune complex deposition were unaffected by the absence of anti-dsDNA and anti-chromatin autoantibodies in autoimmune TLR9$^{-/-}$ mice.

Analysis of TLR3-Deficient Mice on Backcrossed MRL/Mp Background

Because TLR3 appeared to have no effect on autoantibody production, evidence of immune hyperactivation, or clinical disease in Fas-deficient mice in the F2 hybrid generation, we also analyzed a cohort of TLR3-deficient mice from a more homogenous and defined genetic background. Thus, TLR3$^{+/-}$ mice were backcrossed eight generations to MRL/Mp$^{lpr/lpr}$ mice, at which point over 99.8% of the genome was statistically derived

from the MRL/Mp strain. We also verified that all $TLR3^{-/-}$ mice expressed the $MHC^{k/k}$ and $Ig^{a/a}$ haplotypes derived from MRL/Mp (data not shown).

Analysis of $TLR3^{+/+}$ and $TLR3^{-/-}$ littermates on the $MRL/Mp^{lpr/lpr}$ background confirmed that TLR3 did not directly impact autoantibody production or evidence of disease in these mice. Sera from $TLR3^{-/-}$ mice did not exhibit any significant differences in ANA patterns from wild-type serum, although there was an insignificant decrease in speckled ANA patterns in TLR3-deficient sera, which may have suggested a decrease in autoantibodies to RNA-containing antigens (Fig. 8A). Sera from the majority of mice in both groups contained anti-chromatin antibodies, as determined by specific staining of metaphase chromatin in mitotic cells (Fig. 8B). We also performed assays for anti-Sm antibodies to identify specific antibodies to RNA-containing antigens. Despite the potential decrease in speckled ANA staining patterns, $TLR3^{-/-}$ $MRL/Mp^{lpr/lpr}$ mice produced anti-Sm autoantibodies at a level equal to or greater than their wild-type littermates (Fig 8D). Western blotting confirmed that mice in both groups generated antibodies recognizing both the Sm D and B/B' proteins at 14 and 25-30 kD, respectively (Fig. 8E). We therefore conclude that TLR3 has no role in the generation of autoantibodies to the typical RNA-containing antigens of SLE. Circulating levels of total IgG and IgG2a, as well as spleen and lymph node weight and activated T and B cell counts were also not significantly different between $TLR3^{+/+}$ and $TLR3^{-/-}$ mice (Fig. 8C and data not shown).

Discussion

These results demonstrate that TLR9 is required for the generation of anti-dsDNA and anti-chromatin autoantibodies in lupus-prone mice. Although TLRs in general do not recognize endogenous antigens, this central tenet of self versus non-self discrimination appears to breakdown in autoreactive B cells in the context of SLE. This TLR-mediated activation of autoreactive B cells by endogenous nucleic acids has been observed *in vitro* (29, 80, 82), but had not been demonstrated in an *in vivo* system before. We speculate that the synergistic activation of anti-nuclear B cells by both the BCR and TLRs facilitates the specific activation of these cells by self antigens in autoimmunity. Such selective activation of B cells with antigen receptors capable of binding and internalizing endogenous nucleic acids could explain the highly restricted autoantibody repertoire observed in SLE in both humans and mice.

Although TLR9 can shape the autoantibody repertoire in SLE, lack of TLR9 did not ameliorate disease in lupus-prone mice. This was somewhat surprising given the historical association of anti-DNA antibodies with clinical disease activity (9). However, the presence of nephritis in TLR9$^{-/-}$ mice merely confirms previous observations that anti-DNA antibodies per se are not required for the development of disease in general or glomerulonephritis in particular (16, 152). In this sense, it is interesting that TLR9$^{-/-}$ mice in this F2 cohort had both an increase in anti-Sm titers as well as an increase in several markers of immune activation. Because antibodies to RNA complexes may be associated with an increased production of IFN-I by pDCs (87, 114, 117), it is possible that the pathology observed in TLR9$^{-/-}$ mice could be directly attributed to these autoantibodies. It is also possible, however, that either anti-DNA antibodies or TLR9 signaling in other

cell types could have protective or regulatory roles in the context of autoimmune disease. We therefore will analyze the autoantibody repertoire and clinical disease phenotype of TLR9$^{-/-}$ on the homogenous genetic background of the MRL/Mp$^{lpr/lpr}$ strain to further clarify these intriguing findings.

Unlike TLR9, TLR3 had no role in the generation of autoantibodies to DNA or the prototypical RNA-containing Sm antigen. TLR3 also did not affect the clinical development of SLE, either in the initial F2 cohort or in fully backcrossed MRL/Mp$^{lpr/lpr}$ mice. One potential explanation for this is the highly restricted cellular expression of TLR3. TLR3 expression has only been detected in mature dendritic cells of the myeloid lineage (153), and was not observed in B cells by quantitative PCR (72). It is also possible that the specificity of TLR3 for dsRNA is not appropriate for the prototypical RNA-containing autoantigens of lupus, which are composed primarily of single-stranded RNA alternating with regions of intra-strand base pairing. Another candidate for the regulation of autoantibodies to RNA antigens is TLR7, an innate receptor for ssRNA (57, 58). TLR7 is closely related to TLR9 in protein sequence and downstream signaling pathways (51), and, like TLR9, is expressed in endosomal compartments of B cells and pDCs (52, 72). Therefore, we will also analyze the effect of TLR7-deficiency on autoantibody production and disease development in the MRL/Mp$^{lpr/lpr}$ model of SLE.

Materials and Methods

Mice.

Heterozygous TLR9$^{+/-}$ mice (54) of a mixed genetic background (B6 and 129Sv) were generously provided by Shizuo Akira. These mice were bred to MRL/Mp$^{lpr/lpr}$ mice

in our colony under specific pathogen-free conditions. Intercrossing of F1 offspring in 5 mating pairs produced 22 Fas-deficient ($Fas^{lpr/lpr}$) F2 mice, 5 of which were $TLR9^{+/+}$ and 4 of which were $TLR9^{-/-}$. Intercrossing of heterozygous $TLR9^{+/-}$ F2 mice in 4 additional mating pairs produced 56 $Fas^{lpr/lpr}$ mice, 15 of which were $TLR9^{+/+}$ and 13 of which were $TLR9^{-/-}$. The genetic composition of both generations of mice was approximately 50% MRL/Mp. One mouse in each group died before sacrifice at 19-21 weeks of age. In a separate cohort, homozygous $TLR3^{-/-}$ mice, generously provided by Richard Flavell (55), from a mixed genetic background (B6 and 129Sv) were bred to MRL/$Mp^{lpr/lpr}$ mice as above. Intercrossing of F1 offspring in 9 mating pairs produced 33 $Fas^{lpr/lpr}$ mice, 9 of which were $TLR3^{+/+}$ and 11 of which were $TLR3^{-/-}$. Intercrossing of heterozygous $TLR3^{+/-}$ F2 mice in 3 additional mating pairs produced 26 $Fas^{lpr/lpr}$ mice, 8 of which were $TLR3^{+/+}$ and 6 of which were $TLR3^{-/-}$. Two $TLR3^{+/+}$ mice died before sacrifice at 19-21 weeks of age.

To generate $TLR3^{-/-}$ mice of homogenous genetic composition, $TLR3^{+/-}$ from the F1 generation above were backcrossed an additional eight generations to purebred MRL/$Mp^{lpr/lpr}$ mice (Jackson Laboratory), selecting those mice which were homozygous for the $Fas^{lpr/lpr}$ mutation. At this point (>99.8% of genome derived from MRL/Mp strain), $TLR3^{+/-}$ mice were verified to be $MHC^{k/k}$ and $Ig^{a/a}$ haplotypes by FACS analysis of peripheral blood cells. These mice were then intercrossed to produce 11 $TLR3^{+/+}$ and 9 $TLR3^{-/-}$ mice from three different mating pairs. One mouse of each type died before analysis at 18 weeks of age. C57BL/6 mice (Charles River Laboratories) were maintained in our mouse colony to an age of 26 weeks.

ANA and anti-dsDNA immunofluorescence.

Serum was obtained via retro-orbital puncture just prior to sacrifice. For ANA, serum was diluted 1:200 and used for indirect immunofluorescence on fixed Hep-2 ANA slides (Antibodies Incorporated), with fluorescein-conjugated goat anti-mouse IgG (Southern Biotech) as the detection reagent. Slides were read on a fluorescent microscope at 400x magnification and scored as either nuclear homogenous, nuclear speckled, or cytoplasmic staining patterns by a reader blinded to the genotype of the mice. In addition, each serum sample was scored for staining of mitotic chromosomes. Images were captured with a constant exposure time of 4.0 seconds for TLR9 sera and 2.5 seconds for TLR3 sera. For TLR9 F2 mice, endpoint titration of serum was performed at reciprocal dilutions of 50, 200, 800, 2000, 10^4, $4x10^4$, and 10^5, and samples were scored for the presence of nuclear staining, regardless of pattern or cytoplasmic staining. Serum samples from 26 week old C57BL/6 mice were negative for ANA at 1:50 dilution (data not shown).

For anti-dsDNA, 1:10 diluted serum was applied to fixed *Crithidia luciliae* slides (Antibodies Incorporated), with biotin-conjugated goat anti-mouse IgG (Southern Biotech) and Alexa Fluor 555-conjugated streptavidin (Molecular Probes) as detection reagents. *Crithidia* DNA was co-localized with 4',6-diamidino-2-phenylindole (DAPI, Molecular Probes). Slides were read at 1000x magnification and scored 0-4 for intensity of kinetoplast staining by a reader blinded to the genotype of the mice. Images were captured with a constant exposure time of 0.5 seconds in red (IgG) and blue (DAPI) channels, then transferred into green (IgG) and red (DAPI) channels.

Anti-Sm Western blot and ELISA.

For Western blot, purified bovine Sm antigen (Immunovision) was separated by SDS-PAGE, transferred to nitrocellulose membrane, and probed with 1:200 diluted serum, using alkaline phosphatase-conjugated goat anti-mouse IgG (Southern Biotech) and BCIP/NBT substrate (KPL, Inc.) as detection reagents. The monoclonal mouse anti-Sm antibody Y12 (145) was used as a standard. Blots were scored for the presence of visible anti-Sm bands at either 10-15 kD for Sm D protein or 25-35 kD for Sm B/B' proteins. For ELISA, polystyrene plates were coated with Sm antigen, blocked with 1% BSA in PBS, and serial dilutions of serum from 1:50 to 1:36,450 were added. Anti-Sm antibodies were detected with alkaline phosphatase-conjugated goat anti-mouse IgG (Southern Biotech), and absorbance at 405/630nm was compared to the Y12 standard to quantitate.

Anti-cardiolipin ELISA.

Polystyrene plates were coated with cardiolipin by incubation with 100 μg/ml bovine cardiolipin (Avanti Polar Lipids) in 100% ethanol at 4 °C until completely evaporated (12-18 hours). Plates were blocked with 1% BSA in PBS, and serial dilutions of serum from 1:100 to 1:2700 were added. Anti-cardiolipin antibodies were detected with alkaline phosphatase-conjugated goat anti-mouse IgG (Southern Biotech), and absorbance at 405/630nm was compared to the FD1 standard to quantitate. Anti-cardiolipin standards were generously provided by Marc Monestier.

Analysis of lymphocyte subsets and serum IgG.

Spleen and lymph node cells were isolated, counted, and stained with the following antibodies for fluorescence-activated cell sorting analysis: anti-Thy1.2 (30H12), anti-CD4 (GK1.5), anti-CD8 (TIB105), anti-CD44 (IM7), anti-CD62L (Mel-

14), and anti-CD22.2 (Cy34.1). All antibodies except anti-CD22.2 (BD Pharmingen) were made in our laboratory. Total serum IgG and IgG2a were determined by ELISA. Polystyrene plates were coated with goat anti-mouse IgG (Southern Biotech), blocked with 1% BSA in PBS, and serial dilutions of serum from $1:10^4$ to $1:7.3x10^6$ were added. IgG or IgG2a was detected with alkaline phosphatase-conjugated goat anti-mouse IgG or goat anti-mouse IgG2a (Southern Biotech), and absorbance at 405/630nm was compared to known mouse IgG or IgG2a standards to quantitate.

Serum IFN-α ELISA.

Serum was collected at the age of 17-18 weeks for TLR9, or at the time of sacrifice for TLR3 mice, and IFN-α was measured by ELISA. Polystyrene plates were coated with monoclonal rat anti-mouse IFN-α (PBL Biomedical Laboratories), blocked with 1% BSA in PBS, and 1:10 diluted serum was added. IFN-α was detected with rabbit anti-mouse interferon-α (PBL Biomedical Laboratories) and alkaline phosphatase-conjugated goat anti-rabbit IgG (Southern Biotech). Absorbance at 405/630nm was compared to recombinant mouse IFN-αA standard (PBL Biomedical Laboratories) to quantitate. Limit of detection of the assay was 1.0 ng/ml in undiluted serum.

Analysis of kidney disease.

Kidneys were bisected, and one half was fixed in formalin and the other in paraformaldehyde (0.7% in PBS with 1.37% L-lysine and 0.2% sodium periodate). Paraformaldehyde-fixed kidneys were then dehydrated in 30% sucrose and flash-frozen in OCT. Formalin-fixed kidneys were paraffin-embedded, sectioned, and H&E or PAS stained (Histo-Scientific Research Laboratories). Stained sections were scored for glomerular and interstitial disease by a renal pathologist (Michael Kashgarian) who was

blinded to the genotype of the mice. For IgG deposition, frozen kidneys from 8 $TLR9^{+/+}$ and 8 $TLR9^{-/-}$ mice were sectioned and stained with biotin-conjugated goat anti-mouse IgG (γ chain-specific, Southern Biotech, Birmingham, Alabama) and Alexa Fluor 647-conjugated streptavidin (Molecular Probes, Eugene, Oregon). For C3 deposition, frozen kidney sections were stained with monoclonal rat anti-mouse C3 (Connex) and Alexa Fluor 647-conjugated goat anti-rat IgG (cross-adsorbed against mouse IgG, Molecular Probes, Eugene, Oregon). Stained sections were read on a fluorescent microscope at 400x magnification and images were captured with a constant exposure time of 0.5 seconds. To quantitate IgG and C3 deposition, mean fluorescence was calculated from captured images; 2 representative glomeruli per mouse were outlined and mean pixel intensity was calculated with Adobe Photoshop.

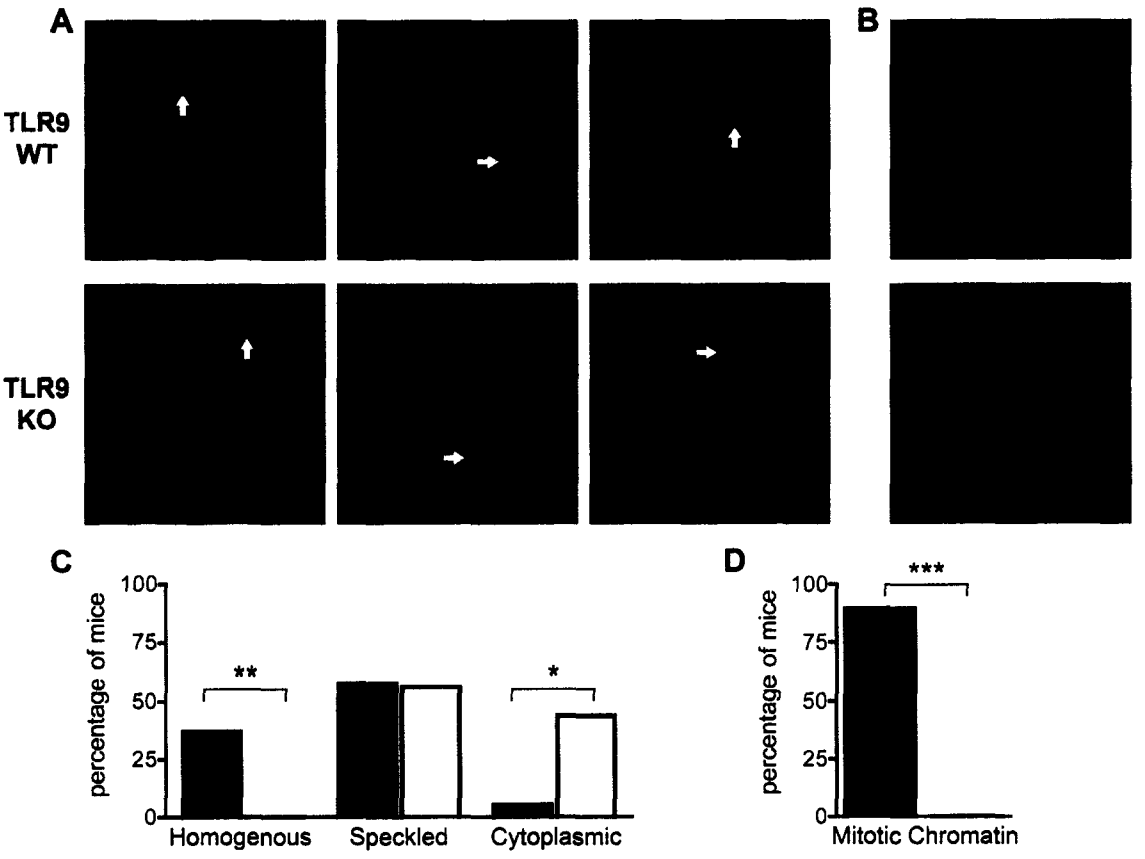

Figure 1. TLR9-deficient sera lack anti-DNA and anti-chromatin staining patterns. (A) ANAs were determined in sera (1:200 dilution) from 20-week old F2 mice. $TLR9^{+/+}$ sera are shown in upper panels (from left: homogenous pattern, speckled pattern, and speckled pattern); $TLR9^{-/-}$ sera are shown in lower panels (from left: speckled pattern, speckled pattern, and cytoplasmic pattern). Some $TLR9^{+/+}$ sera had predominantly speckled patterns superimposed upon faint homogenous staining (middle panel). White arrows indicate cells in metaphase which demonstrate positive (upper panels, $TLR9^{+/+}$) or negative (lower panels, $TLR9^{-/-}$) chromatin staining. Original magnification 400x. (B) Digitally enlarged images of metaphase cells with positive ($TLR9^{+/+}$, upper) or negative ($TLR9^{-/-}$, lower) chromatin staining. (C) Serum ANAs were classified as either nuclear homogenous, nuclear speckled, or cytoplasmic staining patterns. Black bars indicate $TLR9^{+/+}$ sera (n = 19); white bars indicate $TLR9^{-/-}$ sera (n = 16). (D) As in (C), but serum ANAs were classified as either positive or negative for mitotic chromatin staining. $^{*}P < 0.02$, $^{**}P < 0.01$, $^{***}P < 0.0001$, Fisher's exact test.

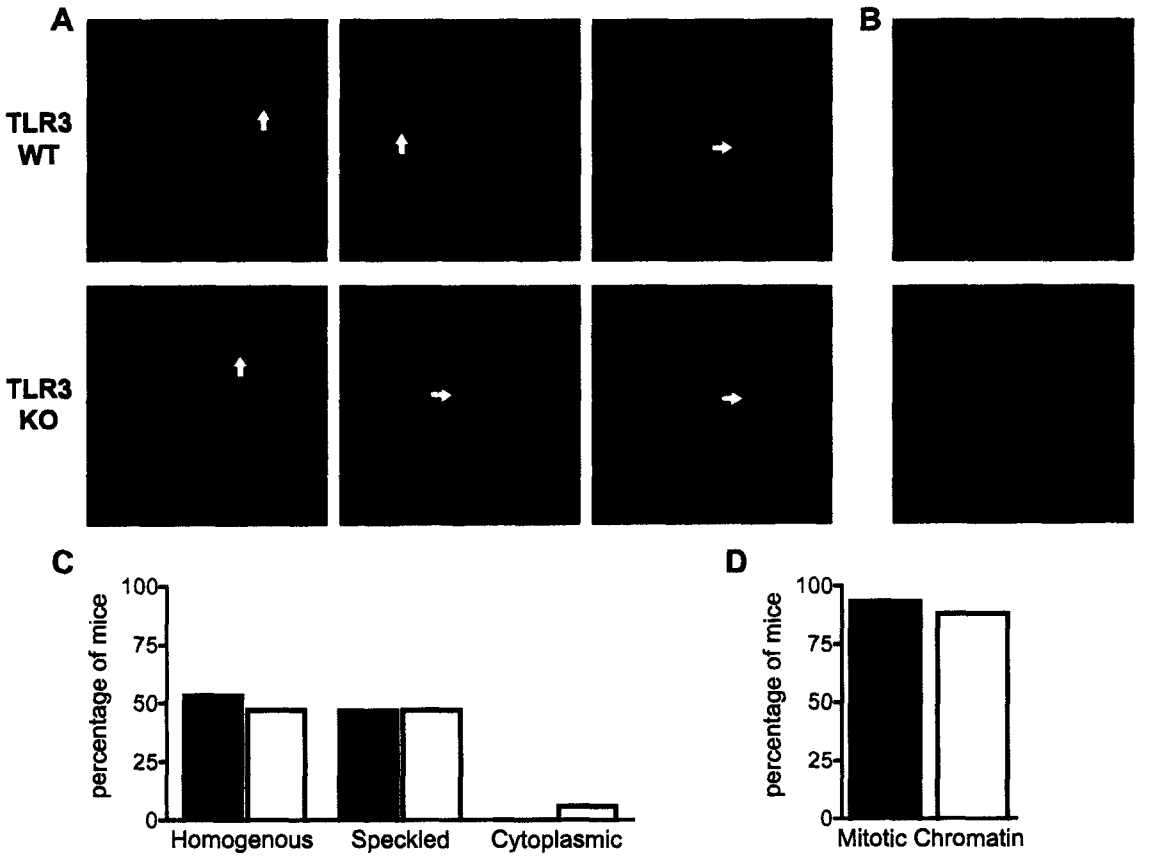

Figure 2. Unaltered ANA patterns in TLR3-deficient sera. (A) Serum ANAs were determined as in Figure 1. $TLR3^{+/+}$ sera are shown in upper panels (from left: homogenous pattern, speckled pattern, and speckled pattern); $TLR3^{-/-}$ sera are shown in lower panels (from left: homogenous pattern, speckled pattern, and speckled pattern). White arrows indicate cells in metaphase which demonstrate positive chromatin staining. Original magnification 400x. (B) Digitally enlarged images of metaphase cells with positive chromatin staining. (C) Serum ANAs were classified as either nuclear homogenous, nuclear speckled, or cytoplasmic staining patterns. Black bars indicate $TLR3^{+/+}$ sera (n = 15); white bars indicate $TLR3^{-/-}$ sera (n = 17). (D) As in (C), but serum ANAs were classified as either positive or negative for mitotic chromatin staining.

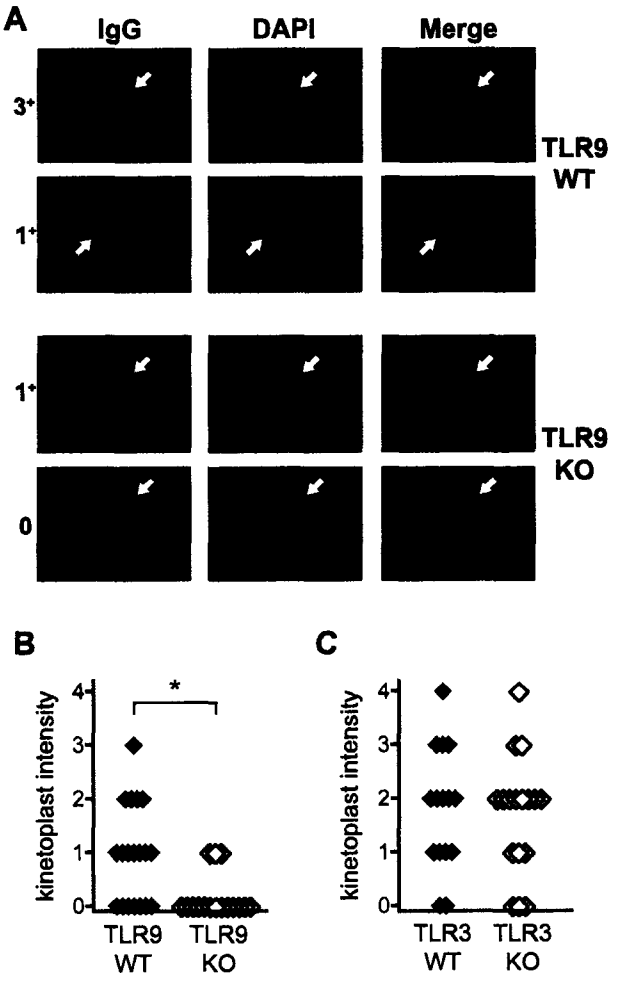

Figure 3. Reduced anti-dsDNA autoantibodies in TLR9$^{-/-}$ but not TLR3$^{-/-}$ mice. (A) Anti-dsDNA antibodies were detected by *Crithidia luciliae* immunofluorescence. IgG antibodies to *C. luciliae* DNA are shown in green (left panels), and DAPI staining of DNA is shown in red (center panels). White arrows indicate the kinetoplast. Specific anti-dsDNA antibodies are identified by co-localization of IgG and DAPI staining in the kinetoplast (yellow, right panels). Representative TLR9$^{+/+}$ sera are shown in upper two rows (intensity scores of 3+ and 1+), and TLR9$^{-/-}$ sera are shown in lower two rows (intensity scores of 1+ and 0). Original magnification 1000x. (B-C) Specific anti-dsDNA staining of *C. luciliae* kinetoplast was scored from 0 to 4 as in (A) for either TLR9$^{+/+}$ (n = 19) and TLR9$^{-/-}$ (n = 16) sera (B), or TLR3$^{+/+}$ (n = 15) and TLR3$^{-/-}$ (n = 17) sera (C). *P < 0.02, Mann-Whitney U test.

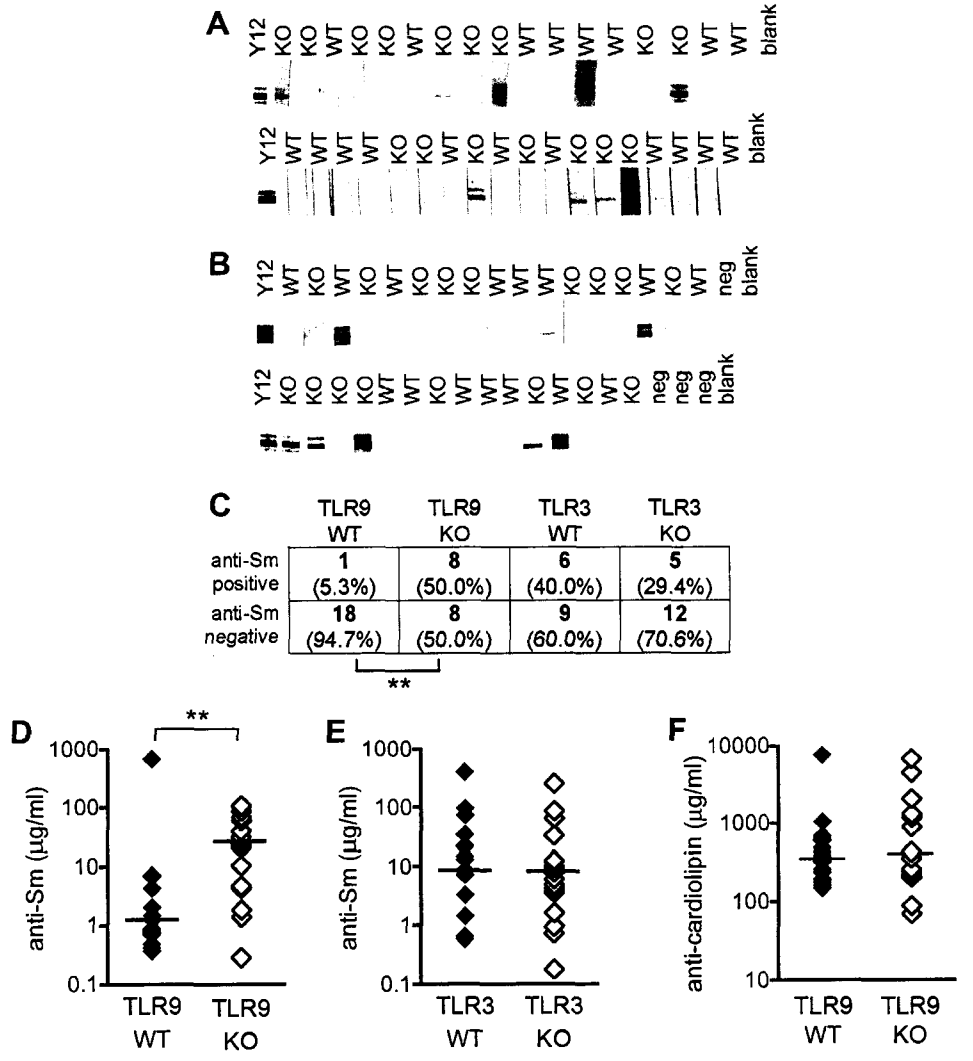

Figure 4. Presence of anti-Sm and anti-cardiolipin autoantibodies in TLR-deficient mice. (A) Anti-Sm antibodies were detected by Western blot in $TLR9^{+/+}$ (WT, n = 19) and $TLR9^{-/-}$ (KO, n = 16) sera. The monoclonal anti-Sm antibody Y12 was used as a positive control. Pictured portion of the gel is from 29-34kD, corresponding to the B and B' cluster of Sm proteins. (B) Anti-Sm antibodies were detected in $TLR3^{+/+}$ (WT, n = 15) and $TLR3^{-/-}$ (KO, n = 17) sera as in (A). Non-autoimmune control sera are also pictured (neg, n = 4). (C) Sera from TLR9 and TLR3 cohorts was scored as either positive or negative for anti-Sm antibodies by Western blot as in (A) and (B). (D-E) Anti-Sm antibodies were confirmed by ELISA in either $TLR9^{+/+}$ (n = 19) and $TLR9^{-/-}$ (n = 16) sera (D), or $TLR3^{+/+}$ (n = 15) and $TLR3^{-/-}$ (n = 17) sera (E). (F) Anti-cardiolipin antibodies were detected in serum from 17-18 week old $TLR9^{+/+}$ (n = 19) and $TLR9^{-/-}$ (n = 16) mice by ELISA. Bars represent median values. **$P < 0.005$, Fisher's exact test (C) or Mann-Whitney U test (D).

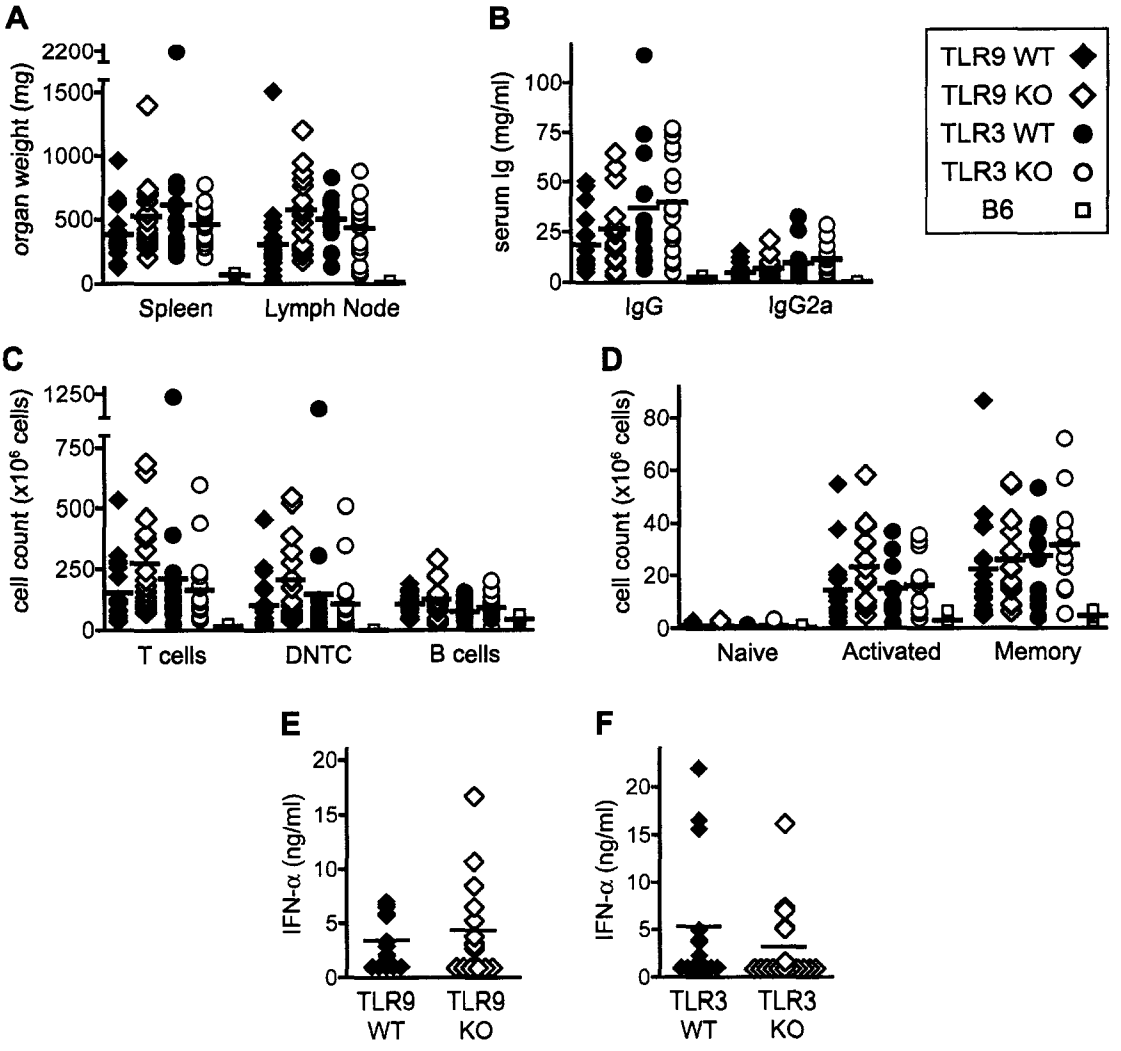

Figure 5. Lymphadenopathy, hypergammaglobulinemia, activated lymphocytes, and circulating interferon in TLR-deficient mice. (A-D) $TLR9^{+/+}$ (filled diamonds, n = 19), $TLR9^{-/-}$ (open diamonds, n = 16), $TLR3^{+/+}$ (filled circles, n = 15), and $TLR3^{-/-}$ (open circles, n = 17) mice were sacrificed at 20 weeks of age and assessed for evidence of aberrant immune activation; non-autoimmune C57BL/6 control mice (open squares, n = 4) were sacrificed at 26 weeks of age. (A) Spleens and the two largest axillary lymph nodes were weighed. (B) Total serum IgG and IgG2a were determined. (C) Splenocyte subsets were enumerated by FACS analysis for T cells (Thy1.2+), DNTC (CD4-/CD8- double-negative T cells), and B cells (CD22+). (D) Splenic CD4+ T cells were classified as either naïve (CD44- CD62L+), activated (CD44+ CD62L+), or memory (CD44+ CD62L-) phenotype. The analysis in (D) was performed on 12 $TLR3^{+/+}$ and 12 $TLR3^{-/-}$ mice. (E) IFN-a levels in serum from 17-18 week-old $TLR9^{+/+}$ (n = 19) and $TLR9^{-/-}$ (n = 16) mice were determined by ELISA. (F) As in (E) for $TLR3^{+/+}$ (n = 15) and $TLR3^{-/-}$ (n = 17) mice at the time of sacrifice. Limit of detection of the assay was 1.0 ng/ml.

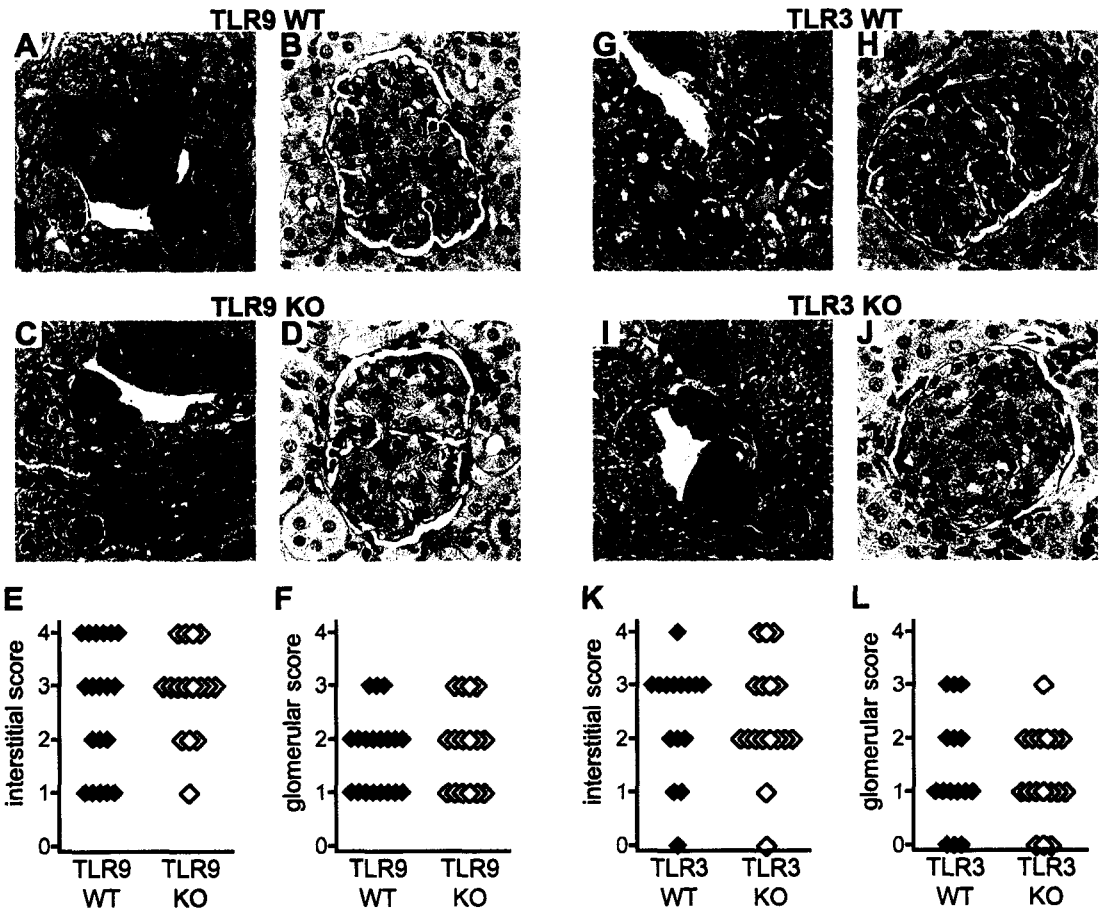

Figure 6. Glomerulonephritis in the absence of anti-DNA autoantibodies. Histological renal disease was assessed in $TLR9^{+/+}$ (n = 19), $TLR9^{-/-}$ (n = 16), $TLR3^{+/+}$ (n = 15) and $TLR3^{-/-}$ (n = 17) mice at 20 weeks of age. (A-F) Paraffin kidney sections from $TLR9^{+/+}$ (A-B) and $TLR9^{-/-}$ (C-D) mice were stained with H&E (A, C) or PAS (B, D). Interstitial infiltrates (E) and glomerular disease (F) were scored from 0-4 for all mice. (G-L) Paraffin kidney sections from $TLR3^{+/+}$ (G-H) and $TLR3^{-/-}$ (I-J) mice were stained with H&E (G, I) or PAS (H, J). Interstitial infiltrates (K) and glomerular disease (L) were scored from 0-4 for all mice. Representative images are shown. Original magnification was 100x for H&E sections (A, C, G, I) and 400x for PAS sections (B, D, H, J).

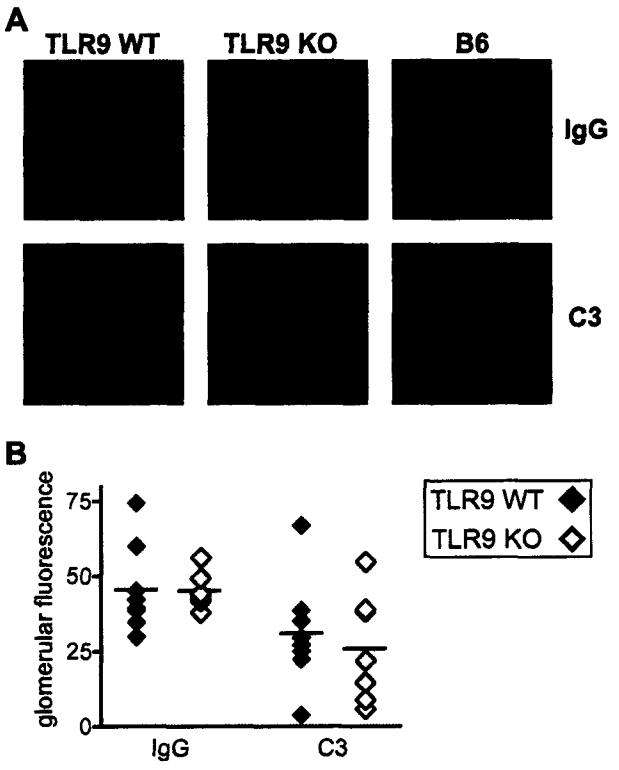

Figure 7. Glomerular immune deposits do not require anti-DNA antibodies. (A) Glomerular immune deposits were detected by direct immunofluorescence for IgG (upper panels) and complement C3 (lower panels) in frozen kidney sections from $TLR9^{+/+}$ (left panels), $TLR9^{-/-}$ (center panels), and non-autoimmune C57BL/6 control mice (right panels). Representative images are shown. Original magnification 400x. (B) Mean glomerular fluorescence intensity (arbitrary units) was determined for IgG and C3 in $TLR9^{+/+}$ (filled diamonds, n = 8) and $TLR9^{-/-}$ (open diamonds, n = 8) mice.

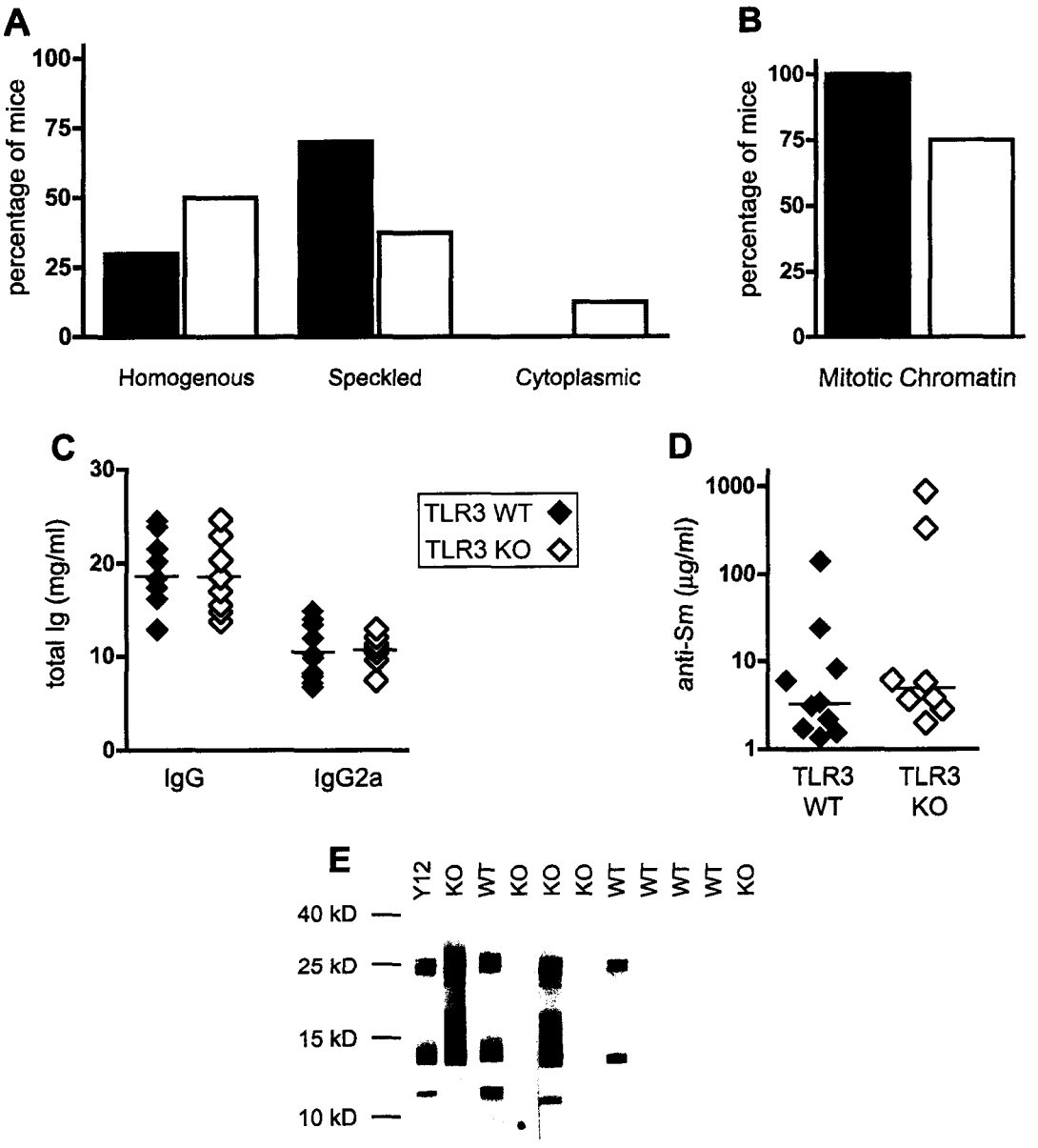

Figure 8. Serum autoantibodies in backcrossed TLR3-deficient MRL/lpr mice. (A) Serum ANAs from 18 week old mice at 1:200 dilution were classified as nuclear homogenous, nuclear speckled, or cytoplasmic staining patterns. Black bars indicate $TLR3^{+/+}$ sera (n = 10), and white bars indicate $TLR3^{-/-}$ sera (n = 8). (B) As in (A), but serum ANAs were classified as either positive or negative for mitotic chromatin staining. (C) Total serum IgG and IgG2a were determined. (D) Serum anti-Sm antibodies were quantitated by ELISA. (E) Antibodies to Sm D protein (14 kD) and Sm B protein cluster (25-30 kD) were verified in representative $TLR3^{+/+}$ (WT) and $TLR3^{-/-}$ (KO) serum by Western blot. The monoclonal anti-Sm antibody Y12 was used as a positive control.

Chapter 3: Contributions of TLR9 and TLR7 to Autoantibody Production and Disease Pathogenesis

Autoantibodies in SLE can be broadly classified as reacting to macromolecular complexes containing either DNA or RNA (7, 20, 22, 24). We observed that in the context of an F2 hybrid genetic background, lupus-prone mice deficient in TLR9 failed to generate autoantibodies to dsDNA and DNA-containing antigens such as chromatin. Despite this lack of a canonical autoantibody specificity, $TLR9^{-/-}$ mice nevertheless developed signs of severe autoimmune disease, including lupus nephritis. Moreover, several markers of immune activation were increased in $TLR9^{-/-}$ mice compared to wild-type controls, and the generation of autoantibodies to RNA-containing antigens such as Sm was similarly enhanced. We questioned whether the absence of TLR9 signaling, or the altered autoantibody repertoire generated in the absence of TLR9 was responsible for the potentially exacerbated disease in autoimmune $TLR9^{-/-}$ mice. In order to address this possibility, TLR9-deficient mice were extensively backcrossed to a homogenous genetic background known to induce spontaneous lupus-like disease. We then confirmed our initial findings on the effect of TLR9 on the autoantibody repertoire, and investigated the role of TLR9 and autoantibodies in autoimmune pathogenesis.

Because TLR9 was found to be critical for the generation of antibodies to DNA-containing antigens, we speculated that another TLR would be required for production of antibodies to RNA-containing antigens. Although TLR3 is a receptor for dsRNA, absence of this receptor in lupus-prone mice did not affect autoantibody production or clinical disease, presumably due to the lack of TLR3 expression on B cells or the paucity

of double-stranded regions in endogenous RNA antigens. A more promising candidate is TLR7, a receptor for ssRNA (56-58). TLR7 is highly homologous to TLR9 (154), and, like TLR9, is expressed in endosomal compartments of B cells and pDCs, and transmits signals exclusively through the adaptor protein MyD88 (51, 72, 107). We therefore generated autoimmune-prone TLR7-deficient mice on a partially defined genetic background, and investigated the requirement for this receptor in the generation of autoantibodies to RNA-containing antigens. In addition, because the absence of TLR9 appeared to modify clinical disease in our initial analysis, we examined the effect that TLR7 deficiency had on the pathogenesis of SLE.

Generation of Lupus-Prone Mice Deficient in TLR9 or TLR7

In order to analyze the effects of TLR9 on SLE in a more controlled genetic experiment, we generated TLR9-deficient autoimmune mice of a homogenous and defined genetic background. $TLR9^{+/-}$ hybrid mice were backcrossed eight generations to Fas-deficient, lupus-prone $MRL/Mp^{lpr/lpr}$ mice (139), at which point over 99.8% of the genome was statistically derived from the MRL/Mp strain. We also verified that all $TLR9^{-/-}$ mice expressed the $MHC^{k/k}$ and $Ig^{a/a}$ haplotypes derived from MRL/Mp (data not shown). To further exclude bias in these studies, we analyzed mice from heterozygous mating pairs, wherein $TLR9^{+/+}$ mice were used as littermate controls for $TLR9^{-/-}$ animals.

Because TLR7 is located on the X chromosome (154), we were able to analyze TLR7-deficient lupus-prone mice on a partially defined genetic background without extensive backcrossing. Hybrid $TLR7^{+/-}$ females were generated, then backcrossed three generations to male $MRL/Mp^{lpr/lpr}$ mice, selecting only those mice which were

homozygous for the $Fas^{lpr/lpr}$ mutation as well as the $MHC^{k/k}$ and $Ig^{a/a}$ haplotypes. After the third backcross generation, $TLR7^{+/y}$ and $TLR7^{-/y}$ male littermates were used for analysis. Importantly, no loci from an undefined genetic background could be homozygous in these mice, as every locus harbored at least one copy of the MRL/Mp allele derived from the male parent.

ANA Profiles in Autoimmune TLR-Deficient Mice

The fluorescent ANA assay is historically the most sensitive detection method for antibodies to both RNA-containing and DNA-containing antigens as they exist *in situ* in their native forms (7, 141). As described in Chapter 2, classification of the nuclear staining pattern as either homogenous (corresponding to anti-DNA antibodies), or speckled (indicative of antibodies to RNA splicing complexes such as Sm and RNP) can also reveal the dominant autoantibody specificity in autoimmune sera (21-23). We therefore began our analysis of the autoantibody repertoire in $TLR9^{-/-}$ $MRL/Mp^{lpr/lpr}$ (hereafter, $TLR9^{-/-}$) mice with the ANA assay. As is typical in the $MRL/Mp^{lpr/lpr}$ strain, the majority of wild-type sera produced a homogenous nuclear staining pattern, and 25 of 26 $TLR9^{+/+}$ mice produced anti-chromatin antibodies, as determined by equatorial staining of chromosomes in metaphase cells (Fig. 9A-C). In contrast, none of the sera from 21 $TLR9^{-/-}$ mice produced homogenous staining, and only 2 mice generated antibodies capable of binding to mitotic chromatin (Fig. 9A-C, $P < 0.0001$). These results confirm our earlier findings in F2 hybrid mice, and indicate a severe impairment in the generation of antibodies to native DNA and chromatin in lupus-prone $TLR9^{-/-}$ mice.

Analysis of the staining patterns generated by TLR9-deficient sera revealed a potential shift in repertoire specificity, favoring antibodies to RNA-containing antigens. An equivalent fraction of sera from both groups produced speckled nuclear staining patterns, but an additional pattern emerged in TLR9-deficient sera that was not observed in wild-type controls. Sera from 15 of 21 $TLR9^{-/-}$ mice stained the HEp-2 cell substrate in a primarily cytoplasmic pattern, accounting for a significant shift in the ANA pattern distribution (Fig. 9A-B, $P < 0.0001$ for comparison of pattern distribution between $TLR9^{+/+}$ and $TLR9^{-/-}$).

Among the multiple specificities that produce cytoplasmic staining, antibodies to RNA and RNA complexes are most common. Fine granular or web-like staining of perinuclear cytoplasm, along with faint speckled nuclear staining (Fig. 9A, lower right panel) is characteristic of antibodies to aminoacyl-tRNA synthetases (anti-Jo-1 antibodies) (23). $TLR9^{-/-}$ sera also produced a more homogenous cytoplasmic staining pattern (data not shown), typical of anti-ribosomal antibodies (23, 26). In addition, the cytoplasmic staining patterns generated by $TLR9^{-/-}$ sera may be due to anti-Ro/SSA or anti-La/SSB antibodies, or even antibodies to naked RNA (26, 82). Although cytoplasmic ANAs can also be produced by antibodies to organelles such as endosomes, the Golgi apparatus, or mitochondria, these antibodies stain discrete regions of the cytoplasm in a characteristic pattern (23) which was not observed in sera from $TLR9^{-/-}$ mice (Fig. 9A and data not shown). Thus, although TLR9-deficient and wild-type sera both produced nuclear speckled patterns characteristic of anti-Sm/RNP antibodies, only $TLR9^{-/-}$ mice generated antibodies reacting with presumed RNA antigens in the cytosol.

Analysis of ANA staining by TLR7-deficient or wild-type sera revealed patterns typical of SLE. The majority of mice in both groups produced anti-DNA antibodies, as determined by homogenous nuclear staining, and all serum samples contained anti-chromatin antibodies (Fig. 10A-C). Although sera from both groups of mice produced nuclear speckled patterns, this characteristic staining of Sm/RNP antigens was observed in only 3 of 20 $TLR7^{-/y}$ mice, compared to 6 of 20 $TLR7^{+/y}$ mice (Fig. 10A-B, $P > 0.05$). Moreover, sera from wild-type mice tended to produce a pure speckled staining in the absence of any other patterns, while speckled patterns in TLR7-deficient sera were obscured by a superimposed homogenous staining (Fig. 10A). Although this was not a statistically significant difference, it suggested an impairment in the generation of antibodies to RNA complexes in $TLR7^{-/y}$ mice, and prompted the analysis of specific autoantibodies to RNA-containing antigens.

Impaired Generation of Specific Autoantibodies in TLR-Deficient Mice

The lack of homogenous nuclear and mitotic chromatin staining patterns in $TLR9^{-/-}$ sera indicated a block on the generation of antibodies to DNA-containing antigens. We sought to confirm this with several assays for anti-DNA antibodies. Because of the high specificity of *Crithidia luciliae* immunofluorescence in the detection of antibodies to dsDNA (143, 144), we began with this assay. $TLR9^{-/-}$ serum showed a substantial decrease in antibodies binding the dsDNA of the *C. luciliae* kinetoplast (Fig. 11A, $P < 0.0001$). Although this decrease was highly significant, there was not a complete block in anti-dsDNA antibody production, as sera from some mice did specifically stain the kinetoplast. This low level of anti-dsDNA antibody production in $TLR9^{-/-}$ mice is in

contrast to the complete absence of antibodies to native DNA/chromatin as determined by the ANA assay. It is probable that this difference reflects the nature of the endogenous antigens in lupus: mammalian DNA exists in a complex with histones and the other protein components of chromatin, and is rarely encountered as naked dsDNA. Thus, the physiologic autoantigen is chromatin, and the presence of antibodies to an artificial antigen such as naked dsDNA may be less relevant to autoimmune pathogenesis (155).

Although immunofluorescent-based assays are useful for the detection of specific autoantibodies, it is difficult to use these assays to determine serum antibody concentrations. We therefore turned to ELISA-based assays to quantitate the decrease in antibodies to DNA-containing antigens in $TLR9^{-/-}$ sera. Using an anti-nucleosome ELISA in which the detection antigen was the combination of histones and dsDNA, we observed an order of magnitude decrease in specific anti-DNA antibodies in $TLR9^{-/-}$ sera (Fig. 11B, $P < 0.0001$). When we employed a standard ELISA for dsDNA in which the detection antigen was the combination of poly-L-lysine and dsDNA, however, there was not a significant decrease in $TLR9^{-/-}$ sera (Fig. 11C). $TLR7^{-/y}$ sera, in contrast, exhibited no defect in the generation of anti-DNA antibodies by either assay (Fig. 11D-E). The apparently conflicting findings in $TLR9^{-/-}$ sera illustrate two points. First, this highlights the low specificity of ELISA-based assays, which are known to be susceptible to high false positive rates (141, 143, 156). Second, this again implicates the chromatin complex of DNA and histones as the endogenous antigen recognized by TLR9 in SLE, while antibodies binding to purified dsDNA may represent cross-reactivity with other nucleic acid autoantigens, or charge-based non-specific association. It is therefore imperative to

use ELISA-based assays in concert with the traditional immunofluorescent ANA to account for both of these potential problems.

We also employed ELISA based assays for anti-RNA complex antibodies to further investigate the suggestive findings from the altered ANA patterns in TLR9- and TLR7-deficient sera. We found no difference between $TLR9^{+/+}$ and $TLR9^{-/-}$ sera for antibodies to either the Sm antigen or the Sm/RNP complex, which agreed with the equivalent incidence of speckled nuclear ANA patterns in the two groups (Fig. 12A-B). Also in agreement with ANA staining patterns was the complete lack of anti-Sm antibodies in $TLR7^{-/y}$ mice (Fig. 12C). However, because anti-Sm antibodies occur with a relatively low prevalence in murine lupus (145) and only 4 of 20 $TLR7^{+/y}$ sera harbored detectable anti-Sm antibodies, the lack of anti-Sm in $TLR7^{-/y}$ sera did not represent a significant difference ($P = 0.106$ by Fisher's exact test). We therefore used a less selective antigen, the complex of Sm and RNP, to detect antibodies to RNA-containing antigens in these mice. Although there was still only a small subset of wild-type mice that produced high titers of anti-Sm/RNP, we nevertheless observed a significant decrease in anti-Sm/RNP autoantibodies in TLR7-deficient sera (Fig. 12D, $P = 0.0454$). We found that all wild-type sera contained anti-Sm/RNP antibodies above the limit of detection, while these antibodies were undetectable in 5 of 20 $TLR7^{-/y}$ sera ($P = 0.0471$ by Fisher's exact test). We therefore conclude that TLR7 can facilitate the production of antibodies to RNA-containing antigens in SLE, as at least one subset of these antibodies was decreased in autoimmune $TLR7^{-/y}$ mice.

Opposing Effects of TLR7 and TLR9 on Clinical Disease and Immune Activation

Having observed the effects of deficiency of TLR7 or TLR9 on autoantibody production, we then determined what impact the absence of these receptors would have on the manifestation of clinical autoimmune disease. Lupus-prone $TLR9^{+/+}$ and $TLR9^{-/-}$ littermates were analyzed for the typical signs of SLE in the $MRL/Mp^{lpr/lpr}$ model at 13-14 weeks of age, when evidence of disease was clearly apparent in most mice. We found that $TLR9^{-/-}$ mice had a significant increase in the incidence and severity of autoimmune skin disease compared to wild-type controls (Fig. 13A, P = 0.0136). Concordant with this was increased lymphadenopathy and splenomegaly in $TLR9^{-/-}$ mice (Fig. 13B, P = 0.0043 and 0.0023, respectively), as had been observed in the initial F2 hybrid analysis.

We also analyzed these parameters in $TLR7^{+/y}$ and $TLR7^{-/y}$ mice, which were sacrificed at 16 weeks of age. This cohort of mice exhibited less accelerated disease than the TLR9 mice, presumably due to the less extensive backcrossing and the fact that all the mice were males. Analysis of skin disease revealed an opposite effect in TLR7-deficient mice that than seen in $TLR9^{-/-}$ animals, as $TLR7^{-/y}$ mice had no apparent skin disease at this time point (Fig. 13A). Although skin disease was evident in $TLR7^{+/y}$ mice, it occurred with a relatively low frequency such that the difference between the two groups did not reach statistical significance (P = 0.0878). Analysis of lymphadenopathy, however, did reveal a significant decrease in both lymph node and spleen weight in $TLR7^{-/y}$ mice compared to wild-type littermates (Fig. 13B, P = 0.0005 and 0.0295, respectively).

Increased spleen and lymph node weight in $MRL/Mp^{lpr/lpr}$ mice is generally a result of uncontrolled lymphocyte activation and failed cell death, as autoreactive

lymphocytes expressing an activated phenotype accumulate in these organs. We therefore enumerated T and B cell subsets in these organs as a measure of global immune activation. As expected from their increased spleen and lymph node weight, $TLR9^{-/-}$ mice had an increased number of $CD4^+$ helper T cells as well as a three-fold increase in the number of $CD4^-$ $CD8^-$ double-negative T cells in the spleen ($P = 0.0096$ and 0.002, respectively), while $CD8^+$ T cells and total B cell numbers were unaffected (Fig. 13C). TLR7-deficient mice, in contrast, exhibited a decrease in this aberrant population of double-negative T cells (Fig. 13C, $P = 0.0155$), thought to arise from the inability to delete activated cells in Fas-deficient animals (139). Analysis of T cell activation status in the lymph node revealed similar phenotypes. $TLR9^{-/-}$ mice had a decrease in naïve phenotype $CD4^+$ cells, with a concomitant increase in activated and memory phenotype cells, while $TLR7^{-/y}$ mice had an increase in naïve cells, which a parallel decrease in cells of a memory phenotype (Fig. 13D, $P = 0.0033$ for TLR9 and 0.0019 for TLR7). Similar results were observed in the spleen (data not shown). Finally, deficiency of these receptors also affected B cell activation. Splenic B cells from $TLR9^{-/-}$ mice expressed higher levels of the activation markers CD44 and CD69 ($P = 0.0002$ and 0.0333, respectively), while B cells in $TLR7^{-/y}$ mice expressed lower levels of CD44 (Fig. 13E, $P = 0.0026$). Taken together, these data indicate that while the lack of TLR9 led to accelerated disease and increased global immune activation, lack of TLR7 had the opposite effect, decreasing disease and immune activation in autoimmune mice.

Divergent Effects of TLR7 and TLR9 on Plasmacytoid Dendritic Cells

We found that TLR7 and TLR9 appeared to have opposing effects on lymphocyte activation in SLE. Since these receptors are expressed not only by B cells but by interferon-producing pDCs as well (52, 72), we hypothesized that the lack of these receptors could similarly influence the activation state of pDCs. Identifying pDCs as $CD11c^{int}$ $pDCA\text{-}1^{+}$ cells (157), we found that splenic pDCs from $TLR9^{-/-}$ mice appeared to be more activated than wild-type pDCs based on the increased expression of MHC class II (Fig. 14A). Conversely, pDCs from $TLR7^{-/y}$ mice had a lower level of class II expression, implying a more immature, un-activated state. This effect was specific to pDCs, as conventional, $CD11c^{hi}$ myeloid dendritic cells (mDCs) did not reveal any change in activation marker expression in the absence of either receptor (Fig. 14A-B). Comparing class II expression across all wild-type and TLR-deficient mice in each cohort revealed a significant increase in $TLR9^{-/-}$ mice and a corresponding decrease in $TLR7^{-/y}$ mice (Fig. 14C, $P < 0.0001$ for TLR9 and $P = 0.0144$ for TLR7). Plasmacytoid DCs from $TLR9^{-/-}$ mice also expressed an increased level of the activation markers B7-1 and B7-2 ($P = 0.0007$ and 0.0002, respectively), an effect which was not observed in TLR7-deficient mice (Fig. 14C).

The altered expression of activation markers by pDCs in TLR-deficient mice suggested a specific effect of these receptors on pDC function in SLE. The major functional consequence of pDC activation by TLRs, however, is the secretion of type I interferons (IFN-I). Because IFN-I has also been implicated in the pathogenesis of autoimmune disease, we determined circulating levels of IFN-α in TLR-deficient lupus-prone mice. In agreement with the increased pDC activation state, we observed an

increase in serum IFN-α in TLR9$^{-/-}$ mice (Fig. 15). Although quantification of systemic IFN may not detect small amounts of IFN produced locally, we nevertheless found that more than half of TLR9$^{-/-}$ sera contained detectable levels of IFN-α, compared with only 2 of 26 wild-type sera (P = 0.0009 by Fisher's exact test). This again indicates an increased level of global activation of pDCs, accompanied by an increase in systemic IFN-α production in autoimmune TLR9$^{-/-}$ mice. Because very few sera from either TLR7$^{+/y}$ or TLR7$^{-/y}$ mice contained detectable levels of IFN-α, we could not determine what effect TLR7 deficiency had on systemic IFN-I production. The decreased pDC activation state observed in TLR7$^{-/y}$ mice, however, did not completely preclude the production of IFN-I, as low levels of IFN-α were detected in some TLR7$^{-/y}$ sera (Fig. 15).

TLR7 and TLR9 Differentially Affect IgG Isotype Production

Activation of TLRs within B cells can lead to the production of class-switched antibodies (74, 75), and factors elaborated by activated mDCs and pDCs can also stimulate B cell antibody production and isotype switch (97, 98, 120). We therefore determined total serum IgG levels as a measure of global B cell activation in TLR-deficient mice. TLR9$^{-/-}$ sera contained elevated levels of every IgG isotype, but the most prominent increases were in IgG2a and IgG3, which were two-fold greater than in wild-type sera (Fig. 16, P = 0.0038 for IgG1, 0.0043 for IgG2a, 0.0006 for IgG2b, and P < 0.0001 for IgG3). Conversely, sera from TLR7$^{-/y}$ mice had decreased levels of total IgG, but this decrease was specific for the inflammatory isotypes IgG2a and IgG3 (Fig. 16, P < 0.0001 for both). Interestingly, the isotypes profoundly and divergently affected by the absence of TLR7 or TLR9 are the immunoglobulin isotypes most potently induced by

IFN-I (97). These findings further support the reciprocal effects of TLR7 and TLR9 on pDC activation, and raise the question of whether the altered IgG isotype profiles in TLR-deficient mice are due to a primary B cell defect or a secondary effect of pDC activation and IFN-I production.

Impact of TLR Deficiency on Lupus Nephritis and Mortality

The definitive measure of end-organ pathology in SLE is the presence of lupus nephritis. In agreement with increased evidence of disease by every other measure, TLR9-deficient mice developed exacerbated kidney disease. We observed increased glomerular size, cellularity, and protein deposition in $TLR9^{-/-}$ kidney sections, leading to a composite glomerulonephritis score that was significantly greater than wild-type littermates (Fig. 17, A and C, $P = 0.0024$). Kidneys from $MRL/Mp^{lpr/lpr}$ mice also show a characteristic interstitial infiltration of lymphocytes and monocytes, primarily centered around major vessels (perivascular infiltrate), but occasionally invading the cortical parenchyma as well. Although we observed a trend toward increased severity of interstitial infiltrates in $TLR9^{-/-}$ mice, this did not reach statistical significance (Fig. 17C). TLR7-deficient mice, in contrast, appeared to have ameliorated renal disease, with decreased glomerular protein deposition and preserved glomerular structure (Fig. 17B). In a reflection of the findings in $TLR9^{-/-}$ mice, $TLR7^{-/y}$ mice exhibited a non-significant trend toward decreased interstitial disease, but showed a significant decrease in glomerular disease (Fig. 17D, $P = 0.019$). The primary effect on glomerular disease and protein deposition may implicate the reciprocally increased or decreased IgG2a/IgG3 titers in TLR9 or TLR7 sera as a critical mediator of nephritis in these mice.

We observed an increase in nearly every marker of disease severity in lupus-prone $TLR9^{-/-}$ mice, along with a reciprocal decrease of several of these markers in $TLR7^{-/y}$ mice. It remained unclear, however, whether these disease markers truly affected mortality in these mice. We therefore allowed a second cohort of $TLR9^{+/+}$, $TLR9^{+/-}$, or $TLR9^{-/-}$ MRL/$Mp^{lpr/lpr}$ littermates to develop spontaneous disease, and monitored them without intervention until the time of death or irreversible morbidity. We found that TLR9-deficient mice had accelerated mortality relative to wild-type controls, as median survival was reduced from 31 weeks in $TLR9^{+/+}$ mice to 16 weeks in $TLR9^{-/-}$ mice (Fig. 18, $P = 0.0261$). $TLR9^{+/-}$ heterozygote mice appeared to have an intermediate phenotype, although we have not yet collected enough data on these mice to make that conclusion. Preliminary analysis of a few $TLR9^{+/-}$ sera revealed ANA patterns similar to wild-type sera (data not shown), but the level of immune activation and clinical disease in these mice has not been determined. It thus remains possible that TLR9 could operate in a dose-dependent manner in SLE, which could have important implications for allelic variation and genetic predisposition to SLE in humans. Finally, our preliminary analysis of TLR7-deficient mice was not designed to assess mortality. As none of the mice in either the $TLR7^{+/y}$ or $TLR7^{-/y}$ groups died before analysis at 16 weeks of age, it is unknown whether the absence of TLR7 will prolong lifespan in lupus-prone mice as a consequence of decreased disease severity.

Association of Disease Severity with Antibodies to RNA Complexes

We observed a decrease in antibodies to the RNA-containing Sm/RNP antigen in TLR7-deficient mice, while ANA patterns in TLR9-deficient mice indicated an increased

incidence of antibodies to other RNA species. At the same time, we found ameliorated disease in TLR7$^{-/y}$ mice and exacerbated disease in TLR9$^{-/-}$ mice. We therefore determined whether the presence of anti-RNA complex antibodies was associated with disease severity in these mice. TLR9$^{+/+}$ and TLR9$^{-/-}$ mice were each subdivided into two groups based on the presence of anti-Sm or anti-Sm/RNP antibodies as determined in Figure 12. Although TLR9$^{-/-}$ mice appear to generate antibodies to other RNA-containing antigens besides Sm/RNP, we reasoned that the presence of these characteristic autoantibodies was at least a first approximation of elevated levels of antibodies to RNA complexes. We then found that the exacerbation of skin disease in TLR9-deficient mice was correlated with the presence of these specific antibodies, as TLR9$^{-/-}$ mice with anti-Sm/RNP antibodies had a significant increase in skin disease compared to TLR9$^{-/-}$ mice without anti-Sm/RNP (Fig. 19A, $P = 0.0069$).

The presence of antibodies to RNA complexes also appeared to enhance global immune activation in these mice. Although the potential increase in lymph node weight in TLR9$^{-/-}$ mice with anti-Sm/RNP did not reach statistical significance (Fig. 19B, $P = 0.07$), these mice did show enhanced T cell activation, with a decreased proportion of splenic CD4^{+} T cells of a naïve phenotype (Fig. 19C, $P = 0.0209$). The presence of antibodies to RNA-containing antigens also correlated with the activation of pDCs, which exhibited an increased activation state in TLR9$^{-/-}$ mice with these antibodies (Fig. 19D, $P = 0.0302$). Finally, TLR9$^{-/-}$ mice with anti-Sm/RNP antibodies also had elevated levels of total IgG2a and IgG3 (Fig. 19E-F, $P = 0.0142$ and 0.0302, respectively). These increased markers of systemic inflammation may be secondary to increased production of IFN-I. Although circulating levels of IFN-α were not associated with anti-Sm/RNP antibodies in

TLR9$^{-/-}$ mice (data not shown), this association has been documented in human lupus patients (117).

The presence of anti-Sm/RNP antibodies in wild-type mice did not appear to affect global immune activation by most of these parameters (Fig. 19, A-C, E-F). It is possible that either the ability to signal through TLR9, or the presence of circulating anti-chromatin antibodies exerted a regulatory effect in these mice and prevented global immune activation by antibodies to RNA-containing antigens. Even in TLR9$^{+/+}$ mice, however, the presence of anti-Sm/RNP antibodies was associated with increased activation of pDCs (Fig. 19D, P = 0.0379). This highlights the potential importance of RNA-containing immune complexes in pDC activation, which have previously been demonstrated to be more potent inducers of IFN-I production than DNA-containing immune complexes (87, 114).

Discussion

We found that the requirement for TLR9 in the production of autoantibodies to DNA-containing antigens, first observed in lupus-prone F2 hybrid mice, also applied to TLR9$^{-/-}$ mice fully backcrossed to the MRL/Mp$^{lpr/lpr}$ strain. There appeared to be a more stringent requirement for TLR9 in the generation of anti-chromatin and anti-nucleosome antibodies than for the generation of antibodies to naked dsDNA. This suggests that the endogenous antigens recognized by TLR9 are complexes of DNA and histones, or at least that these antigens exist as complexes before delivery to TLR9-containing endosomes. ANA patterns from TLR9-deficient mice also suggested a shift in the autoantibody repertoire toward RNA-containing antigens, particularly those that exist in the cytosol.

We also found that TLR7, a receptor for ssRNA, appeared to facilitate the production of antibodies to RNA-containing antigens such as Sm/RNP complexes involved in the processing of nuclear RNA. Although the prevalence of anti-Sm antibodies was not high enough in TLR7 wild-type mice to conclude that TLR7 is required for the generation of these antibodies, we plan to analyze a second cohort of $TLR7^{+/y}$ and $TLR7^{-/y}$ mice. Doubling the sample size of each group will provide the statistical power to definitively answer this question.

Analysis of clinical disease and markers of immune activation in TLR-deficient mice revealed opposing effects of TLR7 and TLR9. In the context of autoimmunity, TLR7 appeared to have a primary inflammatory role, as global immune activation and disease activity were decreased in its absence. TLR9, in contrast, appeared to have a regulatory role inhibiting the pathogenesis of SLE, as disease was exacerbated in TLR9-deficient mice. Because these two receptors are expressed in similar cell types and share downstream signaling pathways (72, 107, 158, 159), it was surprising that they should have such dramatically divergent effects on autoimmune disease. It is possible that the recruitment of additional adaptors or regulators of intracellular signaling by one of these TLRs could explain their disparate phenotypes, although there is currently no evidence for this. Competition between these receptors for shared adaptor molecules could also allow cross-inhibition when both receptors are ligated (160, 161), but this mechanism alone is unlikely to account for the completely opposite phenotypes observed in $TLR7^{-/y}$ and $TLR9^{-/-}$ mice. Instead, the autoantibodies induced by these receptors may be responsible for the phenotypes of their respective genetic knockouts. In this model, antibodies to RNA-containing autoantigens act as potent inducers of inflammation and

IFN-I production, a concept that has been documented in previous studies (117). Decreased anti-Sm/RNP antibodies in TLR7$^{-/y}$ mice and the appearance of additional anti-RNA complex antibodies in TLR9$^{-/-}$ mice could then account for ameliorated or exacerbated disease, respectively. Indeed, the association of anti-Sm/RNP antibodies with disease severity in TLR9$^{-/-}$ mice suggests that the autoantibody repertoire can directly affect SLE pathogenesis.

These findings highlight two critical and potentially pathologic functions of TLRs in SLE. First, activation of the innate immune system by TLRs directs the autoantibody response to the characteristic lupus autoantigens; without appropriate TLR signaling, these antibodies are not generated. Second, TLRs can have a dramatic impact on disease pathogenesis, either by promoting disease in the case of TLR7, or regulating disease in the case of TLR9. The results presented here also illustrate the difficulty of establishing cause-effect relationships in *in vivo* models of autoimmune disease. For example, stimulation of TLRs in B cells could lead to the production of characteristic autoantibody profiles with either inflammatory (in the case of TLR7) or regulatory (in the case of TLR9) effects. These antibodies could then mediate tissue damage and control IFN-I production by pDCs. Alternatively, stimulation of TLRs in pDCs could directly affect IFN-I production, which would then secondarily control T cell activation, tissue damage, and autoantibody production by autoreactive B cells. To distinguish between these two possibilities, we will create an *in vivo* experimental model in which TLR9 deficiency is restricted to B cells. In addition, we will also perform *in vitro* stimulation experiments to dissect the mechanism of increased IFN-α production in TLR9-deficient mice. Integration of data from all these experiments may allow us to discover the causal

relationships between autoantibody production, IFN-I secretion, and clinical disease in SLE.

Materials and Methods

Mice.

To generate TLR9$^{-/-}$ mice of homogenous genetic composition, TLR9$^{+/-}$ from the F1 cross to MRL/Mp$^{lpr/lpr}$ (Chapter 1) were backcrossed an additional eight generations to purebred MRL/Mp$^{lpr/lpr}$ mice (Jackson Laboratory), selecting those mice which were homozygous for the Fas$^{lpr/lpr}$ mutation. At this point (>99.8% of genome derived from MRL/Mp strain), TLR9$^{+/-}$ mice were verified to be MHC$^{k/k}$ and Ig$^{a/a}$ haplotypes by FACS analysis of peripheral blood cells. These backcross generation 8 mice were then intercrossed to produce 26 TLR9$^{+/+}$ mice (14 male and 12 female) and 21 TLR9$^{-/-}$ mice (7 male and 14 female), which were analyzed between 13 and 14 weeks of age. For mortality assessment, additional TLR9$^{+/-}$ mice were intercrossed to produce a second cohort of TLR9$^{+/+}$, TLR9$^{+/-}$, and TLR9$^{-/-}$ mice, which were observed for a period of at least 12 weeks for all mice and up to 33 weeks for some mice. The survival analysis is ongoing.

To generate TLR7-deficient mice of a partially defined genetic background, female TLR7$^{+/-}$ mice of a mixed genetic background (C57BL/6 and 129Sv) were generously provided by Richard Flavell. These were bred to male MRL/Mp$^{lpr/lpr}$ mice (Jackson Laboratory) to produce F1 hybrids. Female TLR7$^{+/-}$ hybrids were then backcrossed an additional three generations to male MRL/Mp$^{lpr/lpr}$ mice. After the first backcross generation, TLR7$^{+/-}$ mice homozygous for the Fas$^{lpr/lpr}$ mutation were selected

for breeding. After the second backcross generation, mice were assayed for MHC and Ig haplotypes by FACS analysis of peripheral blood cells. Only those $TLR7^{+/-}$ mice that were $MHC^{k/k}$ and $Ig^{a/a}$ were selected for breeding. Male $TLR7^{+/y}$ and $TLR7^{-/y}$ offspring (n = 20 each genotype) from the third backcross generation were analyzed at 16 weeks of age. Statistically, 87.5% of genetic loci in these mice are homozygous for MRL alleles, while the remaining 12.5% are heterozygous.

ANA and anti-dsDNA immunofluorescence.

Serum was obtained at the time of sacrifice. ANA immunofluorescence on HEp-2 cells was performed at 1:200 dilution of serum as previously described (Chapter 2). Images were captured at 400X magnification with a constant 2.5 second exposure time. *Crithidia luciliae* immunofluorescence was performed at 1:50 dilution of serum as previously described (Chapter 2). Images were captured at 1000X magnification with a constant 0.7 second exposure time.

Anti-DNA and anti-Sm/RNP ELISA.

For anti-nucleosome ELISA, polystyrene plates were coated with bovine histones (Sigma), then secondarily coated with dsDNA from calf thymus (Sigma) that was phenol-extracted and S1 nuclease treated to remove single-stranded regions. For anti-dsDNA ELISA, polystyrene plates were coated with poly-L-lysine (Sigma), then secondarily coated with dsDNA as above. Plates were then blocked with 1% BSA in PBS, and serial dilutions of serum from 1:200 to 1:5400 were added. Anti-DNA antibodies were detected with alkaline phosphatase-conjugated goat anti-mouse IgG (Southern Biotech), and absorbance at 405/630nm was compared with either PL2-3 anti-nucleosome monoclonal antibody or PL9-6 anti-dsDNA monoclonal antibody to quantitate. PL2-3

had 37-fold lower affinity for poly-L-lysine-dsDNA than for nucleosomes, and PL9-6 had 15-fold lower affinity for nucleosomes than for poly-L-lysine-dsDNA. Anti-Sm ELISA was performed with serial dilutions of serum from 1:200 to 1:5400 as previously described (Chapter 2). Anti-Sm/RNP was performed similarly, but plates were coated with Sm/RNP complex antigen (Immunovision).

Determination of clinical disease.

Skin disease was scored at the time of sacrifice. Mice were scored for the presence and surface area of typical lesions on the dorsum of the head, neck, and back. Lesions generally consisted of alopecia, fibrosis, ulceration, and occasionally active bleeding. Scores ranged from 0-4 for affected area up to 4 cm^2, with up to 1 additional point for the presence of ear dermatitis. Spleen and lymph node weights were determined as previously described (Chapter 2). Analysis of kidney disease was performed as previously described (Chapter 2), except that sections were scored by S. Christensen, who was blinded to the genotype of the mice.

Analysis of lymphocyte and dendritic cell activation.

Spleen and lymph node cells were isolated and T and B cell subsets and activation markers were determined as previously described (Chapter 2). Anti-CD69 antibody (H1.2F3, BD Biosciences) was used as an additional marker for B cell activation. Myeloid and plasmacytoid DCs were identified with anti-CD11c (HL3, BD Biosciences) and anti-mpDCA-1 (Miltenyi Biotec). Anti-MHC class II (M5/114.152, Biolegend), anti-B7-1/CD80 (16-10A1, BD Biosciences), and anti-B7-2/CD86 (GL1, BD Biosciences) were used to assess DC activation.

Serum IFN-α ELISA.

IFN-α ELISA was performed as previously described (Chapter 2), except that serum was added at 1:5 dilution.

Analysis of IgG isotypes.

Levels of IgG isotypes in serum were determined by Beadlyte Mouse Immunoglobulin Isotyping Kit (Upstate) according to the manufacturer's instructions. Serum was tested at 1:250,000 dilution for TLR9 samples and 1:200,000 dilution for TLR7 samples.

Statistics.

Unless otherwise indicated, statistical comparisons between groups of mice were performed with the Mann-Whitney U test. For the comparison of dichotomous variables, Fisher's exact test was used. For the comparison of the ANA pattern distribution between $TLR9^{+/+}$ and $TLR9^{-/-}$ mice (3 potential patterns), a 3x2 Chi square analysis was used. For the analysis of survival curves, the logrank test was used. Statistical analysis was performed with GraphPad Prism version 4.0a or GraphPad InStat version 3.0b for Macintosh, GraphPad Software, San Diego, California.

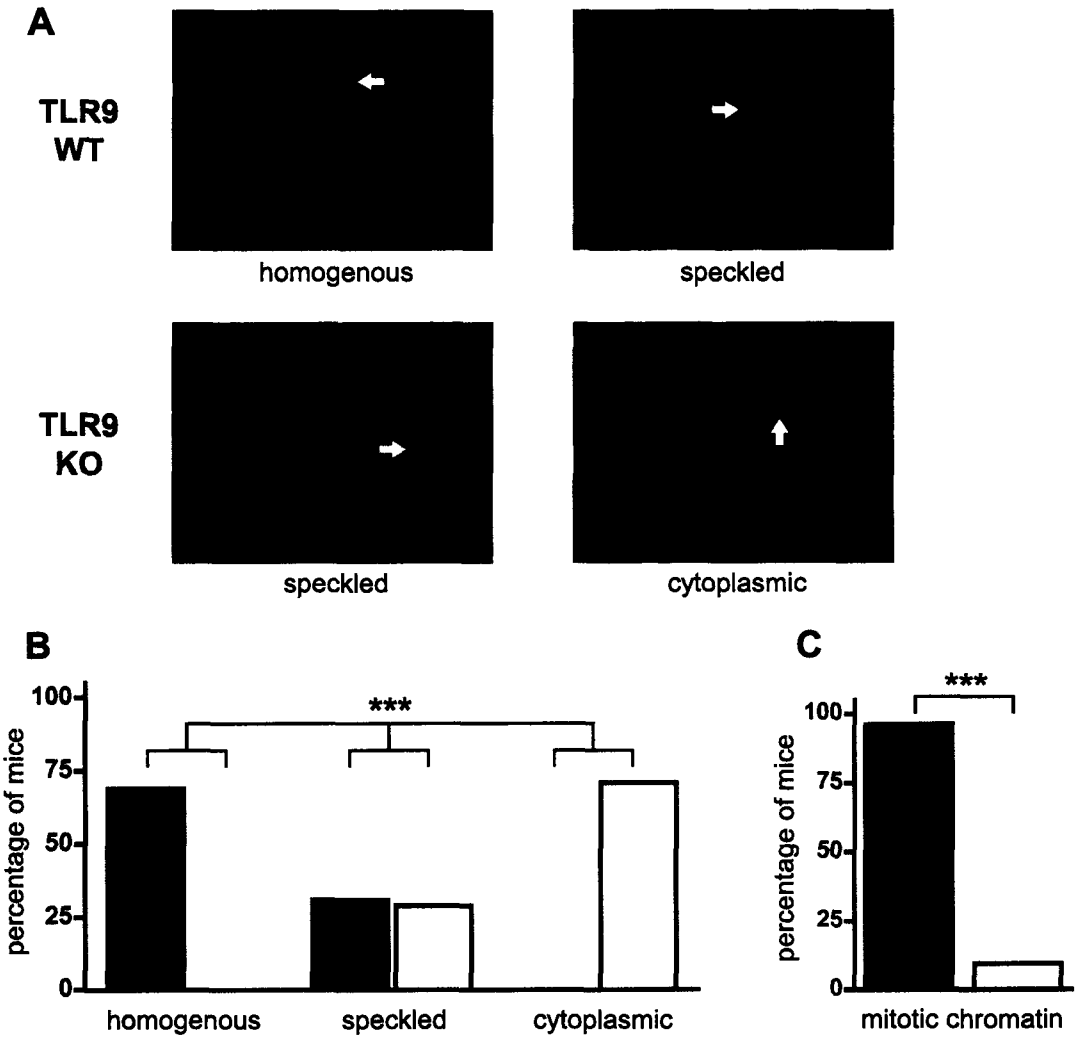

Figure 9. TLR9-deficient sera lack anti-DNA and anti-chromatin staining patterns. (A) ANAs from $TLR9^{+/+}$ (WT) sera are shown in upper panels (left, homogenous nuclear pattern; right, speckled nuclear pattern), and $TLR9^{-/-}$ (KO) sera in lower panels (left, speckled nuclear pattern; right, cytoplasmic pattern). White arrows indicate cells in metaphase that demonstrate positive (upper panels, TLR9 WT) or negative (lower panels, TLR9 KO) staining of mitotic chromatin. (B) Serum ANAs were classified as either nuclear homogenous, nuclear speckled, or cytoplasmic staining patterns. Black bars indicate TLR9 WT sera (n = 26), and white bars indicate TLR9 KO sera (n = 21). (C) As in B, but serum ANAs were classified as either positive or negative for mitotic chromatin staining. ***, $P < 0.0001$ by either Chi square analysis (B), or Fisher's exact test (C).

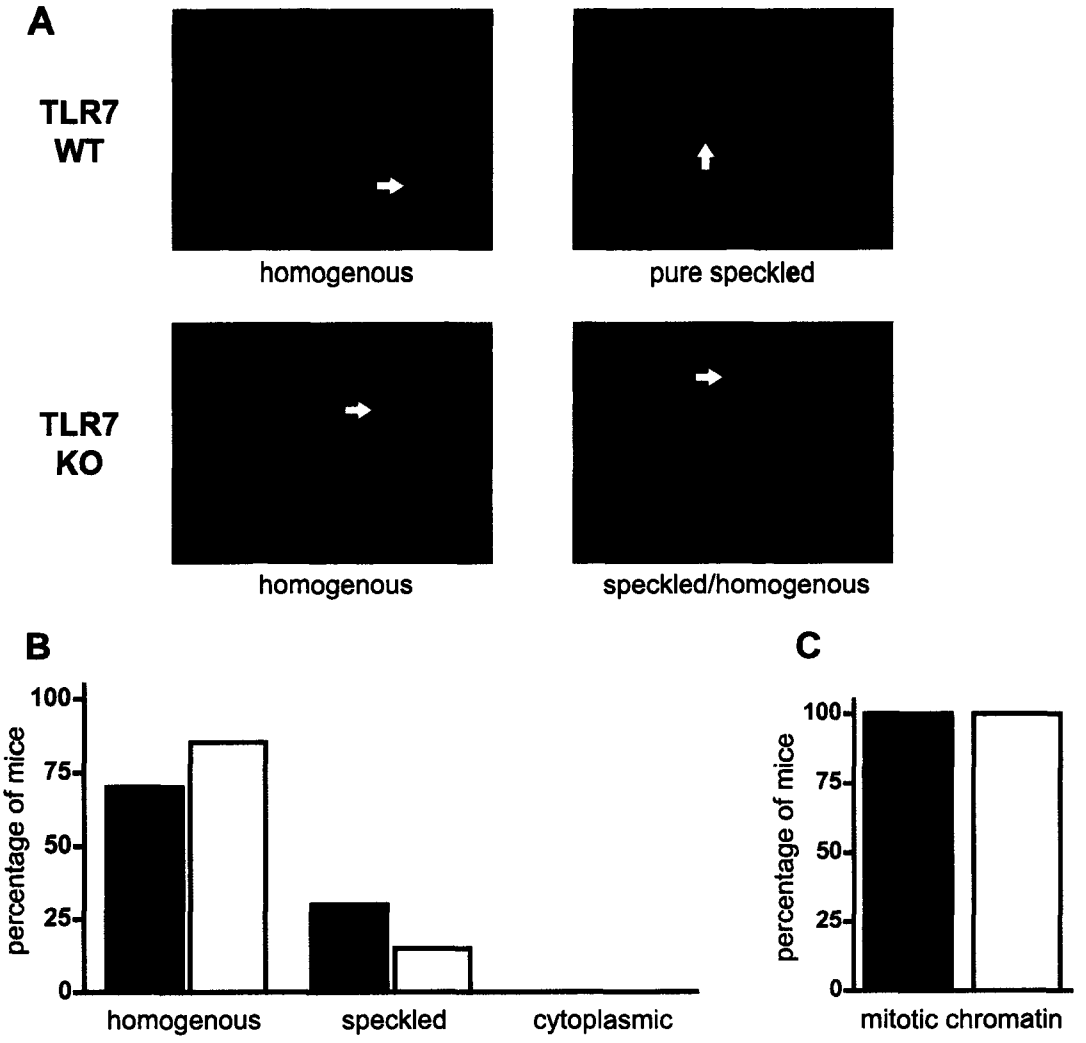

Figure 10. TLR7-deficient sera may have decreased staining of RNA-containing nuclear antigens. (A) ANAs from TLR7$^{+/y}$ (WT) sera are shown in upper panels (left, homogenous nuclear pattern; right, speckled nuclear pattern), and TLR7$^{-/y}$ (KO) sera in lower panels (left, homogenous nuclear pattern; right, speckled nuclear pattern). Speckled patterns in TLR7 KO sera were a mix of speckled staining with superimposed homogenous staining. White arrows indicate cells in metaphase that demonstrate positive staining of mitotic chromatin. (B) Serum ANAs were classified as either nuclear homogenous, nuclear speckled, or cytoplasmic staining patterns. Black bars indicate TLR7 WT sera (n = 20), and white bars indicate TLR7 KO sera (n = 20). (C) As in B, but serum ANAs were classified as either positive or negative for mitotic chromatin staining.

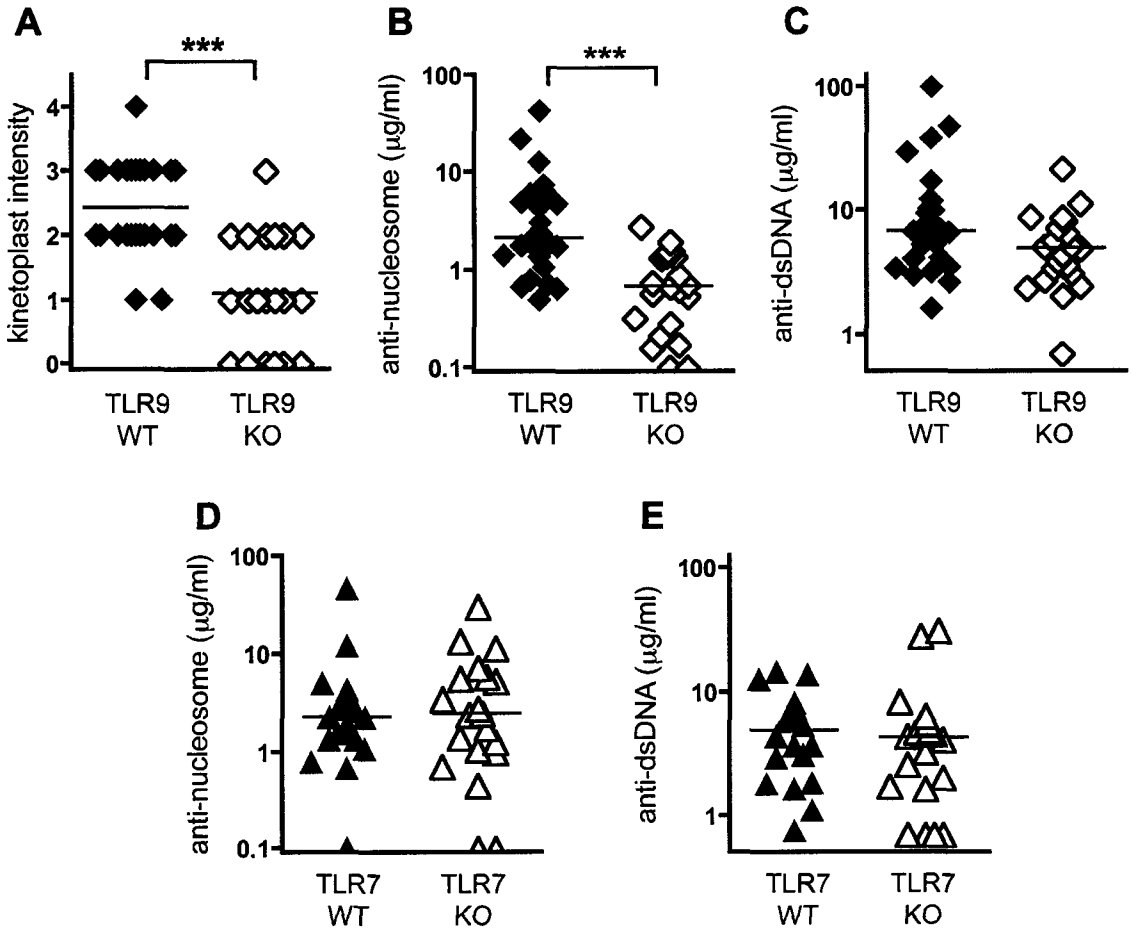

Figure 11. Antibodies to DNA-containing autoantigens are reduced in TLR9-deficient mice. (A) Anti-dsDNA antibodies in TLR9 WT (n = 26) and TLR9 KO (n = 21) sera were detected by *Crithidia luciliae* immunofluorescence. Intensity of staining *C. luciliae* kinetoplast DNA was scored from 0-4. (B-C) Anti-nucleosome (B) or anti-dsDNA (C) antibodies were determined by ELISA in TLR9 WT or TLR9 KO sera. Bars represent median values. (D-E) Anti-nucleosome (D) or anti-dsDNA (E) antibodies were determined by ELISA in TLR7 WT (n = 20) or TLR7 KO (n = 20) sera. Bars represent median values. ***, $P < 0.0001$ by Mann-Whitney U test.

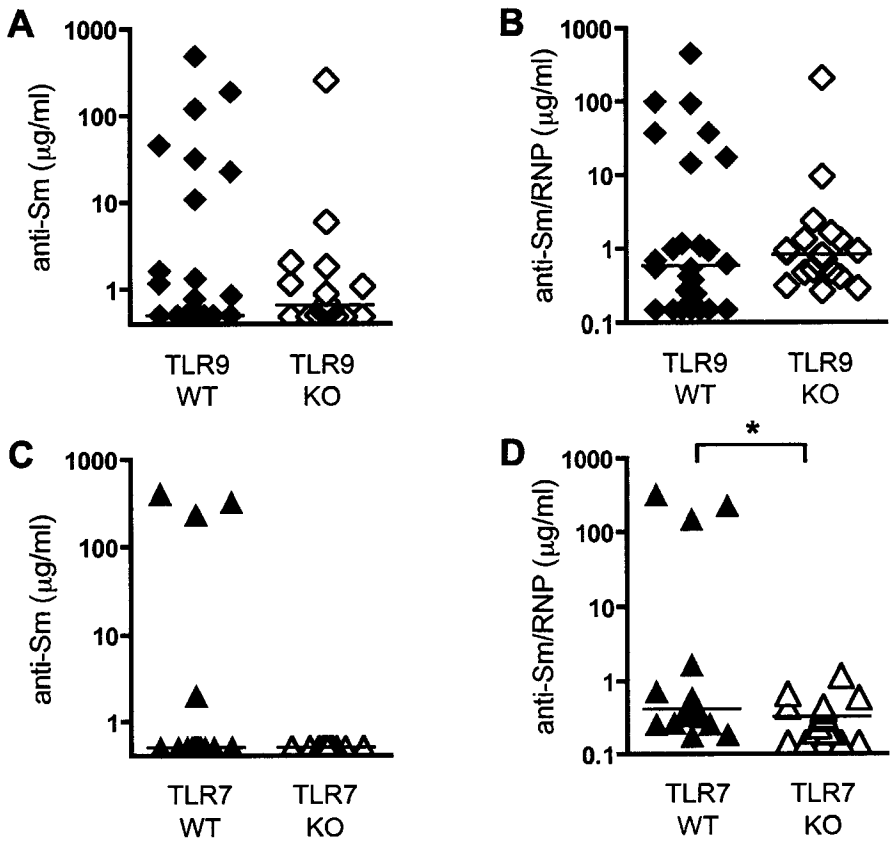

Figure 12. Anti-Sm and anti-RNP autoantibodies in TLR-deficient mice.
(A-B) Anti-Sm (A) or anti-Sm/RNP antibodies were determined by ELISA in TLR9 WT (n = 26) and TLR9 KO (n = 21) sera. Bars represent median values. (C-D). Anti-Sm (C) or anti-Sm/RNP (D) antibodies were determined by ELISA in TLR7 WT (n = 20) or TLR7 KO (n = 20) sera. Bars represent median values.
*, $P < 0.05$ by Mann-Whitney U test.

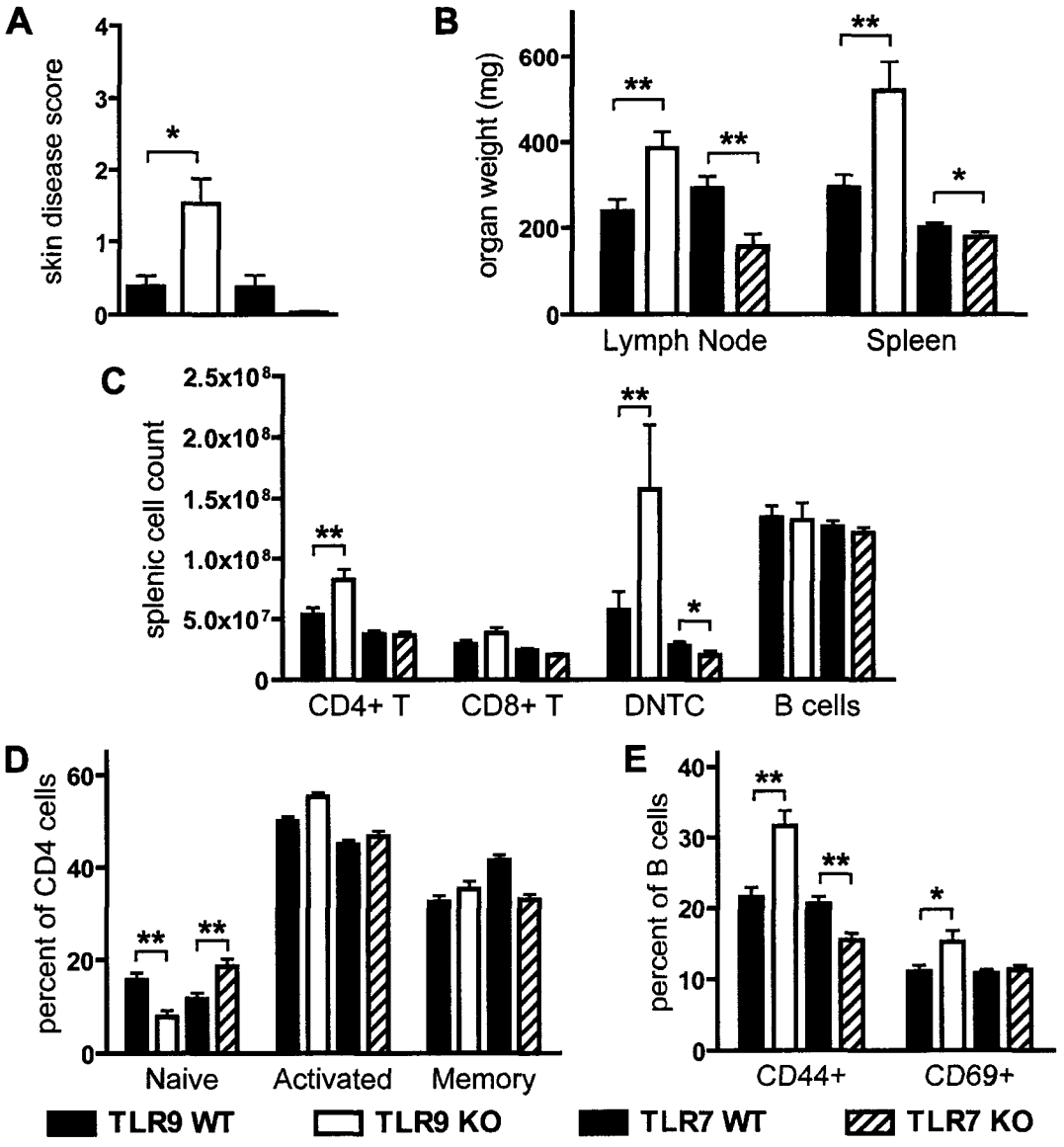

Figure 13. TLR7 and TLR9 have opposing effects on clinical disease and lymphocyte activation. TLR9 WT (black bars, n = 26), TLR9 KO (white bars, n = 21), TLR7 WT (gray bars, n = 20), and TLR7 KO (striped bars, n = 20) mice were assayed for various parameters of clinical disease and immune activation at the time of sacrifice. (A) Severity of skin disease was determined. (B) Spleens and the two largest axillary lymph nodes were removed and weighed. (C) Splenocyte subsets were enumerated by FACS analysis for $CD4^+$ T cells, $CD8^+$ T cells, $CD4^-/CD8^-$ double negative T cells (DNTC), and B cells. (D) Lymph node $CD4^+$ T cells were classified as either naïve ($CD44^-$ $CD62L^+$), activated ($CD44^+$ $CD62L^+$), or memory ($CD44^+$ $CD62L^-$) phenotype. (E) Splenic B cells were assayed for expression of the activation markers CD44 and CD69. Data are presented as mean +/- SEM. *, $P < 0.05$; **, $P < 0.01$ by Mann-Whitney U test.

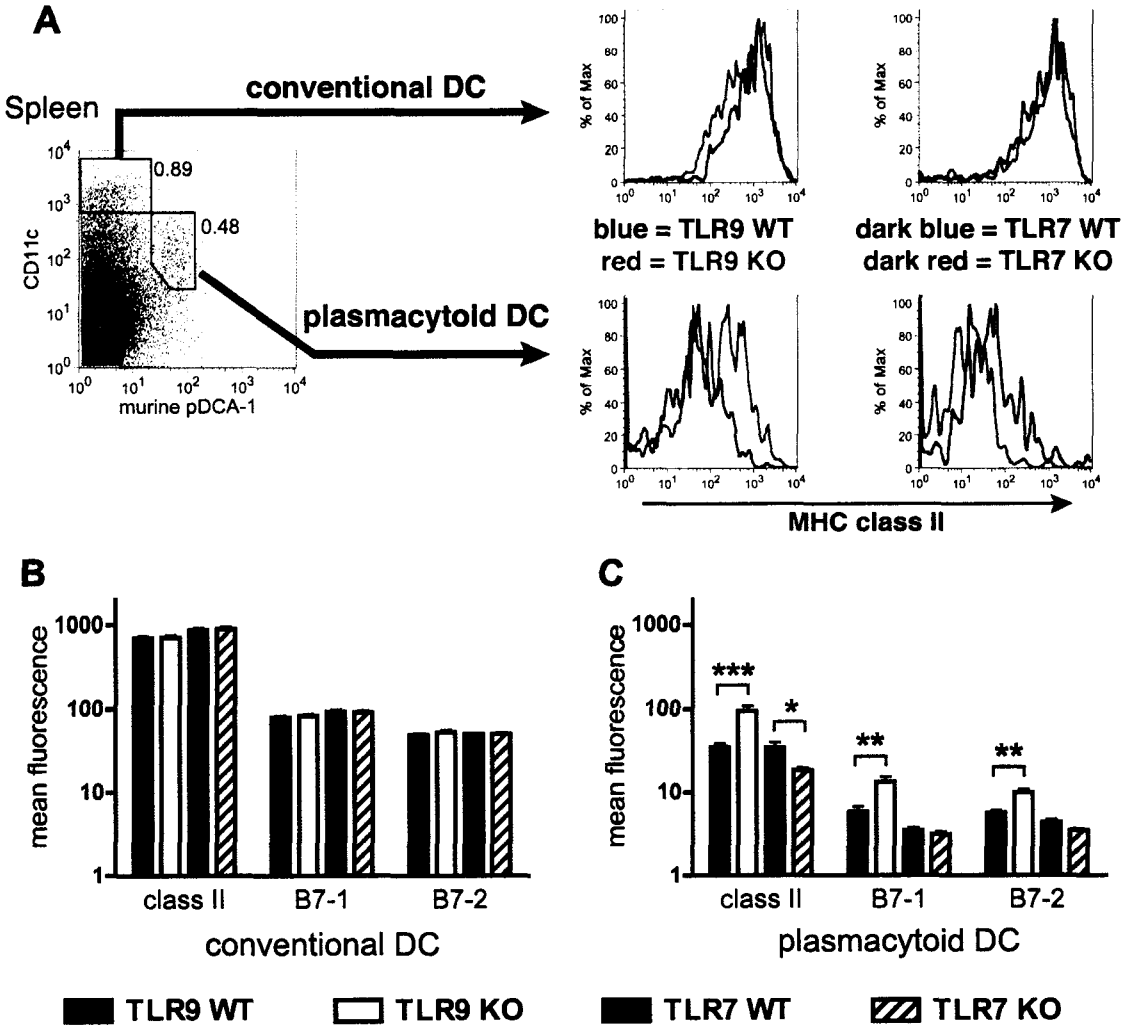

Figure 14. TLR7 and TLR9 have opposing effects on plasmacytoid DC activation. (A) Left panel: splenic conventional DCs ($CD11c^{hi}$ $pDCA\text{-}1^{-}$) and plasmacytoid DCs ($CD11c^{int}$ $pDCA\text{-}1^{+}$) were identified by FACS. Right panels: MHC class II expression was determined in conventional DCs (upper panels) and plasmacytoid DCs (lower panels) from TLR9 WT (blue) and TLR9 KO (red) mice (left histograms) or TLR7 WT (dark blue) and TLR7 KO (dark red) mice (right histograms). Representative samples from the same experiment are shown. (B) Expression of MHC class II, B7-1, and B7-2 was determined in conventional DCs from TLR9 WT (black bars, n = 26), TLR9 KO (white bars, n = 21), TLR7 WT (gray bars, n = 20), and TLR7 KO (striped bars, n = 20) mice. Data are presented as mean +/- SEM. (C) As in B, but activation marker expression was determined in plasmacytoid DCs. *, $P < 0.05$; **, $P < 0.01$; ***, $P < 0.0001$ by Mann-Whitney U test.

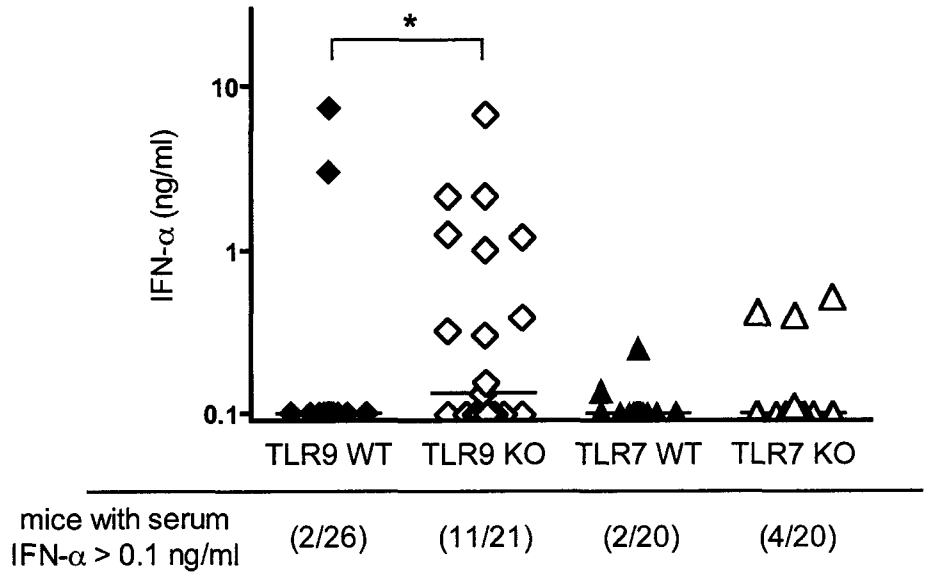

Figure 15. Elevated serum IFN-α in TLR9-deficient mice. Serum IFN-α was determined at the time of sacrifice for TLR9 WT (n = 26), TLR9 KO (n = 21), TLR7 WT (n = 20) and TLR7 KO (n = 20) mice. Limit of detection was 0.1 ng/ml in serum. *, $P < 0.05$ by Mann-Whitney U test.

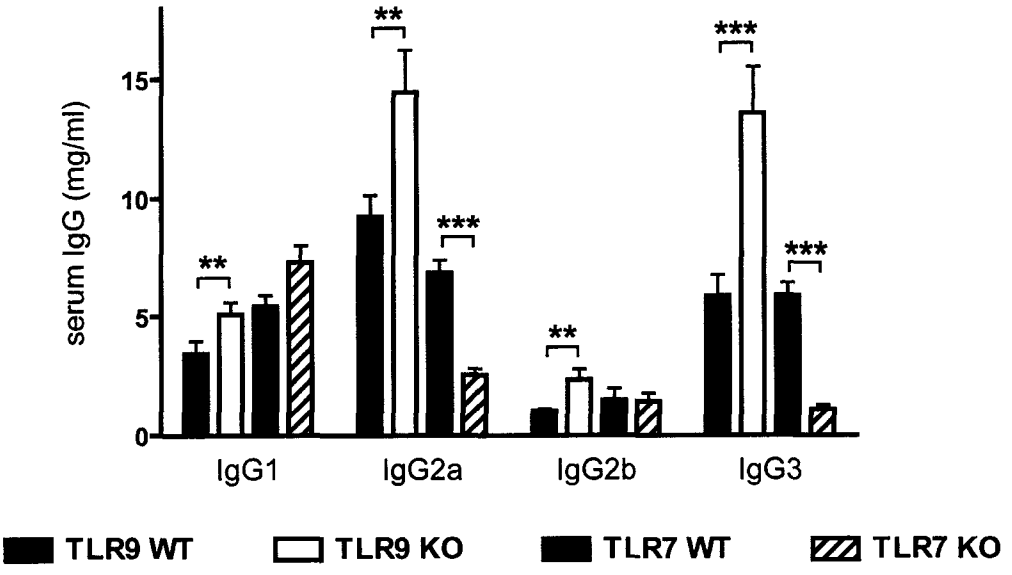

Figure 16. TLR7 and TLR9 differentially affect IgG isotype production. Serum IgG isotypes were determined at the time of sacrifice for TLR9 WT (black bars, n = 26), TLR9 KO (white bars, n = 21), TLR7 WT (gray bars, n = 20), and TLR7 KO (striped bars, n = 20) mice. Data are presented as mean +/- SEM. **, $P < 0.01$; ***, $P < 0.0001$ by Mann-Whitney U test.

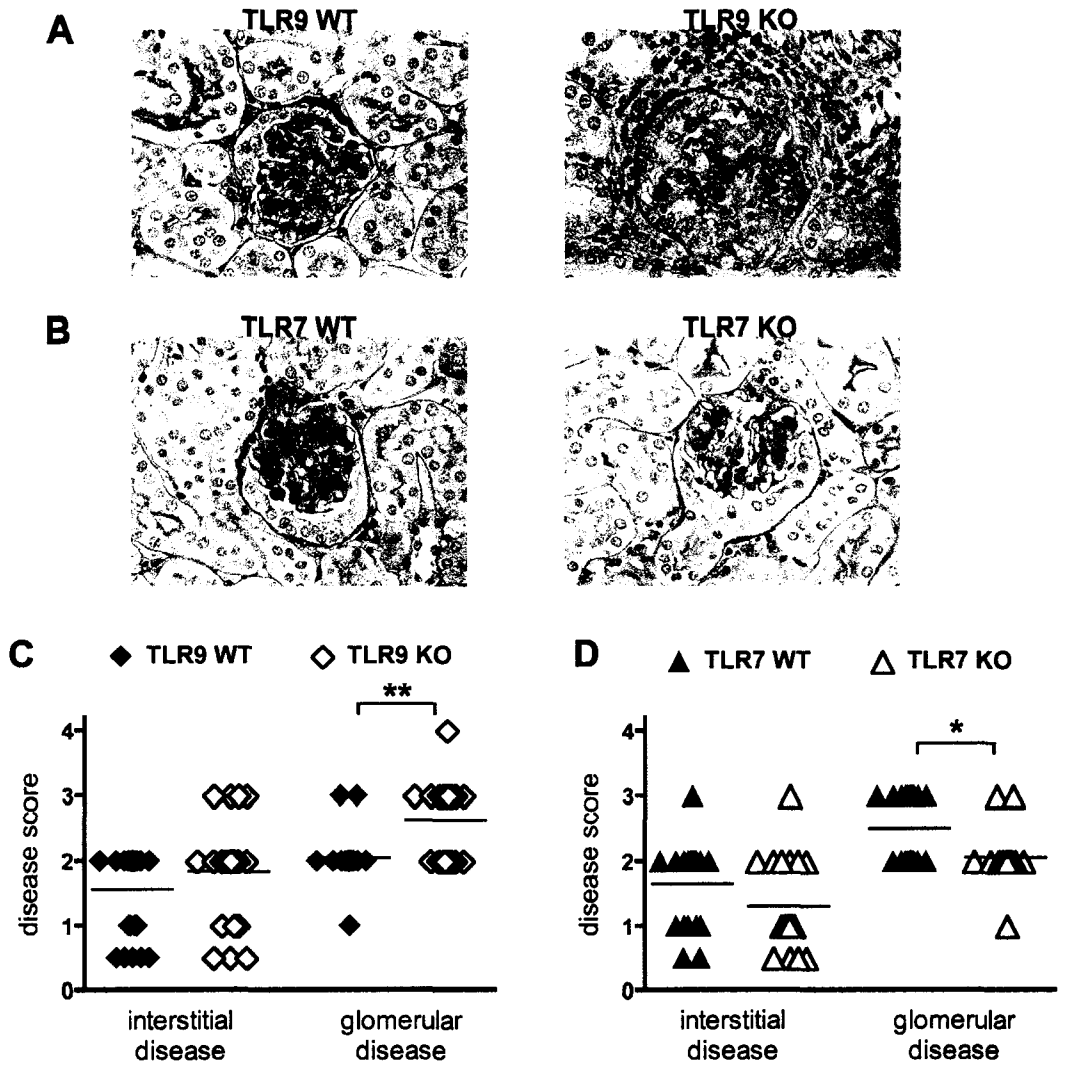

Figure 17. TLR7 and TLR9 have opposing effects on lupus nephritis. (A) Representative TLR9 WT (left panel, glomerular score = 2), and TLR9 KO (right panel, glomerular score = 4) glomeruli are shown. (B) Representative TLR7 WT (left panel, glomerular score = 3), and TLR7 KO (right panel, glomerular score = 2) glomeruli are shown). (C) Interstitial infiltrates and glomerular disease were scored from 0-4 for TLR9 WT (n = 26) and TLR9 KO (n = 21) mice. (D) As in C, but for TLR7 WT (n = 20) and TLR7 KO (n = 20) mice. *, $P < 0.05$; **, $P < 0.01$ by Mann-Whitney U test.

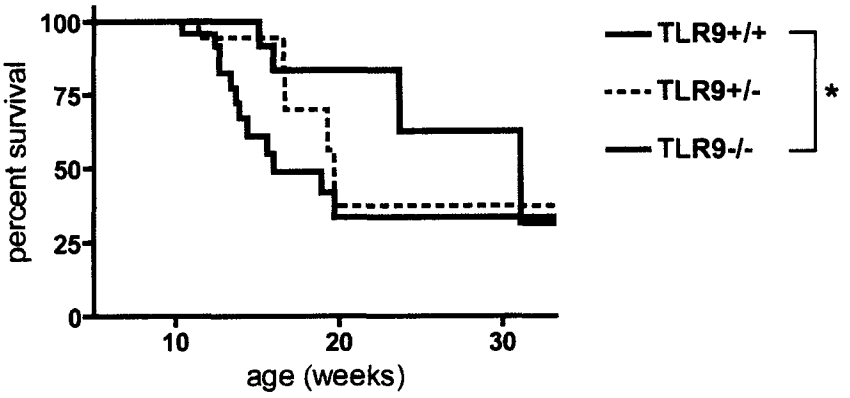

Figure 18. Accelerated mortality in autoimmune TLR9-deficient mice. TLR9 WT (blue line, n = 22), TLR9 heterozygote (black dashed line, n = 18), and TLR9 KO (red line, n = 24) littermates were observed until the time of death. Median survival for WT mice was 31.1 weeks, with 4 deaths during observation period. Median survival for heterozygote mice was 19.7 weeks, with 5 deaths during the observation period. Median survival for KO mice was 16 weeks, with 12 deaths during the observation period. *, $P < 0.05$ for comparison of WT versus KO mice by the logrank test.

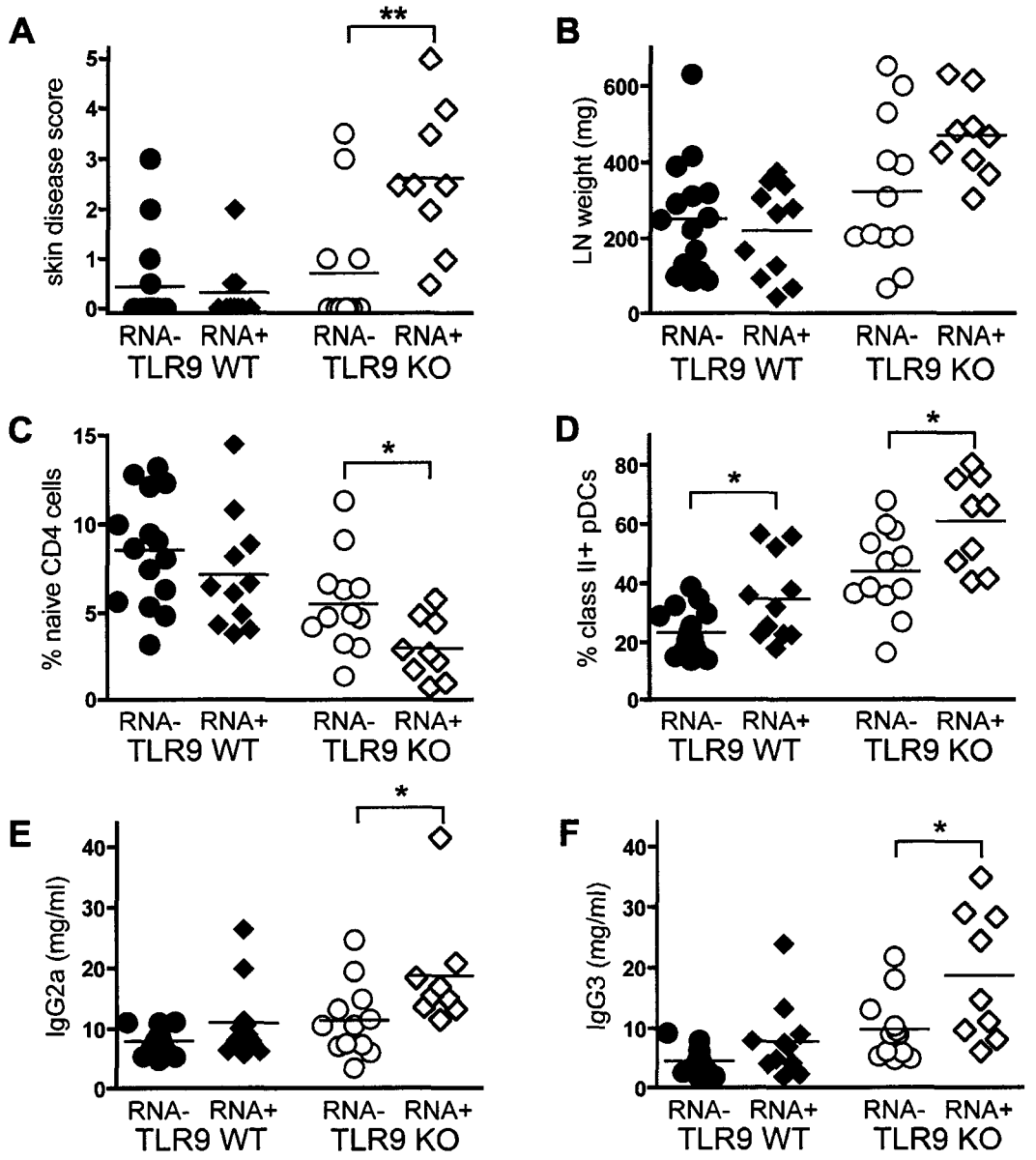

Figure 19. Presence of antibodies to RNA complexes is associated with clinical disease and immune activation. TLR9 WT mice (black symbols) were divided into two subgroups: those with anti-Sm or anti-Sm/RNP antibodies > 1 μg/ml (RNA+, n = 11), and those without (RNA-, n = 15). TLR9 KO mice (white symbols) were similarly classified as anti-Sm or anti-Sm/RNP > 1 μg/ml (RNA+, n = 9) or < 1 μg/ml (RNA-, n = 12). Skin disease (A), and lymph node weight (B) were determined as previously described. (C) Naïve phenotype ($CD62L^+$ $CD44^-$) $CD4^+$ T cells were determined as percentage of splenic $CD4^+$ cells. (D) MHC class II^+ pDCs were determined as percentage of total pDCs. IgG2a (E) and IgG3 (F) were determined as previously described. *, $P < 0.05$; **, $P < 0.01$ by Mann-Whitney U test.

Chapter 4: Mechanism of Autoantibody and Interferon Alpha Production in TLR9-Deficient Autoimmune Mice

Signaling via TLRs is required for the generation of specific autoantibodies in SLE. We have thus far shown, in two different genetic cohorts, that the generation of antibodies to the prototypical DNA-containing autoantigens of lupus cannot occur in the absence of TLR9. The mechanism of TLR9-mediated autoantibody production, however, remains unclear. TLR9 is expressed on multiple cell types including B cells and plasmacytoid and myeloid DCs (72, 162), and all of these cell types can be stimulated by endogenous TLR9 ligands in the context of autoimmunity (80, 116, 118). Thus, although B cell-intrinsic TLR stimulation is a critical aspect of normal immune responses (75), it is possible that anti-DNA B cells are secondarily activated by the ligation of TLR9 on other cells such as pDCs. In this scenario, cognate interactions with or soluble mediators secreted by these proposed accessory cells could provide the necessary costimulation, and TLR expression by autoreactive B cells would then be dispensable. In order to determine the cellular requirements for TLR9 expression in autoantibody production, we generated lupus-prone chimeric mice in which TLR9-deficiency could be restricted to cells of the B lineage.

In addition to the dramatic reduction in autoantibodies to DNA-containing antigens, genetic absence of TLR9 promoted IFN-α production, exacerbated clinical signs of autoimmune disease, and accelerated mortality in lupus-prone mice. As in the case of antibody production, however, the cellular mechanism for this phenotype was unknown. We suspect that the altered autoantibody repertoire contributes to pathogenesis

in TLR9$^{-/-}$ mice, but it is also possible that deficiency of TLR9 in pDCs or other cells of the innate immune system can directly enhance systemic inflammation and disease activity. A synergistic effect of autoantibody specificity and TLR expression within responding cells could also occur, such that TLR9-deficient serum and a lack of TLR9 on DC subsets would both be required for the phenotype of exacerbated SLE in TLR9$^{-/-}$ mice. Analysis of selective TLR9-deficiency in chimeric mice allowed preliminary insight into the mechanism of pathogenesis, but was not conclusive. We therefore devised an experimental system to determine the relative contributions of circulating autoantibodies and DC-intrinsic TLR expression to innate immune activation and inflammatory cytokine production in autoimmunity. We performed controlled stimulation experiments of dendritic cell subsets from wild-type or TLR9$^{-/-}$ mice in the presence of various combinations of TLR ligands and either wild-type or TLR9$^{-/-}$ serum. Our results reveal a primary role for B cells and their autoantibody products in the pathogenesis of SLE in TLR9$^{-/-}$ mice.

Generation of Chimeric Mice

In order to determine whether the TLR9-mediated generation of specific autoantibodies occurs by a B cell-autonomous mechanism, we restricted the genetic knockout of TLR9 to cells of the B lineage in autoimmune mice. This was accomplished with bone marrow chimerism in irradiated recipients. The combination of bone marrow from B cell-deficient $J_H^{-/-}$ donors and TLR9$^{-/-}$ donors created a chimeric mouse in which all B cells were TLR9-deficient, which we designated B.9$^{-/-}$ (Fig. 20A). The use of a 4:1 ratio of the two donors, favoring the $J_H^{-/-}$ marrow, ensured that the majority of non-B cells

expressed a functional TLR9. Controls for this experiment included $B.9^{+/+}$ chimeras, which had the same proportion of B cells as $B.9^{-/-}$ mice but were TLR9 wild-type, and $All.9^{-/-}$ mice, in which all hematopoietic cells were TLR9-deficient with a normal ratio of B cell precursors (Fig. 20A). All donors and recipients were of the lupus-prone $MRL/Mp^{lpr/lpr}$ strain, and all recipients were B cell deficient to prevent potential confounding by surviving B cells in the irradiated hosts, or from pre-existing autoimmune disease.

To verify the expected TLR9-chimerism of experimental mice, we used quantitative polymerase chain reaction (PCR) amplification of TLR9 alleles from genomic DNA of sorted splenocytes. Quantitation of relative levels of the wild-type or knockout allele allowed us to determine the degree of chimerism in various cell types as well as the total spleen. As expected, $B.9^{+/+}$ mice were entirely TLR9 wild-type, with no amplification of the disrupted allele (Fig. 20B). In $B.9^{-/-}$ mice, B cells were completely TLR9-deficient, while other cell types showed varying levels of chimerism. Total splenocytes (of which ~10% were B cells, Fig. 24B below) were less than one-fourth $TLR9^{-/-}$, while only about 10% of macrophages were derived from the TLR9-deficient marrow (Fig. 20B). Plasmacytoid DCs revealed a higher level of $TLR9^{-/-}$ chimerism. This could be due to the technical limitations inherent in isolating and amplifying DNA from this rare subset of cells (<0.5% of total splenocytes in chimeric mice, data not shown), or it could represent a modest but selective expansion of $TLR9^{-/-}$ pDCs. In either case, the majority of pDCs and other non-B cells in $B.9^{-/-}$ mice were TLR9 wild-type. In $All.9^{-/-}$ mice, the vast majority of all cell types were TLR9-deficient, but there was a small fraction of total splenocytes (~8%), as well as macrophages and pDCs (2.3% and 4.5%,

respectively), that retained the wild-type TLR9 (Fig. 20B). These cells may be non-dividing host cells that persisted in the spleen until the mice were analyzed at 16 weeks post-reconstitution, or they may represent the progeny of rare stem cells which survived radiation. As in B.9$^{-/-}$ animals, however, all B cells in All.9$^{-/-}$ mice were TLR9-deficient (Fig. 20B).

B Cell-Intrinsic Requirement for TLR9 in Autoantibody Production

Having created chimeric mice in which deficiency of TLR9 was restricted to the B cell lineage, we then examined the generation of circulating autoantibodies in these mice. We first verified that chimeras had sufficient reconstitution of B cells and serum immunoglobulin after a period of 16 weeks (see analysis below). Analysis of serum ANAs then revealed that B.9$^{-/-}$ sera, like All.9$^{-/-}$ sera, generated ANAs with predominantly cytoplasmic staining patterns (Fig. 21A-B). This indicated a defect in the generation of anti-DNA antibodies, analogous to the autoantibody repertoire in non-chimeric TLR9$^{-/-}$ mice (Chapter 3). This was in stark contrast to sera from B.9$^{+/+}$ controls, the majority of which produced homogenous nuclear staining patterns in the absence of any cytoplasmic staining (Fig. 21A-B). The distribution of ANA patterns in B.9$^{-/-}$ and All.9$^{-/-}$ serum was significantly different from B.9$^{+/+}$ serum ($P < 0.0001$ and $P = 0.0015$ for comparison of B.9$^{+/+}$ versus B.9$^{-/-}$ and All.9$^{-/-}$, respectively). A striking dichotomy was also observed in the staining of chromatin in metaphase cells, with all B.9$^{+/+}$ sera containing antibodies that bound mitotic chromatin, compared to none of the sera from B.9$^{-/-}$ or All.9$^{-/-}$ mice (Fig. 21, A and C, $P < 0.0001$ for comparison of B.9$^{+/+}$ versus either B.9$^{-/-}$ or All.9$^{-/-}$). Thus, sera from mice with TLR9-deficient B cells specifically lacked antibodies capable

of binding the characteristic DNA-containing autoantigens of SLE. Importantly, the failure of B.9$^{-/-}$ sera to produce homogenous nuclear and anti-chromatin staining patterns indicates that the presence of functional TLR9 on the majority of non-B cells in these mice was not sufficient to allow the production of antibodies to DNA-containing antigens.

Analogous to non-chimeric TLR9$^{-/-}$ sera, autoantibodies in B.9$^{-/-}$ and All.9$^{-/-}$ sera stained cytoplasmic antigens in a fine granular to homogenous pattern, highlighting the perinuclear region without staining of specific cytoplasmic organelles (Fig. 21A). Such patterns are characteristic of antibodies to aminoacyl-tRNA synthetases (anti-Jo-1 antibodies) or anti-ribosomal antibodies (23, 26). We also observed a novel nucleolar staining pattern in two of the B.9$^{-/-}$ sera (Fig. 21A and data not shown). Staining of nucleoli, along with coincident cytoplasmic staining and the absence of chromatin staining, can indicate the presence of antibodies to either ribosomal P protein or a protein of unknown function designated polymyositis-scleroderma overlap syndrome (PM/Scl)-related nucleolar protein (23, 163). Because RNA is an inherent component of ribosomes and nucleoli, the autoantibody repertoire of chimeric mice with TLR9-deficient B cells, like that of non-chimeric TLR9$^{-/-}$ mice, appears shifted towards the recognition of endogenous RNA-containing antigens. Moreover, this shift occurs in a B cell autonomous fashion.

The absence of antibodies to DNA and chromatin in chimeric mice with TLR9-deficient B cells was confirmed by specific assays for these autoantibodies. Both B.9$^{-/-}$ and All.9$^{-/-}$ sera contained significantly reduced levels of anti-dsDNA antibodies compared to sera from B.9$^{+/+}$ mice, as determined by immunofluorescent staining of

Crithidia luciliae kinetoplast dsDNA (Fig. 22A, P = 0.0036 and 0.0115 for B.9$^{-/-}$ and All.9$^{-/-}$, respectively). B.9$^{-/-}$ and All.9$^{-/-}$ mice also failed to generate high levels of anti-nucleosome antibodies, which were common in mice with B cells expressing wild-type TLR9 (Fig. 22B, P = 0.0135 and 0.0311 for comparison of B.9$^{+/+}$ with B.9$^{-/-}$ or All.9$^{-/-}$, respectively). There was no difference in the three groups, however, when anti-dsDNA antibodies were measured with a poly-L-lysine-based ELISA (Fig. 22C). This discrepancy between different ELISAs is similar to what was observed in non-chimeric TLR9$^{-/-}$ mice (Chapter 3), and again highlights the lack of specificity of these assays as well as the greater relevance of DNA-histone complexes in the generation of autoantibodies. Taken together, the ANA and specific anti-DNA assays on sera from chimeric mice reveal a requirement for TLR9 expression within B cells for effective production of antibodies to characteristic DNA-containing antigens in SLE. Moreover, the presence or absence of TLR9 on non-B cells did not appear to have any effect on autoantibody production, as B.9$^{-/-}$ and All.9$^{-/-}$ mice generated autoantibody profiles which were indistinguishable.

Creation of Additional Chimeras and B Cell Reconstitution

To help determine if there was a dose-response relationship involving the extent of TLR9 chimerism on non-B cells, we also generated B.9$^{-/-}$ chimeric mice with a higher ratio of TLR9$^{-/-}$ marrow to $J_H^{-/-}$ marrow. Thus, in addition to the B.9$^{-/-}$ (20%) mice previously discussed, we also analyzed a small group of B.9$^{-/-}$ (50%) mice. Quantitative PCR of sorted cells from these mice confirmed that approximately half of non-B cells were TLR9-deficient (data not shown), compared with 10-40% of non-B cells in B.9$^{-/-}$

(20%) mice (Fig. 20B). We then had three increasing levels of TLR9-deficiency on non-B hematopoietic cells: a minority of $TLR9^{-/-}$ cells in $B.9^{-/-}$ (20%) mice, approximately half $TLR9^{-/-}$ cells in $B.9^{-/-}$ (50%) mice, and a vast majority of $TLR9^{-/-}$ cells in $All.9^{-/-}$ mice. As an additional control, we also created $All.9^{+/+}$ mice in which all stem cells were TLR9 wild-type and B cell sufficient. ANA staining patterns and anti-DNA antibodies in these two additional groups were the same as their TLR9-deficient or wild-type counterparts (data not shown).

In order to create the desired degree of TLR9 chimerism, varying proportions of B cell-sufficient bone marrow were used in the different groups (20%, 50%, or 100% as described). It was therefore important to determine the extent of B cell reconstitution in the chimeric mice. At 16 weeks post-reconstitution, B cells were present in the spleen in all chimeric mice. Although there were no significant differences between the groups, there was a trend toward a higher percentage of total splenic B cells in mice that received a higher ratio of B cell-sufficient marrow (Fig. 23A). When we examined the percentages of follicular splenic B cells, however, the greater extent of reconstitution in these mice became significant. Chimeric $All.9^{-/-}$ mice had more splenic follicular B cells than either $B.9^{+/+}$ (20%) or $B.9^{-/-}$ (20%) mice ($P = 0.0229$ and 0.0034, respectively), while the percentage of follicular B cells in $All.9^{+/+}$ mice was comparable to that in $All.9^{-/-}$ mice (Fig. 23B). $B.9^{-/-}$ (50%) mice had a similar percentage of follicular B cells as $B.9^{-/-}$ (20%) mice (Fig. 23B). The ratio of B cell precursors in the donor marrow therefore appeared to determine the extent of B cell reconstitution in the periphery. Importantly, there were similar proportions of peripheral B cell subsets in $B.9^{+/+}$ (20%) and $B.9^{-/-}$ (20%) mice, and

thus the extent of reconstitution was not a confounding variable in comparisons between these two groups.

Clinical Disease and Immune Activation in TLR9 Chimeric Mice

Chimeric TLR9-deficient mice afforded the opportunity to determine the effect of a B cell-specific lack of TLR9 on disease pathogenesis as well as autoantibody production. Two important findings in non-chimeric TLR9$^{-/-}$ mice were the elevated activation state of pDCs and increased circulating levels of IFN-α (Chapter 3). Because circulating immune complexes can activate DCs in a TLR-dependent manner (116, 118), it was unclear whether the altered autoantibody profiles or the lack of TLR9 on DCs was the primary cause of the observed pDC phenotype in TLR9$^{-/-}$ mice. We therefore analyzed the activation state of DCs in chimeric mice, wherein the autoantibody repertoire is dissociated from TLR9 expression on non-B cells. We found a significant increase in MHC class II expression by pDCs in B.9$^{-/-}$ (20%) mice compared to B.9$^{+/+}$ (20%) mice (Fig. 24A-B, P = 0.0076). A similar increase in class II expression was also observed among myeloid dendritic cells (mDCs) in B.9$^{-/-}$ (20%) mice (Fig. 24C, P = 0.0385). Increased DC activation was therefore not due to an intrinsic lack of TLR9 on these cells, since the majority of pDCs and mDCs in B.9$^{-/-}$ (20%) mice were TLR9 wild-type. Furthermore, the absence of TLR9 on pDCs or mDCs did not further increase their activation state in the presence of TLR9-deficient B cells, as B.9$^{-/-}$ (20%), B.9$^{-/-}$ (50%), and All.9$^{-/-}$ mice exhibited similar levels of class II expression among DC subsets (Fig. 24, A and C).

To determine the functional consequences of pDC activation in chimeric mice, we also measured circulating IFN-α levels, but found that none of the chimeric mice in any group had high systemic IFN-α at 8, 12, or 16 weeks post-reconstitution (data not shown). It is unclear if this represents a failure of interferon production by donor-derived pDCs in chimeric mice, or perhaps some effect of radiation non-hematopoietic cells in the recipient animal involved in IFN-I production. Low IFN-α levels were not simply due to a lack of autoimmune disease, however, as skin disease was manifest in most chimeric mice between 12 and 16 weeks post-reconstitution. There was no difference in the incidence or severity of skin disease between experimental groups (data not shown). Similarly, measurement of spot proteinuria at the time of sacrifice (16 weeks) revealed some evidence of kidney disease in most mice without a significant difference between groups (data not shown). The contribution of a B cell-specific deficiency of TLR9 to the pathogenesis of end organ disease cannot be determined from this limited data set, but additional experiments may reveal a specific effect of TLR9 expression within B cells.

Although regulation of specific autoantibody production by TLR9 was a purely B cell-intrinsic phenomenon and the activation of DCs was at least partly attributable to TLR9 expression within B cells, other markers of immune activation were less dependent upon TLR9 expression in B cells. B cell-specific lack of TLR9, for example, was not sufficient to promote exaggerated lymphadenopathy. While B.9$^{+/+}$ (20%) and B.9$^{-/-}$ (20%) mice had comparable lymph node weights, both were significantly less than lymph nodes from All.9$^{-/-}$ mice (Fig. 25A P = 0.0115 and 0.0089, respectively). The apparently intermediate lymph node weight of B.9$^{-/-}$ (50%) mice supports the notion that TLR9-deficiency in non-B cells is required for the induction of severe lymphadenopathy. These

findings on lymph node weight cannot be explained by the extent of B cell reconstitution alone, as chimeric All.$9^{+/+}$ mice, which had the highest level of reconstitution, had low lymph node weights similar to B.$9^{-/-}$ (20%) mice (Fig. 25A). Activation of $CD4^+$ T cells followed a similar pattern, although both B cell-intrinsic and –extrinsic mechanisms of TLR9-deficiency appeared to play a role. While B.$9^{-/-}$ (20%) mice had a smaller fraction of naïve T cells than B.$9^{+/+}$ (20%) mice ($P = 0.0232$), a more profound reduction was observed in B.$9^{-/-}$ (50%) and All.$9^{-/-}$ mice (Fig. 25B, $P = 0.0052$ for comparison of B.$9^{+/+}$ versus All.$9^{-/-}$). The extent of B cell reconstitution may also be a factor in T cell activation, however, as chimeric All.$9^{+/+}$ mice also exhibited a low level of naïve $CD4^+$ T cells (Fig. 25B).

Serum levels of total IgG2a and IgG3 were also determined in TLR9 chimeras, since these were the isotypes with the greatest increase in non-chimeric TLR$9^{-/-}$ mice. We found that B cell-specific deficiency of TLR9 was not sufficient to induce hypergammaglobulinemia (Fig. 26A-B). Particularly for IgG3, All.$9^{-/-}$ mice had increased serum immunoglobulin compared to B.$9^{-/-}$ (20%) mice (Fig. 26B, $P = 0.0324$). Varying degrees of B cell reconstitution in the different groups were unlikely to account for this difference, as the percentage of splenic B cells did not correlate with serum levels of IgG3 in individual mice (Fig. 26C, $P = 0.5218$ by Pearson correlation, $r = 0.1087$). Thus, analysis of markers of disease severity and immune activation in TLR9 chimeric mice suggested that neither B cells nor other hematopoietic cells were exclusively responsible for the effect of TLR9-deficiency on the exacerbation of SLE. While a B cell-specific absence of TLR9 could lead to increased activation of DCs in B.$9^{-/-}$

chimeras, it was not sufficient induce other markers of disease activity such as lymphadenopathy and hypergammaglobulinemia.

Stimulation of IFN-α Production by Autoimmune TLR9$^{-/-}$ Serum

We hypothesized that the autoantibodies produced by TLR9-deficient B cells could be responsible for increased IFN-α production in autoimmune TLR9$^{-/-}$ mice. Although the increased pDC activation state in chimeric B.9$^{-/-}$ mice supported this, the presence of a small percentage of TLR9-deficient DCs in the chimeras as well as the lack of detectable serum IFN-α clouded the interpretation of these experiments. We therefore set up an *in vitro* stimulation of purified pDCs and mDCs from TLR9-deficient or wild-type mice, wherein the autoantibody repertoire could be completely dissociated from TLR9 expression by the responding cells. These cells were then cultured in the presence of autoimmune serum from either wild-type or TLR9-deficient mice, or stimulated with synthetic TLR ligands as positive controls. To create nascent immune complexes of autoantibodies and endogenous DNA or RNA ligands, syngeneic apoptotic thymocytes were also added, either alone or in addition to autoimmune serum. We found that serum from TLR9-deficient mice, but not wild-type serum, induced a high level of IFN-α production in both pDCs and mDCs from wild-type and TLR9-deficient mice (Fig. 27A-B). The addition of apoptotic thymocytes, either alone or in the presence of serum, did not appear to affect IFN-α secretion. Importantly, the IFN-α detected in these cultures was not simply due to circulating interferon from TLR9$^{-/-}$ serum, as both the wild-type and TLR9-deficient serum used contained less than 250 pg/ml IFN-α (data not shown), and serum was diluted ten-fold for these experiments.

The interferon stimulatory capacity of serum from TLR9-deficient mice reveals several important facets of interferon biology in SLE. First, IFN-α production in these experiments was induced by $TLR9^{-/-}$ serum, regardless of the genotype of the responding cells. Thus, the primary defect responsible for elevated IFN-α production by DC subsets in $TLR9^{-/-}$ mice lies in the generation of circulating serum factors, and not in dysregulated IFN-I pathways in pDCs. Second, although $TLR9^{+/+}$ serum did not induce IFN-α in wild-type cells, it did allow a low level of IFN-α secretion in TLR9-deficient pDCs and mDCs. This suggests that an intrinsic increase in IFN-I production by dendritic cells is also present in $TLR9^{-/-}$ mice, although this effect was not observed in the presence of $TLR9^{-/-}$ serum, presumably because the serum alone provided a maximal interferon-inducing stimulus. Third, the ability of TLR9-deficient pDCs to respond to factors in $TLR9^{-/-}$ serum indicates that the stimulatory ligand in these experiments is not likely to be DNA. The failure of $TLR9^{-/-}$ pDCs to produce IFN-α in response to a synthetic C-type CpG oligonucleotide (Fig. 27A) confirms the absence of DNA-sensing TLR pathways in these cells. Fourth, serum from TLR9-deficient mice induced IFN-α not only in pDCs, but also in mDCs. The interferon stimulatory factor in $TLR9^{-/-}$ serum can therefore bypass normal regulatory mechanisms preventing IFN-I secretion in most cell types, perhaps due to altered endosomal trafficking of nucleic acid ligands (109). Finally, we also observed that the addition of apoptotic thymocytes was not required for the stimulatory capacity of $TLR9^{-/-}$ serum. This may be explained by the provision of apoptotic material from the high degree of cell death in these cultures (Fig. 29, below), or it may reflect the presence of pre-formed stimulatory complexes in $TLR9^{-/-}$ serum.

Distinct DC Activation Programs Induced by TLR9 WT or KO Serum

The effect of TLR9-deficient serum on the production of other inflammatory cytokines was also investigated. Serum from both wild-type and TLR9-deficient mice induced modest secretion of IL-12 p40, which was greater than unstimulated cells but an order of magnitude less than the level induced by a C-type CpG oligonucleotide in mDCs (Fig. 28A-B). In both wild-type and TLR9-deficient mDCs, however, $TLR9^{-/-}$ serum was slightly less effective in stimulating IL-12 p40 than wild-type serum (Fig. 28B). Low to undetectable levels of the IL-12 p70 dimer were induced by either wild-type or $TLR9^{-/-}$ serum in these experiments (< 1 pg/ml, data not shown). The lack of IL-12 p70 may indicate pairing of IL12 p40 with IL-23 p19 to create the IL-23 dimer, which appears to have a potent inflammatory role in autoimmunity (164). A somewhat variable level of IL-10 secretion was observed in two different experiments, but unlike the induction of IL-12 p40, $TLR9^{-/-}$ serum tended to produce a slightly higher level of IL-10 than wild-type serum (Fig. C-D). We also measured levels of IL-6, IL-1β and TNF-α in these cultures, and found similar results to IL-12 p40, with low to modest levels of these cytokines induced by both wild-type and TLR9-deficient serum (data not shown). Finally, we found that DCs from both $TLR9^{+/+}$ and $TLR9^{-/-}$ mice produced comparably high levels of inflammatory cytokines (particularly IL-12) in response to the synthetic TLR7 ligand imiquimod (R837), indicating that there was not an inherent increase in TLR7 stimulation pathways in $TLR9^{-/-}$ DCs (data not shown).

We also determined survival and activation marker expression by DCs following these stimulations, and found contrasting effects on these two parameters. While viability was low after 24 hours in unstimulated cells, the presence of $TLR9^{-/-}$ serum

improved survival in wild-type and TLR9-deficient pDCs and mDCs (Figure 29A-B). This improvement in survival was even greater than that induced by stimulatory CpG in wild-type cells. Improved viability was not matched by increased costimulatory molecule expression, however, as $TLR9^{-/-}$ serum-stimulated cells expressed an even lower level of B7-2 than unstimulated cells (Fig. 29C-E). Wild-type serum had the opposite effect on dendritic cells. While serum from $TLR9^{+/+}$ mice induced a partial upregulation of B7-2, it reduced viability in responding cells, particularly in pDCs (Fig. 29A-E). The effect of wild-type or TLR9-deficient serum on expression of MHC class II or CD40 was similar to the effect on B7-2, although CD40 was not as effectively induced on pDCs as on mDCs (data not shown). Circulating factors in autoimmune TLR9-deficient serum thus appeared to enhance DC survival and IFN-α secretion while maintaining the immature phenotype of these cells, suggesting that serum from wild-type or $TLR9^{-/-}$ mice can induce two different activation pathways in dendritic cells.

Discussion

We have thus demonstrated that B cell-intrinsic expression of TLR9 is required for the generation of antibodies to DNA-containing autoantigens in SLE. This B cell-specific requirement for TLR9 was expected from initial studies documenting the TLR-dependent activation of isolated, autoreactive B cells in culture (29, 80, 82). The paradigm that TLR ligation within antigen-specific B cells is required for antibody production in normal immune responses (75) can thus be extended to include autoimmunity and the activation of anti-nuclear B cells. Thus, while multiple cell types express TLRs capable of recognizing endogenous nucleic acids, autoreactive B cells are

unique in the expression of a somatically rearranged surface receptor for these same ligands. On a molecular level, therefore, B cells reside at the interface of innate and adaptive immunity in SLE, and are likely to be responsible for the primary break in tolerance to self nuclear antigens.

The increased activation state of dendritic cells in B.9$^{-/-}$ chimeric mice and the interferon-stimulatory capacity of TLR9$^{-/-}$ serum indicated that circulating factors produced by TLR9-deficient B cells could influence the activation of wild-type DCs. Prior studies have indicated that immune complexes of endogenous nucleic acid bound to autoantibodies can induce cytokine secretion and costimulatory molecule expression by DCs (114-116). In addition to transmitting an activation signal via Fc-gamma receptors, the immunoglobulin portion of the complex appears critical in the delivery of nucleic acids to appropriate endosomal compartments for recognition by intracellular nucleic acid-sensing TLRs (118). Without specific anti-nuclear antibodies acting as vehicles for the transport of endogenous DNA or RNA, innate tolerance of self nucleic acids is maintained in dendritic cells. On a cellular level, therefore, B cells coordinate the interaction of antigen-specific recognition by the adaptive immune system with the potent effector mechanisms of the innate immune system in SLE pathogenesis.

The exact nature of the interferon-stimulatory factor in TLR9$^{-/-}$ serum remains unknown. Because it requires the presence of TLR9-deficient B cells, however, we suspect that the autoantibody repertoire is either directly or indirectly responsible for elevated IFN-α production. Interestingly, an apparent increase in antibodies to RNA-containing antigens was accompanied by increased circulating IFN-α in non-chimeric TLR9$^{-/-}$ mice, while a decrease in anti-Sm/RNP antibodies in TLR7$^{-/y}$ mice was coincident

with a decreased activation state of pDCs (Chapter 3). This suggested that RNA-containing immune complexes could be more potent stimulators of pDCs than DNA complexes, a concept supported by *in vitro* stimulation of pDCs with human lupus serum (87, 114). A related possibility is that DNA-containing immune complexes, by virtue of sub-optimal TLR9 stimulation by mammalian DNA (66), may inhibit IFN-α production by pDCs. The absence of anti-DNA antibodies in $TLR9^{-/-}$ serum could then release responding pDCs from this tonic inhibition, allowing efficient IFN-I secretion. Alternatively, TLR9-deficient mice may generate some other circulating inducer of IFN-α, which requires B cells but is independent of autoantibodies. Further studies on pDC activation by TLR-deficient serum, such as stimulation with serum from TLR7-deficient mice and stimulation with purified IgG from these serum samples, will be critical to further define the interferon-stimulatory factor. Mixing of wild-type serum with $TLR9^{-/-}$ serum in these experiments may also help elucidate an inhibitory effect of antibodies to DNA-containing antigens.

An interesting finding from our *in vitro* experiments was that $TLR9^{-/-}$ serum induced high levels of IFN-α in both myeloid and plasmacytoid dendritic cell subsets. Although mDCs are not traditionally responsible for IFN-I production, these cells can be transformed into efficient interferon-secreting cells under certain conditions (109, 165). Importantly, when intracellular trafficking is altered such that nucleic acids are retained in endosomal, rather than lysosomal compartments in mDCs, signaling via the MyD88-IRF7 axis is facilitated and these cells can produce high levels of IFN-I (109). It is therefore possible that FcR-mediated internalization of RNA-containing immune complexes in $TLR9^{-/-}$ serum can retain these complexes in specialized endosomal vesicles

for efficient IFN-α production. It is also possible, however, that IFN-α induction by serum from TLR9-deficient mice occurs by a TLR-independent mechanism. Several recent findings have identified innate sensors for cytoplasmic RNA and DNA that can induce IFN-I production independently of TLR signaling in multiple cell types (60-63). These sensors are thought to be instrumental in defense against viral infection, but may also be involved in the recognition of endogenous nucleic acids when mechanisms for the clearance of apoptotic cells are overwhelmed (166). Stimulation of MyD88-deficient DCs will allow us to determine the relative contributions of TLR-dependent and –independent mechanisms of IFN-α production in response to autoimmune TLR9$^{-/-}$ serum.

In addition to the induction of IFN-α, serum from TLR9$^{-/-}$ mice appeared to promote a distinct activation program in dendritic cells. This program was characterized by increased survival, decreased expression of costimulatory molecules, minimal secretion of inflammatory cytokines such as IL-6 and IL-12, and a potential increase in IL-10 production. Contrasting effects were observed when DCs were stimulated with wild-type serum. The ability of these cells to persist in an immature state may allow prolonged secretion of IFN-I, facilitating SLE pathogenesis through the prolific effects of this cytokine. Although IL-10 usually functions as a regulatory cytokine to suppress inflammation, the presence of IFN-α can transform IL-10 into a potent inflammatory mediator through the action of STAT1 (167). Thus, increased IL-10 secretion by TLR9$^{-/-}$ serum may also promote immune activation in SLE. The cytokine or cellular milieu may also influence the expression of costimulatory molecules, as serum from TLR9$^{-/-}$ mice inhibited expression of MHC class II and B7-2 in our *in vitro* experiments, but B cell-

derived factors increased class II expression by DCs in B.9$^{-/-}$ chimeric mice. In the context of additional signals *in vivo*, pDCs exposed to the appropriate autoantibody repertoire may mature into efficient antigen-presenting cells and thereby promote autoreactive T cell activation. The lack of TLR9 on B cells can thus have profound effects on autoimmune disease, as autoantibodies produced by these cells induce a specific activation program in dendritic cells, which in turn can facilitate SLE pathogenesis.

Materials and Methods

Generation and verification of chimeric mice.

Bone marrow cells were isolated from MRL/Mp$^{lpr/lpr}$ (TLR9$^{+/+}$), $J_H^{-/-}$ MRL/Mp$^{lpr/lpr}$, and TLR9$^{-/-}$ MRL/Mp$^{lpr/lpr}$ mice between 6-10 weeks of age. All donor and recipient mice were backcrossed at least 9 generations to MRL/Mp$^{lpr/lpr}$. For each experiment in a total of 5 separate experiments, bone marrow was pooled from 1-2 donor mice of each type. A total of $4x10^6$ cells were injected intravenously into recipient $J_H^{-/-}$ MRL/Mp$^{lpr/lpr}$ mice irradiated with 700-800 cGy from an X-Rad 320 X-ray irradiator. Recipient mice were 6-10 weeks of age at the time of reconstitution, and were analyzed at 16 weeks post reconstitution. B.9$^{+/+}$ mice received 20% TLR9$^{+/+}$ and 80% $J_H^{-/-}$ marrow, B.9$^{-/-}$ (20%) mice received 20-25% TLR9$^{-/-}$ and 75-80% $J_H^{-/-}$ marrow, B.9$^{-/-}$ (50%) received 50% TLR9$^{-/-}$ and 50% $J_H^{-/-}$ marrow, All.9$^{-/-}$ received exclusively TLR9$^{-/-}$ marrow, and All.9$^{+/+}$ received exclusively TLR9$^{+/+}$ marrow.

For verification of TLR9 chimerism, B cells (B220$^+$, CD22$^+$, CD11b$^-$, CD11c$^-$, Thy1.2$^-$) and macrophages (B220$^-$, CD22$^-$, CD11b$^+$, CD11c$^-$, Thy1.2$^-$) were sorted from

total splenocytes in 2 of 5 experiments, or B cells ($B220^+$, $CD22^+$, $CD11c^-$, mpDCA-1^-, $Thy1.2^-$) and pDCs ($B220^+$, $CD22^-$, $CD11c^{int}$, mpDCA-1^+, $Thy1.2^-$) were sorted from total splenocytes in 2 of 5 experiments. Antibodies used were as previously described (Chapters 2-3) in addition to anti-B220 (RA3-6B2, BD Biosciences) and anti-CD11b (M1/70, BD Biosciences) antibodies. Sorted cells or total splenocytes were digested at 10^6 cells/ml at 55 degrees in a digest buffer containing 1.5 mg/ml Proteinase K (Novagen).

Amplification of genomic DNA was performed with Brilliant SYBR Green QPCR Master Mix (Stratagene) on the Mx3000P Real-Time PCR System (Stratagene). Amplification of TLR9 wild-type allele was performed with the external primer (5' GCA ATG GAA AGG ACT GTC CAC TTT GTG 3') and the wild-type specific primer (5' GAA GGT TCT GGG CTC AAT GGT CAT GTG 3'). Amplification of TLR9 knockout allele was performed with the external primer above and the knockout specific primer (5' ATC GCC TTC TAT CGC CTT CTT GAC GAG 3'). Amplification of wild-type allele (relative to $TLR9^{+/+}$ control) was compared with amplification of knockout allele (relative to $TLR9^{-/-}$ control) to determine percentage of TLR9 knockout allele in each sample.

Determination of ANA and anti-dsDNA antibodies.

Serum was obtained at the time of sacrifice. ANA immunofluorescence on HEp-2 cells was performed at 1:200 dilution of serum as previously described (Chapter 2). Images were captured at 400X magnification with a constant exposure time of 4.0 seconds. *Crithidia luciliae* immunofluorescence was performed at 1:50 dilution of serum as previously described (Chapter 2). Images were captured at 1000X magnification with

a constant exposure time of 0.8 seconds. Anti-nucleosome and anti-dsDNA ELISAs were performed as previously described (Chapter 3).

Analysis of clinical disease and immune activation.

Skin disease was scored at the time of sacrifice as previously described (Chapter 3). Proteinuria was determined with Albustix reagent strips (Bayer). Spleen and lymph node cells were isolated and T and B cell subsets and activation markers were determined as previously described (Chapter 2). Plasmacytoid and myeloid DC activation status was determined as previously described (Chapter 3). Serum IFN-a ELISA was performed as previously described (Chapter 2), except that serum was added at 1:5 dilution. Levels of IgG isotypes in serum were determined as previously described (Chapter 3).

In vitro stimulation of dendritic cell subsets.

Plasmacytoid DCs (Thy1.2$^-$, CD22$^-$, B220$^+$, Ly6C$^+$, CD11c^{int}) and myeloid DCs (Thy1.2$^-$, CD22$^-$, B220$^-$, Ly6C$^-$, CD11c^{hi}) were sorted from total splenocytes using antibodies described previously in addition to anti-Ly6C antibody (AL-21, BD Biosciences). Sorted cells were stimulated for 24 hours in media supplemented with 10% Ultra-Low IgG Fetal Calf Serum (Gibco) in polystyrene plates at 35,000 cells per 100 μl. Stimuli included C-type CpG oligonucleotide ODN-2395 (Coley Pharmaceuticals) at 0.5 μM, imiquimod (R837, Invivogen) at 1 μg/ml, serum from TLR9$^{+/+}$ or TLR9$^{-/-}$ mice at 10% final concentration, or apoptotic thymocytes at a 1:2 ratio of apoptotic cells to stimulated cells. Serum was pooled from 4 MRL/Mp$^{lpr/lpr}$ mice of each genotype, between 12-18 weeks of age. Apoptotic thymocytes were generated by irradiation of MRL/Mp$^{lpr/lpr}$ thymocytes with 1000 cGy followed by incubation in serum-free media with 1 μM dexamethasone (Sigma) for 6 hours at 37 degrees.

IFN-α ELISA was performed as previously described (Chapter 2), except that culture supernatant was added at 1:1.5 or 1:2 dilution. Determination of inflammatory cytokine secretion was performed with a Bio-Plex mouse cytokine 6-plex kit for IL-1β, IL-6, IL-12 p40, IL-12 p70, and TNF-α (Bio-Rad) according to the manufacturer's instructions. Activation marker expression was determined as previously described (Chapter 3), in addition to the use of anti-CD40 (3/23, BD Pharmingen) antibody.

A

Group	Donor 1 (80%)	Donor 2 (20%)	Irradiated Recipient	Result
B.9$^{+/+}$	$J_H^{-/-}$ MRL/Mp$^{lpr/lpr}$	TLR9$^{+/+}$ MRL/Mp$^{lpr/lpr}$	$J_H^{-/-}$ MRL/Mp$^{lpr/lpr}$	TLR9 wild-type in all hematopoietic cells
B.9$^{-/-}$	$J_H^{-/-}$ MRL/Mp$^{lpr/lpr}$	TLR9$^{-/-}$ MRL/Mp$^{lpr/lpr}$	$J_H^{-/-}$ MRL/Mp$^{lpr/lpr}$	TLR9-deficiency restricted to B cell lineage
All.9$^{-/-}$	TLR9$^{-/-}$ MRL/Mp$^{lpr/lpr}$	none	$J_H^{-/-}$ MRL/Mp$^{lpr/lpr}$	TLR9-deficient in all hematopoitetic cells

B

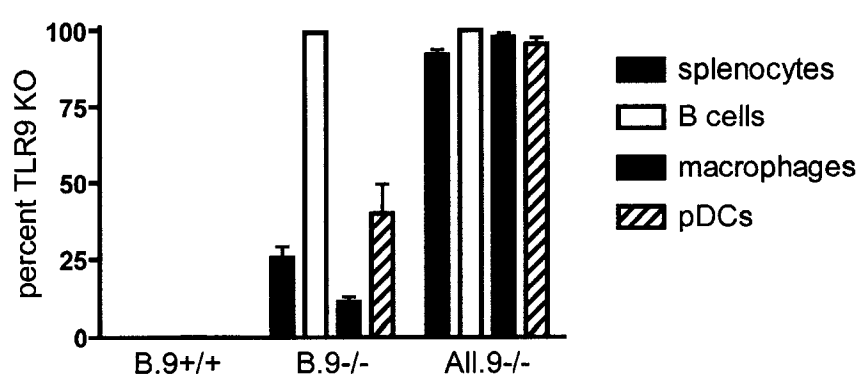

Figure 20. Generation and verification of TLR9-chimeric mice. (A) Generation of radiation chimeras with bone marrow from combination of 1 or 2 donors. (B) Quantitative PCR for TLR9 KO allele on sorted splenocytes from chimeric mice. Black bars indicate total splenocytes, white bars indicate sorted B cells, gray bars indicate macrophages, and striped bars indicate pDCs. Data are presented as mean +/- SEM.

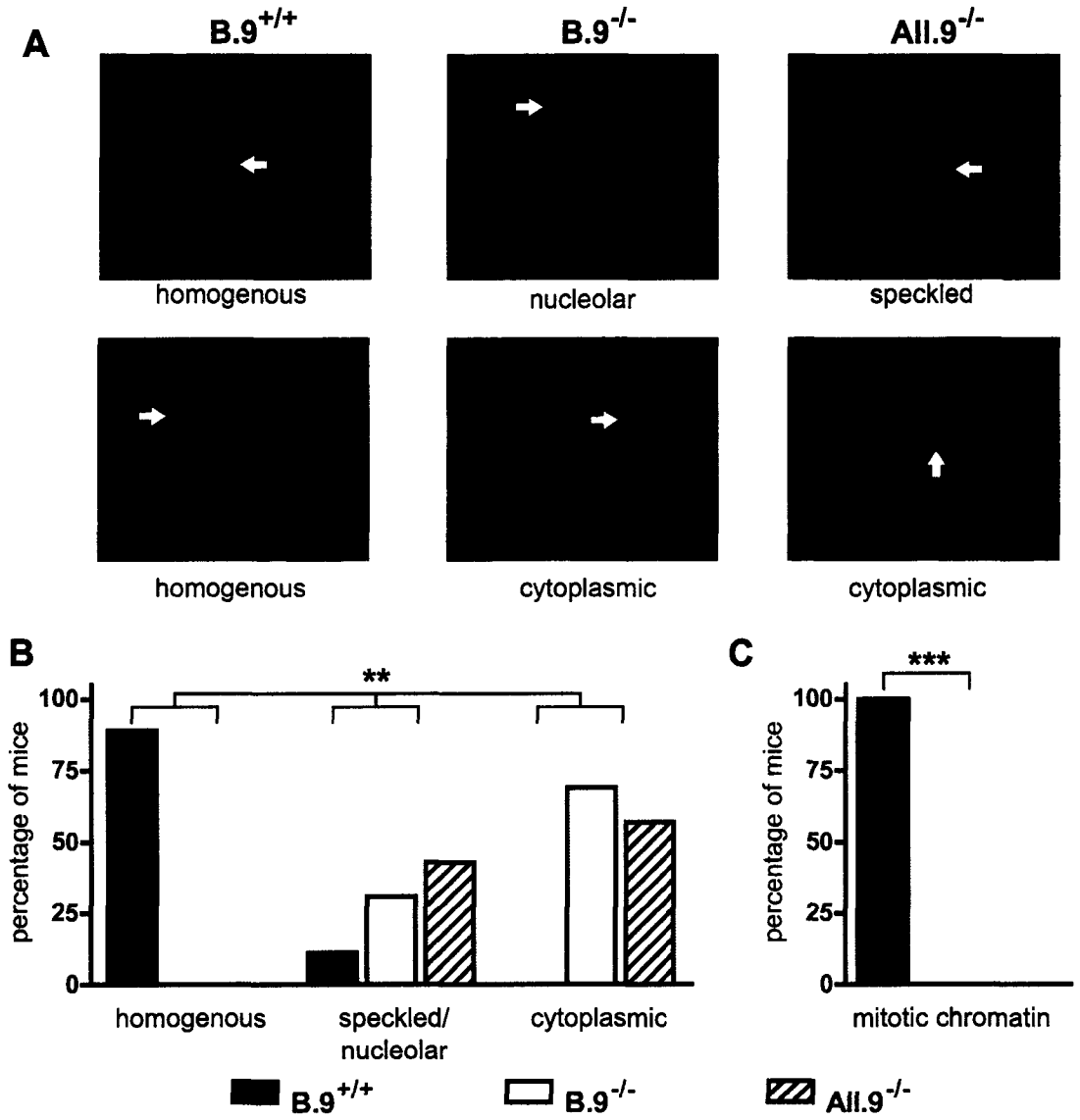

Figure 21. ANA patterns from chimeric mice reveal a B cell-intrinsic requirement for TLR9. (A) ANAs are shown for B.9$^{+/+}$ sera in left-most panels (upper and lower, homogenous nuclear pattern), for B.9$^{-/-}$ sera in middle panels (upper, nucleolar pattern; lower, cytoplasmic pattern), and for All.9$^{-/-}$ sera in right-most panels (upper, speckled nuclear pattern; lower, cytoplasmic pattern). White arrows indicate cells in metaphase that demonstrate positive (left-most panels, B.9$^{+/+}$) or negative (middle and right-most panels, B.9$^{-/-}$ and All.9$^{-/-}$) staining of mitotic chromatin. (B) Serum ANAs were classified as either nuclear homogenous, nuclear speckled and nucleolar, or cytoplasmic staining patterns. Black bars indicate B.9$^{+/+}$ sera (n = 9), white bars indicate B.9$^{-/-}$ sera (n = 13), and striped bars indicate All.9$^{-/-}$ sera (n = 7). (C) As in B, but serum ANAs were classified as either positive or negative for mitotic chromatin staining. **, $P < 0.01$ by Chi square analysis and ***, $P < 0.0001$ by Fisher's exact test for comparison of B.9$^{+/+}$ versus B.9$^{-/-}$ or All.9$^{-/-}$.

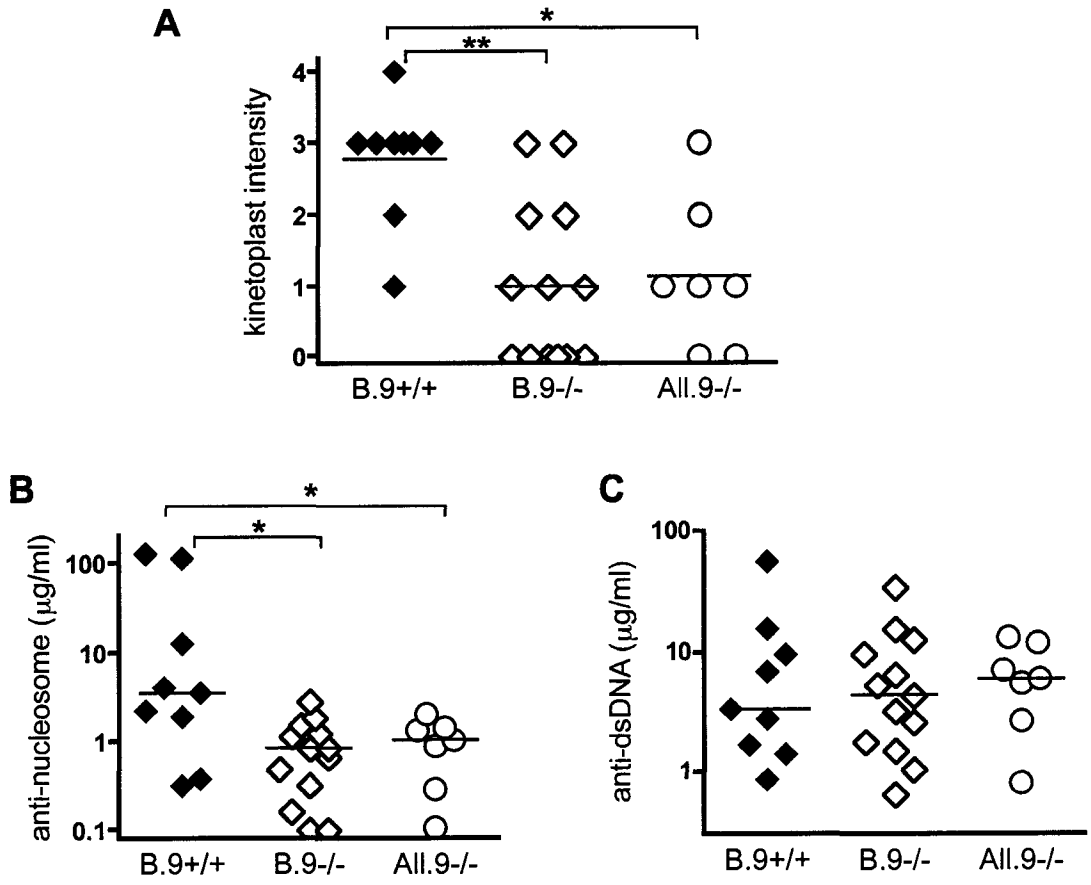

Figure 22. The requirement for TLR9 in the generation of autoantibodies to DNA-containing antigens is B cell-intrinsic. (A) Anti-dsDNA antibodies in B.9$^{+/+}$ (n = 9), B.9$^{-/-}$ (n = 13), and All.9$^{-/-}$ (n = 7) sera were detected by *Crithidia luciliae* immunofluorescence. Intensity of staining *C. luciliae* kinetoplast DNA was scored from 0-4. (B-C) Anti-nucleosome (B) or anti-dsDNA (C) antibodies were determined by ELISA in sera from chimeric mice. Bars represent mean (A) or median (B-C) values. *, $P < 0.05$; **, $P < 0.01$ by Mann-Whitney U test.

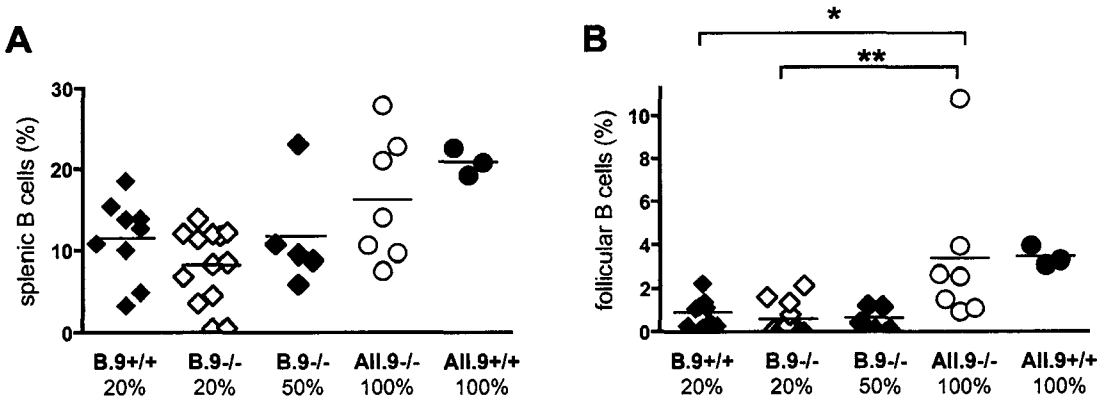

Figure 23. B cell reconstitution in chimeric mice. Total B cells ($CD22^+$, panel A) and follicular B cells ($CD22^+$ $CD23^+$ $CD21^{lo}$, panel B) were determined in spleens of $B.9^{+/+}$ (n = 9), $B.9^{-/-}$ 20% (n = 13), $B.9^{-/-}$ 50% (n = 5), $All.9^{-/-}$ (n = 7), and $All.9^{+/+}$ (n = 3) chimeric mice at 16 weeks post-reconstitution.
*, $P < 0.05$; **, $P < 0.01$ by Mann-Whitney U test.

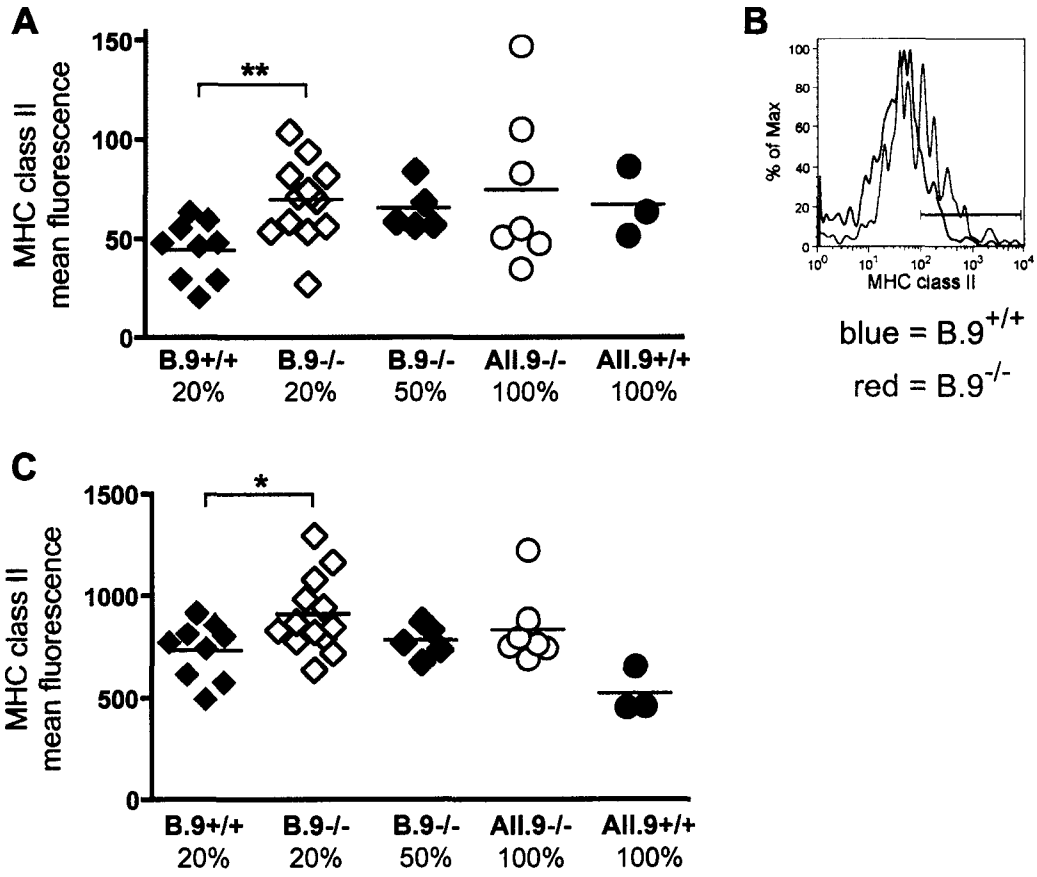

Figure 24. Dendritic cell activation may occur secondary to autoantibody production. (A) Expression of MHC class II was determined in plasmacytoid DCs from B.9$^{+/+}$ (n = 9), B.9$^{-/-}$ 20% (n = 13), B.9$^{-/-}$ 50% (n = 5), All.9$^{-/-}$ (n = 7), and All.9$^{+/+}$ (n = 3) chimeric mice. (B) Representative MHC class II expression on plasmacytoid DCs from B9$^{+/+}$ (blue line) and B.9$^{-/-}$ (red line) mice. (C) As in A, except that activation marker expression was determined in myeloid DCs. *, $P < 0.05$; **, $P < 0.01$ by Mann-Whitney U test.

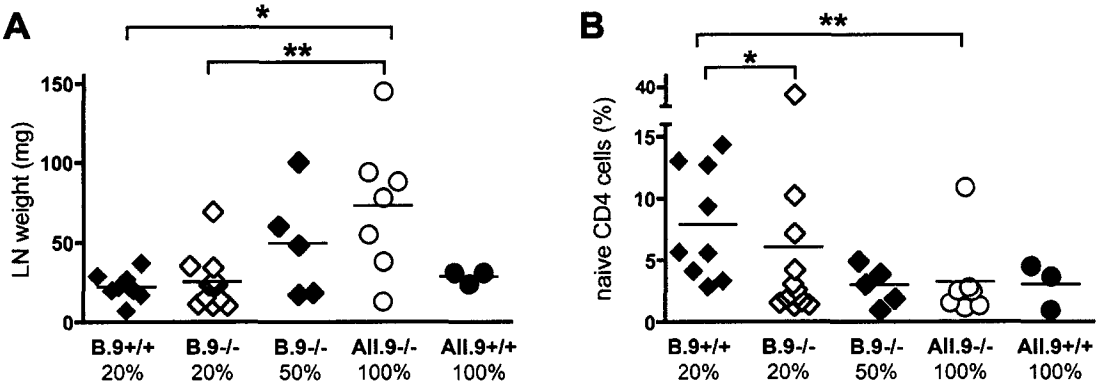

Figure 25. Lymphadenopathy and T cell activation in chimeric mice. $B.9^{+/+}$ (n = 9), $B.9^{-/-}$ 20% (n = 13), $B.9^{-/-}$ 50% (n = 5), $All.9^{-/-}$ (n = 7), and $All.9^{+/+}$ (n = 3) chimeric mice were analyzed at 16 weeks post-reconstitution. (A) Two largest axillary lymph nodes were removed and weighed. (B) Naïve phenotype ($CD62L^+$ $CD44^-$) $CD4^+$ T cells were determined as percentage of splenic $CD4^+$ cells. *, $P < 0.05$; **, $P < 0.01$ by Mann-Whitney U test.

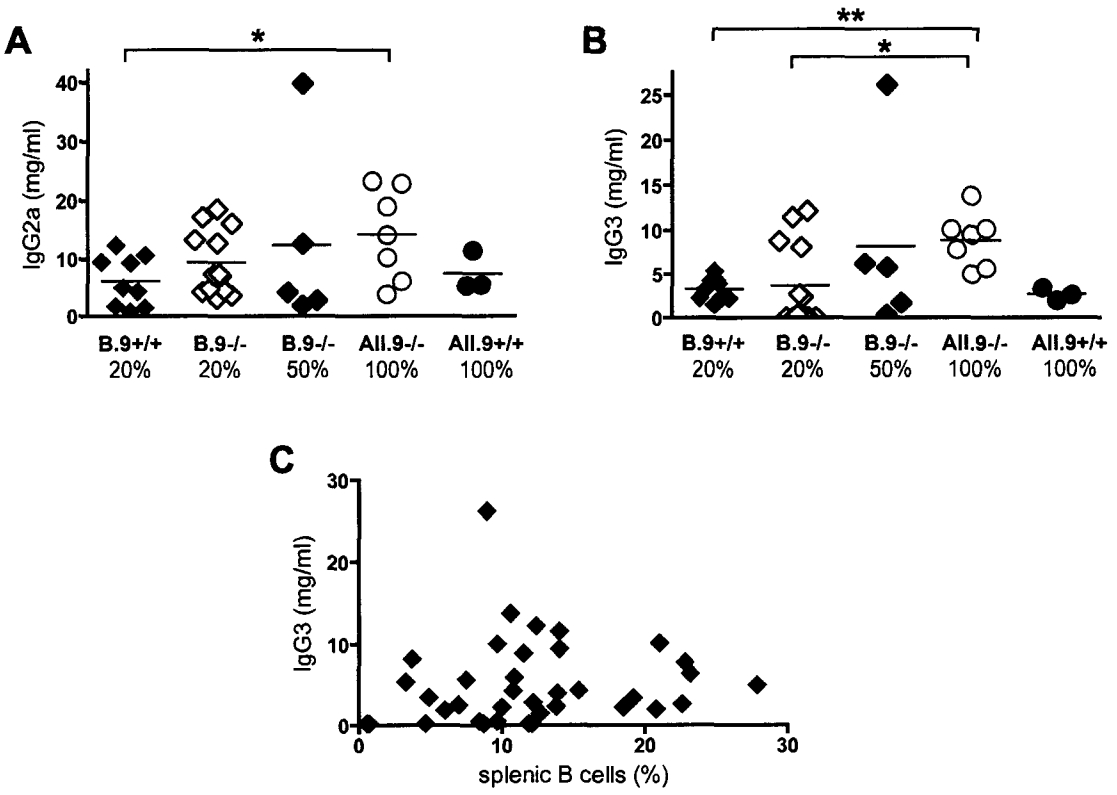

Figure 26. Absence of TLR9 on B cells is not sufficient to induce hypergammaglobulinemia in chimeric mice. Total serum IgG2a (A) and IgG3 (B) were determined at the time of sacrifice for B.9$^{+/+}$ (n = 9), B.9$^{-/-}$ 20% (n = 13), B.9$^{-/-}$ 50% (n = 5), All.9$^{-/-}$ (n = 7), and All.9$^{+/+}$ (n = 3) chimeric mice. (C) Serum IgG3 was not correlated with total splenic B cells for all chimeric mice (n = 37). *, $P < 0.05$; **, $P < 0.01$ by Mann-Whitney U test.

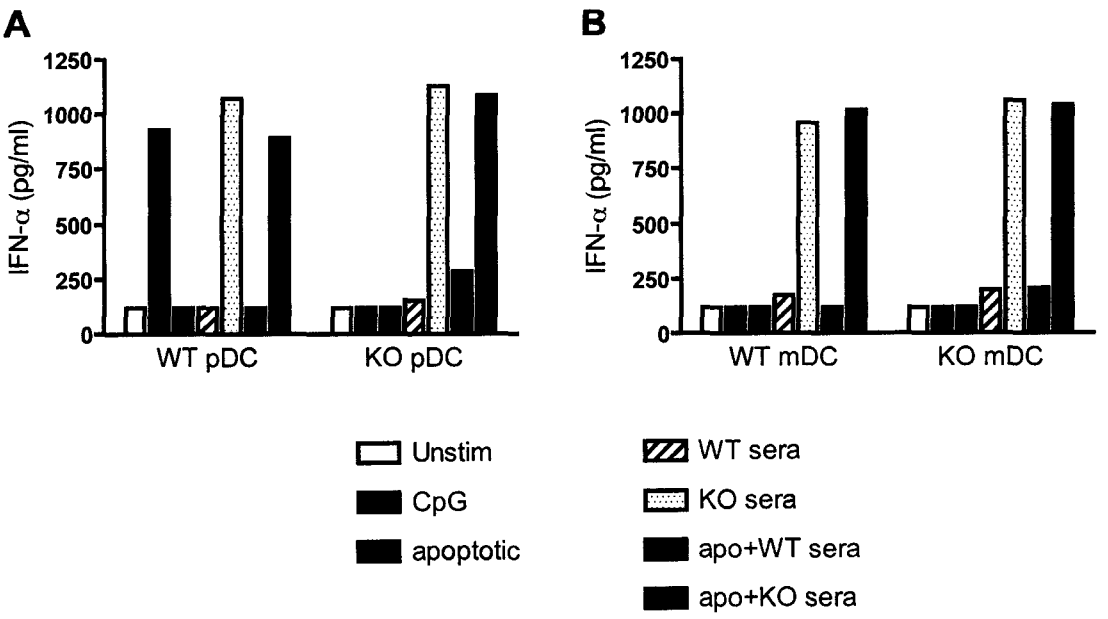

Figure 27. Serum from TLR9-deficient mice induces IFN-α production in dendritic cell subsets. Splenic plasmacytoid DC (pDC, panel A) or myeloid DC (mDC, panel B) were sorted from TLR9 WT or TLR9 KO mice and either unstimulated (white bars) or stimulated with C-type CpG (black bars), apoptotic thymocytes (gray bars), TLR9 WT sera alone (striped white bars), TLR9 KO sera alone (spotted white bars), TLR9 WT sera plus apoptotic thymocytes (striped gray bars), or TLR9 KO sera plus apoptotic thymocytes (spotted gray bars). Secreted IFN-α was measured after 24 hours. Data are representative of two separate experiments.

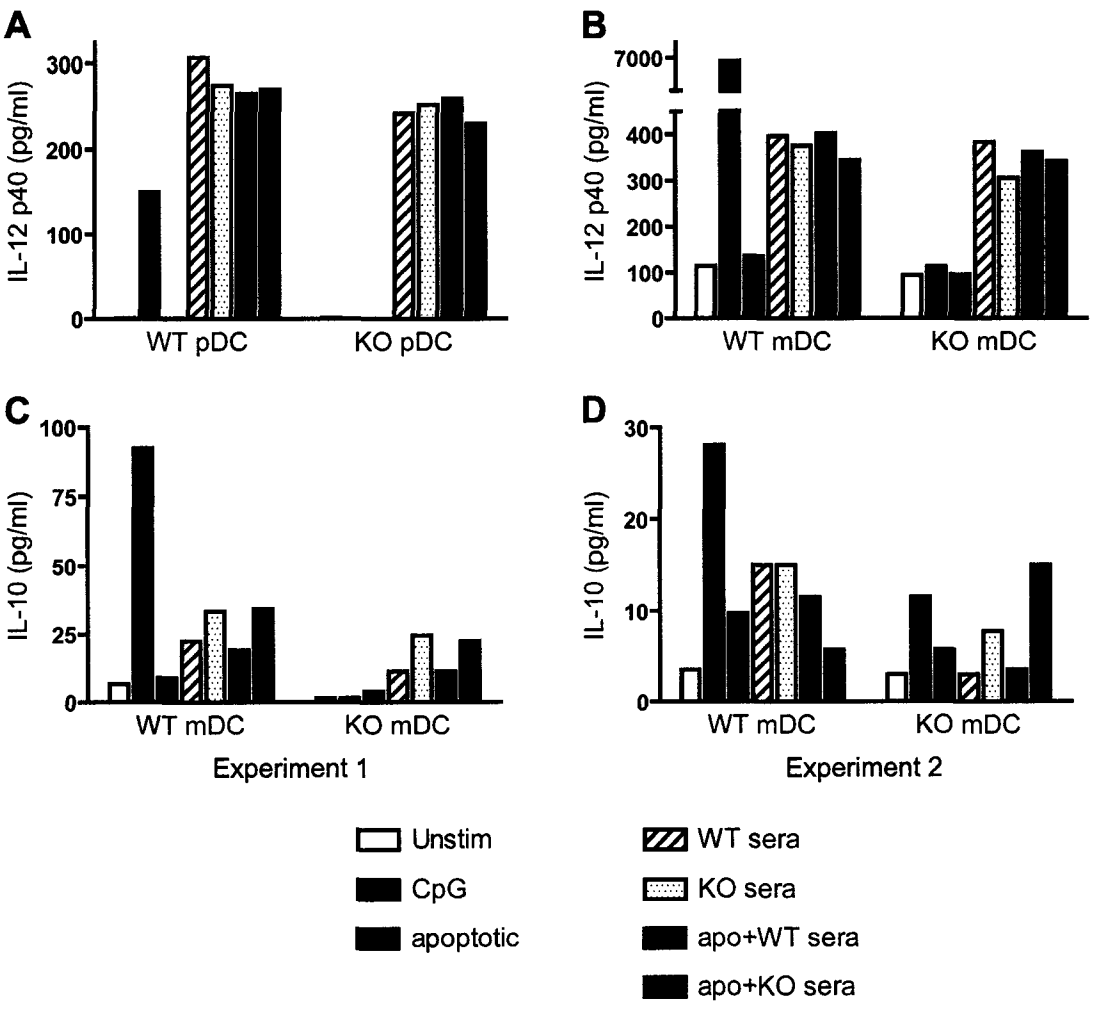

Figure 28. Effect of serum from wild-type or TLR9-deficient mice on cytokine production by dendritic cells. Splenic plasmacytoid DC (pDC, panel A) or myeloid DC (mDC, panels B-D) were sorted from TLR9 WT or TLR9 KO mice and either unstimulated (white bars) or stimulated with C-type CpG (black bars), apoptotic thymocytes (gray bars), TLR9 WT sera alone (striped white bars), TLR9 KO sera alone (spotted white bars), TLR9 WT sera plus apoptotic thymocytes (striped gray bars), or TLR9 KO sera plus apoptotic thymocytes (spotted gray bars). (A-B) Secreted IL-12 p40 was measured after 24 hours. Data are representative of two separate experiments. (C-D) Secreted IL-10 was measured after 24 hours. Each panel represents one experiment.

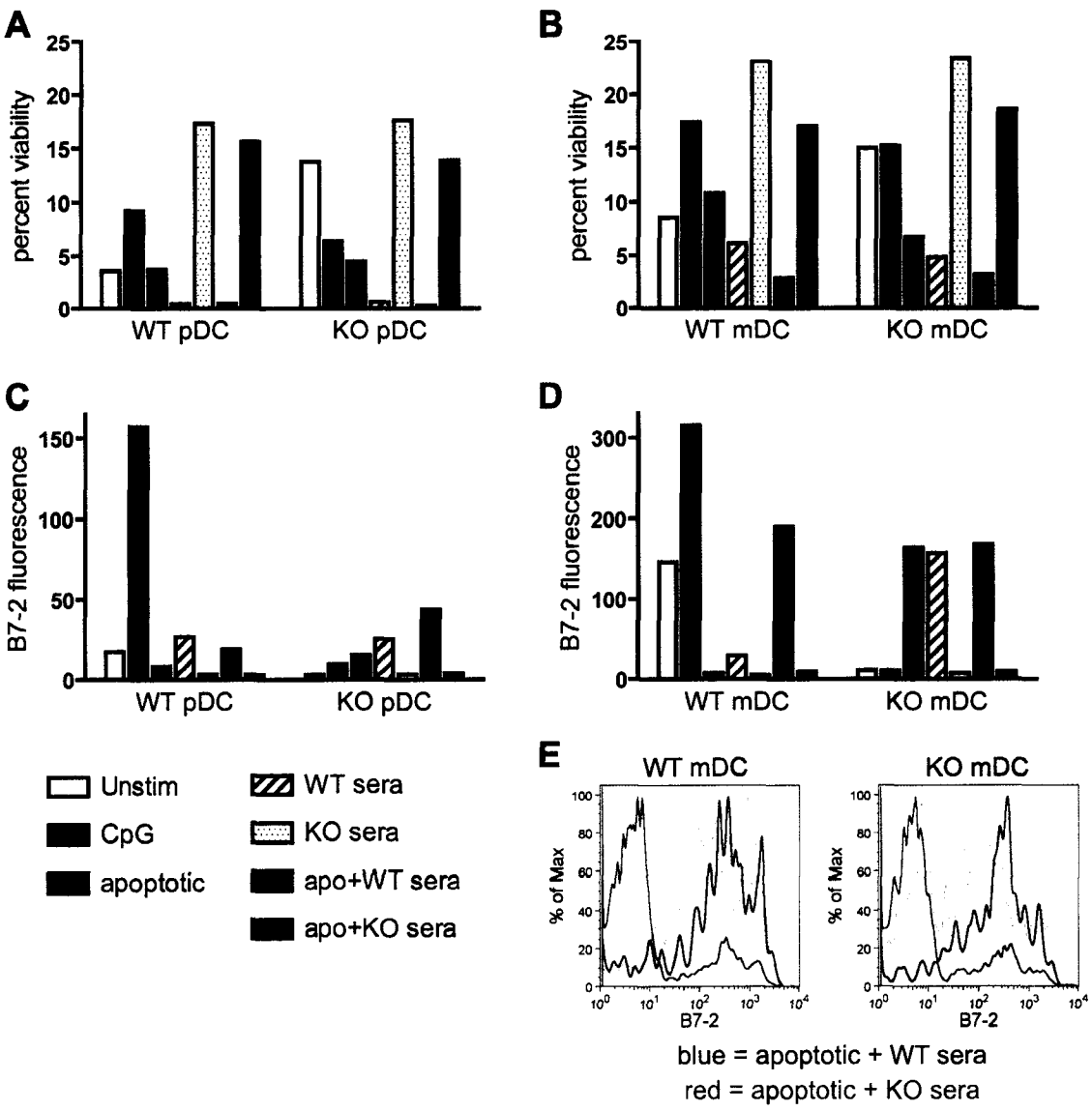

Figure 29. TLR9-deficient serum allows dendritic cells to persist in an immature state. Splenic plasmacytoid DC (pDC, panels A and C) or myeloid DC (mDC, panels B and D) were sorted from TLR9 WT or TLR9 KO mice and either unstimulated (white bars) or stimulated with C-type CpG (black bars), apoptotic thymocytes (gray bars), TLR9 WT sera alone (striped white bars), TLR9 KO sera alone (spotted white bars), TLR9 WT sera plus apoptotic thymocytes (striped gray bars), or TLR9 KO sera plus apoptotic thymocytes (spotted gray bars). Viability (A-B) and B7-2 expression (C-D) were measured after 24 hours. (E) Representative expression levels of B7-2 on WT mDC (left) or KO mDC (right) that were either unstimulated (filled histogram) or stimulated with TLR9 WT sera plus apoptotic thymocytes (blue line), or TLR9 KO sera plus apoptotic thymocytes (red line). Data are representative of two separate experiments.

Chapter 5: Role of TLR9 in Antigen-Specific B Cell Development, Activation and Differentiation

TLR9 is required for the generation of antibodies to DNA-containing antigens in a mouse model of SLE. Moreover, we have demonstrated that signaling through TLR9 must occur within B cells for effective anti-DNA antibody secretion. Yet the precise effect of TLR9 on the development, activation and differentiation of anti-DNA B cells remains unclear. For example, because stimulation with TLR9 ligands is a potent stimulator of antibody secretion and plasma cell differentiation *in vitro* (74, 99), we suspected that activation of TLR9 in anti-DNA B cells would primarily facilitate their differentiation into antibody-secreting cells. Equally plausible is that TLR9 stimulation could be responsible for the initial activation of otherwise anergic B cells, thus permitting the subsequent differentiation of these cells by other mechanisms. Finally, it is also possible that TLR9 directly affects the development of anti-DNA B cells. There is a clear threshold effect in the development of autoreactive B cells, such that high-affinity clones are edited or deleted, while low affinity clones are allowed to exist in the periphery in a partially inactivated or anergic state (78, 168-170). If TLR9 signaling can alter this threshold, or perhaps can rescue autoreactive cells from deletion, it is possible that low-affinity anti-DNA B cells may never escape to the periphery in $TLR9^{-/-}$ mice, and thus prevent anti-DNA antibody formation. Conversely, activation through TLR9 may facilitate the deletion of anti-DNA B cells during development, such that an excess of anergic autoreactive cells could exist in the periphery in $TLR9^{-/-}$ mice.

In order to establish the site of TLR9-mediated production of anti-DNA antibodies, we used established autoreactive BCR transgenic systems. To track the fate of anti-DNA B cells in the presence or absence of TLR9, we used the 3H9 BCR heavy chain transgene, which was initially cloned from an autoimmune MRL/Mp$^{lpr/lpr}$ mouse (171). This heavy chain can create a variety of anti-ssDNA and anti-dsDNA affinities when paired with endogenous kappa and lambda light chains (172, 173). To determine whether the effects of TLR9 on autoreactive B cell activation are specific for the anti-DNA specificity, we also studied B cells from anti-IgG rheumatoid factor transgenic mice. The AM14 heavy chain, also cloned from an autoimmune MRL/Mp$^{lpr/lpr}$ mouse (41), can create the rheumatoid factor anti-IgG2a^{a} specificity when paired with appropriate endogenous Vκ8 light chains (174). Although TLR9 is required *in vitro* for full activation of AM14 B cells by DNA-containing immune complexes (80, 81), these cells can also be stimulated by RNA-containing immune complexes in a TLR7-dependent fashion (82). The AM14 system thus allowed us to study the role of TLR9 *in vivo* in the activation of autoreactive B cells with a BCR specificity not restricted to DNA antigens.

Development and Central Tolerance of Anti-DNA B Cells are Unaffected by TLR9

Developing B cells expressing a BCR with high affinity for endogenous DNA are deleted at the pre-B to immature B cell transition in the bone marrow (170). A lower affinity reactivity to DNA allows developing B cells to exit the bone marrow and exist in the periphery in an inactive state in normal mice (168). Because endogenous light chains can create a wide range of affinity for DNA when paired with the 3H9 heavy chain (172, 173), many light chains are purged from the developing B cell repertoire of 3H9

transgenic mice by deletion and receptor editing. This results in a reduced peripheral B cell frequency and altered light chain repertoire, favoring light chains such as Vλ1 that support low DNA reactivity (175). Importantly, these central tolerance mechanisms appear to be intact in autoimmune-prone mouse strains such as MRL/Mp$^{lpr/lpr}$ (176, 177). To determine whether central tolerance of anti-DNA B cells is altered in the absence of TLR9, we analyzed peripheral B cell populations in TLR9 wild-type and TLR9-deficient 3H9 transgenic mice, as well in non-transgenic wild-type mice of the MRL/Mp$^{lpr/lpr}$ strain. We found that both 3H9 wild-type and TLR9$^{-/-}$ mice exhibited a significant reduction in splenic B cells compared to non-transgenic controls (Fig. 30A, P = 0.0159 for comparison of 3H9 wild-type or TLR9$^{-/-}$ versus non-transgenic). In addition, the frequency of λ1^{+} cells among splenic B cells was increased in both wild-type and TLR9-deficient 3H9 mice compared to non-transgenic controls (data not shown). Thus, these aspects of the central deletion of high-affinity anti-DNA clones (reduced peripheral B cells and shifted light chain repertoire) are not compromised by the absence of TLR9.

While low-affinity λ1^{+} anti-DNA B cells appear developmentally arrested in non-autoimmune mice, these cells assume a mature follicular phenotype and secrete anti-dsDNA antibody in lupus-prone MRL/Mp$^{lpr/lpr}$ mice (177). We determined whether TLR9 signaling played any role in the peripheral development of mature anti-DNA B cells in autoimmune 3H9 transgenic mice. We first observed that λ1^{+} B cells from both wild-type and TLR9$^{-/-}$ mice exhibited a 10-fold decrease in surface levels of λ1 compared to B cells from non-transgenic mice (Fig. 30B). This decreased expression of the BCR has been noted in multiple 3H9 strains, and has been associated with anergy due to prolonged exposure of the cells to specific antigen (177). Although λ1^{+} cells from 3H9

TLR9$^{-/-}$ mice had a slightly lower expression of surface λ1 than 3H9 wild-type (average λ1 MFI = 229.6 for wild-type and 170.8 for TLR9$^{-/-}$, P = 0.0079), it is unclear if this is functionally significant. We did observe a significant difference in peripheral B cell subsets in 3H9 wild-type and TLR9$^{-/-}$ mice, however. TLR9-deficient animals had more λ1^{+} cells of a mature, follicular phenotype (CD21^{lo} CD23^{+}) than wild-type controls (P = 0.0079), accompanied by a corresponding decrease in CD21^{lo} CD23^{-} cells in TLR9$^{-/-}$ mice (Fig. 30C-D). This double-negative population comprises both immature T1 B cells that have not yet acquired these developmental antigens (178), and activated B cells in MRL/Mp$^{lpr/lpr}$ mice that have lost expression of typical B cell markers (179). Examining other markers of immature B cells, we found that less than 5% of λ1^{+} cells in both 3H9 wild-type and TLR9$^{-/-}$ mice expressed the AA4.1 antigen, and that B220 expression was similar between wild-type and TLR9$^{-/-}$ mice (data not shown). Furthermore, many of the CD21^{lo} CD23^{-} cells expressed the activation marker CD44 (data not shown and Fig. 31, below), suggesting that these cells were a product of B cell activation rather than arrested development. Taken together, these data indicate that the absence of TLR9 does not prevent the peripheral maturation of anti-DNA B cells, and may even allow these cells to persist with a mature, follicular phenotype.

Peripheral Tolerance of Anti-DNA B Cells is Maintained in the Absence of TLR9

The lack of effect of TLR9 on central or peripheral development of anti-DNA B cells indicated that TLR9 primarily influenced the activation of mature peripheral B cells. We therefore used surface markers to examine the activation state of λ1^{+} anti-DNA B cells in 3H9 wild-type and TLR9$^{-/-}$ mice. We found that more than half of λ1^{+} cells in

3H9 wild-type mice expressed high levels of the activation marker CD44, and that nearly one fifth had maintained high CD44 expression while losing expression of CD22, an indication of differentiation into antibody-secreting plasmablasts (180). In contrast, the majority of $\lambda 1^+$ cells in TLR9$^{-/-}$ mice were of a naïve phenotype ($CD22^+$ $CD44^{lo}$), with fewer cells expressing CD44 and essentially no detectable plasmablasts (Fig. 31, A and D, P = 0.0079). The presence of some $CD44^{hi}$ $\lambda 1^+$ B cells in 3H9 TLR9$^{-/-}$ mice, along with the lack of $\lambda 1$ plasmablasts, suggests that the primary effect of TLR9 on anti-DNA B cell activation is in the transition from activated B cell to differentiated antibody-secreting cell. However, the decrease in $CD44^{hi}$ B cells, as well as the significant decrease in CD69 expression among TLR9$^{-/-}$ $\lambda 1^+$ cells (Fig. 31E, P = 0.0317) indicates that TLR9 may also play a role in the initial activation of anti-DNA B cells.

To verify the absence of anti-DNA antibody-secreting cells in 3H9 TLR9$^{-/-}$ mice, we assayed for additional markers of plasma cell differentiation. First, analysis of CD138 (Syndecan-1) in wild-type 3H9 mice confirmed that a subset of $CD22^-$ $\lambda 1^+$ cells in these mice expressed this highly specific marker of differentiated antibody-secreting cells (181). CD138 expression on $\lambda 1^+$ cells from 3H9 TLR9$^{-/-}$ mice, by comparison, was significantly decreased (Fig. 31, B and E, P = 0.0079). Similarly, staining for intracellular $\lambda 1$ revealed the presence of anti-DNA antibody-secreting cells in wild-type mice, while $\lambda 1^+$ cells with a high concentration of intracellular antibody were absent in TLR9$^{-/-}$ mice (Fig. 31, C and E, P = 0.0079). Finally, quantification of the number of anti-DNA antibody forming cells in the spleen demonstrated that while 3H9 wild-type mice generated a moderate to high frequency of $\lambda 1$-secreting cells, TLR9$^{-/-}$ mice exhibited a background level of $\lambda 1$ secretion that was similar to that in non-transgenic

mice (Fig. 32, $P < 0.0079$ for comparison of 3H9 wild-type versus TLR9$^{-/-}$). TLR9 thus had a profound effect on the differentiation of effective anti-DNA antibody secreting cells in 3H9 transgenic mice.

Splenic Localization of Anti-DNA B Cells in TLR9-Deficient Mice

Previous reports have indicated that one mechanism for maintaining tolerance of anti-DNA B cells is their exclusion from the B cell follicle: while anti-DNA B cells are clustered at the edges of the T cell zones in normal mice, they can be found within the B cell follicle in lupus-prone MRL/Mp$^{lpr/lpr}$ mice (177). In addition, the break in tolerance of anti-DNA B cells in otherwise normal mice of advanced age is coincident with the entry of these cells into the follicle (182). It is thus possible that the block in anti-DNA antibody secretion in TLR9$^{-/-}$ mice could be due to the exclusion of precursor B cells from follicular locations. However, splenic histology revealed that λ^+ cells were found throughout the B cell follicle in both 3H9 wild-type and TLR9$^{-/-}$ mice (Fig. 33A). Anti-DNA $\lambda1^+$ cells were generally not observed in the marginal zone of the spleen (Fig. 33A), a finding consistent with the low frequency of CD21^{hi} CD23$^-$ cells in both wild-type and TLR9$^{-/-}$ mice (Fig. 30C-D). Although autoreactive B cells can preferentially home to marginal zone compartments (183-185), low affinity anti-DNA B cells appear to be regulated by a different mechanism, at least in MRL/Mp$^{lpr/lpr}$ mice.

Following tolerance breakdown in autoimmunity, anti-DNA B cells appear to migrate into T cell zones of the spleen, where autoreactive antibody-secreting cells have been found to cluster (177, 186). Similarly, we observed the congregation of anti-DNA $\lambda1^+$ cells in the center of T cell-rich peri-arteriolar lymphoid sheaths (PALS) in the spleen

of 3H9 wild-type mice. These cells were also found in extrafollicular sites at T cell zone-red pulp border, and their intense intracellular λ1 staining was indicative of antibody-secreting cells (Figure 33B, left panel). Histologic identification of $\lambda1^+$ cells in $TLR9^{-/-}$ spleens revealed two important differences (Figure 33B, right panel). First, $\lambda1^+$ cells with intense cytoplasmic staining were exceptionally rare, indicating the absence of anti-DNA antibody-secreting cells in these mice. Second, the few $\lambda1^+$ cells found were individual cells residing at the edge of the PALS, as opposed to clusters of cells within the center of the T cell zone. The mechanism of TLR9-mediated anti-DNA antibody production thus appears to be distal to the entry of autoreactive B cells into splenic follicles, but proximal to the differentiation and accumulation of antibody-secreting cells in T cell zones of the spleen.

Rheumatoid Factor B Cell Activation Does Not Require TLR9 *In Vivo*

Our earlier studies of non-transgenic $TLR9^{-/-}$ mice revealed that despite the block in anti-DNA autoantibody production in these mice, antibodies to RNA-containing antigens were produced at comparable or higher levels than in wild-type controls (Chapter 3). The presence of elevated levels of IgG2a and IgG3 further indicated that there was not a global B cell defect imposed by the absence of TLR9. Nevertheless, it was important to determine whether TLR9 could have subtle effects on the activation or differentiation of autoreactive B cells with a BCR specificity not directly related to DNA or chromatin. For this we turned to the AM14 rheumatoid factor system, in which transgenic AM14 B cells break peripheral tolerance only in lupus-prone mice and only in the presence of their specific antigen $IgG2a^a$ (174). AM14 is particularly informative for

studying the role of TLR9 in B cell activation and antibody secretion, as it is a physiologic autoantibody associated with a clinical disease (rheumatoid arthritis), and AM14 B cells have been shown to be activated by TLR signaling. While TLR9 stimulation by chromatin-IgG immune complexes is one mechanism of AM14 activation *in vitro* and has been linked to spontaneous rheumatoid factor secretion *in vivo* (80, 81, 187), these cells can also be stimulated by complexes of IgG and RNA via TLR7 (82). The AM14 system thus allows us to study a population of autoreactive B cells wherein TLRs may be instrumental for effective activation, but TLR9 is not required per se.

Analogous to our study of 3H9 anti-DNA B cell activation, we determined activation marker expression by AM14 transgenic B cells from mice either sufficient or deficient for TLR9. In the majority of these experiments, $TLR9^{+/-}$ heterozygous mice were used as controls with intact TLR9 expression. A smaller group of $TLR9^{+/+}$ and $TLR9^{-/-}$ mice were also compared in separate experiments with identical results. Using CD22 and CD44 to define naïve, activated, and plasmablast B cell populations in $AM14^{+}$ cells, we found a high level of plasmablast differentiation in both TLR9 heterozygous and -deficient mice (Fig. 34, A and C). Not only did the absence of TLR9 not prevent the activation and differentiation of rheumatoid factor B cells, we also observed a significant increase in $AM14^{+}$ cells with an activated phenotype in $TLR9^{-/-}$ mice, along with a corresponding decrease in naïve cells (Fig. 34, A and C, $P = 0.0026$). Analysis of intracellular AM14 confirmed that the majority of $CD22^{-}$ $AM14^{+}$ cells in both groups of mice were antibody-secreting cells with high concentrations of intracellular rheumatoid factor (Fig. 34, B and D). Expression of similar levels of CD69, B7-1, and B7-2 activation markers in wild-type and $TLR9^{-/-}$ $AM14^{+}$ cells further indicated that there was

no defect in autoreactive rheumatoid factor B cell activation in the absence of TLR9 (data not shown).

Functional antibody secretion in AM14 transgenic mice was also determined, and again revealed no defect in the absence of TLR9. The numbers of splenic AM14 antibody-secreting cells were comparable in TLR9 heterozygous and -deficient mice, with both groups of mice exhibiting a wide range of AM14 activation indicative of the stochastic spontaneous rheumatoid factor response (Fig. 35A). We were also able to monitor the kinetics of AM14 activation in live mice using a serum ELISA to identify spontaneous AM14 "seroconversion" (presented in Chapter 6). TLR9-deficient mice did not exhibit any defect in either the magnitude of rheumatoid factor secretion or the kinetics of onset of autoimmunity in the AM14 system (Fig. 35B). In fact, there was a trend toward increased serum levels of AM14 in younger $TLR9^{-/-}$ mice, although this was not statistically significant. Thus neither the initial activation nor the terminal differentiation of AM14 rheumatoid factor B cells was inhibited in the absence of TLR9 *in vivo*.

Discussion

These experiments demonstrate that the ability to generate efficient anti-DNA antibody-secreting cells is blocked in the absence of TLR9, even with forced expression of an anti-DNA BCR transgene. Thus, the lack of antibodies to DNA-containing antigens in non-transgenic $TLR9^{-/-}$ mice is not simply due to a low precursor frequency, or the inability of these cells to compete for sparse survival or activation factors. We also discovered that TLR9 played no clear role in either the central or peripheral development

of anti-DNA B cells. Low-affinity anti-DNA B cells were able to progress to a mature, follicular phenotype in both wild-type and TLR9$^{-/-}$ mice, and the contracted peripheral B cell pool in 3H9 mice of both genotypes indicated that effective central deletion of high-affinity precursors had occurred. It is unclear whether TLR9 is expressed during B cell development, but our findings indicate that TLRs do not play a significant role in shaping the mature B cell repertoire. This could have important implications for the development of autoreactive B cells, suggesting that selection is primarily determined by the affinity of self ligands for the BCR, regardless of their costimulatory capacity.

In contrast to B cell development, the absence of TLR9 had a dramatic impact on the activation and differentiation of peripheral anti-DNA B cells, preventing the formation of antibody-secreting plasmablasts. It has been demonstrated that T cell help is a critical factor in breaking functional tolerance of 3H9 anti-DNA B cells, as provision of cognate CD4^{+} helper cells permits anti-DNA antibody secretion even in non-autoimmune mice (125). It is now clear that a fundamental requirement for TLR9 signaling also exists in these cells. The relationship between TLR-mediated and T cell-mediated costimulation of autoreactive B cells is not yet defined, but our data indicate that in the case of anti-DNA B cells, B cell-intrinsic TLR activation is a final checkpoint for plasmablast differentiation that cannot be overcome by other modes of stimulation. This concept is supported by the fact that while T-independent antibody responses can be mounted against appropriate antigens *in vivo* (188), inability to activate TLRs in B cells prevents effective antibody production (75). In addition to facilitating the differentiation of anti-DNA B cells into efficient producers of antibody, TLR9 also appeared to promote the early activation of these cells. TLR9 may therefore play a role in the initial activation

of otherwise anergic autoreactive B cells. This is an intriguing possibility in light of the demonstration that self-reactive anti-HEL B cells are resistant to TLR9-mediated activation due to tolerogenic signaling through the BCR (79). It is unclear whether anti-DNA B cells are regulated in the same manner, whether co-ligation of the BCR and TLR9 by the same antigen complex can overcome this regulation, or whether other factors such as T cell help are required for effective activation of autoreactive B cells.

Although TLR stimulation can promote the activation of autoreactive AM14 B cells *in vitro* (80, 82), we found that TLR9 was not required for the activation and differentiation of these cells in lupus-prone mice *in vivo*. The requirement for TLR9 in autoantibody production is therefore limited to cells expressing a BCR with appropriate specificity for DNA-containing antigens. In fact, we were surprised to discover that AM14 B cells from TLR9-deficient mice exhibited a level of activation even greater than TLR9-sufficient controls. There are at least three potential explanations for this finding. First, because AM14 B cells can be stimulated by RNA-containing immune complexes via TLR7 (82), and because such complexes appear to be more stimulatory for dendritic cell activation than DNA-containing complexes (Chapter 4), it is possible that TLR7 activation can explain the higher CD44 expression of AM14 B cells from $TLR9^{-/-}$ mice. Second, the increased DC activation and circulating IFN-α that exist in non-transgenic $TLR9^{-/-}$ mice (Chapter 3) could allow for a non-specific increase in the activation state of all B cells. This would then be a tertiary effect of TLR9 on global B cell activation, as production of IFN-α by pDCs appears to be a result of the altered autoantibody repertoire in $TLR9^{-/-}$ mice (Chapter 4). Finally, it is possible that TLR9 could exert a static inhibition of all B cells regardless of BCR specificity, although this possibility has not

been reported in the literature, and it conflicts with the clear stimulatory role of TLR9 in anti-DNA B cells.

Materials and Methods

Mice.

3H9 heavy chain transgenic mice (168) were crossed to TLR9-deficient mice to generate $3H9^{+}$ $TLR9^{-/-}$ and $3H9^{+}$ $TLR9^{+/+}$ strains maintained in separate breeding pairs. AM14 heavy chain transgenic mice (174) were crossed to TLR9-deficient mice to generate $AM14^{+}$ $TLR9^{+/-}$ mice, which were further crossed to $TLR9^{-/-}$ mice to produce $AM14^{+}$ $TLR9^{+/-}$ and $TLR9^{-/-}$ littermates for analysis. Additional experiments were also performed with $AM14^{+}$ $TLR9^{+/+}$ and $AM14^{+}$ $TLR9^{-/-}$ mice from separate breeding pairs. All mice were backcrossed at least 8 generations to $MRL/Mp^{lpr/lpr}$. 3H9 transgenic mice and non-transgenic controls were analyzed at 12 weeks of age. AM14 transgenic mice were analyzed for serum antibody beginning at 8-9 weeks of age, and sacrificed at 16-18 weeks of age.

Analysis of transgenic B cells and activation markers.

Spleen cells were isolated as previously described (Chapter 2). Anti-DNA $\lambda 1^{+}$ cells from 3H9 transgenic mice were identified with anti-$\lambda 1$ antibody (R11-153, BD Biosciences). Rheumatoid factor $AM14^{+}$ cells were identified with 4-44 anti-idiotype antibody produced in our laboratory. Antibodies for B cell activation and differentiation status were used as previously described, in addition to anti-CD21 (7G6), anti-CD23 (B3B4), anti-CD138 (281-2, anti-syndecan-1), and the AA4.1 monoclonal antibody, all obtained

from BD Biosciences. Intracellular λ1 was detected with anti-λ1 antibody (LS136.2) produced in our laboratory.

Quantification of antibody-secreting cells by ELISpot.

Polystyrene plates were coated with polyclonal goat anti-mouse IgM (Chemicon) and blocked with 1% BSA in PBS. Serial dilutions of splenocytes from 100,000 cells per well to 3,700 cells per well were added in media supplemented with 2.5% fetal calf serum (Gemini Bio-Products) and incubated for 5 hours at 37 degrees. Antibodies were detected with either biotin-conjugated R11-153 anti-λ1 antibody (for 3H9 anti-DNA) or biotin-conjugated 4-44 anti-idiotype antibody (for AM14 rheumatoid factor), followed by streptavidin-conjugated alkaline phosphatase (Molecular Probes). Development was performed with bromochloroindoyl phosphate (Amresco) in 0.5% agarose, and spots were counted using a dissecting microscope.

Spleen histology.

Frozen spleens mounted in Tissue-Tek O.C.T. (Sakura) were cut into 7μm sections and thaw-mounted onto positively-charged Superfrost/Plus slides (Fisher). Tissue was blocked with 1% BSA plus 10% rat serum in PBS/0.1% Tween-20, and stained with anti-λ1 (R11-153) or polyclonal goat anti-mouse total λ (Southern Biotech), and CD22.2 or Thy1.2 antibodies. Alkaline phosphatase was developed with naphthol AS-MX (Sigma) and Fast Blue BB Base (Sigma), and horseradish peroxidase was developed with 3-amino-9-ethylcarbazole (Sigma).

Serum AM14 ELISA.

Polystyrene plates were coated with polyclonal goat anti-mouse IgM (Chemicon), blocked with 1% BSA in PBS, and serial dilutions of serum from 1:100 to 1:2700 were

added. AM14 rheumatoid factor antibodies were detected with biotin-conjugated 4-44 anti-idiotype antibody and streptavidin-conjugated alkaline phosphatase (Molecular Probes), and absorbance at 405/630nm was determined. AM14 concentrations in serum were determined by comparison with a known concentration of antibody in supernatant from an AM14-transfected cell line.

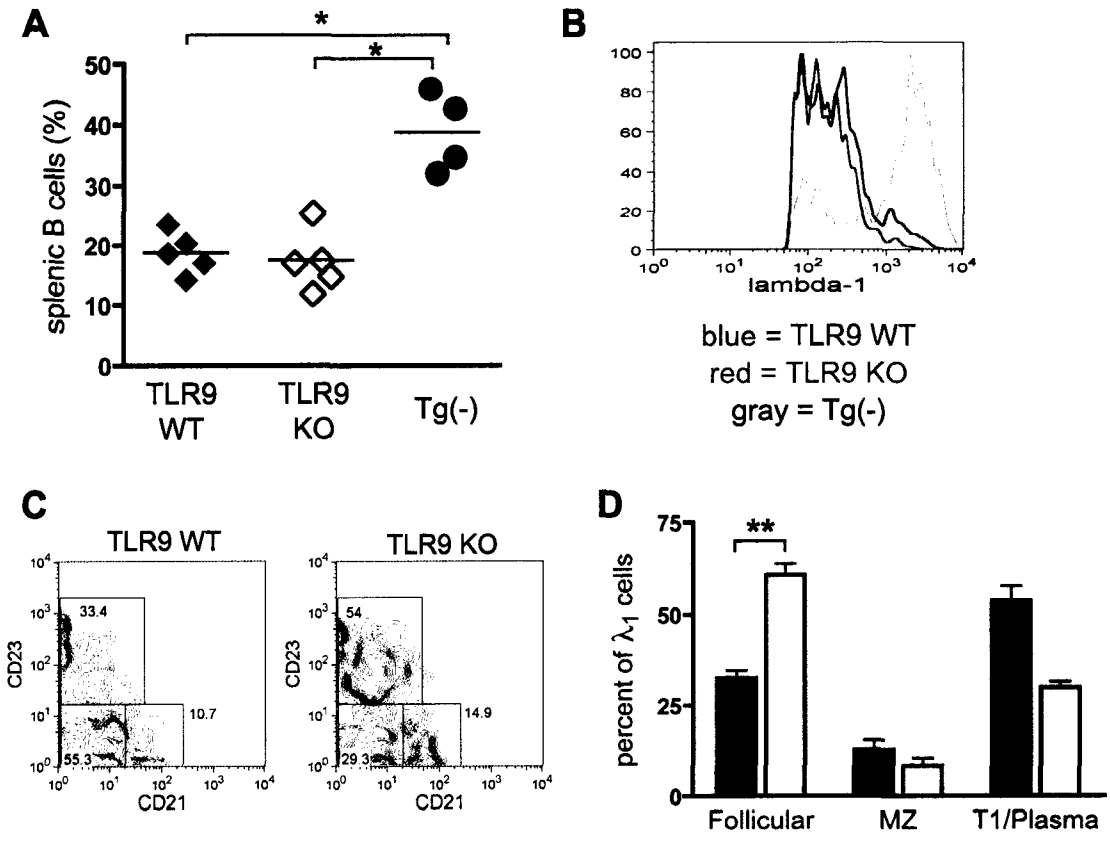

Figure 30. TLR9 does not affect the development of anti-DNA B cells.
(A) Splenic B cells ($CD22^+$) were determined in 3H9 transgenic TLR9 WT (n = 5) or TLR9 KO (n = 5) mice, and in non-transgenic Tg(-) mice (n = 4). (B) Surface expression of lambda-1 was determined in 3H9 TLR9 WT (blue line), 3H9 TLR9 KO (red line) and Tg(-) (filled histogram) mice. Cells shown are $\lambda1^+$ B cells. (C) Expression of CD21 and CD23 was determined on splenic $\lambda1^+$ cells from 3H9 TLR9 WT or TLR9 KO mice. (D) $\lambda1^+$ cells were classified as follicular ($CD21^{lo}$ $CD23^+$), marginal zone (MZ, $CD21^{hi}$ $CD23^-$), or T1/plasmablast phenotype ($CD21^{lo}$ $CD23^-$) for 3H9 TLR9 WT (black bars, n = 5) and 3H9 TLR9 KO (white bars, n = 5) mice. Data are presented as mean +/- SEM. *, $P < 0.05$; **, $P < 0.01$ by Mann-Whitney U test. Because subsets of $\lambda1^+$ cells are interdependent variables, statistical comparisons for one subset are indicative of whole distribution. Data are representative of 2 independent experiments.

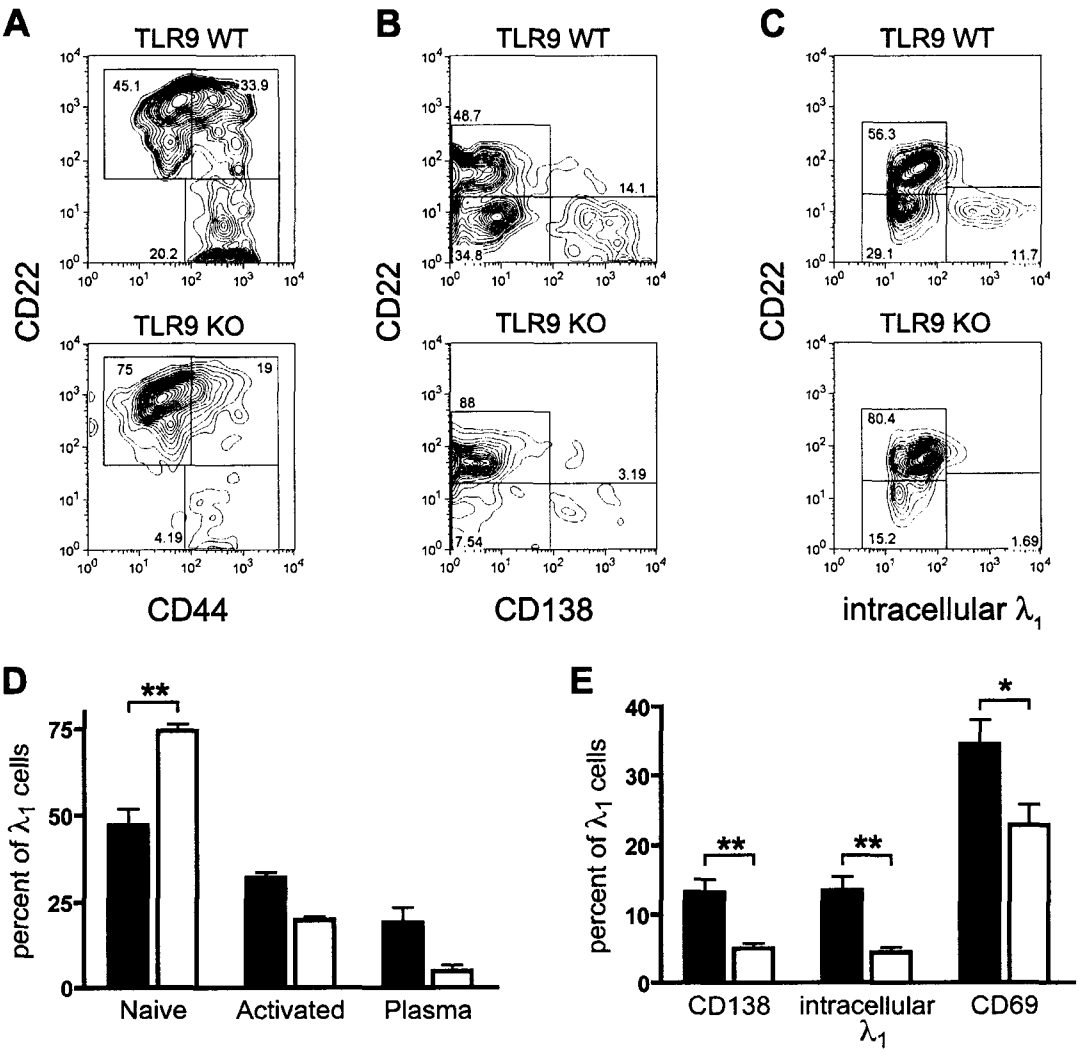

Figure 31. Activation and differentiation of anti-DNA B cells are abrogated in the absence of TLR9. (A-C) CD22 and CD44 (A), CD22 and CD138 (B), or CD22 and intracellular λ1 (C) expression were determined on $\lambda1^+$ cells from spleens of 3H9 TLR9 WT (upper plots) and 3H9 TLR9 KO (lower plots) mice. (D) $\lambda1^+$ cells from 3H9 TLR9 WT (black bars, n = 5) and 3H9 TLR9 KO (white bars, n = 5) mice were classified as naïve ($CD22^+$ $CD44^{lo}$), activated ($CD22^+$ $CD44^{hi}$), or plasmablast phenotype ($CD22^-$ $CD44^{hi}$) based on surface markers as in A. (E) Expression of CD138, intracellular λ1, or CD69 was determined on $\lambda1^+$ cells from 3H9 TLR9 WT (black bars, n = 5) and 3H9 TLR9 KO (white bars, n = 5) mice. Data are presented as mean +/- SEM. *, $P < 0.05$; **, $P < 0.01$ by Mann-Whitney U test. Because subsets of $\lambda1^+$ cells in panel D are interdependent variables, statistical comparisons for one subset are indicative of whole distribution. Data are representative of 2 independent experiments.

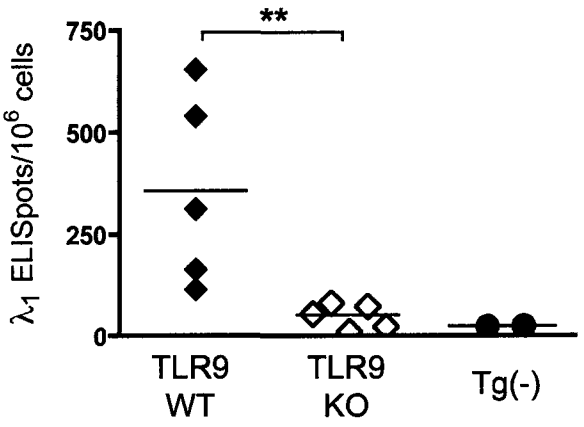

Figure 32. Absence of anti-DNA antibody-secreting cells in TLR9-deficient mice. IgM/λ1 antibody-secreting cells were determined in 3H9 TLR9 WT (n = 5), 3H9 TLR9 KO (n = 5), and non-transgenic Tg(-) (n = 2) mice. Data are presented as ELISpots per million splenocytes. **, $P < 0.01$ by Mann-Whitney U test. Data are representative of 2 independent experiments.

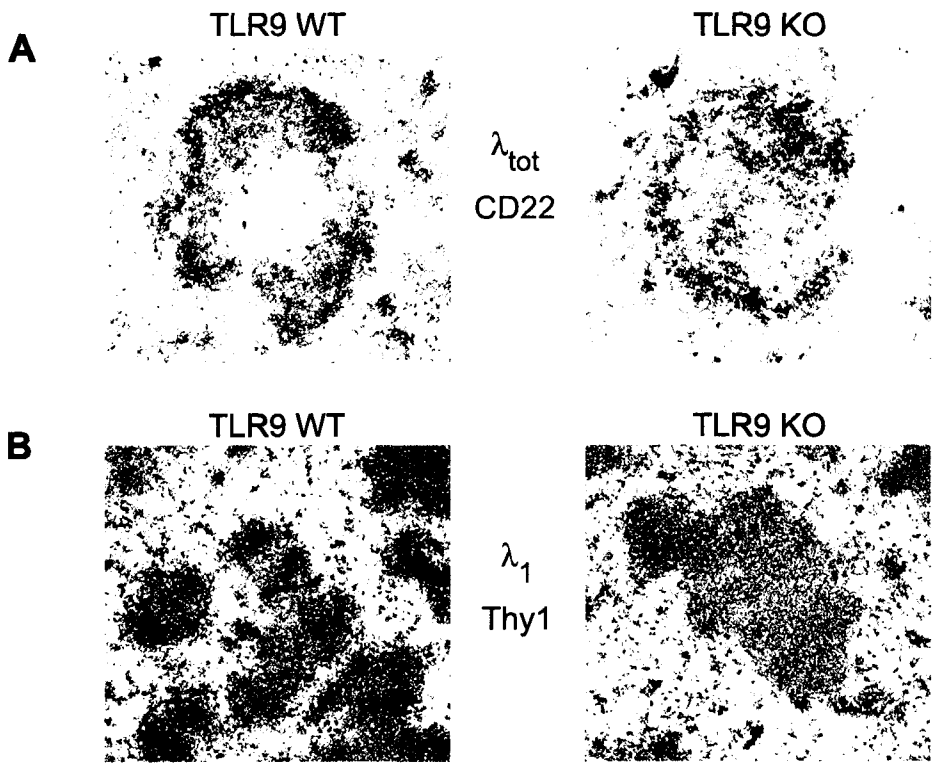

Figure 33. Localization of anti-DNA B cells in TLR9-deficient mice.
(A) Spleen sections from 3H9 TLR9 WT and 3H9 TLR9 KO mice were stained for total λ (blue) and B cell follicles (CD22, red). Anti-DNA λ^+ cells are observed within the B cell follicle in both TLR9 WT and TLR9 KO mice.
(B) As in A, except that sections were stained for λ1 (red) and T cell zones (Thy1, blue). Anti-DNA $\lambda1^+$ antibody-secreting cells accumulate and invade the T cell zone in TLR9 WT, but not TLR9 KO mice. Representative images are shown.

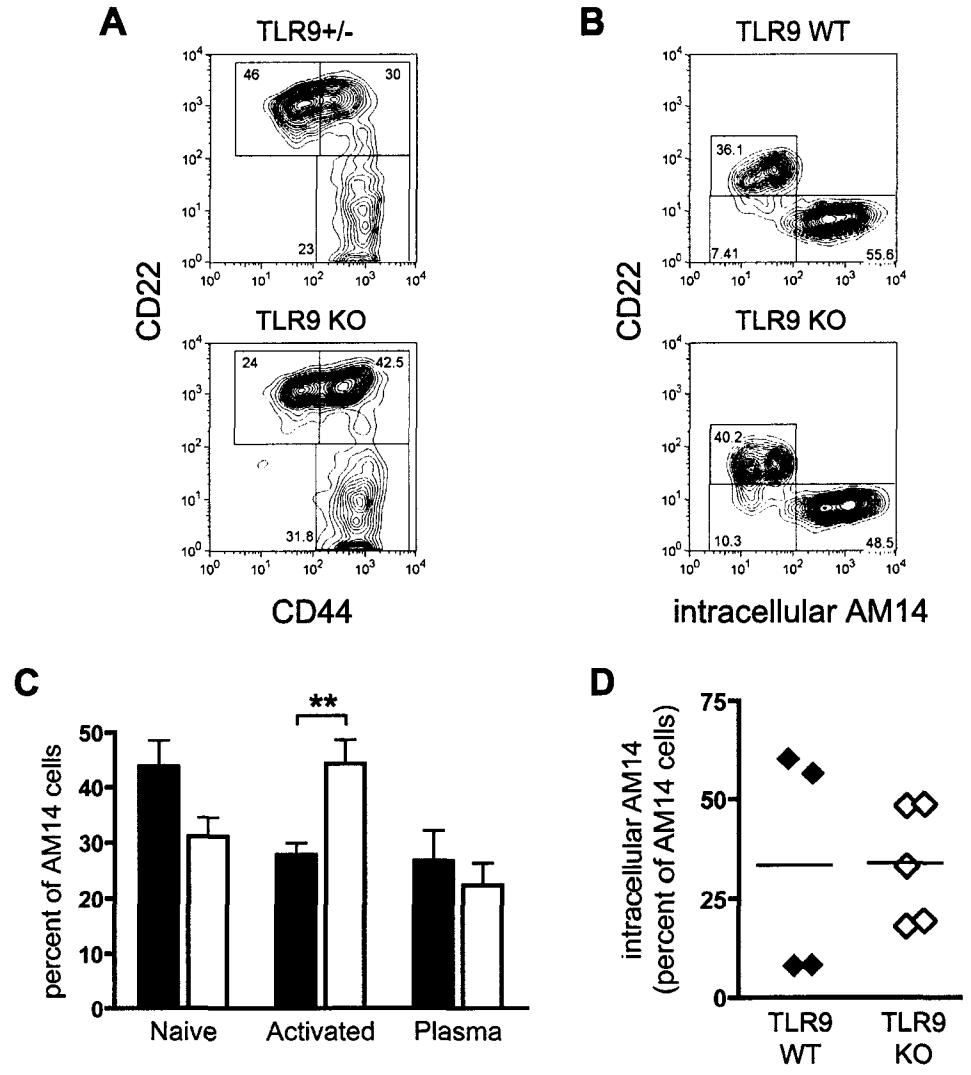

Figure 34. Activation and differentiation of rheumatoid factor B cells in the absence of TLR9. (A) CD22 and CD44 expression was determined on AM14$^+$ cells from spleens of AM14 TLR9$^{+/-}$ heterozygote (upper plot) and AM14 TLR9 KO (lower plot) mice. (B) CD22 and intracellular AM14 expression were determined on AM14$^+$ cells from spleens of AM14 TLR9 WT (upper plot) and AM14 TLR9 KO (lower plot) mice. (C) AM14$^+$ cells from AM14 TLR9$^{+/-}$ heterozygote (black bars, n = 11) and AM14 TLR9 KO (white bars, n = 13) mice were classified as naïve (CD22$^+$ CD44^{lo}), activated (CD22$^+$ CD44^{hi}), or plasmablast phenotype (CD22$^-$ CD44^{hi}) based on surface markers as in A. Data are presented as mean +/- SEM. (D) Expression of intracellular AM14 was determined in AM14$^+$ cells from AM14 TLR9 WT (n = 4) and AM14 TLR9 KO (n = 5) mice. Data in B and D are representative of 3 independent experiments. **, $P < 0.01$ by Mann-Whitney U test. Because subsets of AM14+ cells in panel C are interdependent variables, statistical comparisons for one subset are indicative of whole distribution.

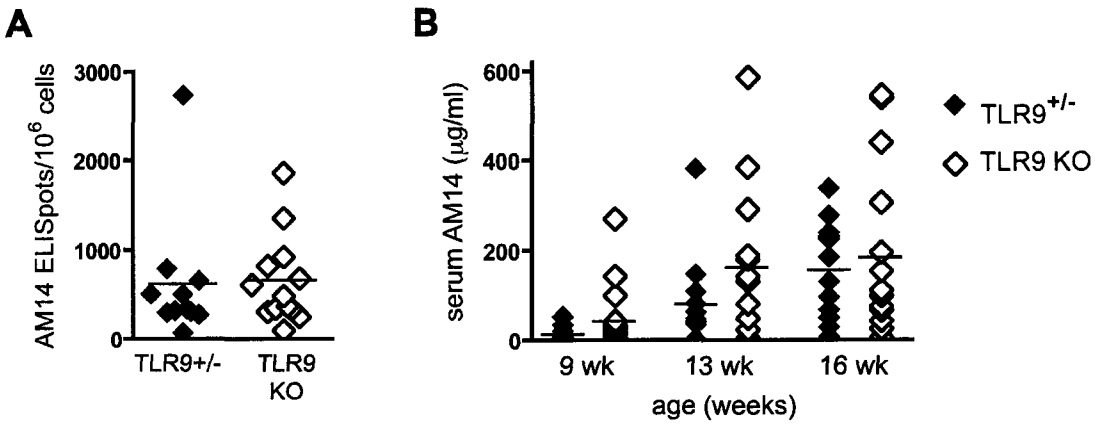

Figure 35. Secretion of rheumatoid factor antibody in the absence of TLR9. (A) AM14 IgM antibody secreting cells were determined in AM14 TLR9$^{+/-}$ heterozygote (n = 11) and AM14 TLR9 KO (n = 13) mice at 16 weeks of age. Data are presented as ELISpots per million splenocytes. (B) Serum AM14 IgM antibody was determined in AM14 TLR9$^{+/-}$ heterozygote (black diamonds, n = 11) and AM14 TLR9 KO (white diamonds, n = 13) mice at varying time points.

Chapter 6: Importance of T Cell Help in Autoreactive B Cell Activation

Our work has revealed that signaling through TLRs is a fundamental requirement for specific activation of autoreactive B cells in SLE. TLR activation alone, however, is unlikely to account for autoantibody production without additional costimulatory signals. Cognate interactions with $CD4^+$ helper T cells are required for effective autoantibody production in autoimmune disease (123, 124), and also appear to be critical for the initiation of autoimmunity in the 3H9 anti-DNA transgenic model (125). Whether continued T cell help is also required for the maintenance or propagation of autoantibody production, however, is unknown. We therefore used the AM14 rheumatoid factor transgenic system (174) to determine the requirements for $CD4^+$ T cells at specific stages of autoreactive B cell activation, after the autoimmune response had already been established.

After the initial activation and expansion of autoreactive B cells, downstream events include heavy chain class-switch to IgG isotypes, somatic hypermutation and affinity maturation of autoreactive clones (41, 189, 190), and the generation of long-lived plasma cells (191), or possibly autoreactive memory cells. Cognate T cell help may be a limiting factor for these potentially pathologic B cell activation pathways. The ability to analyze these later outcomes in antigen-specific autoreactive B cells is limited by the use of conventional transgenic systems. Expression of ectopically-integrated heavy chain transgenes in these B cells does not allow for class switch or somatic hypermutation, and may interfere with terminal plasma cell differentiation. We therefore created a site-directed transgenic animal, inserting the AM14 rheumatoid factor transgene into the

germline IgH locus. Analysis of B cell activation and differentiation in these mice will facilitate the analysis of secondary events in autoreactive B cell biology.

Functional Removal of T Cell Help After Initiation of an Autoimmune Response

Activation and differentiation of AM14 rheumatoid factor (anti-IgG2a^a) transgenic B cells into antibody-secreting plasmablasts occurs spontaneously in lupus-prone mice (174), while these cells do not differentiate or produce antibody in normal mice (192). Generation of AM14 antibody-secreting cells occurs in a stochastic, time-dependent manner in MRL/Mp$^{lpr/lpr}$ mice. Our lab has recently described the abrupt expansion of these cells in the spleen and peripheral blood between 10 and 20 weeks of age (187). We reasoned that activation of AM14 antibody-secreting cells could also be detected by an increase in circulating levels of AM14 IgM antibody. As expected, individual mice exhibited an age-dependent increase in serum AM14 antibody when followed over time (Chapter 5 and data not shown). We then compared serum levels of AM14 with expansion of splenic AM14 plasmablasts by ELISpot, and found that the level of AM14 antibody in terminal serum was a highly specific indicator of splenic plasmablast generation (Figure 36, $P < 0.0001$ for agreement of positive ELISA with positive ELISpot by Fisher's exact test). We were therefore able to track circulating AM14 antibody in live mice over time to identify the point at which the phenomenon of seroconversion occurred.

Depletion of helper T cells with the anti-CD4 monoclonal antibody GK1.5 has been demonstrated to reduce autoantibody secretion in both young and aged lupus-prone mice with established disease (121, 122). The specific consequences of this removal of T

cell help for antigen-specific B cells in an established autoimmune response remained unknown. We therefore used GK1.5 antibody to deplete $CD4^+$ T cells from autoimmune AM14 mice immediately following spontaneous seroconversion. As previously reported, however, $CD4^+$ T cells were resistant to depletion in mice with established disease (122). Treatment of $MRL/Mp^{lpr/lpr}$ mice with varying doses of GK1.5 over a two-week period produced only a 40% depletion of splenic $CD4^+$ T cells and 30% depletion of lymph node $CD4^+$ T cells, although removal of circulating T cells was more effective, with 70% depletion (Fig. 37A-C). Moreover, increasing the dose of administered GK1.5 did not improve depletion efficiency (Fig. 37A-C). Resistance to antibody-mediated depletion was an effect specific to lupus-prone mice, as equivalent or lesser doses of GK1.5 were sufficient to produce 90% depletion of splenic $CD4^+$ T cells and > 99% depletion of circulating $CD4^+$ T cells in BALB/c mice in only one week (data not shown).

Although GK1.5-treated autoimmune mice were not completely depleted of $CD4^+$ T cells, the residual T cells appeared functionally inhibited. There is precedent for a depletion-independent inhibitory effect of GK1.5, as treatment of lupus-prone mice with a non-depleting $F(ab')_2$ fragment of GK1.5 reduced disease to a comparable level as treatment with intact antibody (193). We observed a consistent, order of magnitude decrease in CD4 expression levels among residual T cells in GK1.5-treated mice (Fig. 37D). This effect represented an actual decrease in surface protein levels and was not a result of masking by bound GK1.5, as the RM4-4 antibody used for detection binds to a different epitope on CD4. Moreover, staining of $CD4^+$ cells with GK1.5 *ex vivo* revealed that all GK1.5 epitopes were blocked in treated mice, indicating that residual T cells were completely opsonized with GK1.5 (Fig. 37E). In addition, residual $CD4^+$ T cells were

enriched for naïve, unactivated cells: they expressed lower levels of CD69 (Fig. 37F), had a higher percentage of $CD62L^+$ $CD44^-$ cells (Fig. 37G, $P < 0.0001$), and had a lower level of BrdU incorporation over a 12-hour period (data not shown). These findings all indicated that remaining $CD4^+$ T cells in GK1.5-treated mice were ineffective at providing cognate help to B cells. To directly test this, we treated MRL/$Mp^{lpr/lpr}$ mice with GK1.5 for one week, then immunized with the hapten nitrophenyl (NP) conjugated to chicken gamma-globulin (CGG) and assayed for specific antibody production after an additional 10 days of GK1.5 treatment. Despite the incomplete depletion in these mice (42% reduction in splenic $CD4^+$ T cells, data not shown), treatment with GK1.5 completely inhibited the T-dependent IgG anti-NP response (Fig. 37H). Thus, even in the absence of complete depletion, treatment of lupus-prone mice with GK1.5 effectively eliminates T cell help for antibody-producing B cells.

Reduction in Autoantibody Production in the Absence of T Cell Help

We next determined whether the removal of T cell help with GK1.5 treatment had any effect on the expansion of AM14 antibody-secreting cells. Recently seroconverted AM14 mice were identified by circulating levels of AM14 antibody, and were treated for 2 weeks with either GK1.5 or control antibody. Determination of splenic AM14 plasmablasts by ELISpot then revealed a significant reduction in antibody-secreting cells in GK1.5-treated mice (Fig. 38A, $P = 0.04$). A similar reduction in serum AM14 antibody was also observed, despite the fact that both groups of mice had comparable levels of circulating antibody prior to treatment (Fig. 38B, $P = 0.0056$ for comparison of control versus GK1.5 after 2 weeks of treatment). Although several of the GK1.5-treated

mice had nearly complete reductions in AM14 antibody production, many of these animals maintained a moderate level of autoantibody secretion. To determine whether a more prolonged removal of T cell help would further reduce AM14 antibody production, we also treated a cohort of mice with GK1.5 or control antibody for 4 weeks, and again observed a reduction in splenic AM14 antibody-secreting cells (Fig. 38A, $P = 0.0052$). However, even after 4 weeks without functional $CD4^+$ T cell help, the GK1.5-treated mice had more antibody-producing cells than in age-matched mice that had not yet seroconverted (Fig. 38A, $P = 0.0006$). Examination of circulating AM14 antibody revealed that antibody production increased over time in control mice, but serum levels of AM14 stayed relatively constant in GK1.5-treated mice (Fig. 38C, $P = 0.0002$ for comparison of control versus GK1.5 after 4 weeks of treatment). Taken together, these data indicate that $CD4^+$ T cell help is required for efficient propagation of an established response, but a lower level of autoreactive B cell activation can be maintained in a T-independent manner.

Effects of T Cell Help on AM14 B Cells and Plasmablasts

To determine what effect the removal of T cell help had on autoreactive B cells at various stages of activation, we analyzed the expression of developmental and activation markers on $AM14^+$ B cells. Our lab has previously shown that the spontaneous AM14 response in lupus-prone mice is dominated by a population of rapidly-dividing plasmablasts that have lost expression of the B lineage marker CD22 and express increased levels of multiple activation markers (180). As expected from the decrease in antibody-secreting cells by ELISpot, we observed a marked reduction in $CD22^-$ AM14

plasmablasts in mice treated with GK1.5 (Fig. 39A). Although there was no decrease in the frequency of $CD22^+$ AM14 B cells, there was a decrease in activation marker expression by these cells, which was most prominent for the early activation marker CD69 (Fig. 39B-E, $P < 0.0001$ for CD69 expression). Expression of some activation markers by $CD22^-$ plasmablasts was not affected by the removal of T cell help, as AM14 plasmablasts from both GK1.5- and control antibody-treated mice expressed high levels of CD44 and CD69 (Fig. 39, B and D). We did observe a significant reduction in B7-1 expression in AM14 plasmablasts from GK1.5-treated mice ($P = 0.0142$), an effect that was not observed in $CD22^+$ AM14 B cells (Fig. 39, C and E). Thus, costimulation from $CD4^+$ T cells appeared to have different functional outcomes in $CD22^+$ B cells and $CD22^-$ plasmablasts.

The high level of activation marker expression by $CD22^-$ AM14 plasmablasts, even in the absence of T cell help, suggested that maintenance of these cells could occur in a T cell-independent manner. It was unclear whether the disappearance of these plasmablasts after GK1.5 treatment was due to direct inhibition of these cells or whether the formation of antibody-secreting cells from naïve $CD22^+$ precursors was blocked. To determine how these two autoreactive B cell subsets were affected by the removal of T cell help, we assessed 5-bromo-2'-deoxyuridine (BrdU) incorporation after a 12 hour labeling period. After two-week treatment with GK1.5, proliferation of both $CD22^+$ AM14 B cells and $CD22^-$ AM14 plasmablasts was reduced by approximately two-fold (Fig. 40, $P = 0.0142$ for $CD22^+$ and 0.0008 for $CD22^-$). Thus, the provision of $CD4^+$ T cell help is required for the continued proliferation of both $CD22^+$ autoreactive B cells and differentiated $CD22^-$ plasmablasts in an established autoimmune response. We also

examined the rate of cell death in these two populations of AM14 cells. An intrinsically high level of apoptosis was found in $CD22^-$ plasmablasts as previously demonstrated (180), but we observed no difference in the death rate between cells from GK1.5-treated or control mice (data not shown). Interestingly, the residual level of AM14 proliferation, both for $CD22^+$ and $CD22^-$ cells, was not further reduced after 4 weeks of GK1.5 treatment (Fig. 40). This again suggests the presence of T-independent mechanisms for maintenance of autoantibody production in SLE.

Splenic Localization of Residual Plasmablasts in the Absence of T Cell Help

We have previously shown that AM14 plasmablasts proliferate in extrafollicular locations in the spleen, clustering around bridging channels adjacent to T cell zones (180, 187, 189). We found that the functional removal of T cell help did not significantly alter the splenic localization of these cells. Although there were reduced numbers of cells with intense cytoplasmic staining for AM14 in mice treated with GK1.5, these smaller clusters of plasmablasts were still found primarily at the T zone-red pulp border. This was true in mice treated for a period of either 2 weeks (Fig. 41A) or 4 weeks (Fig. 41B). In fact, a greater invasion into the red pulp was observed in controls than in GK1.5-treated mice, in which AM14 cells were closely associated with T cell zones (Fig. 41A-B). It is likely that other factors besides interaction with T cells, such as chemokine gradients or cytokines produced by dendritic cells, are responsible for the selective retention of antibody-secreting cells at the edge of T cell zones in the spleen.

Inhibition of CD40L Does Not Reduce AM14 Plasmablasts

Stimulation by CD40L expressed on activated $CD4^+$ T cells has been shown to be a critical component of T cell help for cognate B cells (126, 127), and has also been demonstrated to facilitate autoantibody production in the context of autoimmunity (128). To determine whether T cell help for AM14 rheumatoid factor B cells was mediated by CD40L, we treated recently seroconverted mice with either MR-1 anti-CD40L antibody or control antibody for 2 weeks. Inhibition of CD40L with MR-1 *in vivo* has previously been shown to block the development of short-lived antibody-secreting cells in T-dependent immunization protocols (194). Unlike the analogous experiment with GK1.5, treatment of AM14 mice with MR-1 did not reduce AM14 antibody-secreting cells over a 2-week period (Fig. 42A). Analysis of AM14 cell subsets in these mice revealed that while inhibition of CD40L did significantly reduce CD69 expression among $CD22^+$ AM14 B cells ($P = 0.0159$), there was no effect on expression of CD44, CD69, or B7-1 among $CD22^-$ plasmablasts (Fig 42B and data not shown). This suggests that CD40L is critical for the early activation of autoreactive B cells, while other T cell derived factors may be more important for the maintenance of differentiated plasmablasts in an established response. Important caveats of these experiments, however, are that we have not verified the complete inhibition of CD40L with this treatment regimen, and that our group sizes were not large enough to detect a subtle effect on autoantibody production. It is thus possible that CD40L may contribute to the generation or maintenance of autoreactive plasmablasts, but it does not appear to be absolutely required, as suggested by the partial effect of genetic ablation of CD40L in $MRL/Mp^{lpr/lpr}$ mice (128).

Generation of AM14 Site-Directed Transgenic Mice

Analysis of AM14 activation and antibody secretion in the absence of T cell help revealed that different aspects of the autoreactive B cell response could be differentially stimulated by T cell-derived factors. It is thus probable that downstream events in B cell activation such as somatic hypermutation, class-switching, and long-lived plasma cell or memory formation could also require costimulation from $CD4^+$ T cells. In order to study these later stages of B cell activation in the AM14 model, we created an AM14 site-directed transgenic (AM14-sdTg), in which the rearranged VDJ gene segments of the AM14 heavy chain were inserted into the J_H region of the germline immunoglobulin heavy chain (IgH) locus. The presence of upstream V_H and D_H gene segments in site-directed BCR transgenes renders them particularly susceptible to RAG-mediated V_H replacement during B cell development. This process of gene replacement occurs as upstream V_H or D_H gene segments undergo recombination signal sequence (RSS)-mediated recombination with an internal heptamer in the 3' coding region of the inserted transgene (195). In the AM14-sdTg, recombination could potentially occur with this internal heptamer found in the V_H J558 gene segment, or with the 5' heptamer from the J_H4 gene segment, since AM14 is rearranged to J_H3 (Figure 43A). We therefore mutated the heptamers of these two RSS in order to improve stability of the transgene during B cell development. The J_H4 heptamer was mutated from 5'-CACAATA (on the antisense strand) to 5'-TGCAATA, and the internal heptamer was mutated from 5'-CACAATA (on the antisense strand) to 5'-CTCAATA. Mutation of the internal heptamer was a silent mutation that did not alter the protein sequence of the transgene.

We then transfected the AM14-sdTg targeting construct into murine embryonic stem (ES) cells and screened for homologous recombination of the transgene into the germline IgH locus (Fig. 43A). Initial screening was done by PCR amplification of a region spanning the 1.2 kb of 5' overlap between the targeting construct and the germline locus (black arrows in Fig. 43A). Of 223 independent ES clones screened, three were PCR-positive for correct upstream integration. Genomic DNA from these three clones was digested with EcoRI and hybridized to a J_H4 probe by Southern blot. A 6.2 kb band corresponding to the native germline IgH locus was seen in all three clones, and a 9.4 kb band corresponding to the correct integration of the transgene was observed in only one clone (Fig. 43B). This ES cell clone was then injected into blastocysts, which were transferred into pseudopregnant female mice. Breeding of chimeric offspring resulted in transmission of the AM14-sdTg transgene to progeny mice in Mendelian ratios.

Expression of the AM14 rheumatoid factor idiotype was confirmed in AM14-sdTg mice after one backcross generation to Fas-intact MRL/Mp mice. Approximately 3-4% of splenocytes expressed the AM14 idiotype created by pairing of the AM14-sdTg heavy chain with appropriate endogenous light chains, and expression was restricted to $CD22^+$ B cells (Fig. 44A). Expression was also found in less than 1% of bone marrow cells, and was restricted to $B220^{hi}$ B cells (Fig. 44B). Significant expression of the AM14 idiotype was not observed in spleen or bone marrow of non-transgenic mice (Fig. 44A-B). The majority of splenic $AM14^+$ cells in AM14-sdTg mice were IgM^{lo} IgD^{hi}, indicative of a mature, follicular phenotype (Fig. 44C). Expression of high levels of CD23 and lower levels of CD21 on most $AM14^+$ cells also indicated a follicular phenotype (Fig. 44C). Approximately 10-15% of splenic $AM14^+$ cells in AM14-sdTg

mice exhibited a marginal zone B cell phenotype (IgM^{hi} IgD^{lo} $CD21^{hi}$ $CD23^{lo}$, Fig. 44C). These findings indicate that the AM14-sdTg is expressed appropriately during B cell development, allowing normal expression of IgM and IgD, and favoring development towards follicular phenotype peripheral B cells.

Production of IgG Rheumatoid Factor Antibodies in AM14-sdTg Mice

We next determined whether spontaneous activation and antibody production by AM14-sdTg B cells could occur in lupus-prone mice. AM14-sdTg mice were backcrossed seven generations to $MRL/Mp^{lpr/lpr}$ mice, and AM14 antibody-secreting cells in the spleen were identified after 21 weeks, an age at which nearly all conventional AM14-transgenic $MRL/Mp^{lpr/lpr}$ mice have undergone spontaneous seroconversion (187). We found that aged AM14-sdTg mice harbored AM14 antibody-secreting cells of IgM, IgG2a, and IgG2b + IgG3 isotypes (Fig. 45A). All three isotypes were significantly increased relative to 7 week-old mice, indicating that spontaneous production of rheumatoid factor antibody is an age-dependent phenomenon (Fig. 45A, $P = 0.0041$ for IgM, 0.0095 for IgG2a, and 0.0035 for IgG2b + IgG3). The presence of antibody-secreting cells of multiple isotypes indicates that AM14-sdTg B cells can indeed class switch to IgG isotypes in the context of autoimmunity. Moreover, there appeared to be either a selective expansion or a more effective generation of IgG-producing cells, as aged mice produced more AM14 antibody-secreting cells of IgG2b + IgG3 isotype than IgM isotype (Fig. 45A, $P = 0.0327$). Analysis of circulating IgG AM14 antibody confirmed the age-dependent expansion of class-switched AM14 cells, with a significant increase in serum AM14 from an age of < 12 weeks to an age of 15 weeks (Figure 45B, P

= 0.0004). An age-dependent increase in circulating IgM AM14 antibody was not observed, with both young and old mice producing generally low levels of IgM AM14 (< 10 μg/ml, data not shown).

Finally, we determined whether the spontaneous activation of AM14-sdTg cells produced a population of antibody-secreting plasmablasts analogous to those observed in AM14 conventional transgenic mice (180). Surprisingly, even in mice with high levels of AM14 antibody-secreting cells by ELISpot, we found very few cells with the typical plasmablast phenotype: surface $AM14^+$ $CD22^-$ (Figure 46A). This was in contrast to staining for intracellular antibody, which revealed an expansion of intracellular $AM14^+$ $CD22^-$ cells in seroconverted mice (Figure 46B). Suspecting that the antibody-secreting cells in AM14-sdTg mice had lost surface expression of the BCR, we then compared expression of surface AM14 with intracellular AM14. This confirmed that the majority of intracellular $AM14^+$ cells in these mice were indeed surface $AM14^-$ (Figure 46C). This was in contrast to antibody-secreting cells from AM14 conventional transgenic mice, which were predominantly intracellular $AM14^+$ and surface $AM14^+$ (Figure 46D). Thus, antibody-secreting cells from AM14-sdTg mice exhibit a different phenotype than the previously described AM14 plasmablasts in conventional transgenic mice (180, 187, 189), and may represent a more complete transition to terminally-differentiated plasma cells. It is unclear whether the ability to switch to IgG isotype production is directly responsible for this difference, although we were able to identify IgG2a-expressing surface $AM14^+$ cells in these mice (data not shown).

Discussion

We have shown that even after the initiation of a robust autoantibody response, $CD4^+$ helper T cells are still required for the efficient propagation of that response. Within as little as two weeks, the number of rheumatoid factor-producing cells in the spleen decreased by nearly three-fold in GK1.5-treated mice compared to controls. T cells played important roles in multiple stages of autoreactive B cell activation, as they were required both for the early activation of B cells and to maintain a high level of proliferation among differentiated plasmablasts. Nevertheless, a low but significant level of autoantibody-secreting cells was maintained for as long as four weeks in the absence of T cell help. The fact that splenic plasmablasts, serum AM14 antibody, and AM14 proliferation rates did not further decrease from 2 to 4 weeks indicates that this T cell-independent maintenance of antibody secretion is stable over time. We suspect that TLR stimulation is the driving force for T-independent autoantibody production, as AM14 B cells can be activated by both TLR9 and TLR7 (82), and we have shown that TLR9 activation is required for the efficient generation of anti-DNA antibody-secreting cells *in vivo* (Chapter 5). Dendritic cell-derived factors may also be important, such as IFN-I (97-99) or the B cell activating factor BAFF (119). The restricted location of AM14 plasmablasts at defined sites in the spleen—even in the absence of $CD4^+$ T cell help—suggests that cell types such as DCs could be involved in the maintenance of autoantibody-producing cells in SLE.

In addition to facilitating the expansion of autoreactive plasmablasts, T cells are likely to be required for subsequent stages of B cell differentiation, including antibody class switch and the generation of long-lived plasma cells or memory cells. To allow

study of these downstream events, we have created a rheumatoid factor site-directed transgenic model, AM14-sdTg. Like conventional AM14 transgenic mice, AM14-sdTg mice do not exhibit any defect in B cell development, and also experience an age-dependent expansion of rheumatoid factor-secreting cells in the spleen. Importantly, the ability of AM14-sdTg B cells to class switch was demonstrated by the fact that the majority of antibody-secreting cells in aged mice produced IgG isotypes. We observed a different phenotype of antibody-producing cells in AM14-sdTg mice than that described previously for conventional AM14 transgenics (180), as very few of these cells in AM14-sdTg mice expressed detectable surface AM14. Because most antibody-secreting cells from AM14-sdTg mice were class-switched to IgG, it is possible that the inability to class switch to IgG in conventional transgenic mice prevents IgM-producing plasmablasts from fully differentiating to surface Ig-negative plasma cells. This could have important implications for the lifespan of these cells and the durability of autoantibody production. The AM14-sdTg will therefore be an important tool to study the generation of antigen-specific, long-lived plasma cells and memory B cells in autoimmunity.

Materials and Methods

Transgenic Mice.

AM14 heavy chain conventional transgenic mice (174) were backcrossed at least 12 generations to MRL/Mp$^{lpr/lpr}$ mice. All seroconverted mice used for depletion of CD4$^+$ T cells were between 10-20 weeks of age.

AM14-sdTg mice were created as described above, in consultation with the Animal Genomics Gene Targeting Service at Yale University. The targeting construct

was created from the original AM14 conventional transgene, except that a 1.2 kb region of homology to the germline D_H region was added at the 5' terminus and a thymidine kinase cassette was added at the 3' terminus. Mutagenesis of RSS heptamers was performed with the Quick-Change Site-Directed Mutagenesis Kit (Stratagene) according to the manufacturer's instructions. PCR screening of transfected ES cell clones was performed with primers within the germline D_H region (5' ATC TAC ATA GCT AGA GAG CTA GAG G 3') and the neomycin resistance cassette (5' GCA TCG CAT TGT CTG AGT AGG TGT CA 3'). Southern blotting of EcoRI digests of genomic ES cell DNA was performed with radiolabeled J_H4 probe. The 1.6 kb HindIII-EcoRI fragment from the targeting construct was labeled with ^{32}P-dCTP (Amersham), using the Random-Primed DNA Labeling Kit (Roche) according to the manufacturer's instructions. Chimeric pups derived from blastocyst injection of ES cells were first bred to Fas-intact MRL/Mp mice to confirm germline transmission of the AM14-sdTg transgene. Mice were then backcrossed 7 generations to Fas-deficient MRL/Mp$^{lpr/lpr}$ mice for analysis of seroconversion.

Depletion of $CD4^+$ T cells and inhibition of CD40L.

$CD4^+$ T cells were depleted with GK1.5 anti-CD4 monoclonal antibody, either produced in our laboratory or in a bioreactor system at the Iowa State University Hybridoma Facility. Hybridoma culture supernatants were purified over Protein G columns (Amersham) dialyzed into PBS, and filter sterilized. Purified GK1.5 was tested for the ability to label $CD4^+$ T cells and concentration was determined by optical density at 280nm and by ELISA for rat IgG. Mice were injected i.p. with GK1.5 or control rat gamma globulin (Rockland) at 1.5 or 2.0 mg/ml. For most experiments, mice were

injected with 2.0 mg of antibody twice per week (4.0 mg/week). For dose titration, mice were injected with either 1.0 mg twice per week (2.0 mg/week), 2.0 mg twice per week (4.0 mg/week), or 2.5 mg twice per week plus 3.0 mg once per week (8.0 mg/week). For inhibition of the T-dependent response to NP-CGG, mice were treated with 4.0 mg/week for one week then immunized with 100 μg NP-CGG emulsified in alum, prepared in our laboratory as previously described (196). Mice were then treated with GK1.5 (4.0 mg/week) for an additional 10 days, at which time T cell depletion and antibody production were determined. For depletion of $CD4^+$ T cells in non-autoimmune mice, BALB/c mice were injected with a single injection of 1.0 mg or two injections of 1.0 mg over a one week period.

CD40L was inhibited with MR-1 anti-CD40L monoclonal antibody produced in our laboratory. Hybridoma culture supernatants were ammonium sulfate precipitated, purified with QAE anion-exchange beads (Amersham), dialyzed into PBS, and filter sterilized. Purified MR-1 was tested for the ability to label activated T cells and concentration was determined by optical density at 280nm and by ELISA for hamster IgG. Mice were injected i.v. with 0.4 mg of MR-1 or control hamster gamma globulin (Rockland) three times per week for a period of 2 weeks.

Quantification of antibody production by ELISpot and serum ELISA.

ELISpot for AM14 IgM plasmablasts was performed as previously described (Chapter 5). For detection of IgG-producing plasmablasts, plates were coated with either anti-mouse $IgG2a^a$ (20.8.3 monoclonal antibody produced in our laboratory) or a cocktail of polyclonal goat anti-mouse IgG2b + anti-mouse IgG3 (Southern Biotech).

Serum levels of AM14 IgM antibody were determined by ELISA as described previously (Chapter 5). For initial correlation of serum antibody and splenic plasmablasts, mice were sacrificed and splenic AM14 plasmablasts determined by ELISpot within 2 days of serum antibody determination. For identification of seroconverted mice, a cohort of AM14 mice was screened every 2-3 weeks by serum ELISA for AM14 antibody, and conversion was determined by serum AM14 > 40 μg/ml. Treatment with GK1.5, MR-1, or control antibodies was then begun within 3 days of screening. Serum levels of AM14 IgG antibody were determined by ELISA as described previously, except that plates were coated with a cocktail of polyclonal goat anti-mouse IgG2b + anti-mouse IgG3 (Southern Biotech). Relative levels of IgG were determined by comparison to optical density produced by supernatant from an AM14 IgM-transfected cell line in a parallel IgM ELISA.

Anti-NP antibody was determined by ELISA. Polystyrene plates were coated with NP-conjugated BSA (produced in our laboratory), blocked with 1% BSA in PBS, and serial dilutions of serum from 1:50 to 1:156,000 were added. IgG antibodies were detected with alkaline phosphatase-conjugated goat anti-mouse IgG (Southern Biotech), and absorbance at 405/630nm was compared with 23.3 anti-NP monoclonal antibody (produced in our laboratory) to quantitate.

Analysis of lymphocyte subsets, activation markers and proliferation rates.

Spleen cells were isolated as previously described (Chapter 2). $CD4^+$ T cells were identified with RM4-4 monoclonal antibody (BD Biosciences) which does not cross-react with GK1.5. Identification of $AM14^+$ cells and activation marker expression was determined as previously described (Chapter 5). IgM and IgD, and IgG2a-expressing

AM14-sdTg B cells were detected with anti-IgM^a (RS3.1, produced in our laboratory), anti-IgD (11-26, eBioscience), and anti-IgG2a^a (20.8.3, produced in our laboratory) antibodies. For determination of proliferation rates, mice were given a single i.p. injection of 3 mg of BrdU (Sigma) 12 hours prior to sacrifice. BrdU incorporation was detected with anti-BrdU antibody (PRB-1, Phoenix Flow) as previously described (197). Apoptosis was determined with the CaspGLOW fluorescein active caspase staining kit (Biovision) according to the manufacturer's instructions.

Spleen histology.

Spleen histology was performed as previously described (Chapter 5), except that AM14 cells were detected with 4-44 monoclonal antibody produced in our laboratory.

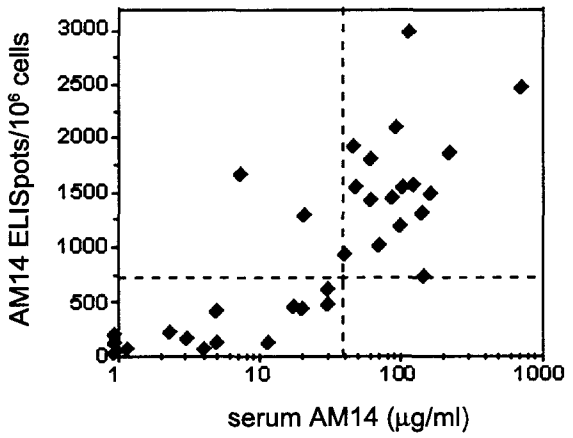

Figure 36. Serum levels of AM14 antibody correlate with expansion of AM14 plasmablasts in the spleen. A cohort of AM14 transgenic mice (n = 33) was serially bled every two weeks and assayed for serum AM14 antibody by ELISA. Mice were sacrificed between 10 and 25 weeks of age, within 2 days of the last serum assay, and AM14 expansion in the spleen was determined by ELISpot for AM14-secreting plasmablasts. Dashed lines indicate cutoff points for what was considered a positive assay. $P < 0.0001$ by Fisher's exact test.

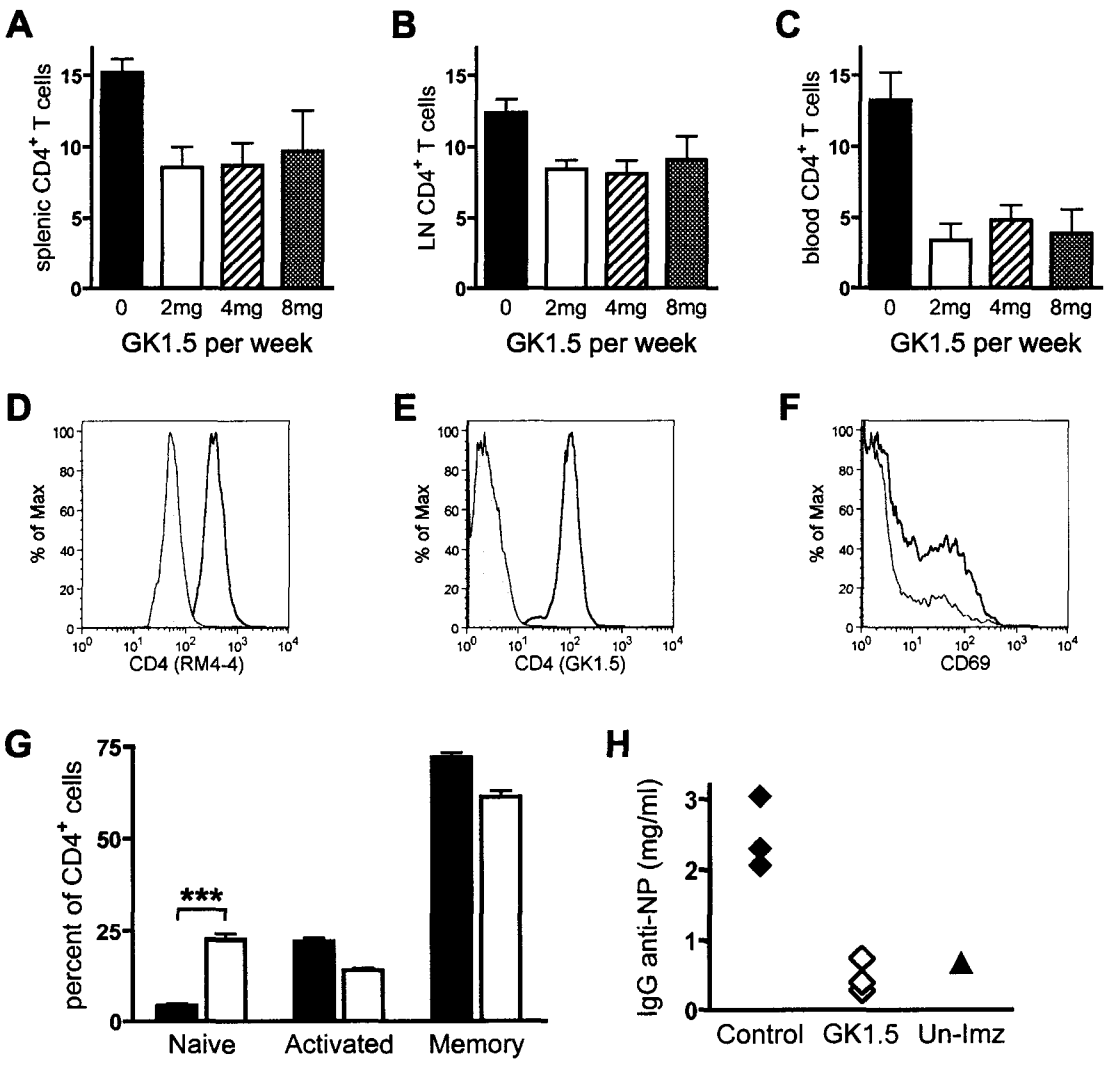

Figure 37. GK1.5 inhibits CD4⁺ T cell function without complete depletion. (A-C) MRL/Mp$^{lpr/lpr}$ mice were injected with either control antibody (n = 4) or GK1.5 anti-CD4 antibody at 2 mg/week (n = 2), 4 mg/week (n = 6), or 8 mg/week (n = 3) over a 2 week period. Percentages of CD4⁺ T cells were determined in spleen (A), lymph node (B), and peripheral blood (C). (D-F) Histograms show CD4⁺ T cells from control (black line) or GK1.5-treated mice (4 mg/week, filled histogram). (D) Decreased surface levels of CD4 in treated mice were determined with RM4-4 antibody. (E) Complete opsonization of CD4⁺ T cells with GK1.5 in vivo was determined by ex vivo staining with GK1.5. (F) Activation of CD4⁺ T cells was determined by levels of CD69. (G) Splenic CD4⁺ T cells from control (black bars, n = 9) or GK1.5-treated mice (4 mg/week, white bars, n = 9) were classified as naïve (CD44⁻ CD62L⁺), activated (CD44⁺ CD62L⁺), or memory (CD44⁺ CD62L⁻) phenotype. (H) Control or GK1.5-treated mice were immunized with NP-CGG, and serum anti-NP IgG titers were determined 10 days later (Un-Imz = unimmunized control). ***, $P < 0.0001$ by Mann-Whitney U test.

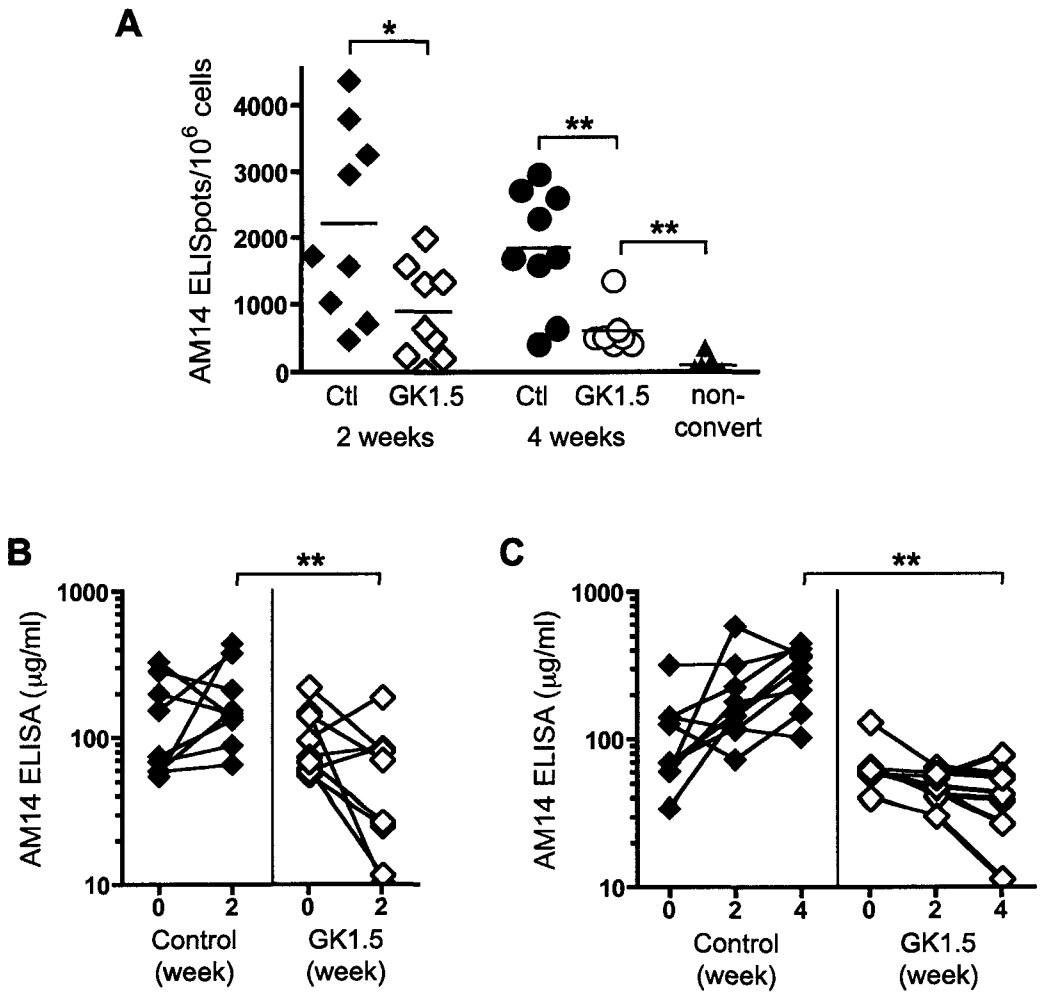

Figure 38. Removal of CD4⁺ T cell help reduces AM14 rheumatoid factor antibody secretion. (A) AM14 antibody-secreting cells were determined in seroconverted mice treated with GK1.5 (n = 9) or control antibody (n = 9) for 2 weeks, or GK1.5 (n = 7) or control antibody (n = 9) for 4 weeks, or age-matched non-seroconverted mice (n = 7). Data are presented as ELISpots per million splenocytes. (B-C) Serum AM14 antibody was determined in mice treated with GK1.5 or control antibody as in A for 0, 2, or 4 weeks. *, $P < 0.05$; **, $P < 0.01$ by Mann-Whitney U test.

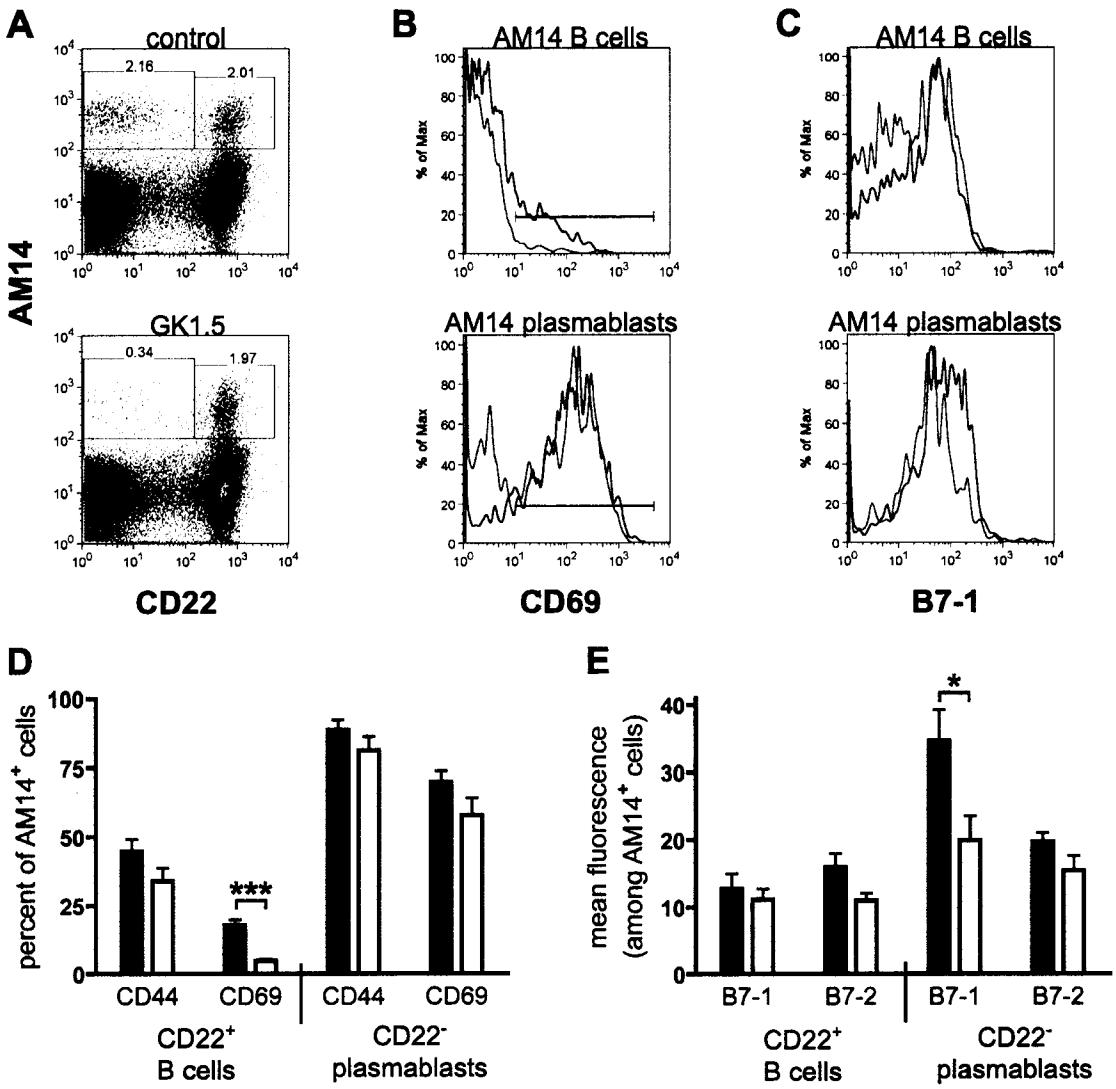

Figure 39. Differential effects of CD4+ T cell help on AM14 B cells and plasmablasts. (A) Splenic AM14 CD22+ B cells and CD22- plasmablasts were identified in mice treated with control antibody (upper plot) or GK1.5 (lower plot). (B-C) CD69 (B) and B7-1 (C) expression were determined in AM14 CD22+ B cells (upper plots) and CD22- plasmablasts (lower plots) from mice treated with control antibody (blue lines) or GK1.5 (red lines). (D) CD44 and CD69 expression were determined in AM14 CD22+ B cells and CD22- plasmablasts from mice treated with control antibody (black bars, n = 9) or GK1.5 (white bars, n = 9). (E) As in D, except for B7-1 and B7-2 expression. Data presented are mice treated for 2 weeks; similar results were observed with 4 week treatment.
*, $P < 0.05$; ***, $P < 0.0001$ by Mann-Whitney U test.

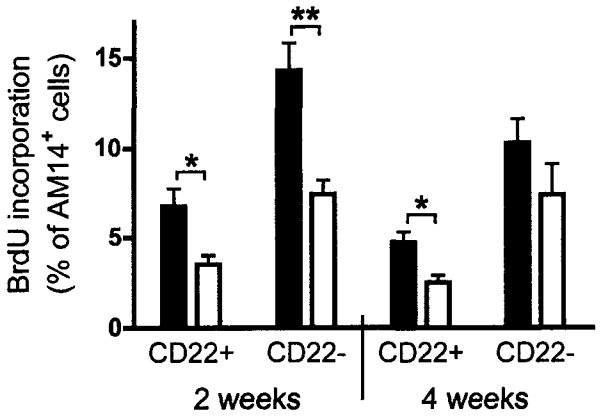

Figure 40. Residual proliferation of AM14 B cells and plasmablasts after removal of CD4⁺ T cell help. 12-hour BrdU incorporation was determined in AM14 $CD22^+$ B cells and $CD22^-$ plasmablasts from mice treated for 2 or 4 weeks with control antibody (black bars, n = 9 for 2 weeks and 4 weeks) or GK1.5 (white bars, n = 9 for 2 weeks, n = 7 for 4 weeks). *, $P < 0.05$; **, $P < 0.01$ by Mann-Whitney U test.

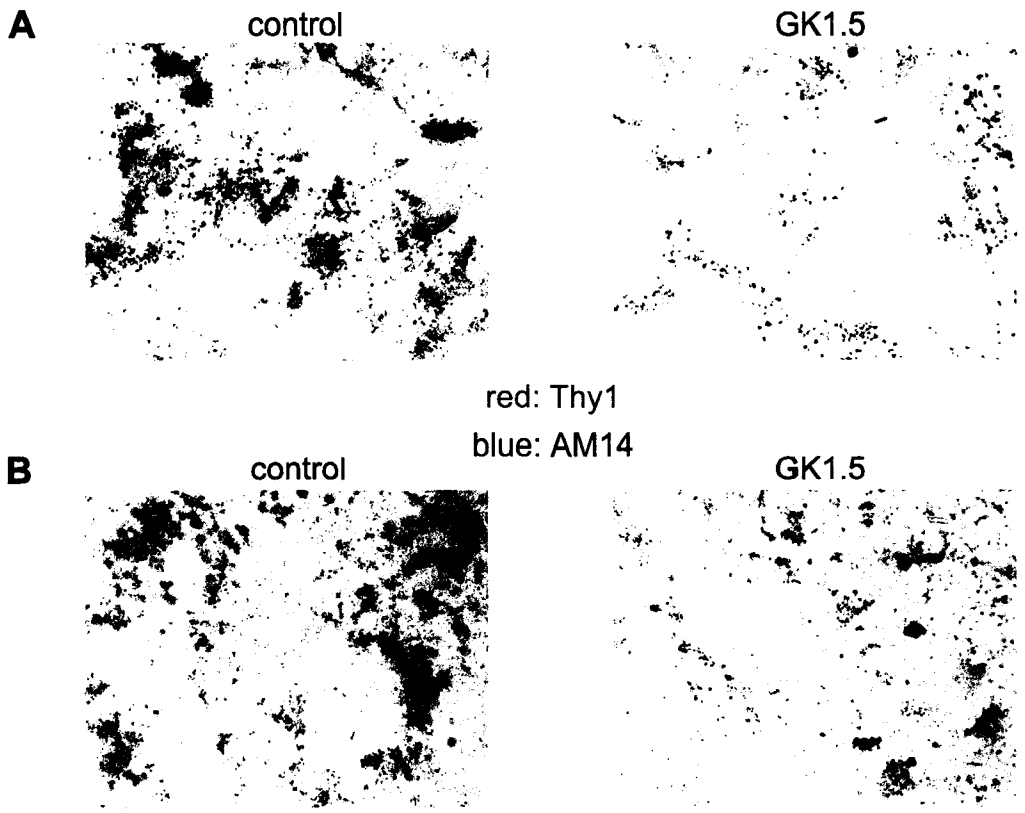

Figure 41. Reduced numbers of AM14 plasmablasts remain adjacent to T cell zones after removal of CD4⁺ T cell help. (A) Spleen sections from mice treated for 2 weeks with either control antibody (left panel) or GK1.5 (right panel) were stained for T cell zones with Thy1 (red) and AM14 plasmablasts (blue). (B) As in A, except that mice were treated for 4 weeks with either control antibody (left panel) or GK1.5 (right panel).

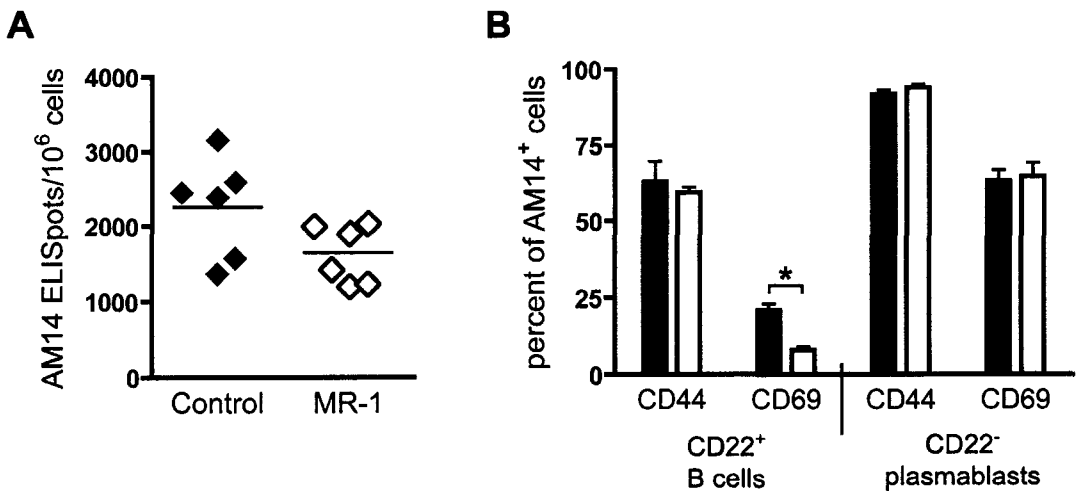

Figure 42. Inhibition of CD40L does not eliminate AM14 plasmablasts. (A) AM14 antibody-secreting cells were determined in serconverted mice treated with anti-CD40L antibody MR-1 (n = 6) or control antibody (n = 6) for 2 weeks. Data are presented as ELISpots per million splenocytes. (B) Expression of CD44 and CD69 were determined in splenic AM14 $CD22^+$ B cells or $CD22^-$ plasmablasts from mice treated with control antibody (black bars, n = 5) or MR-1 (white bars, n = 4). *, $P < 0.05$ by Mann-Whitney U test.

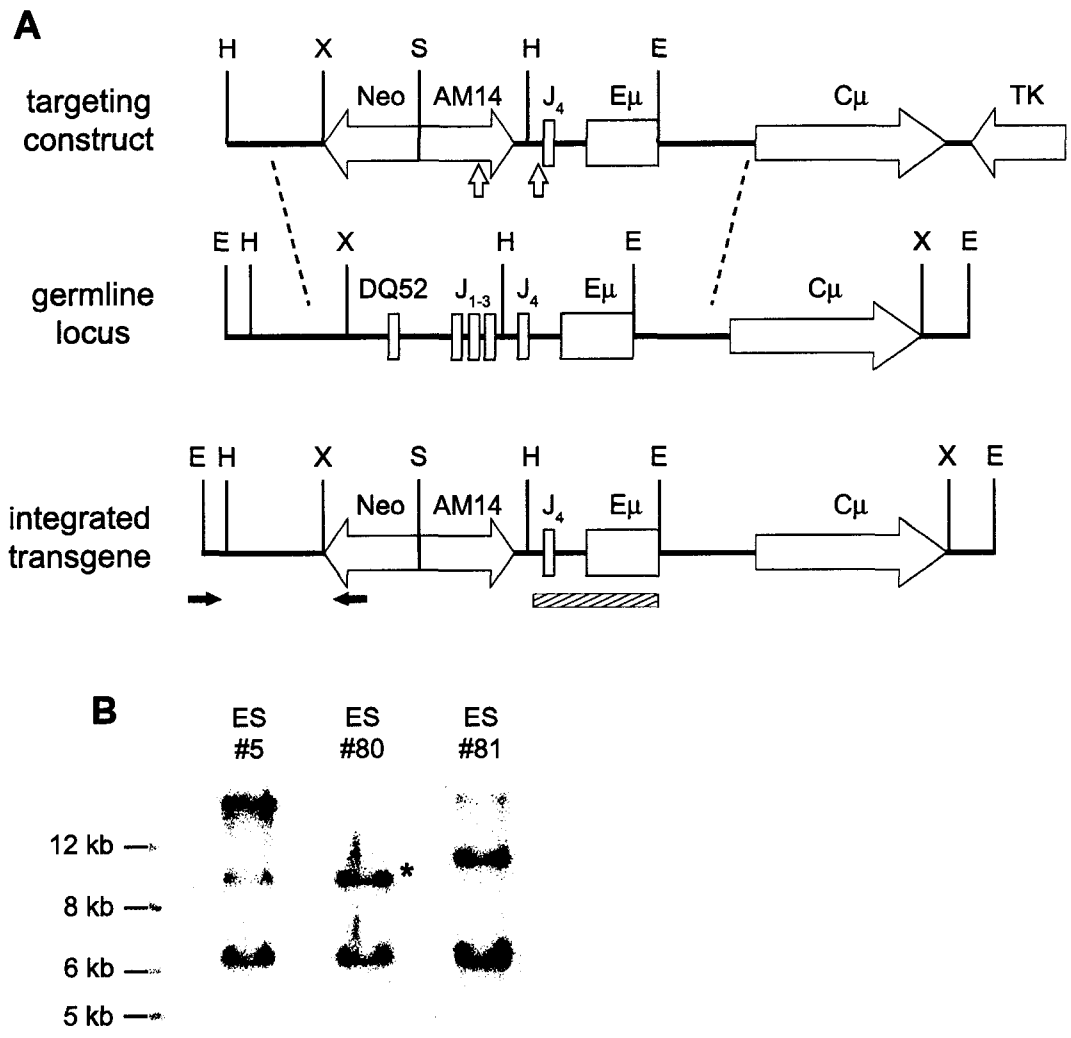

Figure 43. Construction of AM14 site-directed transgenic mice. (A) Targeting construct, germline IgH locus, and final integrated transgene are shown. Neo = neomycin resistance cassette; AM14 = rearranged AM14 VDJ_3; DQ52 = 3' germline D_H gene segment; J_{1-3} and J_4 = germline J_H gene segments; Eμ = IgM enhancer; Cμ = IgM C region exons; TK = thymidine kinase cassette. Vertical lines indicate restriction sites: EcoRI (E), HindIII (H), SalI (S), and XhoI (X). Dashed lines indicate regions of homologous recombination with germline IgH locus. White arrows indicate site-directed mutagenesis of RSS heptamers. Black arrows indicate PCR primers to screen for correct upstream integration. Striped bar indicates J_4 probe used in Southern blot. (B) Southern blot of EcoRI digest of genomic DNA from 3 ES cell clones which were PCR-positive for correct upstream integration. Germline IgH band is 6.2 kb, correct integration of transgene produces 9.4 kb band, indicated by asterisk in ES #80.

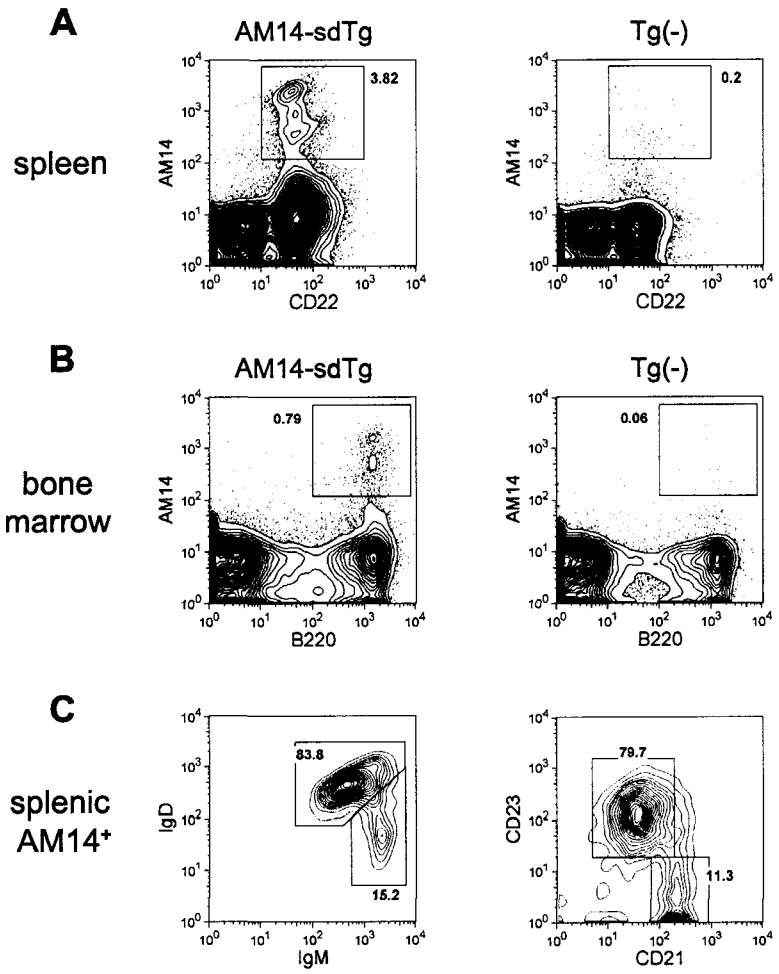

Figure 44. Expression of AM14-sdTg in spleen and bone marrow B cells. (A) Expression of CD22 and AM14 idiotype was determined in spleen cells from AM14 site-directed transgenic (AM14-sdTg, left panel) or transgene-negative littermates (right panel). (B) Expression of B220 and AM14 idiotype was determined in bone marrow cells from mice as in A. (C) Expression of IgM and IgD (left panel) or CD21 and CD23 (right panel) was determined on splenic AM14$^+$ cells from AM14-sdTgic mice. Most AM14$^+$ cells are IgD-expressing CD21^{lo} CD23^{hi} follicular B cells.

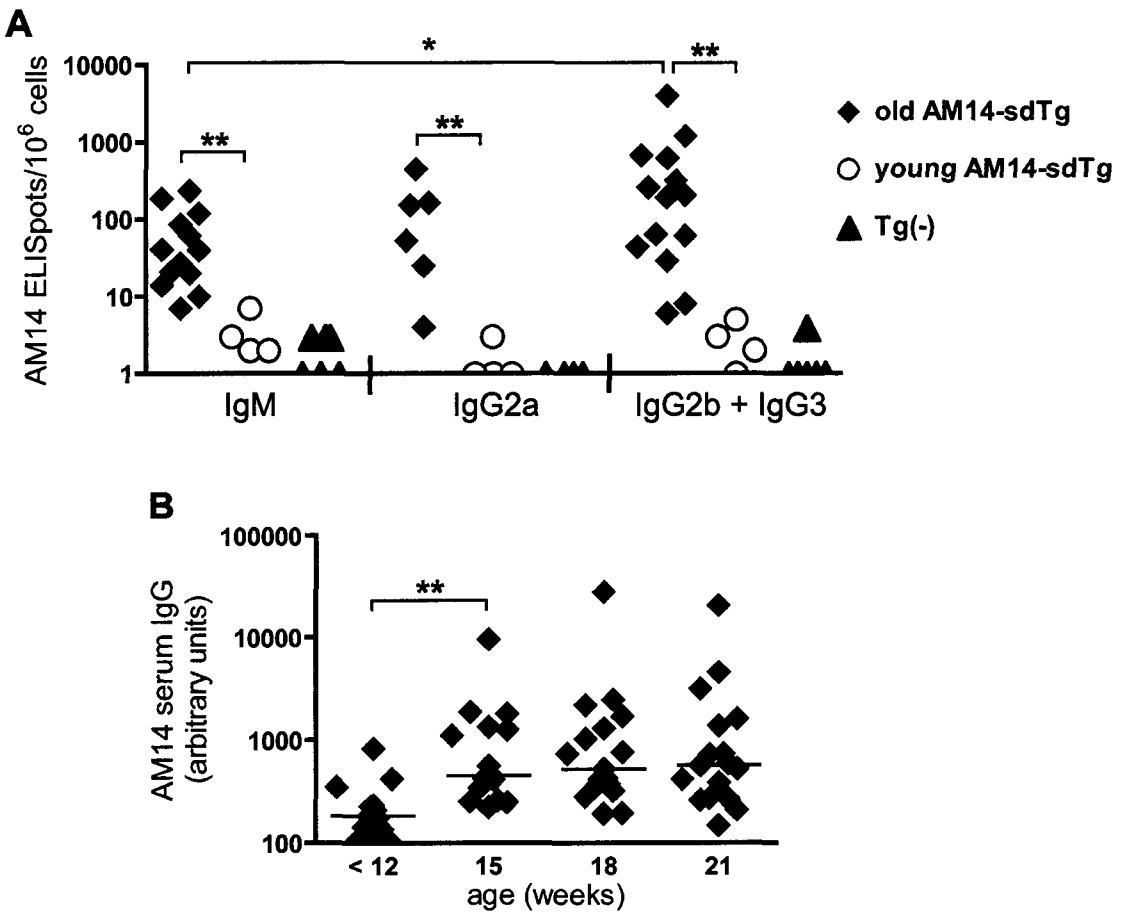

Figure 45. Spontaneous expansion of IgG AM14 antibody-secreting cells is age-dependent. (A) AM14 antibody-secreting cells of IgM, IgG2a, or IgG2b + IgG3 isotypes were determined in old AM14-sdTg mice (black diamonds, n = 14 for all except IgG2a n = 6); young AM14-sdTg mice (white circles, n = 4), or non-transgenic mice (gray triangles, n = 6 for all except IgG2a n = 4). Old mice were 21 weeks of age, young mice were 7 weeks of age. (B) Serum AM14 IgG2b + IgG3 was determined in AM14-sdTg mice at multiple different time points (n = 17 for all time points except < 12 weeks n = 13). *, $P < 0.05$; **, $P < 0.01$ by Mann-Whitney U test.

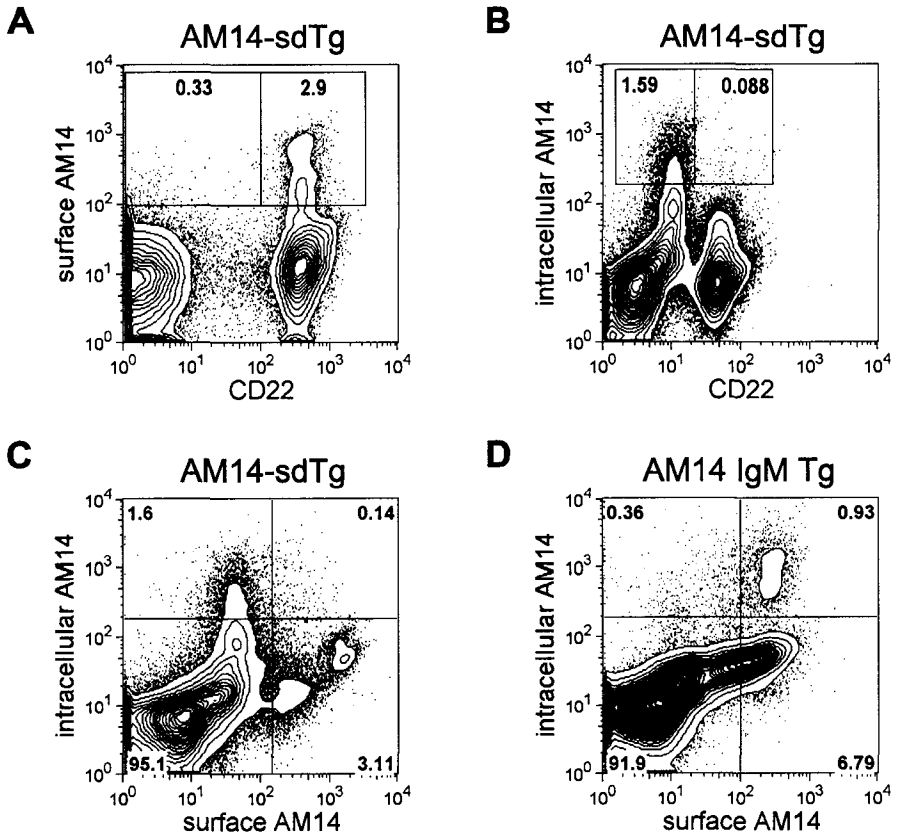

Figure 46. Antibody-secreting cells in AM14-sdTg mice do not express surface antibody. (A-C) AM14 antibody-secreting cells were identified in an aged AM14-sdTg mouse with many splenic AM14 ELISpots. (A) Surface staining of CD22 and AM14 revealed few typical $CD22^-$ plasmablasts. (B) Intracellular staining for AM14 revealed many $CD22^-$ antibody-secreting cells. (C) The majority of intracellular $AM14^+$ cells in AM14-sdTg mice are negative for surface AM14. (D) The majority of intracellular $AM14^+$ cells in a seroconverted AM14 conventional transgenic (IgM-only) mouse are surface $AM14^+$.

Chapter 7: Conclusions and Future Studies

The findings presented here have begun to identify the factors required for the activation of autoreactive B cells. We have identified TLRs as critical factors in the production of autoantibody-secreting cells. Individual TLRs are required for the generation of specific antibodies to self nuclear components, with TLR9 controlling antibodies to DNA-containing antigens, and TLR7 promoting the formation of antibodies to RNA-containing antigens. The observations that TLR3 did not affect autoantibody production and that TLR9 was not required for production of rheumatoid factor autoantibodies highlight the specificity of the interactions between TLRs and autoantibody targets. We have further shown that TLR expression within B cells is required for autoantibody secretion, and that TLRs facilitate the differentiation of mature, peripheral B cells into efficient antibody-producing cells. TLRs are not the sole source of autoreactive B cell activation, however. We also discovered that $CD4^+$ T cell help contributes to the continued activation of both early-activated B cells and differentiated plasmablasts, even after a robust response has been established.

Our work has also illustrated some of the consequences of autoreactive B cell activation for global immune activation and clinical disease in the context of SLE. We found that in the absence of TLR9 and anti-DNA autoantibody production, lupus-prone mice developed exacerbated disease with accelerated mortality. This was associated with an increased activation state of lymphocytes and dendritic cells, as well as elevated levels of circulating IFN-α. Our studies of TLR9-chimeric mice revealed that these effects on immune activation were at least partly due to factors elaborated in the absence of TLR9

expression in B cells. Moreover, the ability of serum from TLR9-deficient, but not wild-type, mice to induce high levels of IFN-α production by pDCs further suggested that circulating autoantibodies played a causative role in promoting inflammation and exacerbated disease. The opposite was true for mice deficient in TLR7, as genetic ablation of this receptor ameliorated clinical disease and immune activation. Because the autoantibody repertoire of TLR7-deficient mice was shifted away from RNA antigens and the autoantibody repertoire of TLR9-deficient mice was shifted toward RNA antigens, it is possible that the relative level of antibodies to RNA complexes dictates—or potentially reflects—the severity of immune activation and clinical disease. The observation that antibodies to Sm/RNP were correlated with disease activity in TLR9-deficient mice supports this hypothesis.

Pathogenic Activation Cycles Centered Around B Cells and TLRs in SLE

Positive feedback activation cycles have evolved within the immune system to rapidly mount effective responses against invading pathogens. These amplification loops between B cells, T cells, and dendritic cells become dysregulated in autoimmune disease, in which the constant presence of self antigen allows continued expansion and propagation of the immune response. In SLE, positive feedback between autoreactive B and T cells may be particularly important for chronic progression of clinical disease, as well as the phenomenon of epitope spreading to target an increasing array of endogenous antigens (149). Our findings further support this model of self-reinforcing activation, and emphasize the importance of innate immune activation via TLRs in SLE pathogenesis. In addition, we have also identified dendritic cell subsets as important mediators of

inflammation and immune activation. In all these various interactions and activation cycles, B cells and their autoantibody products play a critical role, as diagrammed in Figure 47.

An initiating event in systemic autoimmunity may be the release of endogenous nucleic acid antigens from apoptotic or necrotic cells, and the subsequent dual recognition of these antigens by B cells with anti-nuclear BCR specificity and appropriate TLRs. An increased predisposition to autoimmune disease has been documented in multiple experimental systems wherein clearance of apoptotic or necrotic debris is impaired (36-38), and also in humans lacking complement pathways for apoptotic clearance (39). The recognition of RNA or DNA ligands by TLRs can occur in a B cell-intrinsic manner, and can then facilitate differentiation of autoreactive B cells to antinuclear antibody-secreting cells. Autoantibodies produced by these cells can have direct pathogenic effects (4, 11), promoting tissue damage, cell death, and the release of additional endogenous TLR ligands. These TLR ligands could then promote additional B cell activation, creating a B cell autonomous activation cycle involving apoptotic cells, nucleic acid-sensing TLRs, and autoantibodies.

We have also found that circulating factors produced when TLR9 is absent on B cells (presumably autoantibodies) can mediate the activation of pDCs and promote efficient secretion of IFN-I. The ability of IFN-I to promote antibody production (97-99) then completes a second activation cycle, this one between B cells and pDCs. IFN-I can also induce the maturation of monocytes and immature DCs into efficient antigen-presenting cells (88, 100), facilitating the activation of otherwise tolerant autoreactive T cells. These T cells could then provide the cognate help necessary for effective

expansion and differentiation of autoreactive B cells. In addition, because BCR-mediated endocytosis can be coupled to antigen-processing pathways, B cells can also function as APCs for autoreactive T cells (149). This then creates two additional activation cycles, one involving B cells, DCs, and T cells, and the other a involving a reciprocal activation of autoreactive B and T cells.

Finally, an important interaction between B cells and myeloid DCs may also exist in autoimmune disease. Immune complexes of autoantibodies and endogenous DNA have been shown to induce maturation and cytokine secretion by mDCs (118), and our results indicate that B cell-derived serum factors from wild-type or TLR9-deficient mice can have distinct effects on DC activation. Autoreactive B cells may therefore directly promote the generation of mature DCs, without a requirement for IFN-I production (198). Reciprocally, cytokines produced by activated DCs, particularly the TNF family member BAFF (199, 200), can promote autoreactive B cell survival and antibody secretion to complete an activation cycle between mDCs and B cells. Thus, by virtue of the integration of signals from receptors of the innate and adaptive immune system, and by the ability to coordinate the actions of both innate and adaptive effector cells, B cells reside at the center of multiple activation loops in the etiology and pathogenesis of SLE.

TLRs and the Evolution of Innate Tolerance to Self Antigens

We found that in the absence of anti-DNA antibodies in TLR9-deficient mice, autoimmune disease was not prevented but was actually exacerbated. This raised the possibility that these antibodies do not directly contribute to pathology in SLE, and furthermore, that anti-DNA antibodies could be protective against autoimmune disease.

Similar to studies of human lupus serum (87, 114), we also found that a higher prevalence of antibodies to RNA-containing antigens in $TLR9^{-/-}$ serum was associated with a more potent induction of IFN-I than that induced by anti-DNA antibodies present in wild-type serum. It thus appeared that the recognition of endogenous DNA by TLR9 had different effects in B cells and pDCs. While TLR9 was clearly stimulatory for antibody production by anti-DNA B cells, it was less effective in activating IFN-I secretion by pDCs. This could provide insight into the evolution of nucleic acid-sensing TLRs and how defense against infection is tempered by the risk of autoimmunity.

Anti-DNA and anti-chromatin antibodies are the most prevalent specificities in multiple autoimmune syndromes, and there is an inherent predisposition toward anti-DNA reactivity in the germline V gene repertoire of the BCR (201). This suggests that the immune system is permissive for the development of these autoantibodies, at least relative to other anti-nuclear specificities. In addition, because of the inherently short half-life of RNA, DNA is more likely to persist in the extracellular milieu, and therefore more likely to encounter nucleic acid-sensing TLRs than RNA. Moreover, the same molecular modifications that increase the stability of mammalian RNA appear to inhibit its recognition by TLRs, thereby further decreasing the probability of TLR activation by endogenous RNA (67). Assuming that autoantibody complexes can facilitate dendritic cell activation by endogenous nucleic acids, the high frequency of anti-DNA antibodies coupled with the prevalence of DNA ligands *in vivo* thus pose a significant risk of aberrant DC activation in normal individuals. Yet this risk appears to be mitigated by a decreased stimulatory capacity of DNA-containing complexes in the activation of pDCs

to produce IFN-I. In other words, a high sensitivity to TLR9 ligands in B cells may have co-evolved with a decreased sensitivity to these ligands in pDCs.

The TLR7-mediated IFN-I response of pDCs to RNA-containing antigens, in contrast, is particularly robust. As described above, RNA antigens released from apoptotic cells or contained in serum immune complexes are potent inducers of IFN-I. From an evolutionary perspective, the potentially dire consequences of pDC activation by endogenous RNA may be acceptable in light of the low prevalence of anti-RNA antibodies and the rapid degradation of endogenous RNA *in vivo*. Thus, tolerance to RNA is enforced not by pDCs, but mainly by the B cell antibody repertoire and the efficient clearance of extracellular RNA. In this respect, it is interesting that expression of TLR7 in B cells is strictly regulated, unlike the constitutive expression of TLR9 in these cells (202). In contrast to the common occurrence of anti-DNA antibodies, the suppression of antibodies to RNA-containing antigens appears particularly effective, even in individuals with autoimmune disease.

The relative levels of antibodies to DNA- or RNA-containing antigens, produced by B cells in response to ligation of TLR9 or TLR7, may therefore determine the functional consequences of autoreactive B cell activation. While the secretion of anti-DNA antibodies could be compatible with self tolerance and immune homeostasis, the generation of high titer antibodies to RNA-containing antigens is likely to induce autoimmune disease. Our findings further suggest that the regulated production of anti-DNA antibodies may even prevent low levels of anti-RNA antibodies from achieving a stimulatory capacity. Of course, SLE can and does develop in the absence of detectable antibodies to endogenous RNA antigens. It is possible that the lack of these antibodies in

some individuals may be attributable to technical difficulties in their detection. It is clear, however, that anti-DNA antibodies can also exert pathogenic effects, such as direct deposition and tissue injury (11), and effective production of IFN-I by pDC under appropriate conditions (203).

Therapeutic Implications in SLE

The studies presented here also have important implications for the treatment of human autoimmune disease. First, our findings in TLR-deficient mice implicate TLRs as important mediators of immune activation and disease, and highlight these receptors as potential candidates for therapeutic inhibition in SLE. However, our demonstration of exacerbated disease in TLR9-deficient mice provides a note of caution for TLR inhibition in the context of autoimmunity. Although interventions to decrease TLR9 signaling in human lupus patients may be able to reduce anti-DNA B cell activation and autoantibody secretion, such interventions may also increase the prevalence of antibodies to RNA-containing antigens, promote elevated IFN-I production, and lead to heightened clinical disease in these patients. Selective inhibitors of TLR7 would be much more promising therapeutic candidates. Alternatively, dual inhibition of both receptors could have more profound effects on autoantibody production and clinical disease than inhibition of either receptor alone.

We have also identified IFN-I as a potential mediator of pathogenesis in SLE, adding to the long history of this family of cytokines in autoimmunity (88-92). Although the pathogenic nature of IFN-I in autoimmune disease is not a novel concept, we have discovered an important role for serum factors produced in the absence of TLR9

(presumably a shifted autoantibody repertoire) in the production of these cytokines *in vivo*. It may therefore be possible to decrease IFN-I production by preventing the autoantibody-mediated delivery of endogenous TLR ligands to appropriate compartments in DC subsets. This could be accomplished either by altering the autoantibody repertoire at the level of B cells, or by inhibiting recognition of autoantibody complexes at the level of responding DCs. In the case of the latter, Fc receptor-mediated endocytosis and intracellular activation signals are candidates for therapeutic inhibition, as are TLR signaling pathways. In addition, pharmacologic agents such as chloroquine, which inhibits the endosomal acidification required for the activation of intracellular TLRs, could also reduce DC-mediated inflammation in SLE. Although chloroquine has been used clinically for decades to treat SLE and rheumatoid arthritis, continued investigation of this and related compounds may provide new insights and treatment options in systemic autoimmunity.

Finally, our studies on the role of $CD4^+$ T cell help in autoreactive B cell activation point towards T cells as additional targets of therapeutic intervention. Although a requirement for T cells in SLE was not unexpected, the dramatic decrease in antibody-secreting cells that we observed after a brief period of T cell inhibition illustrates the dynamic, short-lived nature of the autoantibody response. The fact that removal of $CD4^+$ T cell help affected antibody secretion even after the initiation of a robust autoimmune response makes this approach particularly relevant to the treatment of human disease. Therapeutic inhibition of helper T cells may be most effective during disease flares, when a brief treatment window can reduce inflammation back to baseline levels without causing excessive immunosuppression. Although pharmacologic

inhibition of T cell function has yet to prove beneficial in human lupus patients, this is an area of active research (204).

Future Studies

The more we have learned about B cells and TLRs in autoimmunity, the more questions we have generated. Although the findings presented here represent an important contribution to understanding the mechanisms and consequences of autoantibody production in SLE, several aspects of these mechanisms remain unresolved. For example, we have demonstrated a shift in ANA patterns of TLR9-deficient mice toward cytoplasmic, presumably RNA-containing, antigens, but we have not precisely identified these antigens. Treatment of the ANA substrate with RNase may abolish these staining patterns from TLR9-deficient serum, and thereby confirm the presence of autoantibodies to RNA-containing complexes. In addition, we have also begun studies to identify specific antibodies to characteristic autoantigen targets in TLR9-deficient mice. Preliminary work suggests that anti-ribosomal antibodies, identified by immunoprecipitation of RNA from whole-cell lysates, may become more prominent in the absence of TLR9. Similarly, we have presented evidence of a decrease in anti-Sm/RNP antibodies in TLR7-deficient mice, but were unable to determine whether TLR7 was absolutely required for the generation of antibodies to RNA antigens. We are therefore preparing a second cohort of TLR7-deficient mice, which should provide the statistical power to detect a block in anti-Sm antibodies. In addition, we can extend our analysis to include other RNA-containing antigens such as those which appear to be targeted in TLR9-deficient mice.

Another area of uncertainty is the mechanism of exacerbated or ameliorated disease in the absence of TLR9 or TLR7, respectively. Although we have provided evidence that the circulating autoantibody repertoire in TLR-deficient mice can influence dendritic cell activation and cytokine secretion, we have not established a molecular mechanism for this, nor have we documented how it translates to clinical disease activity. Because we suspect that immune complexes of autoantibodies and endogenous nucleic acids induce IFN-I production, we can utilize existing genetic models to establish a mechanism of disease pathogenesis. Genetic ablation of Fc gamma receptors in $TLR9^{+/+}$ or $TLR9^{-/-}$ mice can be achieved by breeding with $Fcerg1^{tm1}$ mice (118), and the requirement for FcR signaling in mediating exacerbated disease can then be determined. AM14-sdTg mice may also provide insights into the requirement for IgG immune complexes in disease. Comparison of conventional AM14 transgenic mice with AM14-sdTg mice, which should have the same repertoire of autoantibody specificity, should allow us to determine what role class-switching to IgG isotypes plays in disease pathogenesis. Finally, combining TLR9-deficiency with IFN-I-deficiency in IFNAR-$1^{-/-}$ mice (92) will allow us to identify the potential role of IFN-I in disease pathogenesis.

Another mechanism for increased disease severity in TLR9-deficient mice could be the failed clearance of apoptotic debris. The ability of IgM antibody to promote phagocytosis of apoptotic cells has been recently reported (205), and it is possible that anti-DNA antibodies fulfill a physiologic role in promoting the clearance of exposed DNA on fragments of dead and dying cells. The absence of anti-DNA antibodies in TLR9-deficient serum could then lead to an increase in circulating nucleic acid antigens derived from apoptotic cells, thereby facilitating TLR-mediated recognition of these

antigens and promoting generalized inflammation. In a series of preliminary experiments, we have yet to identify any defect in phagocytosis of apoptotic cells in $TLR9^{-/-}$ mice or an impairment of $TLR9^{-/-}$ serum in promoting phagocytosis. More studies are planned to further evaluate this potential mechanism, such as quantification of circulating DNA in $TLR9^{-/-}$ serum, and identification of apoptotic cells *in situ* within secondary lymphoid organs.

As discussed in chapter 4, the nature of the interferon-stimulatory factor in serum from TLR9-deficient mice remains an enigma. Because of the high probability that autoantibodies are central to pDC stimulation, an initial first step will be to purify IgG fractions from serum, and ascertain whether interferon-stimulatory capacity is retained. Digestion of serum samples with RNase or DNase will also reveal whether pre-formed nucleic acid complexes are required for stimulation, or whether nascent complexes are formed during culture conditions. Additionally, stimulation with serum from TLR7-deficient mice will reveal what role the autoantibody repertoire has in promoting IFN-I secretion. At the level of the responding cells, it is clear that TLR9 expression is not required for IFN-I production. We suspect that TLR7-mediated recognition of RNA antigens is the mechanism of pDC activation, and that the IFN-I response will be abrogated in TLR7-deficient DCs. It is also possible that either TLR7 or TLR9 can promote IFN-I production, and we therefore plan to generate mice doubly-deficient for both of these receptors. Analysis of DC stimulation as well as clinical disease and autoantibody production in these mice will be highly informative.

Finally, several groups have recently reported the existence of novel innate sensors of cytosolic RNA and DNA that can induce IFN-I production by a TLR-

independent mechanism (60-63), and that this pathway may be activated by endogenous DNA under appropriate conditions (166). It will thus be important to determine whether IFN-α production induced by TLR9-deficient serum, or the exacerbated clinical disease in TLR9-deficient mice can be attributed to these TLR-independent pathways of immune activation. Analysis of clinical disease and IFN-I production in mice deficient for MyD88, the shared adaptor protein required for signaling through TLR7 and TLR9, will allow us to identify the relative contribution of TLR-dependent and –independent sensors of endogenous nucleic acid antigens. It is possible that the study of these TLR-independent activation pathways will reveal another dimension in the pathogenesis of SLE. If so, this could uncover yet another mechanism whereby innate immune signals instruct and regulate the activity of the adaptive immune system in health and disease.

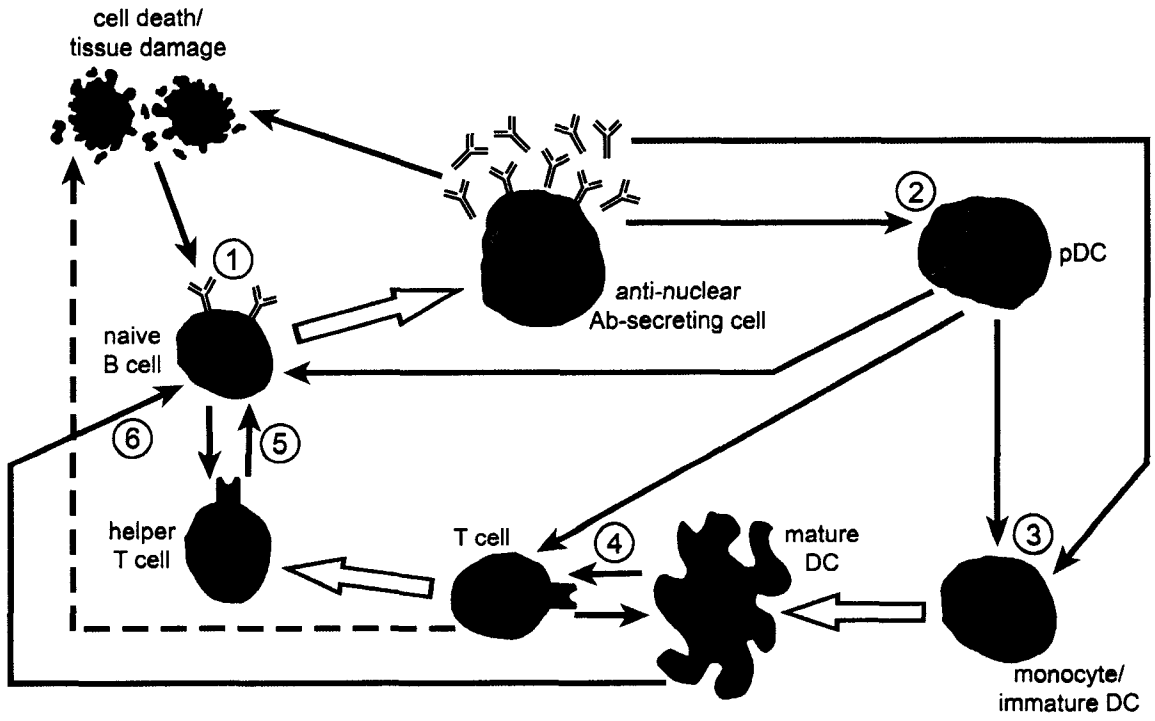

Figure 47. B cells at the center of immune activation cycles in SLE.
(1) Endogenous DNA- and RNA-containing antigens released by apoptotic and necrotic cells activate TLRs within autoreactive B cells, allowing differentiation to anti-nuclear antibody-secreting cells. Autoantibodies produced by these cells (blue arrows) can have direct pathogenic effects, releasing additional endogenous TLR ligands and promoting autoreactive B cell activation (B cell autonomous activation cycle). (2) Autoantibody immune complexes activate pDCs, inducing production of IFN-I (red arrows). IFN-I then acts upon B cells to promote antibody secretion (B cell-pDC activation cycle). (3) IFN-I induces maturation of monocytes or immature DCs into effective antigen presenting cells. Autoantibody immune complexes can also facilitate myeloid DC activation. (4) Mature dendritic cells activate cognate T cells (purple arrows) to produce autoreactive effector T cells, and IFN-I promotes T cell polarization to inflammatory T_H1 effectors. Activated T cells may have direct cytotoxic effects on host tissues (dashed arrow). (5) Activated helper T cells provide additional stimulation to autoreactive B cells (purple arrows) for efficient antibody production (B cell-DC-T cell activation cycle). B cells can also reciprocally present antigen to cognate T cells (B cell-T cell activation cycle). (6) Cytokines such as BAFF produced by activated dendritic cells (green arrow) promote autoreactive B cell survival and antibody secretion (B cell-DC activation cycle).

References

1. Janeway, C.A., Travers, P., Walport, M., Shlomchik, M. 2001. Immunobiology: The Immune System in Health and Disease. Garland Publishing, 732 pp.

2. Amital, H., Shoenfeld, Y. 2004. Autoimmunity and Autoimmune Diseases like Systemic Lupus Erythematosus. In Systemic Lupus Erythematosus. R.G. Lahita, editor Elsevier Academic Press, 3-27.

3. Lahita, R.G. 2004. The Clinical Presentation of Systemic Lupus Erythematosus. In Systemic Lupus Erythematosus. R.G. Lahita, editor Elsevier Academic Press, 435-448.

4. Alarcon-Segovia, D., Alarcon-Riquelme, M. E. 2004. Etiopathogenesis of Systemic Lupus Erythematosus. In Systemic Lupus Erythematosus. R.G. Lahita, editor Elsevier Academic Press, 93-107.

5. Gladman, D.D. 2004. Epidemiology of Systemic Lupus Erythematosus. In Systemic Lupus Erythematosus. R.G. Lahita, editor Elsevier Academic Press, 697-715.

6. Hargraves, M.M., Richmond, H., Morton, R. 1948. Presentation of Two Bone Marrow Elements: the "Tart" Cell and the "L.E." Cell. *Proc. Staff Meet. Mayo Clin.* 23:25-28.

7. Tan, E.M., A.S. Cohen, J.F. Fries, A.T. Masi, D.J. McShane, N.F. Rothfield, J.G. Schaller, N. Talal, and R.J. Winchester. 1982. The 1982 revised criteria for the classification of systemic lupus erythematosus. *Arthritis Rheum* 25:1271-1277.

8. Kotzin, B. 1996. Systemic lupus erythematosus. *Cell* 85:303-306.

9. Hahn, B.H. 1998. Antibodies to DNA. *N Engl J Med* 338:1359-1368.

10. Amoura, Z., H. Chabre, S. Koutouzov, C. Lotton, A. Cabrespines, J.F. Bach, and L. Jacob. 1994. Nucleosome-restricted antibodies are detected before anti-dsDNA and/or antihistone antibodies in serum of MRL-Mp lpr/lpr and +/+ mice, and are present in kidney eluates of lupus mice with proteinuria. *Arthritis Rheum* 37:1684-1688.

11. Vlahakos, D.V., M.H. Foster, S. Adams, M. Katz, A.A. Ucci, K.J. Barrett, S.K. Datta, and M.P. Madaio. 1992. Anti-DNA antibodies form immune deposits at distinct glomerular and vascular sites. *Kidney International* 41:1690-1670.

12. Shlomchik, M.J., M.P. Madaio, D. Ni, M. Trounstine, and D. Huszar. 1994. The role of B cells in lpr/lpr-induced autoimmunity. *J. Exp. Med.* 180:1295-1306.

13. Chan, O.T., M.P. Madaio, and M.J. Shlomchik. 1999. B cells are required for lupus nephritis in the polygenic, Fas-intact MRL model of systemic autoimmunity. *J Immunol* 163:3592-3596.

14. Lin, R.H., M.J. Mamula, J.A. Hardin, and C.A. Janeway, Jr. 1991. Induction of autoreactive B cells allows priming of autoreactive T cells. *J Exp Med* 173:1433-1439.

15. Mamula, M.J., S. Fatenejad, and J. Craft. 1994. B cells process and present lupus autoantigens that initiate autoimmune T cell responses. *J Immunol* 152:1453-1461.

16. Chan, O.T., L.G. Hannum, A.M. Haberman, M.P. Madaio, and M.J. Shlomchik. 1999. A novel mouse with B cells but lacking serum antibody reveals an antibody-independent role for B cells in murine lupus. *J Exp Med* 189:1639-1648.

17. Leandro, M.J., J.C. Edwards, G. Cambridge, M.R. Ehrenstein, and D.A. Isenberg. 2002. An open study of B lymphocyte depletion in systemic lupus erythematosus. *Arthritis Rheum* 46:2673-2677.

18. Martin, F., and A.C. Chan. 2004. Pathogenic roles of B cells in human autoimmunity; insights from the clinic. *Immunity* 20:517-527.

19. Sfikakis, P.P., J.N. Boletis, and G.C. Tsokos. 2005. Rituximab anti-B-cell therapy in systemic lupus erythematosus: pointing to the future. *Curr Opin Rheumatol* 17:550-557.

20. Notman, D.D., N. Kurata, and E.M. Tan. 1975. Profiles of antinuclear antibodies in systemic rheumatic diseases. *Ann Intern Med* 83:464-469.

21. Bradwell, A., Stokes, RP, and Johnson, GD. 1995. Atlas of Hep-2 Patterns. AR Bradwell,

22. Egner, W. 2000. The use of laboratory tests in the diagnosis of SLE. *J Clin Pathol* 53:424-432.

23. Muro, Y. 2005. Antinuclear antibodies. *Autoimmunity* 38:3-9.

24. Plotz, P.H. 2003. The autoantibody repertoire: searching for order. *Nat Rev Immunol* 3:73-78.

25. Pettersson, I., M. Hinterberger, T. Mimori, E. Gottlieb, and J.A. Steitz. 1984. The structure of mammalian small nuclear ribonucleoproteins. Identification of multiple protein components reactive with anti-(U1)ribonucleoprotein and anti-Sm autoantibodies. *J Biol Chem* 259:5907-5914.

26. Reichlin, M. 2004. Anticytoplasmic Antibodies in SLE. In Systemic Lupus Erythematosus. R.G. Lahita, editor Elsevier Academic Press, 315-324.

27. Alba, P., L. Bento, M.J. Cuadrado, Y. Karim, M.F. Tungekar, I. Abbs, M.A. Khamashta, D. D'Cruz, and G.R. Hughes. 2003. Anti-dsDNA, anti-Sm antibodies, and the lupus anticoagulant: significant factors associated with lupus nephritis. *Ann Rheum Dis* 62:556-560.

28. Reeves, W.H., Sato, M., Richards, H.B. 2004. Origins of Antinuclear Antibodies. In Systemic Lupus Erythematosus. R.G. Lahita, editor Elsevier Academic Press, 401-431.

29. Viglianti, G.A., C.M. Lau, T.M. Hanley, B.A. Miko, M.J. Shlomchik, and A. Marshak-Rothstein. 2003. Activation of autoreactive B cells by CpG dsDNA. *Immunity* 19:837-847.

30. Casciola-Rosen, L.A., G. Anhalt, and A. Rosen. 1994. Autoantigens targeted in systemic lupus erythematosus are clustered in two populations of surface structures on apoptotic keratinocytes. *J Exp Med* 179:1317-1330.

31. Cocca, B.A., A.M. Cline, and M.Z. Radic. 2002. Blebs and apoptotic bodies are B cell autoantigens. *J Immunol* 169:159-166.

32. Mevorach, D., J.L. Zhou, X. Song, and K.B. Elkon. 1998. Systemic exposure to irradiated apoptotic cells induces autoantibody production. *J Exp Med* 188:387-392.

33. Qiao, B., J. Wu, Y.W. Chu, Y. Wang, D.P. Wang, H.S. Wu, and S.D. Xiong. 2005. Induction of systemic lupus erythematosus-like syndrome in syngeneic mice by immunization with activated lymphocyte-derived DNA. *Rheumatology (Oxford)* 44:1108-1114.

34. Madaio, M.P., S. Hodder, R.S. Schwartz, and B.D. Stollar. 1984. Responsiveness of autoimmune and normal mice to nucleic acid antigens. *J Immunol* 132:872-876.

35. Gilkeson, G.S., J.P. Grudier, D.G. Karounos, and D.S. Pisetsky. 1989. Induction of anti-double stranded DNA antibodies in normal mice by immunization with bacterial DNA. *J Immunol* 142:1482-1486.

36. Bickerstaff, M.C., M. Botto, W.L. Hutchinson, J. Herbert, G.A. Tennent, A. Bybee, D.A. Mitchell, H.T. Cook, P.J. Butler, M.J. Walport, and M.B. Pepys. 1999. Serum amyloid P component controls chromatin degradation and prevents antinuclear autoimmunity. *Nat Med* 5:694-697.

37. Napirei, M., H. Karsunky, B. Zevnik, H. Stephan, H.G. Mannherz, and T. Moroy. 2000. Features of systemic lupus erythematosus in Dnase1-deficient mice. *Nat Genet* 25:177-181.

38. Cohen, P.L., R. Caricchio, V. Abraham, T.D. Camenisch, J.C. Jennette, R.A. Roubey, H.S. Earp, G. Matsushima, and E.A. Reap. 2002. Delayed apoptotic cell clearance and lupus-like autoimmunity in mice lacking the c-mer membrane tyrosine kinase. *J Exp Med* 196:135-140.

39. Manderson, A.P., M. Botto, and M.J. Walport. 2004. The role of complement in the development of systemic lupus erythematosus. *Annu Rev Immunol* 22:431-456.

40. Clifford, B.D., D. Donahue, L. Smith, E. Cable, B. Luttig, M. Manns, and H.L. Bonkovsky. 1995. High prevalence of serological markers of autoimmunity in patients with chronic hepatitis C. *Hepatology* 21:613-619.

41. Shlomchik, M.J., A. Marshak-Rothstein, C.B. Wolfowicz, T.L. Rothstein, and M.G. Weigert. 1987. The role of clonal selection and somatic mutation in autoimmunity. *Nature* 328:805.

42. Shan, H., M.J. Shlomchik, A. Marshak-Rothstein, D.S. Pisetsky, S. Litwin, and M.G. Weigert. 1994. The mechanism of autoantibody production in an autoimmune MRL/lpr mouse. *J. Immunol.* 153:5104-5120.

43. Wardemann, H., S. Yurasov, A. Schaefer, J.W. Young, E. Meffre, and M.C. Nussenzweig. 2003. Predominant autoantibody production by early human B cell precursors. *Science* 301:1374-1377.

44. Janeway, C.A., Jr. 1989. Approaching the asymptote? Evolution and revolution in immunology. *Cold Spring Harb Symp Quant Biol* 54 Pt 1:1-13.

45. Medzhitov, R. 2001. Toll-like receptors and innate immunity. *Nature Reviews. Immunology.* 1:135-145.

46. Medzhitov, R., P. Preston-Hurlburt, and C.A. Janeway, Jr. 1997. A human homologue of the Drosophila Toll protein signals activation of adaptive immunity. *Nature* 388:394-397.

47. Poltorak, A., X. He, I. Smirnova, M.Y. Liu, C. Van Huffel, X. Du, D. Birdwell, E. Alejos, M. Silva, C. Galanos, M. Freudenberg, P. Ricciardi-Castagnoli, B. Layton, and B. Beutler. 1998. Defective LPS signaling in C3H/HeJ and C57BL/10ScCr mice: mutations in Tlr4 gene. *Science* 282:2085-2088.

48. Hoshino, K., O. Takeuchi, T. Kawai, H. Sanjo, T. Ogawa, Y. Takeda, K. Takeda, and S. Akira. 1999. Cutting edge: Toll-like receptor 4 (TLR4)-deficient mice are

hyporesponsive to lipopolysaccharide: evidence for TLR4 as the Lps gene product. *J Immunol* 162:3749-3752.

49. Schnare, M., G.M. Barton, A.C. Holt, K. Takeda, S. Akira, and R. Medzhitov. 2001. Toll-like receptors control activation of adaptive immune responses. *Nat Immunol* 2:947-950.

50. Akira, S., K. Takeda, and T. Kaisho. 2001. Toll-like receptors: critical proteins linking innate and acquired immunity. *Nat Immunol* 2:675-680.

51. Takeda, K., T. Kaisho, and S. Akira. 2003. Toll-like receptors. *Annu Rev Immunol* 21:335-376.

52. Iwasaki, A., and R. Medzhitov. 2004. Toll-like receptor control of the adaptive immune responses. *Nat Immunol* 5:987-995.

53. Zhang, D., G. Zhang, M.S. Hayden, M.B. Greenblatt, C. Bussey, R.A. Flavell, and S. Ghosh. 2004. A toll-like receptor that prevents infection by uropathogenic bacteria. *Science* 303:1522-1526.

54. Hemmi, H., O. Takeuchi, T. Kawai, T. Kaisho, S. Sato, H. Sanjo, M. Matsumoto, K. Hoshino, H. Wagner, K. Takeda, and S. Akira. 2000. A Toll-like receptor recognizes bacterial DNA. *Nature* 408:740-745.

55. Alexopoulou, L., A.C. Holt, R. Medzhitov, and R.A. Flavell. 2001. Recognition of double-stranded RNA and activation of NF-kappaB by Toll-like receptor 3. *Nature*. 413:732-738.

56. Hemmi, H., T. Kaisho, O. Takeuchi, S. Sato, H. Sanjo, K. Hoshino, T. Horiuchi, H. Tomizawa, K. Takeda, and S. Akira. 2002. Small anti-viral compounds activate immune cells via the TLR7 MyD88-dependent signaling pathway. *Nat Immunol* 3:196-200.

57. Diebold, S.S., T. Kaisho, H. Hemmi, S. Akira, and C. Reis e Sousa. 2004. Innate antiviral responses by means of TLR7-mediated recognition of single-stranded RNA. *Science* 303:1529-1531.

58. Heil, F., H. Hemmi, H. Hochrein, F. Ampenberger, C. Kirschning, S. Akira, G. Lipford, H. Wagner, and S. Bauer. 2004. Species-specific recognition of single-stranded RNA via toll-like receptor 7 and 8. *Science* 303:1526-1529.

59. Jurk, M., F. Heil, J. Vollmer, C. Schetter, A.M. Krieg, H. Wagner, G. Lipford, and S. Bauer. 2002. Human TLR7 or TLR8 independently confer responsiveness to the antiviral compound R-848. *Nat Immunol* 3:499.

60. Yoneyama, M., M. Kikuchi, T. Natsukawa, N. Shinobu, T. Imaizumi, M. Miyagishi, K. Taira, S. Akira, and T. Fujita. 2004. The RNA helicase RIG-I has an essential function in double-stranded RNA-induced innate antiviral responses. *Nat Immunol* 5:730-737.

61. Kato, H., S. Sato, M. Yoneyama, M. Yamamoto, S. Uematsu, K. Matsui, T. Tsujimura, K. Takeda, T. Fujita, O. Takeuchi, and S. Akira. 2005. Cell type-specific involvement of RIG-I in antiviral response. *Immunity* 23:19-28.

62. Ishii, K.J., C. Coban, H. Kato, K. Takahashi, Y. Torii, F. Takeshita, H. Ludwig, G. Sutter, K. Suzuki, H. Hemmi, S. Sato, M. Yamamoto, S. Uematsu, T. Kawai, O. Takeuchi, and S. Akira. 2006. A Toll-like receptor-independent antiviral response induced by double-stranded B-form DNA. *Nat Immunol* 7:40-48.

63. Stetson, D.B., and R. Medzhitov. 2006. Recognition of cytosolic DNA activates an IRF3-dependent innate immune response. *Immunity* 24:93-103.

64. Latz, E., A. Schoenemeyer, A. Visintin, K.A. Fitzgerald, B.G. Monks, C.F. Knetter, E. Lien, N.J. Nilsen, T. Espevik, and D.T. Golenbock. 2004. TLR9 signals after translocating from the ER to CpG DNA in the lysosome. *Nat Immunol* 5:190-198.

65. Barton, G.M., J.C. Kagan, and R. Medzhitov. 2006. Intracellular localization of Toll-like receptor 9 prevents recognition of self DNA but facilitates access to viral DNA. *Nat Immunol* 7:49-56.

66. Krieg, A.M. 2002. CpG motifs in bacterial DNA and their immune effects. *Annu Rev Immunol* 20:709-760.

67. Kariko, K., M. Buckstein, H. Ni, and D. Weissman. 2005. Suppression of RNA recognition by Toll-like receptors: the impact of nucleoside modification and the evolutionary origin of RNA. *Immunity* 23:165-175.

68. Ishii, K.J., K. Suzuki, C. Coban, F. Takeshita, Y. Itoh, H. Matoba, L.D. Kohn, and D.M. Klinman. 2001. Genomic DNA released by dying cells induces the maturation of APCs. *J Immunol* 167:2602-2607.

69. Kariko, K., H. Ni, J. Capodici, M. Lamphier, and D. Weissman. 2004. mRNA is an endogenous ligand for Toll-like receptor 3. *J Biol Chem* 279:12542-12550.

70. Vollmer, J., S. Tluk, C. Schmitz, S. Hamm, M. Jurk, A. Forsbach, S. Akira, K.M. Kelly, W.H. Reeves, S. Bauer, and A.M. Krieg. 2005. Immune stimulation mediated by autoantigen binding sites within small nuclear RNAs involves Toll-like receptors 7 and 8. *J Exp Med* 202:1575-1585.

71. Krieg, A.M., A.K. Yi, S. Matson, T.J. Waldschmidt, G.A. Bishop, R. Teasdale, G.A. Koretzky, and D.M. Klinman. 1995. CpG motifs in bacterial DNA trigger direct B-cell activation. *Nature* 374:546-549.

72. Hornung, V., S. Rothenfusser, S. Britsch, A. Krug, B. Jahrsdorfer, T. Giese, S. Endres, and G. Hartmann. 2002. Quantitative expression of toll-like receptor 1-10 mRNA in cellular subsets of human peripheral blood mononuclear cells and sensitivity to CpG oligodeoxynucleotides. *J Immunol* 168:4531-4537.

73. Shirota, H., K. Sano, N. Hirasawa, T. Terui, K. Ohuchi, T. Hattori, and G. Tamura. 2002. B cells capturing antigen conjugated with CpG oligodeoxynucleotides induce Th1 cells by elaborating IL-12. *J Immunol* 169:787-794.

74. Jung, J., A.K. Yi, X. Zhang, J. Choe, L. Li, and Y.S. Choi. 2002. Distinct response of human B cell subpopulations in recognition of an innate immune signal, CpG DNA. *J Immunol* 169:2368-2373.

75. Pasare, C., and R. Medzhitov. 2005. Control of B-cell responses by Toll-like receptors. *Nature* 438:364-368.

76. Goeckeritz, B.E., M. Flora, K. Witherspoon, Q. Vos, A. Lees, G.J. Dennis, D.S. Pisetsky, D.M. Klinman, C.M. Snapper, and J.J. Mond. 1999. Multivalent cross-linking of membrane Ig sensitizes murine B cells to a broader spectrum of CpG-containing oligodeoxynucleotide motifs, including their methylated counterparts, for stimulation of proliferation and Ig secretion. *Int Immunol* 11:1693-1700.

77. Wang, Y., and A.M. Krieg. 2003. Synergy between CpG- or non-CpG DNA and specific antigen for B cell activation. *Int Immunol* 15:223-231.

78. Goodnow, C.C. 1996. Balancing immunity and tolerance: deleting and tuning lymphocyte repertoires. *Proc Natl Acad Sci U S A* 93:2264-2271.

79. Rui, L., C.G. Vinuesa, J. Blasioli, and C.C. Goodnow. 2003. Resistance to CpG DNA-induced autoimmunity through tolerogenic B cell antigen receptor ERK signaling. *Nat Immunol* 4:594-600.

80. Leadbetter, E.A., I.R. Rifkin, A.M. Hohlbaum, B.C. Beaudette, M.J. Shlomchik, and A. Marshak-Rothstein. 2002. Chromatin-IgG complexes activate B cells by dual engagement of IgM and Toll-like receptors. *Nature* 416:603-607.

81. Marshak-Rothstein, A., L. Busconi, C.M. Lau, A.S. Tabor, E.A. Leadbetter, S. Akira, A.M. Krieg, G.B. Lipford, G.A. Viglianti, and I.R. Rifkin. 2004. Comparison of CpG s-ODNs, chromatin immune complexes, and dsDNA fragment immune complexes in the TLR9-dependent activation of rheumatoid factor B cells. *J Endotoxin Res* 10:247-251.

82. Lau, C.M., C. Broughton, A.S. Tabor, S. Akira, R.A. Flavell, M.J. Mamula, S.R. Christensen, M.J. Shlomchik, G.A. Viglianti, I.R. Rifkin, and A. Marshak-Rothstein. 2005. RNA-associated autoantigens activate B cells by combined B cell antigen receptor/Toll-like receptor 7 engagement. *J Exp Med* 202:1171-1177.

83. Beutler, B. 2004. Inferences, questions and possibilities in Toll-like receptor signalling. *Nature* 430:257-263.

84. Anders, H.J. 2005. A Toll for lupus. *Lupus* 14:417-422.

85. Martin, D.A., and K.B. Elkon. 2005. Autoantibodies make a U-turn: the toll hypothesis for autoantibody specificity. *J Exp Med* 202:1465-1469.

86. Andreakos, E., B. Foxwell, and M. Feldmann. 2004. Is targeting Toll-like receptors and their signaling pathway a useful therapeutic approach to modulating cytokine-driven inflammation? *Immunol Rev* 202:250-265.

87. Barrat, F.J., T. Meeker, J. Gregorio, J.H. Chan, S. Uematsu, S. Akira, B. Chang, O. Duramad, and R.L. Coffman. 2005. Nucleic acids of mammalian origin can act as endogenous ligands for Toll-like receptors and may promote systemic lupus erythematosus. *J Exp Med* 202:1131-1139.

88. Theofilopoulos, A.N., R. Baccala, B. Beutler, and D.H. Kono. 2005. Type I interferons (alpha/beta) in immunity and autoimmunity. *Annu Rev Immunol* 23:307-336.

89. Hooks, J.J., H.M. Moutsopoulos, S.A. Geis, N.I. Stahl, J.L. Decker, and A.L. Notkins. 1979. Immune interferon in the circulation of patients with autoimmune disease. *N Engl J Med* 301:5-8.

90. Baechler, E.C., F.M. Batliwalla, G. Karypis, P.M. Gaffney, W.A. Ortmann, K.J. Espe, K.B. Shark, W.J. Grande, K.M. Hughes, V. Kapur, P.K. Gregersen, and T.W. Behrens. 2003. Interferon-inducible gene expression signature in peripheral blood cells of patients with severe lupus. *Proc Natl Acad Sci U S A* 100:2610-2615.

91. Bennett, L., A.K. Palucka, E. Arce, V. Cantrell, J. Borvak, J. Banchereau, and V. Pascual. 2003. Interferon and granulopoiesis signatures in systemic lupus erythematosus blood. *J Exp Med* 197:711-723.

92. Santiago-Raber, M.L., R. Baccala, K.M. Haraldsson, D. Choubey, T.A. Stewart, D.H. Kono, and A.N. Theofilopoulos. 2003. Type-I interferon receptor deficiency reduces lupus-like disease in NZB mice. *J Exp Med* 197:777-788.

93. Braun, D., P. Geraldes, and J. Demengeot. 2003. Type I Interferon controls the onset and severity of autoimmune manifestations in lpr mice. *J Autoimmun* 20:15-25.

94. Hron, J.D., and S.L. Peng. 2004. Type I IFN protects against murine lupus. *J Immunol* 173:2134-2142.

95. Ronnblom, L.E., G.V. Alm, and K.E. Oberg. 1991. Autoimmunity after alpha-interferon therapy for malignant carcinoid tumors. *Ann Intern Med* 115:178-183.

96. Gota, C., and L. Calabrese. 2003. Induction of clinical autoimmune disease by therapeutic interferon-alpha. *Autoimmunity* 36:511-518.

97. Le Bon, A., G. Schiavoni, G. D'Agostino, I. Gresser, F. Belardelli, and D.F. Tough. 2001. Type i interferons potently enhance humoral immunity and can promote isotype switching by stimulating dendritic cells in vivo. *Immunity* 14:461-470.

98. Jego, G., A.K. Palucka, J.P. Blanck, C. Chalouni, V. Pascual, and J. Banchereau. 2003. Plasmacytoid dendritic cells induce plasma cell differentiation through type I interferon and interleukin 6. *Immunity* 19:225-234.

99. Poeck, H., M. Wagner, J. Battiany, S. Rothenfusser, D. Wellisch, V. Hornung, B. Jahrsdorfer, T. Giese, S. Endres, and G. Hartmann. 2004. Plasmacytoid dendritic cells, antigen, and CpG-C license human B cells for plasma cell differentiation and immunoglobulin production in the absence of T-cell help. *Blood* 103:3058-3064.

100. Santini, S.M., C. Lapenta, M. Logozzi, S. Parlato, M. Spada, T. Di Pucchio, and F. Belardelli. 2000. Type I interferon as a powerful adjuvant for monocyte-derived dendritic cell development and activity in vitro and in Hu-PBL-SCID mice. *J Exp Med* 191:1777-1788.

101. Blanco, P., A.K. Palucka, M. Gill, V. Pascual, and J. Banchereau. 2001. Induction of dendritic cell differentiation by IFN-alpha in systemic lupus erythematosus. *Science* 294:1540-1543.

102. Nguyen, K.B., W.T. Watford, R. Salomon, S.R. Hofmann, G.C. Pien, A. Morinobu, M. Gadina, J.J. O'Shea, and C.A. Biron. 2002. Critical role for STAT4 activation by type 1 interferons in the interferon-gamma response to viral infection. *Science* 297:2063-2066.

103. Colonna, M., G. Trinchieri, and Y.J. Liu. 2004. Plasmacytoid dendritic cells in immunity. *Nat Immunol* 5:1219-1226.

104. Asselin-Paturel, C., and G. Trinchieri. 2005. Production of type I interferons: plasmacytoid dendritic cells and beyond. *J Exp Med* 202:461-465.

105. Liu, Y.J. 2005. IPC: professional type 1 interferon-producing cells and plasmacytoid dendritic cell precursors. *Annu Rev Immunol* 23:275-306.

106. Lund, J., A. Sato, S. Akira, R. Medzhitov, and A. Iwasaki. 2003. Toll-like receptor 9-mediated recognition of Herpes simplex virus-2 by plasmacytoid dendritic cells. *J Exp Med* 198:513-520.

107. Kawai, T., S. Sato, K.J. Ishii, C. Coban, H. Hemmi, M. Yamamoto, K. Terai, M. Matsuda, J. Inoue, S. Uematsu, O. Takeuchi, and S. Akira. 2004. Interferon-alpha induction through Toll-like receptors involves a direct interaction of IRF7 with MyD88 and TRAF6. *Nat Immunol* 5:1061-1068.

108. Honda, K., H. Yanai, H. Negishi, M. Asagiri, M. Sato, T. Mizutani, N. Shimada, Y. Ohba, A. Takaoka, N. Yoshida, and T. Taniguchi. 2005. IRF-7 is the master regulator of type-I interferon-dependent immune responses. *Nature* 434:772-777.

109. Honda, K., Y. Ohba, H. Yanai, H. Negishi, T. Mizutani, A. Takaoka, C. Taya, and T. Taniguchi. 2005. Spatiotemporal regulation of MyD88-IRF-7 signalling for robust type-I interferon induction. *Nature* 434:1035-1040.

110. Nestle, F.O., C. Conrad, A. Tun-Kyi, B. Homey, M. Gombert, O. Boyman, G. Burg, Y.J. Liu, and M. Gilliet. 2005. Plasmacytoid predendritic cells initiate psoriasis through interferon-alpha production. *J Exp Med* 202:135-143.

111. Ronnblom, L., and G.V. Alm. 2001. A pivotal role for the natural interferon alpha-producing cells (plasmacytoid dendritic cells) in the pathogenesis of lupus. *J Exp Med* 194:F59-63.

112. Vallin, H., S. Blomberg, G.V. Alm, B. Cederblad, and L. Ronnblom. 1999. Patients with systemic lupus erythematosus (SLE) have a circulating inducer of interferon-alpha (IFN-alpha) production acting on leucocytes resembling immature dendritic cells. *Clin Exp Immunol* 115:196-202.

113. Bave, U., G.V. Alm, and L. Ronnblom. 2000. The combination of apoptotic U937 cells and lupus IgG is a potent IFN-alpha inducer. *J Immunol* 165:3519-3526.

114. Lovgren, T., M.L. Eloranta, U. Bave, G.V. Alm, and L. Ronnblom. 2004. Induction of interferon-alpha production in plasmacytoid dendritic cells by immune complexes containing nucleic acid released by necrotic or late apoptotic cells and lupus IgG. *Arthritis Rheum* 50:1861-1872.

115. Bave, U., M. Magnusson, M.L. Eloranta, A. Perers, G.V. Alm, and L. Ronnblom. 2003. Fc gamma RIIa is expressed on natural IFN-alpha-producing cells

(plasmacytoid dendritic cells) and is required for the IFN-alpha production induced by apoptotic cells combined with lupus IgG. *J Immunol* 171:3296-3302.

116. Means, T.K., E. Latz, F. Hayashi, M.R. Murali, D.T. Golenbock, and A.D. Luster. 2005. Human lupus autoantibody-DNA complexes activate DCs through cooperation of CD32 and TLR9. *J Clin Invest* 115:407-417.

117. Kirou, K.A., C. Lee, S. George, K. Louca, M.G. Peterson, and M.K. Crow. 2005. Activation of the interferon-alpha pathway identifies a subgroup of systemic lupus erythematosus patients with distinct serologic features and active disease. *Arthritis Rheum* 52:1491-1503.

118. Boule, M.W., C. Broughton, F. Mackay, S. Akira, A. Marshak-Rothstein, and I.R. Rifkin. 2004. Toll-like Receptor 9-Dependent and -Independent Dendritic Cell Activation by Chromatin-Immunoglobulin G Complexes. *J Exp Med* 199:1631-1640.

119. Mackay, F., P. Schneider, P. Rennert, and J. Browning. 2003. BAFF AND APRIL: A Tutorial on B Cell Survival. *Annu Rev Immunol* 21:231-264.

120. Balazs, M., F. Martin, T. Zhou, and J. Kearney. 2002. Blood dendritic cells interact with splenic marginal zone B cells to initiate T-independent immune responses. *Immunity* 17:341-352.

121. Wofsy, D., and W.E. Seaman. 1985. Successful treatment of autoimmunity in NZB/NZW F1 mice with monoclonal antibody to L3T4. *J Exp Med* 161:378-391.

122. Wofsy, D., and W.E. Seaman. 1987. Reversal of advanced murine lupus in NZB/NZW F1 mice by treatment with monoclonal antibody to L3T4. *J Immunol* 138:3247-3253.

123. Sobel, E.S., V.N. Kakkanaiah, M. Kakkanaiah, R.L. Cheek, P.L. Cohen, and R.A. Eisenberg. 1994. T-B collaboration for autoantibody production in lpr mice is cognate and MHC-restricted. *J Immunol* 152:6011-6016.

124. Peng, S.L., M.P. Madaio, D.P. Hughes, I.N. Crispe, M.J. Owen, L. Wen, A.C. Hayday, and J. Craft. 1996. Murine lupus in the absence of alpha beta T cells. *J Immunol* 156:4041-4049.

125. Seo, S.J., M.L. Fields, J.L. Buckler, A.J. Reed, L. Mandik-Nayak, S.A. Nish, R.J. Noelle, L.A. Turka, F.D. Finkelman, A.J. Caton, and J. Erikson. 2002. The impact of T helper and T regulatory cells on the regulation of anti- double-stranded DNA B cells. *Immunity* 16:535-546.

126. Renshaw, B.R., W.C. Fanslow, 3rd, R.J. Armitage, K.A. Campbell, D. Liggitt, B. Wright, B.L. Davison, and C.R. Maliszewski. 1994. Humoral immune responses in CD40 ligand-deficient mice. *J Exp Med* 180:1889-1900.

127. Xu, J., T.M. Foy, J.D. Laman, E.A. Elliott, J.J. Dunn, T.J. Waldschmidt, J. Elsemore, R.J. Noelle, and R.A. Flavell. 1994. Mice deficient for the CD40 ligand. *Immunity* 1:423-431.

128. Ma, J., J. Xu, M.P. Madaio, Q. Peng, J. Zhang, I.S. Grewal, R.A. Flavell, and J. Craft. 1996. Autoimmune lpr/lpr mice deficient in CD40 ligand: spontaneous Ig class switching with dichotomy of autoantibody responses. *J Immunol* 157:417-426.

129. Borriello, F., M.P. Sethna, S.D. Boyd, A.N. Schweitzer, E.A. Tivol, D. Jacoby, T.B. Strom, E.M. Simpson, G.J. Freeman, and A.H. Sharpe. 1997. B7-1 and B7-2 have overlapping, critical roles in immunoglobulin class switching and germinal center formation. *Immunity* 6:303-313.

130. Liang, B., R.J. Gee, M.J. Kashgarian, A.H. Sharpe, and M.J. Mamula. 1999. B7 costimulation in the development of lupus: autoimmunity arises either in the absence of B7.1/B7.2 or in the presence of anti-b7.1/B7.2 blocking antibodies. *J Immunol* 163:2322-2329.

131. Dong, C., U.A. Temann, and R.A. Flavell. 2001. Cutting edge: critical role of inducible costimulator in germinal center reactions. *J Immunol* 166:3659-3662.

132. McAdam, A.J., R.J. Greenwald, M.A. Levin, T. Chernova, N. Malenkovich, V. Ling, G.J. Freeman, and A.H. Sharpe. 2001. ICOS is critical for CD40-mediated antibody class switching. *Nature* 409:102-105.

133. Vinuesa, C.G., M.C. Cook, C. Angelucci, V. Athanasopoulos, L. Rui, K.M. Hill, D. Yu, H. Domaschenz, B. Whittle, T. Lambe, I.S. Roberts, R.R. Copley, J.I. Bell, R.J. Cornall, and C.C. Goodnow. 2005. A RING-type ubiquitin ligase family member required to repress follicular helper T cells and autoimmunity. *Nature* 435:452-458.

134. Daikh, D.I., B.K. Finck, P.S. Linsley, D. Hollenbaugh, and D. Wofsy. 1997. Long-term inhibition of murine lupus by brief simultaneous blockade of the B7/CD28 and CD40/gp39 costimulation pathways. *J. Immunol.* 159:3104-3108.

135. Wang, X., W. Huang, M. Mihara, J. Sinha, and A. Davidson. 2002. Mechanism of action of combined short-term CTLA4Ig and anti-CD40 ligand in murine systemic lupus erythematosus. *J Immunol* 168:2046-2053.

136. Sakaguchi, S. 2004. Naturally arising CD4+ regulatory t cells for immunologic self-tolerance and negative control of immune responses. *Annu Rev Immunol* 22:531-562.

137. Bystry, R.S., V. Aluvihare, K.A. Welch, M. Kallikourdis, and A.G. Betz. 2001. B cells and professional APCs recruit regulatory T cells via CCL4. *Nat Immunol* 2:1126-1132.

138. Will, C.L., and R. Luhrmann. 2001. Spliceosomal UsnRNP biogenesis, structure and function. *Curr Opin Cell Biol* 13:290-301.

139. Cohen, P.L., and R.A. Eisenberg. 1991. Lpr and gld: single gene models of systemic autoimmunity and lymphoproliferative disease. *Annu Rev Immunol* 9:243-269.

140. Izui, S., V.E. Kelley, K. Masuda, H. Yoshida, J.B. Roths, and E.D. Murphy. 1984. Induction of various autoantibodies by mutant gene lpr in several strains of mice. *J Immunol* 133:227-233.

141. Emlen, W., and L. O'Neill. 1997. Clinical significance of antinuclear antibodies: comparison of detection with immunofluorescence and enzyme-linked immunosorbent assays. *Arthritis Rheum* 40:1612-1618.

142. Aarden, L.A., E.R. de Groot, and T.E. Feltkamp. 1975. Immunology of DNA. III. Crithidia luciliae, a simple substrate for the determination of anti-dsDNA with the immunofluorescence technique. *Ann N Y Acad Sci* 254:505-515.

143. Isenberg, D.A., C. Dudeney, W. Williams, I. Addison, S. Charles, J. Clarke, and A. Todd-Pokropek. 1987. Measurement of anti-DNA antibodies: a reappraisal using five different methods. *Ann Rheum Dis* 46:448-456.

144. Kavanaugh, A., R. Tomar, J. Reveille, D.H. Solomon, and H.A. Homburger. 2000. Guidelines for clinical use of the antinuclear antibody test and tests for specific autoantibodies to nuclear antigens. American College of Pathologists. *Arch Pathol Lab Med* 124:71-81.

145. Bloom, D.D., J.L. Davignon, M.W. Retter, M.J. Shlomchik, D.S. Pisetsky, P.L. Cohen, R.A. Eisenberg, and S.H. Clarke. 1993. V region gene analysis of anti-Sm hybridomas from MRL/Mp-lpr/lpr mice. *J Immunol* 150:1591-1610.

146. Cocca, B.A., S.N. Seal, P. D'Agnillo, Y.M. Mueller, P.D. Katsikis, J. Rauch, M. Weigert, and M.Z. Radic. 2001. Structural basis for autoantibody recognition of phosphatidylserine-beta 2 glycoprotein I and apoptotic cells. *Proc Natl Acad Sci U S A* 98:13826-13831.

147. Arbuckle, M.R., M.T. McClain, M.V. Rubertone, R.H. Scofield, G.J. Dennis, J.A. James, and J.B. Harley. 2003. Development of autoantibodies before the clinical onset of systemic lupus erythematosus. *N Engl J Med* 349:1526-1533.

148. Laderach, D., S. Koutouzov, J.F. Bach, and A.M. Yamamoto. 2003. Concomitant early appearance of anti-ribonucleoprotein and anti-nucleosome antibodies in lupus prone mice. *J Autoimmun* 20:161-170.

149. Shlomchik, M.J., J. Craft, and M.J. Mamula. 2001. From T to B and back again: positive feedback in systemic autoimmune disease. *Nature Reviews Immunology* 1:147-153.

150. Lian, Z.X., K. Kikuchi, G.X. Yang, A.A. Ansari, S. Ikehara, and M.E. Gershwin. 2004. Expansion of bone marrow IFN-alpha-producing dendritic cells in New Zealand Black (NZB) mice: high level expression of TLR9 and secretion of IFN-alpha in NZB bone marrow. *J Immunol* 173:5283-5289.

151. Yamamoto, M., S. Sato, H. Hemmi, K. Hoshino, T. Kaisho, H. Sanjo, O. Takeuchi, M. Sugiyama, M. Okabe, K. Takeda, and S. Akira. 2003. Role of adaptor TRIF in the MyD88-independent toll-like receptor signaling pathway. *Science* 301:640-643.

152. Waters, S.T., M. McDuffie, H. Bagavant, U.S. Deshmukh, F. Gaskin, C. Jiang, K.S. Tung, and S.M. Fu. 2004. Breaking tolerance to double stranded DNA, nucleosome, and other nuclear antigens is not required for the pathogenesis of lupus glomerulonephritis. *J Exp Med* 199:255-264.

153. Muzio, M., D. Bosisio, N. Polentarutti, G. D'Amico, A. Stoppacciaro, R. Mancinelli, C. van't Veer, G. Penton-Rol, L.P. Ruco, P. Allavena, and A. Mantovani. 2000. Differential expression and regulation of toll-like receptors (TLR) in human leukocytes: selective expression of TLR3 in dendritic cells. *J Immunol* 164:5998-6004.

154. Roach, J.C., G. Glusman, L. Rowen, A. Kaur, M.K. Purcell, K.D. Smith, L.E. Hood, and A. Aderem. 2005. The evolution of vertebrate Toll-like receptors. *Proc Natl Acad Sci U S A* 102:9577-9582.

155. Losman, M.J., T.M. Fasy, K.E. Novick, and M. Monestier. 1992. Monoclonal autoantibodies to subnucleosomes from a MRL/Mp(-)+/+ mouse. Oligoclonality of the antibody response and recognition of a determinant composed of histones H2A, H2B, and DNA. *J Immunol* 148:1561-1569.

156. Takeuchi, Y., O. Ishikawa, and Y. Miyachi. 1997. The comparative study of anti-double stranded DNA antibody levels measured by radioimmunoassay and enzyme-linked immunosorbent assay in systemic lupus erythematosus. *J Dermatol* 24:297-300.

157. Krug, A., A.R. French, W. Barchet, J.A. Fischer, A. Dzionek, J.T. Pingel, M.M. Orihuela, S. Akira, W.M. Yokoyama, and M. Colonna. 2004. TLR9-dependent recognition of MCMV by IPC and DC generates coordinated cytokine responses that activate antiviral NK cell function. *Immunity* 21:107-119.

158. Akira, S. 2003. Toll-like receptor signaling. *J Biol Chem* 278:38105-38108.

159. Uematsu, S., S. Sato, M. Yamamoto, T. Hirotani, H. Kato, F. Takeshita, M. Matsuda, C. Coban, K.J. Ishii, T. Kawai, O. Takeuchi, and S. Akira. 2005. Interleukin-1 receptor-associated kinase-1 plays an essential role for Toll-like receptor (TLR)7- and TLR9-mediated interferon-{alpha} induction. *J Exp Med* 201:915-923.

160. Sato, S., O. Takeuchi, T. Fujita, H. Tomizawa, K. Takeda, and S. Akira. 2002. A variety of microbial components induce tolerance to lipopolysaccharide by differentially affecting MyD88-dependent and -independent pathways. *Int Immunol* 14:783-791.

161. Napolitani, G., A. Rinaldi, F. Bertoni, F. Sallusto, and A. Lanzavecchia. 2005. Selected Toll-like receptor agonist combinations synergistically trigger a T helper type 1-polarizing program in dendritic cells. *Nat Immunol* 6:769-776.

162. Edwards, A.D., S.S. Diebold, E.M. Slack, H. Tomizawa, H. Hemmi, T. Kaisho, S. Akira, and C. Reis e Sousa. 2003. Toll-like receptor expression in murine DC subsets: lack of TLR7 expression by CD8 alpha+ DC correlates with unresponsiveness to imidazoquinolines. *Eur J Immunol* 33:827-833.

163. Bluthner, M., and F.A. Bautz. 1992. Cloning and characterization of the cDNA coding for a polymyositis-scleroderma overlap syndrome-related nucleolar 100-kD protein. *J Exp Med* 176:973-980.

164. Hunter, C.A. 2005. New IL-12-family members: IL-23 and IL-27, cytokines with divergent functions. *Nat Rev Immunol* 5:521-531.

165. Diebold, S.S., M. Montoya, H. Unger, L. Alexopoulou, P. Roy, L.E. Haswell, A. Al-Shamkhani, R. Flavell, P. Borrow, and C. Reis e Sousa. 2003. Viral infection switches non-plasmacytoid dendritic cells into high interferon producers. *Nature* 424:324-328.

166. Okabe, Y., K. Kawane, S. Akira, T. Taniguchi, and S. Nagata. 2005. Toll-like receptor-independent gene induction program activated by mammalian DNA escaped from apoptotic DNA degradation. *J Exp Med* 202:1333-1339.

167. Sharif, M.N., I. Tassiulas, Y. Hu, I. Mecklenbrauker, A. Tarakhovsky, and L.B. Ivashkiv. 2004. IFN-alpha priming results in a gain of proinflammatory function

by IL-10: implications for systemic lupus erythematosus pathogenesis. *J Immunol* 172:6476-6481.

168. Erikson, J., M.Z. Radic, S.A. Camper, R.R. Hardy, C. Carmack, and M. Weigert. 1991. Expression of anti-DNA immunoglobulin transgenes in non-autoimmune mice. *Nature* 349:331-334.

169. Gay, D., T. Saunders, S. Camper, and M. Weigert. 1993. Receptor editing: An approach by autoreactive B cells to escape tolerance. *J. Exp. Med.* 177:999-1008.

170. Chen, C., Z. Nagy, M.Z. Radic, R.R. Hardy, D. Huszar, S.A. Camper, and M. Weigert. 1995. The site and stage of anti-DNA B-cell deletion. *Nature* 373:252-255.

171. Shlomchik, M., M. Mascelli, H. Shan, M.Z. Radic, D. Pisetsky, A. Marshak-Rothstein, and M. Weigert. 1990. Anti-DNA antibodies from autoimmune mice arise by clonal expansion and somatic mutation. *J Exp Med* 171:265-292.

172. Radic, M.Z., M.A. Mascelli, J. Erikson, H. Shan, and M. Weigert. 1991. Ig H and L chain contributions to autoimmune specificities. *J Immunol* 146:176-182.

173. Ibrahim, S.M., M. Weigert, C. Basu, J. Erikson, and M.Z. Radic. 1995. Light chain contribution to specificity in anti-DNA antibodies. *J Immunol* 155:3223-3233.

174. Wang, H., and M.J. Shlomchik. 1999. Autoantigen-specific B cell activation in Fas-deficient rheumatoid factor immunoglobulin transgenic mice. *J Exp Med* 190:639-649.

175. Mandik-Nayak, L., A. Bui, H. Noorchashm, A. Eaton, and J. Erikson. 1997. Regulation of anti-double-stranded DNA B cells in nonautoimmune mice: localization to the T-B interface of the splenic follicle. *J Exp Med* 186:1257-1267.

176. Rubio, C.F., J. Kench, D.M. Russell, R. Yawger, and D. Nemazee. 1996. Analysis of central B cell tolerance in autoimmune-prone MRL/lpr mice bearing autoantibody transgenes. *J Immunol* 157:65-71.

177. Mandik-Nayak, L., S.J. Seo, C. Sokol, K.M. Potts, A. Bui, and J. Erikson. 1999. MRL-lpr/lpr mice exhibit a defect in maintaining developmental arrest and follicular exclusion of anti-double-stranded DNA B cells. *J Exp Med* 189:1799-1814.

178. Hardy, R.R., and K. Hayakawa. 2001. B cell development pathways. *Annu Rev Immunol* 19:595-621.

179. Takahashi, K., Y. Kozono, T.J. Waldschmidt, D. Berthiaume, R.J. Quigg, A. Baron, and V.M. Holers. 1997. Mouse complement receptors type 1 (CR1;CD35) and type 2 (CR2;CD21): expression on normal B cell subpopulations and decreased levels during the development of autoimmunity in MRL/lpr mice. *J Immunol* 159:1557-1569.

180. William, J., C. Euler, and M.J. Shlomchik. 2005. Short-lived plasmablasts dominate the early spontaneous rheumatoid factor response: differentiation pathways, hypermutating cell types, and affinity maturation outside the germinal center. *J Immunol* 174:6879-6887.

181. Kallies, A., J. Hasbold, D.M. Tarlinton, W. Dietrich, L.M. Corcoran, P.D. Hodgkin, and S.L. Nutt. 2004. Plasma cell ontogeny defined by quantitative changes in blimp-1 expression. *J Exp Med* 200:967-977.

182. Eaton-Bassiri, A.S., L. Mandik-Nayak, S.J. Seo, M.P. Madaio, M.P. Cancro, and J. Erikson. 2000. Alterations in splenic architecture and the localization of anti-double-stranded DNA B cells in aged mice. *Int Immunol* 12:915-926.

183. Li, Y., H. Li, D. Ni, and M. Weigert. 2002. Anti-DNA B cells in MRL/lpr mice show altered differentiation and editing pattern. *J Exp Med* 196:1543-1552.

184. Martin, F., and J.F. Kearney. 2002. Marginal-zone B cells. *Nat Rev Immunol* 2:323-335.

185. Viau, M., and M. Zouali. 2005. B-lymphocytes, innate immunity, and autoimmunity. *Clin Immunol* 114:17-26.

186. Sekiguchi, D.R., S.M. Jainandunsing, M.L. Fields, M.A. Maldonado, M.P. Madaio, J. Erikson, M. Weigert, and R.A. Eisenberg. 2002. Chronic Graft-Versus-Host in Ig Knockin Transgenic Mice Abrogates B Cell Tolerance in Anti-Double-Stranded DNA B Cells. *J Immunol* 168:4142-4153.

187. William, J., C. Euler, E. Leadbetter, A. Marshak-Rothstein, and M.J. Shlomchik. 2005. Visualizing the onset and evolution of an autoantibody response in systemic autoimmunity. *J Immunol* 174:6872-6878.

188. Alugupalli, K.R., J.M. Leong, R.T. Woodland, M. Muramatsu, T. Honjo, and R.M. Gerstein. 2004. B1b lymphocytes confer T cell-independent long-lasting immunity. *Immunity* 21:379-390.

189. William, J., C. Euler, S. Christensen, and M.J. Shlomchik. 2002. Evolution of autoantibody responses via somatic hypermutation outside of germinal centers. *Science* 297:2066-2070.

190. Wellmann, U., M. Letz, M. Herrmann, S. Angermuller, J.R. Kalden, and T.H. Winkler. 2005. The evolution of human anti-double-stranded DNA autoantibodies. *Proc Natl Acad Sci U S A* 102:9258-9263.

191. Hoyer, B.F., K. Moser, A.E. Hauser, A. Peddinghaus, C. Voigt, D. Eilat, A. Radbruch, F. Hiepe, and R.A. Manz. 2004. Short-lived plasmablasts and long-lived plasma cells contribute to chronic humoral autoimmunity in NZB/W mice. *J Exp Med* 199:1577-1584.

192. Hannum, L.G., D. Ni, A.M. Haberman, M.G. Weigert, and M.J. Shlomchik. 1996. A disease-related RF autoantibody is not tolerized in a normal mouse: implications for the origins of autoantibodies in autoimmune disease. *J. Exp. Med.* 184:1269-1278.

193. Carteron, N.L., C.L. Schimenti, and D. Wofsy. 1989. Treatment of murine lupus with F(ab')2 fragments of monoclonal antibody to L3T4. Suppression of autoimmunity does not depend on T helper cell depletion. *J Immunol* 142:1470-1475.

194. Han, S., K. Hathcock, B. Zheng, T.B. Kepler, R. Hodes, and G. Kelsoe. 1995. Cellular interaction in germinal centers. Roles of CD40 ligand and B7-2 in established germinal centers. *J Immunol* 155:556-567.

195. Chen, C., Z. Nagy, E.L. Prak, and M. Weigert. 1995. Immunoglobulin heavy chain gene replacement: a mechanism of receptor editing. *Immunity* 3:747-755.

196. Rossbacher, J., and M.J. Shlomchik. 2003. The B cell receptor itself can activate complement to provide the complement receptor 1/2 ligand required to enhance B cell immune responses in vivo. *J Exp Med* 198:591-602.

197. Allman, D.M., S.E. Ferguson, V.M. Lentz, and M.P. Cancro. 1993. Peripheral B cell maturation. II. Heat-stable antigen(hi) splenic B cells are an immature developmental intermediate in the production of long-lived marrow-derived B cells. *J Immunol* 151:4431-4444.

198. Bayry, J., S. Lacroix-Desmazes, M.D. Kazatchkine, O. Hermine, D.F. Tough, and S.V. Kaveri. 2005. Modulation of dendritic cell maturation and function by B lymphocytes. *J Immunol* 175:15-20.

199. MacLennan, I., and C. Vinuesa. 2002. Dendritic cells, BAFF, and APRIL: innate players in adaptive antibody responses. *Immunity* 17:235-238.

200. Litinskiy, M.B., B. Nardelli, D.M. Hilbert, B. He, A. Schaffer, P. Casali, and A. Cerutti. 2002. DCs induce CD40-independent immunoglobulin class switching through BLyS and APRIL. *Nat Immunol* 3:822-829.

201. Li, H., Y. Jiang, E.L. Prak, M. Radic, and M. Weigert. 2001. Editors and editing of anti-DNA receptors. *Immunity* 15:947-957.

202. Bekeredjian-Ding, I.B., M. Wagner, V. Hornung, T. Giese, M. Schnurr, S. Endres, and G. Hartmann. 2005. Plasmacytoid dendritic cells control TLR7 sensitivity of naive B cells via type I IFN. *J Immunol* 174:4043-4050.

203. Vallin, H., A. Perers, G.V. Alm, and L. Ronnblom. 1999. Anti-double-stranded DNA antibodies and immunostimulatory plasmid DNA in combination mimic the endogenous IFN-alpha inducer in systemic lupus erythematosus. *J Immunol* 163:6306-6313.

204. Kalunian, K.C., J.C. Davis, Jr., J.T. Merrill, M.C. Totoritis, and D. Wofsy. 2002. Treatment of systemic lupus erythematosus by inhibition of T cell costimulation with anti-CD154: a randomized, double-blind, placebo-controlled trial. *Arthritis Rheum* 46:3251-3258.

205. Ogden, C.A., R. Kowalewski, Y. Peng, V. Montenegro, and K.B. Elkon. 2005. IGM is required for efficient complement mediated phagocytosis of apoptotic cells in vivo. *Autoimmunity* 38:259-264.